THE GEOGRAPHY AND RECENT ACTIVITY OF LAKE MICHIGAN'S COASTAL SAND DUNES

By

Kevin G. McKeehan

A DISSERTATION

Submitted to
Michigan State University
in partial fulfillment of the requirements
for the degree of

Geography – Doctor of Philosophy

2022

ABSTRACT

THE GEOGRAPHY AND RECENT ACTIVITY OF LAKE MICHIGAN'S COASTAL SAND DUNES

By

Kevin G. McKeehan

This dissertation attempts to fill a gap in knowledge regarding conditions amongst the dunefields of Lake Michigan's eastern shore. Much is now known about the evolution and geochronology of these unique freshwater dune systems. The region's coastal dunes began forming during the Nipissing high stand phase (~5.5ka) of ancestral Lake Michigan. Since then, according to the chronology constructed from several studies, the coastal dunes then underwent several periods of stability and instability along the entire shoreline. However, questions remain regarding dune conditions and variability since ~1900. The goal of this dissertation was to determine if changes have occurred to the region's coastal dune systems in the last ~120 years and what might be driving those changes. Given that dune systems are sensitive to biotic and abiotic variables, examining the last ~120 years of dune behavior could potentially reveal how Lake Michigan coastal dunes are responding to anthropogenic climate change and human development.

Three studies, each comprising a dissertation chapter (Chapters 2-4), were conducted to help close this knowledge gap. Each chapter is broadly linked through an ecogeomorphic lens, particularly through the relationship between dunes and vegetation, which are interconnected in important ways. In Chapter 2, changes in dunefield vegetation and morphology were determined at several locations along the eastern Lake Michigan shoreline through the use of ground-level repeat photography. The second dissertation study – Chapter 3 – concerns the spatiotemporal analysis of historical changes of blowouts, which are important indicators of significant disturbance in the dunes. In this chapter, blowouts were mapped from aerial images at three timestamps – 1938, 1986-8, and 2018 – and the changes quantified. Chapter 4, the final

dissertation study, explores the relationship between terrain ruggedness and vegetation in a coastal dunefield along Lake Michigan by calculating two terrain indices – Riley's Terrain Ruggedness Index (TRI) and Sappington's Vector Ruggedness Measure (VRM) – and the Soil-Adjusted Vegetation Index (SAVI). Through a land systems framework, the results were compared to determine if any correlation exists between the ruggedness of dunes and vegetation.

In the first two dissertation studies, the results show a clear expansion of vegetation at the expense of previously bare sand. In the final study, the values from TRI and VRM and the values from the Soil-Adjusted Vegetation Index (SAVI) were not correlated overall, especially where one type of vegetation was dominant. However, within one land system – the dune barrens -- a moderate-to-strong negative correlation existed between terrain ruggedness and vegetation. Moreover, evidence suggests that vegetation has transformed the dune barrens land system area within the modern period. Overall, the results of these three studies demonstrate that vegetation is expanding over previously bare surfaces in coastal dunes along the eastern shore of Lake Michigan and has a considerable influence on regional dune conditions. While the precise driver(s) of this transformation is unclear, the regional-scale nature of these results suggests a uniform control is affecting these changes. As described in this dissertation, it is possible that an increase in precipitation since the 1930s, elevated atmospheric CO_2 and N concentrations, a reduction in wind power, some other change in climate drivers, or a combination of many factors is responsible for the expansion in vegetation. It is also possible the trend in vegetation growth in Lake Michigan's coastal dunes is a lagged response to an earlier climate event.

For Kellan, Finley, and Noah

ACKNOWLEDGEMENTS

Many people have contributed to the development of this dissertation and to my progress as a scientist. I am grateful to all of them. In particular, I'd like to thank Dr. Alan F. Arbogast, who served as my adviser and the chair of my dissertation committee. Dr. Arbogast provided the impetus and funding for the first dissertation study focusing on ground-level repeat photography, which largely shaped the tone and focus of the remaining dissertation components. Additionally, I'd like to thank the members of my dissertation committee: Drs. Kyla Dahlin and Ethan J. Theuerkauf, with MSU's Department of Geography, Environment, and Spatial Science, and Dr. Robert B. Richardson, with MSU's Department of Community Sustainability. Each of them provided valuable advice and encouragement through this process. I am also grateful for the support from the department faculty, including Drs. Nathan Moore, Shiyuan Zhong, Jeffery A. Andresen, and Morris Thomas. Graduate Academic Program Coordinators Joni Burns and Sharon Ruggles helped me overcome any administrative difficulties and assisted with the funding to attend conferences at which I presented aspects of this dissertation.

Financial assistance for the research in Chapter 2 was provided, in part, by the Michigan Coastal Management Program, Water Resources Division; and the Michigan Department of Environment, Great Lakes, and Energy (EGLE), under the National Coastal Zone Management Program, through a grant from the National Oceanic and Atmospheric Administration (NOAA), U.S. Department of Commerce (Grant #RC109434). The project was managed by the Michigan Environmental Council (MEC) and Michigan State University (MSU). In addition, I was financially supported by the department for all four years of my doctoral residence, of which I am appreciative.

I would also like to express my deepest gratitude to my parents, Gene and Vickie McKeehan, for their continued support and to my boys – Kellan, Finley, and Noah – who have inspired me to do

good things in this world. Finally, I'd like to offer my deepest appreciation to Dr. Menglin Wang for support, guidance, and friendship; to paraphrase: the domains of time and space are vast and it is a comfort to share the planet and epoch with her.

TABLE OF CONTENTS

LIST OF TABLES

LIST OF FIGURES

KEY TO ABBREVIATIONS

3DEP – USGS's 3D Elevation Program

BW – black and white

C – Chepil's C

C_3 – three-year running average of C

CE – common era

CIR – color infrared

cm – centimeter

CO_2 – carbon dioxide

D – Delgado-Fernandez et al.'s disturbance parameter

DEM – digital elevation model

Dfb – continental, no dry season, warm-summer climate

DNR – Michigan Department of Natural Resources

DP – drift potential

ECMWF – European Centre for Medium-Range Weather Forecasts

EGLE – Michigan Department of Environment, Great Lakes, and Energy

e.g. – exempli gratia (for example)

ESRI – Environmental Systems Research Institute

et al. – et aliī (and others)

GCP – ground control point

GEE – Google Earth Engine

GIS – geographic information system

HCO – Holocene Climate Optimum

HD – Melton's ruggedness index

IBL – internal boundary layer

i.e. – id est (that is)

ISODATA – iterative self-organizing data analysis technique

km – kilometer

LAI – leaf area index

LIA – Little Ice Age

LiDAR – light detection and ranging

LULC – land use land cover

m – meter

M – Lancaster's M

MCO – Medieval Climate Optimum

MEC – Michigan Environmental Council

MI – Michigan

mi – mile

MIS 1 – marine isotope stage 1

ML – machine learning

mm – millimeter

MRCC – Midwestern Regional Climate Center

MSU – Michigan State University

N – nitrogen

NAIP – National Agricultural Imagery Program

NDVI – normalized difference vegetation index

NHAP – National High Altitude Photography

NOAA – National Oceanic and Atmospheric Administration, U.S. Department of Commerce

p./pp. – page or pages

P – annual precipitation

P-E – Thornthwaite's effective precipitation index

PET – potential evapotranspiration

PLS – U.S. Public Lands Survey

PRC – People's Republic of China

R^2 – coefficient of determination

RCO -- Roman Climate Optimum

ρ – Spearman's ρ (Rho, correlation)

RMSE – root mean square error

SAVI – soil-adjusted vegetation index

SBDNL – Sleeping Bear Dunes National Lakeshore

SD – standard deviation

SSE – sum of the squared residuals

SSR – sum of the squares regression

STAMP – spatial–temporal analysis of moving polygons

TPI – topographic position index

TRI – Riley's terrain ruggedness index

TWI – topographic wetness index

U.S./USA – United States of America

USDA – United States Department of Agriculture

USGS – United States Geological Survey

V – Delgado-Fernandez et al.'s vegetation parameter

VRM – Sappington's vector ruggedness measure

z – elevation

Z – Z-statistic

z_o – surface roughness

CHAPTER 1.
INTRODUCTION, THE GEOGRAPHY AND RECENT ACTIVITY OF LAKE MICHIGAN'S COASTAL SAND DUNES

1.1 Introduction

Coastal sand dunes line much of the eastern shore of Lake Michigan. These magnificent dunes provide the recreational setting and economic engine for many communities. The region's dunes often are featured in the state of Michigan's *Pure Michigan* tourism campaigns, while Sleeping Bear Dunes National Lakeshore, with its distinctive perched dunes, was even listed as "The Most Beautiful Place in America" by *Good Morning America* in 2011. Dunes here are also the source of considerable foundry sand (Schrotenboer and Arbogast, 2010). Yet, beyond their esthetic and economic value, these coastal dune systems are important for geomorphological reasons. The coastal dunes of Lake Michigan's eastern shore are an unique aeolian system, comprising of ~3.5M acres of dunes (Arbogast et al., 2018). This expansive landscape represents possibly the largest freshwater dune system in the world (Peterson and Dersch, 1981) and developed under conditions distinctive from most other coastal dune systems (Hansen et al., 2010). Specifically, the Lake Michigan coastal dune systems developed without the influence of tectonic or tidal activity (Hansen et al., 2010). Instead, Lake Michigan's coastal dunes formed mostly due to reworking of sandy glacial and lacustrine deposits by forces related to climatic and lake level variability (Hansen et al., 2010; Loope and Arbogast, 2000; Lovis et al., 2012; Thompson et al., 2011).

Due to work over the last 25 years, much is now known about the evolution and geochronology of these landscapes. Research clearly demonstrates that the coastal dunes began forming during the Nipissing high stand phase (~5.5ka) of ancestral Lake Michigan, although in some locations, dune building may have started later (Lovis et al., 2012). According to the chronology constructed from several studies, the coastal dunes then underwent several periods of stability and instability along the entire shoreline in the late Holocene, culminating in a time of pronounced stability from

~2ka to ~1ka in which vegetation expanded across the previously mobile dunes (Lovis et al., 2012). Six such phases of dune stability or instability were identified by Hansen et al. (2010) based upon a synthesis of geomorphic analyses and the dating of soil and aeolian deposits. Driving these distinct events – and the corresponding dune response – are changes in climate, specifically temperature and precipitation, and Lake Michigan water levels, which occur at multiple spatiotemporal scales.

Yet, despite this illuminating geochronology and a basic understanding of the landscape's geomorphic process-response regime, questions remain regarding this unique dune system. Most prominently for this dissertation, is the question of the geomorphic variability of dune behavior in the modern period. Specifically, this dissertation sought to address the gap in knowledge with regards to the ecogeomorphic variability of dune along Lake Michigan's eastern shoreline since ~1900, the time when our ability to observe and record our world began to improve. The goal of this dissertation was to determine if changes in vegetation and terrain have occurred to the region's coastal dune systems in the last ~120 years and what might be driving those changes. Given that dune systems are sensitive to biotic and abiotic changes, examining the last ~120 years of dune behavior could potentially reveal how Lake Michigan coastal dunes are responding to anthropogenic climate change and human development. After all, the region's dunefields are a complex process-response system in which dune behavior is based upon the interaction of Lake Michigan with coastal landforms, the availability of littoral and foredune sand, the ability and power of wind to entrain that sand inland, and a series of interrelated ecogeomorphic feedback mechanisms involving vegetation and dune morphology (van Dijk, 2004, 2014; Walker et al., 2017). Change in any one variable within this system affects the other variables, driving dune behavior between different possible modes – active, stabilized, mixed – within a dynamic multiple-state system. In other words, if we can observe how dune are changing in the modern

period and assign possible drivers to those changes, then we may be able to better understand dune behavior for the last ~5.5k years. Additionally, we might also be able to predict how Lake Michigan's dune systems could evolve in the coming years. Beyond that, however, coastal managers along the eastern shore of Lake Michigan may find the results of this dissertation of interest, as it may be up to them to address the implications of a changing dune system.

I approached these questions of modern dune variability in three related studies, each representing a distinctive dissertation chapter. Each chapter is broadly linked through an ecogeomorphic lens, particularly through the relationship between dunes and vegetation. This relationship is critical to our understanding of Lake Michigan's coastal dunes because vegetation is a dominant control on dune behavior, while dune morphology has the capacity to influence how vegetation develops (Delgado-Fernandez et al., 2019; Schwarz et al., 2018). In the first dissertation study, I used ground-level repeat photography to demonstrate how the coastal dunes of Lake Michigan's eastern shore have changed since the 19th century. Hundreds of photographs of the region's dunes were collected, taken between the years 1885 and 2018, from archives and citizen scientists. I then located the photograph sites in the field and took new photographs from the same spot, replicating the original images. The photographic pairs were compared for changes in vegetation extent, as one recent study suggested an expansion of vegetation was underway in the dunefields along the eastern shore of Lake Michigan (White et al., 2019). That study comports with evidence that dunefields globally have recently become more stabilized due to vegetation (Gao et al., 2020). The changes in vegetation extent between the original photographs and rephotographs were calculated and we assigned likely divers to the changes we observed.

Similarly, the second dissertation study concerns the spatiotemporal analysis of historical changes of blowouts, which are important indicators of significant disturbance in the dunes. In this chapter,

blowouts were mapped from aerial images at three timestamps – 1938, 1986-8, and 2018 – using an unsupervised classification algorithm known as iso-clustering. I then compared the blowout geographies through a technique known as a spatial–temporal analysis of moving polygons (STAMP) model, which permitted an assessment of how each individual blowout changed in time and space. Understanding the spatiotemporal changes of these landforms is important, as blowouts are erosional depressions or troughs which have "blown out" through existing dunes due to natural or anthropogenic forcing (Hesp, 2002) and are particularly sensitive to changes in their environment (Schwarz et al., 2018). In other words, blowouts are excellent indicators of changing conditions in the region's coastal dunefields. Thus, if blowouts are growing geographically in size or if new ones have formed, this could be indicative of changes in lake levels, regional climate, or human disturbance. Likewise, if blowouts are becoming stabilized or fragmented by vegetation, this condition could suggest different biotic and abiotic shifts are underway. We examined the spatiotemporal changes of blowouts from our aerial image analyses and, like the first dissertation chapter, assigned possible drivers to the changes we observed.

Clearly, these first two dissertation studies are closely linked. Both use some type of repeat photography and both are concerned with ecogeomorphic changes of dunes in the modern period. The final dissertation study is linked to the first two more subtly as it considers the ecogeomorphic relationship between vegetation and dune morphology from a different perspective. Here, I explored the relationship between terrain ruggedness and vegetation in a coastal dunefield at Ludington State Park along Lake Michigan's eastern shore. If dunes and dunefields are the product of a complex, multivariate process-response system which result in nonlinear ecogeomorphic outcomes (Lichter, 2000; Miyanishi and Johnson, 2021; Schwarz et al., 2018; Sherman and Bauer, 1993; Stallins and Parker, 2003; Walker et al., 2017; Wright and Thom, 1977), then understanding the relationship between vegetation and dune form is important

to comprehending coastal dunefield morphodynamics. For example, it has been observed that vegetation can serve as a control on sand supply to downwind dune landforms with consequences to their ecogeomorphic mode (Cooper, 1958; Gares, 1992; Schwarz et al., 2018). To better understand this relationship, I calculated two terrain indices – Riley's Terrain Ruggedness Index (TRI) and Sappington's Vector Ruggedness Measure (VRM) – and compared them to a common measure of vegetation in dune environments – the Soil-Adjusted Vegetation Index (SAVI).

For all three dissertation studies, I hypothesize that vegetation is expanding in Lake Michigan's dunefields and exerting an important influence on the geomorphology of dunes. We believe that the results of our studies will show vegetation is expanding in dunes generally (Chapter 2), stabilizing and fragmenting blowouts (Chapter 3), and changing the terrain variability of dune land systems (Chapter 4). Driving these trends is possibly an increase in annual precipitation regionally since the 1930s, which White et al. (2019) described. While we hypothesize that White et al. (2019) were correct in identifying this control, we also believe other drivers may be involved. For example, it is possible the region's dunefields are midstream of a nonlinear ecogeomorphic lag from the stormier Little Ice Age period or the proceeding, drier Medieval Warm Period. The goal of this dissertation, then, is to test our hypotheses regarding dune behavior along the lakeshore in the modern period and attempt to identify possible variables driving any changes we observe.

REFERENCES

REFERENCES

Arbogast, A.F., Garmon, B., Sterrett Isely, E., Jarosz, J., Kreiger, A., Nicholls, S., Queen, C., Richardson, R.B., 2018. Valuing Michigan's Coastal Dunes: GIS Information and Economic Data to Support Management Partnerships.

Cooper, W.S., 1958. Coastal Sand Dunes of Oregon and Washington. Geological Society of America - Memoir 72.

Delgado-Fernandez, I., O'Keeffe, N., Davidson-Arnott, R.G.D., 2019. Natural and human controls on dune vegetation cover and disturbance. Sci. Total Environ. 672, 643–656. https://doi.org/10.1016/j.scitotenv.2019.03.494

Gao, J., Kennedy, D.M., Konlechner, T.M., 2020. Coastal dune mobility over the past century: A global review. Prog. Phys. Geogr. Earth Environ. 44, 814–836. https://doi.org/10.1177/0309133320919612

Gares, P.A., 1992. Topographic changes associated with coastal dune blowouts at island beach state park, New Jersey. Earth Surf. Process. Landforms 17, 589–604. https://doi.org/10.1002/esp.3290170605

Hansen, E.C., Fisher, T.G., Arbogast, A.F., Bateman, M.D., 2010. Geomorphic history of low-perched, transgressive dune complexes along the southeastern shore of Lake Michigan. Aeolian Res. 1, 111–127. https://doi.org/10.1016/j.aeolia.2009.08.001

Hesp, P., 2002. Foredunes and blowouts: Initiation, geomorphology and dynamics. Geomorphology 48, 245–268. https://doi.org/10.1016/S0169-555X(02)00184-8

Lichter, J., 2000. Colonization constraints during primary succession on coastal Lake Michigan sand dunes. J. Ecol. 88, 825–839.

Loope, W.L., Arbogast, A.F., 2000. Dominance of an ~150-year cycle of sand-supply change in late Holocene dune-building along the eastern shore of Lake Michigan. Quat. Res. 54, 414–422. https://doi.org/10.1006/qres.2000.2168

Lovis, W.A., Arbogast, A.F., Monaghan, G.W., 2012. The Geoarchaeology of Lake Michigan Coastal Dunes. Michigan State University Press, East Lansing, Mich.

Miyanishi, K., Johnson, E.A., 2021. Coastal dune succession and the reality of dune processes, in: Plant Disturbance Ecology. Elsevier, pp. 253–290. https://doi.org/10.1016/B978-0-12-818813-2.00007-1

Peterson, J., Dersch, E., 1981. guide to sand dune and coastal ecosystem functional relationships, Michigan State University Extension Bulletin EMICHU-SG-81-501. East Lansing, Mich.

Schrotenboer, B.R., and Arbogast, A.F., 2010. Locating alternative sand sources for Michigan's foundry industry: A geographical approach. Applied Geography 30, 697-719.

Schwarz, C., Brinkkemper, J., Ruessink, G., 2018. Feedbacks between Biotic and Abiotic Processes Governing the Development of Foredune Blowouts: A Review. J. Mar. Sci. Eng. 7, 2. https://doi.org/10.3390/jmse7010002

Sherman, D.J., Bauer, B.O., 1993. Dynamics of beach-dune systems. Prog. Phys. Geogr. Earth Environ. 17, 413–447. https://doi.org/10.1177/030913339301700402

Stallins, J.A., Parker, A.J., 2003. The influence of complex systems interactions on barrier island dune vegetation pattern and process. Ann. Assoc. Am. Geogr. 93, 13–29.

Thompson, T.A., Lepper, K., Endres, A.L., Johnston, J.W., Baedke, S.J., Argyilan, E.P., Booth, R.K., Wilcox, D.A., 2011. Mid Holocene lake level and shoreline behavior during the Nipissing phase of the upper Great Lakes at Alpena, Michigan, USA. J. Great Lakes Res. 37, 567–576. https://doi.org/10.1016/j.jglr.2011.05.012

van Dijk, D., 2014. Short- and long-term perspectives on the evolution of a Lake Michigan foredune, in: Coastline and Dune Evolution along the Great Lakes. Geological Society of America, pp. 195–216. https://doi.org/10.1130/2014.2508(11)

van Dijk, D., 2004. Contemporary geomorphic processes and change on Lake Michigan coastal dunes: an example from Hoffmaster State Park, Michigan. Mich. Acad. 35.

Walker, I.J., Davidson-Arnott, R.G.D., Bauer, B.O., Hesp, P.A., Delgado-Fernandez, I., Ollerhead, J., Smyth, T.A.G., 2017. Scale-dependent perspectives on the geomorphology and evolution of beach-dune systems. Earth-Science Rev. 171, 220–253. https://doi.org/10.1016/j.earscirev.2017.04.011

White, R.A., Piraino, K., Shortridge, A., Arbogast, A.F., 2019. Measurement of vegetation change in critical dune sites along the eastern shores of Lake Michigan from 1938 to 2014 with object-based image analysis. J. Coast. Res. 35, 842. https://doi.org/10.2112/jcoastres-d-17-00141.1

Wright, L.D., Thom, B.G., 1977. Coastal depositional landforms. Prog. Phys. Geogr. Earth Environ. 1, 412–459. https://doi.org/10.1177/030913337700100302

CHAPTER 2.
REPEAT PHOTOGRAPHY OF LAKE MICHIGAN COASTAL DUNES: EXPANSION OF VEGETATION SINCE 1900 AND POSSIBLE DRIVERS

Kevin G. McKeehan[a*] and Alan F. Arbogast[a]

a: Department of Geography, Environment, and Spatial Sciences, Michigan State University, Geography Building, 673 Auditorium Rd, East Lansing, MI 48824, United States.
mckeeha2@msu.edu and dunes@msu.edu

2.1 Abstract

Coastal dunes are prominent features along the Lake Michigan shoreline, especially along Michigan's Lower Peninsula. Numerous studies in recent years have reconstructed the geomorphic history of these dune systems, from their initial formation in the mid-Holocene to about 300 years ago. These studies have suggested linkages between past dune behavior and climatic variability and fluctuating lake levels. Less is known, however, about how these dune systems change on shorter-temporal scales in the modern era and the potential drivers of that change. Using repeat photography, this paper attempts to demonstrate how the coastal dunes of Lake Michigan's eastern shore have changed since the 19th century. We collected hundreds of photographs of these dunes, taken between the years 1885 and 2018, from archives and citizen scientists. In the spring and summer of 2019, we took ~70 new photographs replicating the original images. The changes between coastal dune conditions in the original photographs and in the 2019 re-photographs show a general expansion of vegetation across formerly barren and active surfaces along the entire shoreline. Although human development has also played a role in reshaping the coastal dune systems, the most pronounced difference between historical and current dune conditions where repeat photography was conducted is the expansion of vegetation – grasses, shrubs, and even trees. Here, we present the 20 photograph pairs most representative of these trends, explore these changes, and discuss the likely causes, including the increase in precipitation in Michigan in the past ~80 years.

Keywords: Coastal dunes, Lake Michigan, repeat photography, bare sand, vegetation, climate trends, Holocene

Citation: McKeehan, K.G., and Arbogast, A.F., 2021. Repeat Photography of Lake Michigan Coastal Dunes: Expansion of Vegetation Since 1900 and Possible Drivers. *Journal of Great Lakes Research* 47(6), 1518-1537. doi: 10.1016/j.jglr.2021.09.016

2.2 Introduction

The coastal dunes along the eastern shoreline of Lake Michigan comprise a unique aeolian system. They are the largest freshwater coastal dunes in the world (Peterson and Dersch, 1981) and developed under different conditions than most coastal dune systems elsewhere, as they are not associated with tectonic or tidal activity (Hansen et al., 2010). Instead, as successive studies from the last ~25 years have shown, Lake Michigan's coastal dunes formed mostly due to reworking of sandy glacial and lacustrine deposits by forces related to climatic and lake level variability (Hansen et al., 2010; Loope and Arbogast, 2000; Lovis et al., 2012; Thompson et al., 2011). This understanding followed the dating of aeolian sands and buried soils at many dune sites (e.g., Arbogast and Loope, 1999; Kilibarda et al., 2014; Loope and Arbogast, 2000) that was paired with robust reconstructed lake level chronologies (e.g., Baedke and Thompson, 2000). Accordingly, the coastal dunes began forming during ancestral Lake Michigan's Nipissing high phase (~5.5ka) (Lovis et al., 2012), although in some locations, especially along the southern shore, dune development may have started later (e.g., Argyilan et al., 2014; Kilibarda et al., 2014). Periods of dune stability and instability followed along much of the shoreline in the mid and late Holocene, culminating in a time of pronounced stability from ~2ka to ~1ka during which vegetation expanded across the previously mobile dunes (Arbogast et al., 2004; Lovis et al., 2012). This period of stability resulted in the Holland Paleosol, which is an Inceptisol present in dunes along Lake Michigan's southeastern coast. Subsequently, dunes reactivated ~1ka (Lovis et al., 2012)and again ~0.5 ka (Hansen et al., 2010).

Reconstructed geomorphic histories from several sites indicated similar patterns of dune activity followed by sometimes brief periods of stability (e.g., Arbogast et al., 2002; Argyilan et al., 2014; Blumer et al., 2012; Hansen et al., 2004; Kilibarda et al., 2014; Lepczyk and Arbogast, 2005; Van Oort et al., 2001). From this, six phases of dune behavior since the Nipissing transgression were identified by Hansen et al. (2010), each characterized by distinct periods of

dune stability or instability. These distinct phases were likely driven by a complex system of climate and lake-level changes, which either increased or restricted the supply of sand (Anderton and Loope, 1995; Arbogast et al., 2004; Dow, 1937; Loope and Arbogast, 2000; Lovis et al., 2012). Since then, a more complex explanation has emerged (van Dijk, 2004). Loope and Arbogast (2000) found dune building overall occurred during ~150-year cyclical lake-level fluctuations detected over the last 4,700 years on Lake Michigan through an examination of beach ridges and swale sediments (Baedke and Thompson, 2000; Thompson and Baedke, 1997).

On shorter temporal scales, additional variables were found to be critical in understanding Lake Michigan coastal dune behavior. In a series of related studies focusing on decadal changes in dune behavior at Indiana Dunes National Park, Olson (1958a, b, c) observed the relationships between wind, vegetation, lake levels, sand transport and deposition. In three related studies, Olson 1) tested the manner in which wind, topography, and different types of vegetation built and eroded dunes primarily through the changes in surface roughness (Olson, 1958a), 2) examined the stabilizing geomorphic force of vegetation in more detail (Olson, 1958b), and 3) formulated a dune-building model tailored for Lake Michigan's coastal environments (Olson, 1958c). The model demonstrated how exposed offshore bars could be stabilized by pioneering grass assemblages during periods of low lake levels, leading to the development of a dune cap or incipient foredune (Olson, 1958c). Subsequent higher lake levels might then erode the newly formed foredunes, reworking the sandy sediment and increasing sand supply in the aeolian system, unless the incipient foredune stabilized sufficiently and became new foreshore-backshore margin. Olson's model comports somewhat to later dating research showing a time-transgressive structure exists in Lake Michigan's dunefields, with older dunes inhabiting the backshore areas and younger dunes forming lakeward (Hansen et al., 2010; Lovis et al., 2012).

Other studies identified wind energy in conjunction with human interventions as a primary factor in dune behavior (Bennett and Olyphant, 1998, 1993), while Loope and Arbogast (2000) found dune building on Lake Michigan's eastern shore is somewhat irregular and largely governed locally by differences in littoral geomorphology, available sand, wind regimes, and wave energy. In two related studies at P.J. Hoffmaster State Park south of Muskegon, indirect variables on foredune behavior, such as seasonality, proved to have more influence than variables directly impacting the landforms, such as wind velocity and direction, beach width, surface moisture, snow, ice, ground freezing, and dune vegetation (van Dijk, 2014, 2004). These two studies concluded that aeolian processes were strongest during autumn and winter months, when storms were stronger and vegetation less prevalent, and that further research regarding the relationships between important variables and aeolian landform response needed to be conducted. Similarly, Lepczyk and Arbogast (2005), in their ~4,800-year geochronology of dune behavior at Petoskey State Park, called for better understanding of modern dune conditions in an attempt to validate the accepted dune building models proposed by various workers.

Vegetation plays an important role in dune behavior and can be indicative of changes in the regimes of several variables, including precipitation. According to two classic studies from the region, vegetation affects geomorphic form, but specific species of grass and trees affect form in different ways, with some species more effective than others (Cowles, 1899; Olson, 1958b). This geomorphic variance by species has been confirmed in other, later dune vegetation studies (e.g., Lee et al., 2019; Ruggiero et al., 2018). The amount of vegetation coverage can also determine a dune's susceptibility to aeolian erosion (Hesp et al., 2021; Pelletier et al., 2009). The impetus for the establishment of coastal dune vegetation is dependent on several factors (Hesp et al., 2021), principally climate (Doing, 1985; Tsoar, 2005), favorable edaphic conditions (Baldwin and Maun, 1983; Cowles, 1899; Gardner and McLaren, 1999), and the availability of seed and

rhizomes along with stochastic events (Hesp, 2002; Lichter, 2000). Seasonal variations of these and other factors play a role as well. For example, the summer establishment of grasses on bare dunes does not necessarily portend an expansion of vegetative coverage, as increased deposition of sand in autumn and winter buries the previous summer's new growth (Olson, 1958b; van Dijk, 2014). In the Lake Michigan-Huron basin, the establishment of vegetation was seen as a classic successional process involving pioneering plant species reliant on the amount of soil moisture, bare sand albedo and upper soil horizon temperature, and topographic position of colonization, among other factors (Cowles, 1899). Alternatively, the factors governing establishment and dune succession are multifaceted and often random, reflective of the varied and harsh conditions of a complex coastal dunefield (Lichter, 2000, 1998). For example, dune succession is sometimes dependent on topographic aspect, the size of the rodent population, frequency of storms, and whether leaf litter is present, amongst other considerations. Importantly for our study, a recent paper examining dune landforms along the west African and the Canary Islands coasts linked vegetation density and dune stability closely with rainfall amounts (Hesp et al., 2021). This relationship also was suggested by White et al. (2019) with regards to changes in vegetation density on Lake Michigan's eastern shore.

As reported by White et al. (2019), vegetation appears to have expanded at many dune sites in state parks and Sleeping Bear Dunes National Lakeshore (SBDNL) along Lake Michigan's eastern shore since the 1930s. Aerial images from 1938 and 2014 of 16 dune park sites were compared to determine the change in vegetation coverage (White et al., 2019). Vegetation coverage expanded at 13 of the 16 sites, with vegetation growth by 2014 at Holland State Park and SBDNL exceeding 30% over coverage in 1938. It was speculated based upon meteorological data from Muskegon that precipitation may be driving the change in vegetation coverage in these dunefields (White et al., 2019). One site where White et al. (2019) did not

detect an expansion of vegetation was P.J. Hoffmaster State Park. In an earlier study at this location, Belford et al. (2014) reported that bare sand expanded slightly at the park and an adjacent site at the expense of vegetation.

The goal of this paper is to further fill the gap in knowledge that exists within current literature about changes in general vegetation patterns in Lake Michigan coastal dunes during the modern era, defined here as the last ~200 years. We also aimed to quantify those changes as much as possible and determine potential drivers of these changes if they indeed occurred. Such findings may also shed light on past drivers of dune changes and place the Lake Michigan coastal dunes in current context of dune stabilization trends elsewhere, such as northern Europe, where bare and mobile sand dunes are declining at the expense of vegetated, immobile dunes (Provoost et al., 2011). Our paper attempts to determine if the changes reported by White et al. (2019) are occurring elsewhere on Lake Michigan's eastern shore using a different methodology – repeat photography – that is rarely employed east of the Mississippi River. After recapturing historical photographs of dune sites, we measured the amount of vegetative change between the original photos and those photos we captured in 2019 using a semi-quantified categorization.

Having evaluated the changes in dune vegetation, we then attempted to identify possible drivers of those dunefield changes by examining a wider array of meteorological data, including hourly wind reanalysis data from the European Centre for Medium-Range Weather Forecasts (ECMWF), and by calculating three dune mobility indices – Lancaster's *M*, Chepil's C, and Drift Potential (*DP*) (Chepil et al., 1963; Fryberger and Dean, 1979; Lancaster, 1988). Each of these indices weighs meteorological data differently. Thus, relative changes or inertia over time amongst the indices could inform regarding the possible drivers of Lake Michigan dune conditions. We also applied Mann-Kendall tests to determine if any of the trends in the meteorological or dune mobility data are statistically significant. Additionally, we also examined the original land survey notes from

the 19th century to understand if longer trends in vegetation coverage could be deduced, especially as those surveys were conducted in the closing years of the Little Ice Age.

2.3 Methodologies

2.3.1 Repeat Photography

Repeat photography has been a tool in the physical sciences for over 100 years (Rogers et al., 1984). The first documented series of photographs taken from the same location in a temporal sequence (i.e., repeat photography) was in 1888 in Switzerland, when Sebastian Finsterwalder first began surveying and photographing alpine glaciers in the eastern Alps (Hattersley-Smith, 1966; Rogers et al., 1984). A review of repeat photography studies since Finsterwalder reveals fewer studies have been set in the eastern United States than in the more arid, less tree-covered western United States. However, a few notable Michigan dune studies did accentuate photography (e.g., Cowles, 1899; Olson, 1958a, 1958b, 1958c), including Gates' study of the "disappearing" Sleeping Bear Dune (Gates, 1950). For our purposes, the results of White et al. (2019), coupled with other research regarding recent dune behavior (e.g., Abhar et al., 2015; Belford et al., 2014; Kilibarda and Shillinglaw, 2015; Millington et al., 2009), suggest that employing the practice of repeat photography, both ground-level and aerial, is a useful approach to determining trends in coastal dune systems, even in areas where more dense vegetation can be a photographic limitation. Most of these studies, including the White et al. (2019) paper in Michigan, employed the use of repeat aerial photography. We used ground-level repeat photography by obtaining historical photographs, evaluating each photograph's usefulness, recapturing the photos in the field, and then analyzing the results (Figure 1). The process involved libraries, archives, citizen scientists, several field trips to perform repeat photography, and software to analyze photographs digitally.

The first step in this process was to locate caches of historical photographs. An effort was made to search several known archives, including those in counties along the Lake Michigan shoreline.

The primary sources for historical photographs were the Archives of Michigan, the Bentley Historical Library at the University of Michigan, the Photographic Archive at the University of Chicago, which included images from scientist Henry Chandler Cowles' coastal Michigan field trips, and the Saugatuck-Douglas Historical Society Museum. Another fruitful repository of historical dune photographs was the Michigan Department of Environment, Great Lakes, and Energy (EGLE), where several binders of photographic slides documenting coastal conditions from approximately 1965 to 1995 were discovered. Once suitable photographs were gleaned from these repositories, they were subsequently downloaded digitally into a database if online or a picture was taken of the photo with a digital camera. Additional photographs in various media were forwarded to researchers from citizen scientists, who answered appeals for their vacation photographs by local and social media through the *Sands of Time* project coordinated through the Michigan Environmental Council (Arbogast et al., 2020).

Eventually, 207 photographs were considered as potential candidates to be recaptured as part of this study. For a candidate to be truly viable, however, its precise location had to be identifiable and the photograph of good quality. Additionally, for the purposes of temporal analyses, it was necessary to know the approximate year the photograph was taken. All 207 candidates were documented in a database with information such as the year of the photograph, the image source, photographer (if known), year, and a description of the likely location, which was determined either through archival notes associated with the photograph or through an investigation using online and topographic maps.

Of the 207 candidates for repeat photography, 193 photographs were selected for field investigation. A total of seven field trips were made to the Lake Michigan coast to visit the locations where these photographs were originally acquired. Some photograph locations proved somewhat easy to find, while others were never located, as the human-built environment or other

forces had altered the site beyond recognition. In addition, the aeolian nature of the landscape made it sometimes impossible to reshoot from exactly the same elevation as the original photograph. Once the approximate location of the photograph was found, care was taken to obtain the correct focal height, or camera's distance above the ground, angle, and light. Three cameras were used to take multiple photographs, including a 1974 Bell & Howell FD35 film camera, a Nikon Coolpix S6000 digital camera, and a personal cellphone. Multiple pictures from a variety of angles and *z* heights were taken with each camera.

2.3.2 Measuring Vegetation Expansion

Quantifying landscape change detected in repeat photographs is a challenge (Kull, 2005) as the process encompasses many variables. For instance, the precise location of the photographer of the original image is often impossible to determine in the field, while important camera variables such as focal length, *z* distance above the ground, tilt, roll, and azimuth are unknown unless recorded by the original photographer, which was unlikely. Taken together, these variables and others are often referred to as the projection matrix (Harley et al., 2019; Kohek et al., 2017). If too many variables in the projection matrix are unknown, then it is difficult to perform the pixel-to-pixel analysis between photographs. Moreover, there are often questions of resolution with the digital camera, the processing computer, and the output format all potentially having different resolutions (Hall, 2001). To accomplish the pixel-to-pixel effect, camera stations – known locations with a fixed stand and a camera cradle – were established to provide the repetitive conditions necessary for the process. Early glacial geomorphologists were amongst those who pioneered this process (Hattersley-Smith, 1966) and other disciplines, such as coastal geomorphology (e.g., Harley et al., 2019), have followed. Absent a camera station, researchers have either developed qualitative means for measuring landscape change, created a constrained quantitative methodology that focuses on only what can be measured with certainty, or crafted a mixed-methods approach (Bayr, 2021; Kull, 2005; Manier and Laven, 2002).

For our study, we estimated the change in vegetation by measuring the amount of bare dune sand visible in both the historical photographs and the re-photographs. To do this, we used ESRI ArcGIS software to georeference both photographs to each other in a local Cartesian coordinate system using control points visible in each (Figure 2). Then, the photos were cropped to include only the overlapping areas and the bare sand portions mapped as polygon feature classes. The unitless areas of bare sand were calculated and compared, with a percentage increase or decrease in bare sand computed. The final pixel analysis effect appears similar to other studies (e.g., Bayr, 2021 fig. 9). Rather than report the exact or even approximate percentage change between the year the original photograph was captured and 2019, the year of the re-photograph, we rolled all results into broad categorial bins. We used this more qualitative reporting approach as we had neither camera stations nor fully known projection matrix values. These categorical bins are somewhat similar to those used by Kull (2005). Further, we measured bare sand, rather than vegetation, using heuristics due to sand's reflectiveness, which we felt was less subjectively observed. A machine learning process was not employed because of the wide variability and quality of the historical photographs.

2.3.3 U.S. Public Lands Survey (PLS)

Our study focuses on dune behavior in the modern era, roughly since 1830 when European patterns of settlement began in the region. To help estimate the coastal dune behavior just prior to the earliest photographs taken in our database, we used the U.S. General Office Public Lands Survey (PLS) notebooks kept by the field surveyors who walked the land in the 19th century to prepare the areas for formal settlement. Surveyors were instructed to inspect the land down to the quarter-section level, which was a ½ mi. x ½ mi. slice of a 36 mi^2 township area, and report on the soil quality, trees and vegetation, and topography, amongst other features (Delcourt and Delcourt, 1996). For our purposes, the focus by the surveyors on these three landscape variables should yield information about the state of dunes on Lake Michigan's eastern shore at the time of

the original survey, at least along quarter-section lines. Other geomorphologists and physical scientists have used the PLS notebook descriptions or similar texts to reconstruct pre-European settlement environments. For example, the diary descriptions of early European explorers were employed to reconstruct dune conditions on the Great Plains during the early 1800s (Muhs and Holliday, 1995), while PSL surveyor notebooks were used to determine that presettlement forests in Michigan's Upper Peninsula were more heterogenous than present (Delcourt and Delcourt, 1996). While there are concerns regarding the quality of some PLS notebook descriptions, the source overall has been considered "quantitative" (Schulte and Mladenoff, 2001) and "one of the best records of the pre-European settlement" (Manies and Mladenoff, 2000). We accessed PLS notebook descriptions for the nearest survey to each of our repeat photograph locations from Michigan History Center, then examined the records for indications of bare sand or dune vegetation. We recorded the surveyor's words for each site, along with the year, and created a word cloud to gauge dune conditions at the time of the original survey in the study area prior to the era of our photographs. The notebooks are sprawling datasets; as such, we confined ourselves to reporting descriptions associated with the nearest section line boundary or meander survey.

2.3.4 Meteorological Data

To determine possible drivers of dune vegetation trends, we obtained meteorological data from the Midwestern Regional Climate Center (MRCC) for three sites that are geographically distributed along the Lake Michigan coast – South Bend, Ind., and Muskegon and Traverse City in Michigan. These three sites were chosen for two reasons. Firstly, they are geographically well-distributed across our study area (Figure 3). Secondly, they possess the longest, most complete meteorological records for the eastern shore of Lake Michigan. From the MRCC data, we were able to extract 79 years' worth of uninterrupted precipitation and temperature data for South Bend, 91 years of data with some gaps for Muskegon, and 111 years for Traverse City. Other

stations, including Benton Harbor and Grand Haven, did not possess such unbroken, complete datasets. Neither South Bend nor Traverse City are on Lake Michigan, although the latter is on the West Arm of Grand Traverse Bay. Both sites, however, are ~35km from the eastern shore of Lake Michigan. These stations are the closest stations to the lake we could find that had the most complete records.

Unfortunately, hourly observational wind data are often incomplete. Reanalysis data, which are often utilized in atmospheric and climate models, attempt to solve this problem by blending known, historic weather observations with modeled data to fill in the gaps (Hayes et al., 2021). The dune mobility indices we are utilizing in this study require complete wind data as an input without any gaps. As a result, we obtained hourly wind reanalysis data from the European Centre for Medium-Range Weather Forecasts' (ECMWF) the ERA5 dataset, which are stored in grib messages in a 0.25°x0.25° or ~1,000km^2 grid (Bell et al., 2020; Hersbach, H. et al., 2018). The hourly wind speed represents the wind speed at the given hourly interval averaged for the entire reanalysis grid (Yan et al., 2020). To process the grib messages and extract the 10m-height *u* and *v* wind components, we used the PyGrib 2.1.3 interface module with Python 3.9.1, NumPy 1.20.0, and Pandas 1.2.3 in the Google Colaboratory environment. After translating the grib messages, we were able to determine hourly wind speed in m/s and use these data to feed into the dune mobility indices.

2.3.5 Dune Mobility Indices

Dune mobility indices can evaluate the capacity of sand to mobilize based upon a location's climatic conditions (Abbasi et al., 2019; Lancaster and Helm, 2000). Each index considers and emphasizes a different set of variables when determining dune mobility potential. We calculated three different indices – Lancaster's *M*, Chepil's C, and Drift Potential (*DP*) (Chepil et al., 1963; Fryberger and Dean, 1979; Lancaster, 1988) – for each year beginning in 1950 for the three

abovementioned meteorological stations – South Bend, Muskegon, and Traverse City. Our goal was to determine if any trends in the indices correspond to trends in dune vegetation change. Lancaster's M was developed to measure mobility in desert continental dunes and has been applied as such in several studies (e.g., Cordova et al., 2005; Muhs and Maat, 1993). Lancaster's M has also been applied novelly to studies of coastal dunes in northwest England (Delgado-Fernandez et al., 2019), Wales (Rodgers et al., 2019), and the Canary Islands (Smith et al., 2017), although never to our knowledge in the study of inland coastal dunes like those found along Lake Michigan. The index considers sand mobility to be a function of the annual percentage of time the wind is above the threshold for sand transport (W), which is determined to be 4.5 m/s, and the ratio between annual precipitation (P) (mm) and adjusted potential evapotranspiration (PET) (mm) as calculated using the Thornthwaite method (Lancaster, 1988; Lancaster and Helm, 2000; Thornthwaite, 1948; Thornthwaite and Mather, 1957):

$$M = W/(P/PET) \tag{1}$$

As mentioned earlier, annual precipitation across Lower Michigan appears to have increased since 1930 (White et al., 2019). Thus, as an index, we hypothesize that Lancaster's M, as it is attuned somewhat to precipitation, might reflect this increase by returning diminished mobility over time, especially since Lancaster's M performs well at decadal timescales (Rodgers et al., 2019). However, it is also possible temperatures have risen since the 1930s, perhaps due to anthropogenic climate change. This would drive PET higher, potentially offsetting any index changes attributed to precipitation.

Chepil's C, or average annual wind erosion climatic index (Chepil et al., 1963), is the second mobility index we calculated. Developed after studying wind erosion and dust storms on the Great Plains, Chepil's C attempts to measure wind erosion capacity by dividing the cube of average annual wind velocity (v) by the square of soil surface moisture or by Thornthwaite's effective precipitation index (P-E) (Chepil et al., 1963; Talbot, 1984). Thornthwaite's effective precipitation index is defined as precipitation divided by evaporation and is sometimes written as P-E (Thornthwaite, 1931). The formula for Chepil's C is (Chepil et al., 1963):

$$C = v^3/(P\text{-}E)^3 \quad (2)$$

Chepil's C was used to understand potential dune mobility in the mostly vegetated Sahel of West Africa (Talbot, 1984). Its emphasis is somewhat distinct from Lancaster's M, in that Chepil's C uses Thornthwaite's effective precipitation index to approximate soil moisture (Skidmore, 1974; Talbot, 1984) and considers the effect of wind differently, using the average annual wind velocity instead of the annual percentage of time the wind is above the threshold for sand transport. Moreover, Chepil et al. (1963) concluded that the index values could track with annual episodes of storminess and created an iteration of C that accounted for the lag in landscape response to years with a high number of storms. This iteration, which is known as C_3, is a three-year running average of C (Chepil et al., 1963). Thus, if a decrease in storminess has occurred on the eastern shore of Lake Michigan and is driving dune stabilization, Chepil's C may be the vehicle that detects such a change, although we hypothesize that the values of C_3 will largely be unchanged since 1950. A decrease in C_3 could also be interpreted as an increase in dune soil moisture, although Thornthwaite's index has issues in this regard (Talbot, 1984). We feel these

features make Chepil's C_3 unique from Lancaster's M, which focuses on precipitation and temperature, as C_3 attempts to gauge storminess and soil moisture indirectly. Here, we report C_3 as Chepil et al. (1963) did. Moreover, we adhere to the unnormalized, simplified formula seen above that was used by Talbot et al. (1984) and reported by Abbasi et al. (2019).

The final dune mobility index we calculated is Drift Potential (DP), which considers the potential for sand transport by focusing solely on wind power (Fryberger and Dean, 1979; Yizhaq et al., 2007). DP as constructed by Fryberger and Dean (1979) uses a higher sand mobilization threshold (6 m/s) than Lancaster's M and was first reported as Q. DP is expressed as the squared observed hourly wind value multiplied by the wind value minus the sand mobilization threshold (V_t), the result of which is multiplied by $1/n$ of the number of observations, a value originally reported as t (Fryberger and Dean, 1979). Here, we have simplified the DP formula from that reported by Fryberger and Dean (1979):

$$DP = V^2(V - V_t) \cdot 1/n \tag{3}$$

We did not calculate other associated DP statistics, such as resultant drift potential (RDP), as we are concerned with overall wind power only. Based upon our knowledge of regional meteorological trends, we hypothesize that there has been no significant change in wind power along the Lake Michigan shore that could explain a possible expansion of dune vegetation. However, there are indications that some locations in the Great Lakes basin are becoming windier (Desai et al., 2009). Nevertheless, windier conditions would somewhat preclude dune stabilization as erosion would increase (Pye et al., 2014), although it is unclear how much influence wind power

alone has in determining dune, vegetation, or erosion conditions (Mason et al., 2008; Smalley, 1970). Taken together, we hypothesize that none of the three dune mobility indices will have changed relatively in ways which can explain a possible increase in vegetation since the 1930s, suggesting a complex forcing similar to studies elsewhere that found some changes in climate may not be enough to explain vegetation gains (e.g., Delgado-Fernandez et al., 2019). In fact, some indices may trend in ways which suggest Lake Michigan's coastal dunes should be mobilizing, rather than stabilizing. In that case, we will be left to explain the expansion of vegetation through alternative explanations.

2.3.6 Determining Trends and Statistical Significance

Mann-Kendall tests can be calculated to determine if trends exist with an observed variable over time by evaluating Kendall's τ and its significance (Helsel and Hirsch, 2002; Mann, 1945). If monotonic trends in the aforementioned meteorological and dune mobility metrics exist, Mann-Kendall tests could detect their strength and if they are statistically significant, helping us establish possible drivers for dune conditions. While similar to a regression analysis, the Mann-Kendall tests does not assume a normal distribution of residuals and, thus, is nonparametric (Helsel and Hirsch, 2002). Mann-Kendall tests trends by calculating the *S*-statistic (Pohlert, 2020a):

$$S = \sum_{k=1}^{n-1} \sum_{j=k+1}^{n} sgn\left(X_j - X_k\right) \tag{4}$$

The properties of the *S*-statistic can be transferred into two other metrics, both of which we will report instead of *S*. The *Z*-statistic, which is occasionally reported in geoscience studies (e.g.,

Gocic and Trajkovic, 2013), detects the existence of trends through the *Z*-transformation of *S* (Gocic and Trajkovic, 2013; Pohlert, 2020a):

$$Z = \begin{cases} \frac{S-1}{\sqrt{Var(S)}} & if \quad S > 0 \\ 0 & if \quad S = 0 \\ \frac{S+1}{\sqrt{Var(s)}} & if \quad S < 0 \end{cases}$$

(5)

Additionally, Kendall's τ_b, a measure of rank correlation and association (Kendall, 1938) which is often reported in studies along with or instead of other metrics (Corbella and Stretch, 2013; e.g., Mason et al., 2008; Reyes et al., 2020), is derived from its relationship to the *S*-statistic (Pohlert, 2020a):

$$\tau = \frac{S}{D}$$

(6)

Where:

$$D = \left[\frac{1}{2}n(n-1) - \frac{1}{2}\sum_{j=1}^{P} t_j\left(t_j - 1\right)\right]^{\frac{1}{2}} \left[\frac{1}{2}\, n\,(n-1)\right]^{\frac{1}{2}}$$

(7)

The Mann-Kendall test is relatively common in hydrological studies (Yue et al., 2002b) and even has been used to evaluate the factors behind dune mobility (e.g., Mason et al., 2008) and arid land conditions (Li et al., 2015; e.g., Wang et al., 2017). Here, we utilized the "trend" r package to produce three metrics: the Z statistic, Kendall's τ, and P-values (two-tailed) (Pohlert, 2020b).

However, one of the assumptions regarding the proper application of the Mann-Kendall test is that the data are free of serial correlation, also known as autocorrelation (Yue et al., 2002b). In other words, since Mann-Kendall evaluates a variable Y over a time series, it is possible that Y accumulates or dissipates over time naturally, resulting in a statistical influence on the reported trend (Ezekiel and Fox, 1959). This condition could induce Type I errors in Mann-Kendall tests (Bayazit and Önöz, 2007), or make the test too "liberal" in its trend analysis (Kulkarni and von Storch, 1995). One approach in reducing serial correlation is to perform a process known as "pre-whitening", which seeks to model the time series data as an autoregressive (AR1) model with a mean of 0 by subtracting the time-accumulated "memory" of the data (Kulkarni and von Storch, 1995). This procedure makes any time series more "orthogonal" (Box and Jenkins, 1976). While some studies suggest a trend analysis involving atmospheric phenomenon should contain a pre-whitening procedure (e.g., Collaud Coen et al., 2020), others have suggested the process introduces significant Type 2 error by not detecting trends when they exist (Bayazit and Önöz, 2007; Razavi and Vogel, 2018). In fact, alternative pre-whitening techniques have been proposed to address these issues (e.g., Yue et al., 2002b). However, Bayazit and Önöz (2007) determined that pre-whitening was unnecessary in data with more than 50 observations, a threshold all our data achieves.

To determine if pre-whitening our data was necessary, we employed a different approach and calculated serial correlation within our Y variables by conducting a series of Durbin-Watson tests. Although a less common approach, other studies have employed a Durbin-Watson test of serial correlation in conjunction with a Mann-Kendall trend analysis. This includes, most relevantly, a study of precipitation trends in Brazil in which the authors performed the Mann-Kendall test after finding no serial correlation in their data from the Durbin-Watson test (Blain and Bardim-Camparotto, 2014). We employed a similar approach.

The Durbin-Watson test is an evaluation of serial correlation through the calculation of the *d*-statistic (Durbin and Watson, 1951):

$$d = \frac{\sum(\Delta z)^2}{\sum z^2} \tag{8}$$

We calculated the Durbin-Watson test using the dwtest function within the "lmtest" r package (Zeileis and Hothorn, 2002). As Chepil's C_3 is a moving average and, consequently, inherently autocorrelated, we ran Durbin-Watson tests on the raw Chepil's C instead.

2.4 Results

2.4.1 Repeat Photography

Of the 193 candidates, a total of 72 repeat photographic pairs were created (Figure 3). Citizen scientists contributed a handful of photo candidates and only 2 of those were part of the 72 eventual pairs. Here, we report on 20 pairs (Table 1) that best represent the trends seen in dune systems along Lake Michigan's eastern shore. These 20 pairs are also relatively well-distributed geographically north to south along the coast. The remaining 52 repeat photographic pairs were

set aside for a variety of reasons. For example, some photographic pairs were not used because the site had changed so much that a vegetation analysis was impossible; others were not used because the re-photograph was taken at the correct vicinity, but at the wrong tilt, roll, *z* height, or distance from the original camera location.

Of the 20 pairs we report here in this article, we visually present the 6 most representative repeat photographic pairs in Figures 4 – 9, while the remaining 14 are available in an online appendix. Additional photographs can be viewed on the Michigan Environmental Council's Learning to Live in Dynamic Dunes website (Learning to Live in Dynamic Dunes, 2020). In most of the paired photographs, two distinct trends have emerged – one extensive, the other less so. In most of the historical photographs, regardless of their year, bare sand is abundant, while in the 2019 re-photographs, vegetation has expanded considerably. This expansion of grasses and, in some cases, invasive species, trees, and other woody vegetation is a considerable trend, one which we evaluated (see below). At some of the sites, the presence of vegetation allowed the landscape to aggrade, or become slightly convex. This is likely due to the ability of grasses and trees to trap additional entrained and saltating mobile sand. The other, less ubiquitous trend involves the advent of the human-built environment, in the form of beachside homes, barriers, buildings, roads, and trash. This human intervention is not seen at all or even most sites, but it is pronounced south of Warren Dunes, around Holland, and near Muskegon. Perhaps the best example of human intervention in the dune environment can be seen in the far south at Grand Beach (Figure 4), where a dune known as Eiffel Tower Dune was flattened partially and made into homesites, not all of which contain homes.

2.4.2 Measuring Vegetation Expansion

We categorized the trends in dune vegetation expansion seen in Figures 4 – 9, as well as the other 14 photos in the appendix. An example of the results of the process can be seen in Figure

10. At no site did bare dune sand expand overall at the expense of vegetation (Table 2). Most sites lost much of their bare dune sand. Moreover, there was no geographic distribution amongst the results; sites that lost the least bare sand (i.e., Big Sable Point) or the most bare sand (i.e., Laketown Beach), were found in the southern, mid, and northern sections of the coast. These semi-quantified results confirm the trends seen visually in the repeat photograph pairs.

2.4.3 U.S. Public Lands Survey (PLS)

PLS notebooks revealed many sites contained bare sand in the early- to mid-19th century (Table 3). While it is difficult to draw conclusions based upon historical or qualitative data, some patterns do emerge. First, bare sand is mentioned at 15 of 20 sites by the PLS surveyors and at least once by each of the 6 different surveyors. Second, "bare sand" becomes more ubiquitous and vegetation less so in the notebooks as the surveys move north and forward in time, lending the results the veneer of a spatio-temporal pattern. Specifically, north of Holland and after 1832, trees species are mentioned only once by the surveyors – at Sleeping Bear Point in 1850. This is somewhat reflected in an analysis of the words and phrases the surveyors used to describe the landscape (Figure 11). The words "sand" and "hills" or "hilly" appeared most frequently in the notebooks, as did other dune-associated descriptions. There were 78 total dune-related words or phrases out of 105 that we recorded, while the word "sand" appears 17 times in PLS notebooks for our sites. Additionally, an addendum added in the 1950s to the PLS notebooks by the U.S. Geological Survey (USGS) noted that surveying irregularities in the Sleeping Bear area were due to the difficult conditions encountered by the surveyors, especially near the Dune Climb (Figure 9).

2.4.4 Meteorological Data

We compared annual mean temperature, annual total precipitation, annual total PET, and average annual wind speed for our three meteorological stations (Figure 12). Results for South Bend, at the southern end of our study area, show that conditions on the southeastern Lake

Michigan shore have been warmer, wetter, and less windy than the other stations since the early- to mid-20th century. Conversely, conditions at Traverse City, which is a proxy for coastal dunefields in the north of the Lower Peninsula, have been cooler, drier, and windier than the other stations. South Bend and Muskegon have seen similar tendencies in temperature, precipitation, PET, and wind. Average annual wind speed has declined since 1950 for both locations, while mean annual temperatures have risen nearly 1°C. Precipitation has increased over 100mm and PET ~50mm in the same time period (Figure 12). Traverse City's mean annual temperature, total annual precipitation, and total annual PET have changed less since the early- to mid-20th century than was experienced in South Bend and Muskegon, while the region's average yearly wind speed has largely remained unchanged (Figure 12).

2.4.5 Dune Mobility Indices

The spatial and temporal patterns present in the meteorological data are somewhat evident in the results from our dune mobility calculations (Figure 13). Overall, the capacity for dune mobility in coastal dunefields nearest South Bend was lower than the other sites and has declined by all metrics since 1950. Conversely, Traverse City, a proxy for dunefields on the northeastern Lake Michigan shoreline, had a higher potential dune mobility that increased over time by all metrics. Nevertheless, these results should be put into perspective; compared to inland semi-arid dunefields worldwide, these results represent a low capacity for dune activity. For example, Lancaster (1988) provided guidance on how to interpret *M* results; any dunefield *M* value below 50 should be considered "inactive" with vegetation cover >20% (Figure 14). All *M* data points for all three stations since 1950 with the exception of one – Traverse City in 2007 – were <50. The relatively high *M* value for Traverse City in 2007, a spike which was also captured by Chepil's C_3, appears predicated on an exceptionally dry year as the Traverse City meteorological station recorded the least amount of annual precipitation since the 1920s. This coincided with low lake levels, as by December 2007 levels on Lake Michigan-Huron were near

record lows at 175.7m (Indiana DNR, 2020). Still, the dune mobility critical value for 2007 at Traverse City was $50<M<100$, which is interpreted as "crestal areas only active (vegetation cover 10-20%)" (Lancaster, 1988). These results for Lancaster's *M* reflect similar findings from the application of this dune mobility metric in the temperate coastal dunes in northwest England, where the *M* values never exceeded 50 (Delgado-Fernandez et al., 2019). The results for *DP*, which are directly immune from swings in precipitation, are largely unchanged through time since 1950 for all three stations. Moreover, as interpreted from Fryberger and Dean (1979), any site returning *DP* values in vector units (vu) <200 should be interpreted as having "low" drift potential. Results for Lancaster's *M* and Chepil's C_3 do demonstrate trends and these were evaluated for strength and significance, along with all the other variables.

2.4.6 Determining Trends and Statistical Significance

Based on the *d*-statistic returns from the Durbin-Watson tests, our meteorological and dune mobility data are without serial correlation, except for one variable (annual mean temperature) for Traverse City (Table 4). The *d*-statistic ranges from 0 to 4, with the value of 2 denoting the absence of serial correlation (Draper and Smith, 1998). The closer the time series data are to 2, the less first-order serial correlation exists (Draper and Smith, 1998). For the 1% significance levels with one regressor and between 70 and 111 observations, any *d*-statistic value within a bounding range of ~1.5 to ~2.5 should indicate a lack of serial correlation (Savin and White, 1977) and would suggest that pre-whitening is unnecessary, although the range gets slightly narrower as observations increase (Durbin and Watson, 1951).

All other variables possess *d*-statistic scores at 1% significance levels between the acceptable bounding range for serial correlation (Savin and White, 1977). The lower bounding limit for a dataset with $n=100$ observations with 1 regressor is 1.522, which the *d*-statistic for the temperature variable for Traverse City exceeds at 1.452. However, the violation of the Durbin-

Watson test for this variable may be an artifact of the test itself, which narrows the acceptable bounding range as *n* increases (Draper and Smith, 1998). Considering this, the severity of the test violation, which amounts to ~0.07 on a 4-point scale, and the lack of violations amongst the other variables, we decided to avoid the pre-whitening process and proceed to the Mann-Kendall test stage.

Understanding the results of our Mann-Kendall tests (Table 5) requires interpreting Kendall's τ_b and the *Z*-statistic, which can both be used to determine trends. The *Z*-statistic is rather straightforward as the no trend hypothesis is rejected if $Z > \pm 1.96$ at the 5% significance level (Gocic and Trajkovic, 2013), which we use here as it seems to be standard. Interpreting Kendall's τ_b, even if it is employed more frequently, is more difficult, as it has "no direct probability interpretation" (Somers, 1962). Kendall's τ_b yields a value $-1 \leq \tau_b \leq 1$, with a higher absolute value equating to a stronger trend association (Puth et al., 2015). The determination of what Kendall's τ_b value signifies as a weak versus strong association is somewhat subjective. There are many approaches, including evaluating Kendall's τ_b in a manner similar to Spearman's ρ (Akoglu, 2018) and several informal thresholds (Botsch, 2011; e.g., van den Berg, 2021). In some cases, Kendall's τ_b is visualized spatially as a choropleth map rather than binned into groupings (e.g., Reyes et al., 2020). If Kendall's τ_b is correlated to Spearman's ρ, as is suggested (Khamis, 2008; Yue et al., 2002a), then it follows that we could utilize a Spearman's correlation coefficient table to describe our results. Thus, we use as a base the groupings reported by Corder and Foreman (2009, pg. 123) and modify it slightly based on the findings of Tabari et al.'s (2014) PET study in Iran. For this study, we consider trend strength to be trivial if $\tau_b < \pm 0.1$, weak if $\pm 0.1 \leq \tau_b < \pm 0.25$, moderate if $\pm 0.25 \leq \tau_b < \pm 0.5$, and strong thereafter (Corder and Foreman, 2009, p. 123; Tabari et al., 2014).

Based on those interpretations, the Mann-Kendall test results fail to show a clear picture of potential drivers for the changes in dune bare sand and vegetation seen in our repeat photographic analyses. Trends, as represented by the *Z*-statistic are present, especially for temperature, precipitation, PET, and Lancaster's *M* for South Bend and Muskegon; no trends exist in the data for Traverse City. Relatively stronger trends, as measured by Kendall's τ_b, were found for only two variables – mean annual wind speed at South Bend and PET at Muskegon. Yet, there was no variable that trended either positively or negatively across all three stations. Relatively weak-to-moderate positive statistically significant trends for temperature and PET at South Bend and Muskegon are interesting, but theoretically would be driving toward reactivation not stabilization through vegetation maintenance.

2.5 Discussion

The mixed results of our statistical analysis leave open speculation for possible drivers of the expansion of coastal dune vegetation on Lake Michigan's eastern shoreline. What is clear is that vegetation has expanded at the expense of bare dune sand in the modern era. It is unclear why, but there are possibilities. For example, a regional increase in annual precipitation remains a possible driver. While it may not have signaled a strong trend, a weak positive statistically significant trend in precipitation was evident for South Bend and Muskegon. Moreover, annual precipitation did increase at those two stations by ~175mm on average since the 1940s and by ~75mm since the 1900s in Traverse City. It is possible that these gains, or a shift in how precipitation is delivered, could have provided enough water to the vadose zone of these aeolian sand dunes to affect changes in vegetation. Specifically, an increase in annual precipitation may have expanded the typical wetting front patterns and raised the soil moisture percentage above a threshold at which available water increased and plant growth began.

Sand response to water is "an extremely complex phenomenon" (Dincer et al., 1974) and is characterized by the rapidity with which it conducts water through the profile (Salisbury, 1952). In fact, Dincer et al. (1974) concluded that "no universal theory" exists that predicts water behavior in sand. Yet, we can understand sand response to water broadly as a function of climate, soil texture, topography, the presence of laminae, and vegetation (Bagnold, 1941; Dincer et al., 1974). When precipitation falls on unsaturated sand and infiltrates it, a wetting front extends downward through the soil profile (Gardner and McLaren, 1999). This front moves quickly downward under the influence of gravity and the matric suction gradient, then more slowly as the edge effects of an extended wetting front begin to exert their influence and the gravitational and matric forces diminish (Gardner and McLaren, 1999). Sands with a coarser texture tend to conduct the water downward through the profile more efficiently due to larger and fewer pores between particles, amongst other factors (O'Geen, 2013). Additionally, moisture in the top ~30cm of sandy soil quickly is reduced due to the effects of evapotranspiration (Mehta et al., 1994), meaning the upper horizons of dune sand possess a rapid response to both percolation and evapotranspiration (Gardner and McLaren, 1999). This is the phenomenon Cowles (1899) identified in conjunction with the albedo and the associated higher temperature of bare dune sand in Michigan. Yet, dune response changes with the delivery of persistent episodes of precipitation. Bare sand dunes are sensitive to as little as 2-3mm of rainfall and more sensitive to larger amounts, especially lower in the profile (Gardner and McLaren, 1999). Given such sensitivity, it is not difficult to imagine that dune vegetation has expanded due to the gains in precipitation we have presented in this study.

If a soil moisture threshold has been exceeded because of an increase in precipitation, it is possible dune vegetation will continue to expand based upon the theory of the temporal stability of soil moisture (*TS SM*) (Vachaud et al., 1985), especially under a positive trend in precipitation

and after vegetation has already established itself (Wang et al., 2008). The presence of vegetation increases the amount of organic material and finer-grained particles in soil. Further, cycles of wetting and drying in coastal sand dunes are extended from mere days under bare sand to weeks in vegetated dunes (Gardner and McLaren, 1999), likely perpetuating a feedback loop that helps maintain and promote vegetation. In a study of Lake Huron dunes, field capacity of water was higher on vegetated back dunes than on younger foredunes (Baldwin and Maun, 1983). Soil moisture clearly is an important component for our study area, for even though PET increased according to our findings, the region still is an Udic soil moisture regime, where P>PET and dry conditions are rare (Schaetzl and Anderson, 2005). Additionally, it is important to note that recent research found precipitation to be a controlling factor of dune vegetation and morphology along a ~3,500km reach of the African shore (Hesp et al., 2021).

The reduction in mean annual wind speed since 1950 may also play a role in dune stabilization through vegetation expansion, although this is unlikely to be a primary driver. A moderate negative statistically significant trend in wind speed was found at South Bend, but the effect is not uniform and tapers farther north along the shore. This supports recent findings of less frequent strong winds in Minnesota (Klink, 2002) and the Great Plains (Hugenholtz and Wolfe, 2005), and contrasts with a study of Lake Superior winds (Desai et al., 2009). Wind affects dune behavior (Lancaster, 1988), foredune morphology in conjunction with other factors (Davidson-Arnott et al., 2018; Duran and Moore, 2013), and even dune vegetation dynamics, as sand and burial tolerant species are promoted at the expense of those species less tolerant of sand burial, according to a Lake Huron dune study (Dech and Maun, 2005). As Tsoar's (2005) hysteresis model of wind power and vegetation coverage demonstrated, a reduction in wind has a greater impact on vegetation expansion than an increase in wind does on dune remobilization. According to the model, once vegetation has established itself in dunes, the *DP* necessary to remobilize stabilized,

vegetated dunes is significantly higher than the reduction of power necessary to foster vegetation growth (Tsoar, 2005). Yet, in a study from China, a sharp reduction in wind power and *DP* proved to be a smaller factor than land use changes in dune stabilization there (Mason et al., 2008). In our study, the reduction in annual wind speed was not uniform and only significant in one location. Thus, in our estimation, the reduction in mean annual wind speed is likely here to be a minor, local control, contributing to dune stabilization by reducing erosion and the burial of vegetation, but is not regionally uniform to affect the broad changes captured in our repeat photo pairs.

Other local controls could be influencing dune and vegetation behavior. These fall into two categories – 1) controls operating at short- and meso-term temporal scales, and 2) those controls operating at longer scales from which a lag in landscape response delayed changes in dune vegetation. In the former category are fire suppression, the importation of invasive species – especially baby's breath *(Gypsophila paniculata*) – and dune stabilization planting programs. The suppression of fire would allow the accumulation of biomass on the land (Bowman et al., 2011) and it is also tied to the behavior and control of invasive species. Studies have shown fires can exacerbate invasive species proliferation (D'Antonio and Vitousek, 1992) or help control it (Emery and Gross, 2005). *G. paniculata* has established itself in dune areas mostly northeast of Point Betsie since its introduction there (Emery et al., 2013), although it has also been found at Arcadia Dunes to the south (Leimbach-Maus et al., 2020). By their nature, dunes are disturbed landscapes and, as such, can be susceptible to invasive species colonization. *G. paniculata*, with its deep taproot and large seed disbursement, has successfully directly competed for limited resources from more sensitive native species such as Pitcher's thistle (*Cirsium pitcher*) (Leimbach-Maus et al., 2020; Yang et al., 2019). Grass planting programs, such as those around Ottawa Beach in the 1980s, have accomplished much the same effect, as one of our repeat photo pairs from that area

demonstrates. One such program, which directed the planting of ~25,000 non-native Austrian pines (*Pinus nigra*) in and around Saugatuck Dunes State Park from the 1950s to the 1970s, was both a planting program and an invasive species introduction (Leege and Murphy, 2001, 2000). Planting programs, dune restoration efforts, and the advent of invasive species were shown to contribute to the stabilization of coastal dunes in northwest England (Delgado-Fernandez et al., 2019). Unfortunately, other than documenting their presence, there has not been, to our knowledge, any study systemically investigating the dune fixation properties or trends associated with these invasive species introductions or planting programs along the Lake Michigan coast.

The second category of local controls includes the effects of logging and agricultural clearing which mostly occurred in the 19th century. Our PLS investigation was an attempt to understand the prevalence of these practices. If they were widespread and present at a majority of our repeat photography sites, then it would be possible that the dune systems along Lake Michigan's eastern shore were responding in an asymmetrical and lagged manner to the removal of natural landcover ~100+ years ago in an attempt to reach its vegetated steady state. While Native American agriculture was present near Saugatuck in the 1830s, only 6 of 20 survey sites we present in this paper showed signs of vegetation or trees. Certainly, there was logging and agricultural activity in the region, but there is no evidence it played a substantial role in the expansion of vegetation. In fact, PLS survey notes indicate the prevalence of bare sand long before European agricultural practices or logging would have impacted the landscape.

Despite the questions regarding invasive species and timber activities in dunes, these factors are local controls operating at a site-specific scale, one that cannot influence the broad, longitudinal, long-term geographic trend evident in our repeat photography analysis. A uniformity must be exhibiting some control regionally to account for the trend in vegetation. Either it is precipitation, a combination of factors, or another factor operating at high levels. One such uniform factor is

the increased atmospheric concentration of $C0_2$ through anthropogenic means, although much of the direct impact of this phenomenon on regional ecosystems is unclear. Atmospheric $C0_2$ has grown from ~280ppm from the pre-industrial era, just before the PLS was conducted, to over 400ppm at current (Baso et al., 2021). By some measures, this has caused and will continue to cause the growth of vegetation globally (Thompson et al., 2004). One early estimate using a review of greenhouse experiments predicted a 33% increase in vegetation productivity with a doubling of mid-20th century atmospheric $C0_2$ (Kimball, 1983). A more recent estimate determined that the leaf area index (LAI) or greening had grown in 25-50% of the global environment, including in the Lower Peninsula of Michigan, between 1982 and 2009 and that ~70% of that growth was due to increased $C0_2$ fertilization (Zhu et al., 2016). Certainly, these findings and others fit the pattern demonstrated in our analysis, especially given the stabilization of European coastal dunes through vegetation expansion since ~1900 (Provoost et al., 2011). Unfortunately, much is uncertain with regards to the coupling between regional vegetation productivity and increased atmospheric $C0_2$. Ultimately, if the expansion of coastal dune vegetation in our study area is being driven by higher atmospheric $C0_2$, then the future persistence of this trend will be based on the physiological tradeoffs presented by this phenomenon: Increased amounts of $C0_2$ drive photosynthesis and facilitate water efficiency in plant, while the higher temperatures associated with most climate change scenarios will cause plant stress, increased water usage, and less photosynthesis (Sperry et al., 2019). Much like the effects of increased atmospheric $C0_2$, greater atmospheric nitrogen deposition from anthropogenic means might also be uniformly driving N enrichment of dune soils across the region. Greater atmospheric N deposition would foster plant growth and influence the composition of dune grassland ecosystems (van den Berg et al., 2005), although more work needs to be done with respect to this topic in North American dunefields.

An additional, if intriguing, uniform control on dune vegetation is the possibility that the expansion of plants in coastal dunes along Lake Michigan is a lagged response to the colder and stormier conditions of the Little Ice Age (LIA), the most recent global Holocene cooling event (Jackson et al., 2019). This event, defined broadly as from 1300–1900 CE in the Northern Hemisphere with regional variations (Nordstrom, 2015), coincided with well-documented, episodic coastal dune activity in western and northern Europe (Jackson et al., 2019; Provoost et al., 2011). While conditions during the LIA were often asynchronous and varied, climate reconstructions show the core of the LIA to be particularly cool conditions from 1580-1880 CE that were fully reversed only in the last 50 years (PAGES 2k Consortium, 2013). The causes of the LIA were complex, but workers generally have focused on solar forcing and volcanic activity as the primary drivers (Jackson et al., 2019; PAGES 2k Consortium, 2013). With regards to LIA aeolian activity, coastal dunes displayed transgressive behavior at several locations from Portugal (e.g., Clarke and Rendell, 2006), to the Aquitaine Coast in the southwest of France (e.g., Clarke et al., 2002), the British Isles (e.g., Wintle et al., 1998), and into Scandinavia (Clemmensen et al., 2015), amongst other areas. There is disagreement as to whether the LIA aeolian activity in Europe was primarily the consequence of an increased supply of sand in foreshore due to storminess and sea level fluctuation or a reactivation of existing dunes in the backshore (Clarke et al., 2002; Jackson et al., 2019; Nordstrom, 2015; Szkornik et al., 2008). Regardless, there is little doubt that the LIA was a period of coastal dune activity in much of Europe.

In the Great Lakes region, there is evidence of the effects of the LIA, but not necessarily in dune environments. The LIA began a few hundred years after a pronounced ~1,000-year period of stability amongst Lake Michigan's dunes, as evidenced by the development of the Holland Paleosol (Lovis et al., 2012). Hansen et al. (2010) in their study of eastern Lake Michigan dunes suggested that the ~6,000-year record of dune behavior in the region could only be explained

by something "in addition to lake level and modern land use practices." One factor they considered as a uniform control was storminess (Hansen et al., 2010), noting a study from Green Mountain Beach south of Holland where much of the annual sand transport was in response to strong storms (Hansen et al., 2009) along with similar findings at P.J. Hoffmaster State Park (van Dijk, 2004). Storminess was a suspected hallmark of LIA dune behavior in Europe, but a link to dune behavior in Michigan and the LIA was not explored in those studies.

In a non-dune study, geochemical and radiocarbon analysis on Lake Michigan sediment showed that an abrupt change in deposition occurred around ~1400 CE (Colman et al., 2000). Lake deposits had been coarse-grained and consistent with river and lake bluff erosion, but became finer-grained and consistent with soil erosion around 1400 CE (Colman et al., 2000). Pollen records from the Lower Peninsula of Michigan for the LIA found a significant decline in the wet-mesic conifer *Thuja* genus of trees, while genera typically found farther north – specifically *Pinus* and *Tsuga* – increased, in a clear response to cooler and drier conditions (Hupy and Yansa, 2009). A new study examined tree ring data from South Manitou Island in Lake Michigan just off Sleeping Bear Point for roughly the same period and determined that the LIA period contained multiple decadal severe droughts, especially in the late 1500s CE, which coincided with an event known as the Late 16th-Century Megadrought (Warner et al., 2021), a ~25-year period driven by one of the most intense occurrences of cold tropical Pacific Ocean sea surface temperatures (Cook et al., 2018). Climate reconstructions show that the drought indices may have been slightly elevated along the middle and northern sections of the Lake Michigan eastern shoreline (Cook et al., 2018, Fig. 1), aligning somewhat with our PLS findings, where surveyors noted bare sand at sites in the middle and northern sections of the coast. In this regard, the PLS notebooks could be interpreted as windows into a landscape emerging from the cooler ~500+ year LIA event and a related megadrought. Moreover, a long lag in dune soil response to increasingly mesic conditions

over the last ~100 years is more plausible given Salisbury's (1952, pg. 161) observations from cold dunes in England that the mere "passage of time" eventually provides the conditions for beneficial pedogenesis, especially if dune migration slows. Thus, it is conceivable that the dune systems of Lake Michigan operate as a dynamic multiple state system that is still in nonequilibrium in response to conditions of the LIA.

The idea of landscape steady state or equilibrium is contested (Huggett, 2007; Perry, 2002; Thorn and Welford, 1994; Turner et al., 1993), but as Turner et al. (1993) argued the concept has merit if the spatial and temporal scales of landscape disturbance and recovery are understood. There is much about the Lake Michigan dune systems which is not well understood. Yet, we have presented evidence of a landscape response on a coastal scale over several decades, possibly as a system that is returning to a steady state, fluctuating between alternative states, or in nonequilibrium. In other words, based upon the evidence we presented here, Lake Michigan's coastal dunes are either returning to their natural vegetated steady state – a condition punctuated only by the storminess of the LIA – or transitioning between two natural alternative states (bare sand and vegetated) based upon current drivers or something more chaotic. A more chaotic geomorphological circumstance would involve multiple uniform and local factors interacting in dynamic ways to drive landform response, perpetuating a state of nonequilibrium (Huggett, 2011; Phillips, 2007).

Thus, the results of a study from coastal dunes in northwest England may be instructive. There, Delgado-Fernandez et al. (2019) concluded that the loss of bare sand and the increase in vegetation was the result of the "interaction of multiple drivers" that "act together with different degrees of predominance depending on the location and characteristics of the coastal dune field." Yet, perhaps climate was ultimately responsible for most of the changes, acting as a uniform "primary control on dune vegetation cover" (Delgado-Fernandez et al., 2019). Evidence

presented from our study demonstrates that a type of ecogeomorphic regime shift may be underway, possibly due, as is often the case, to external controls such as climate interacting with the internal dynamics of a system (Andersen et al., 2009), such as dune sand soil. Nonlinear regime shifts owing to threshold response, as is perhaps occurring, "are typically rapid" and "difficult to foresee" (Ratajczak et al., 2014), especially in complex systems which exhibit high degrees of connectivity and homogeneity (Scheffer et al., 2012), which might describe Lake Michigan coastal dune systems.

The most likely driver of the changes presented in our study is a uniform control operating at the meso and macro spatio-temporal scales, with a combination of local controls and feedbacks providing variability and heterogeneity of dune conditions at microscales. One of the candidates of increased dune stability is a modest increase in annual precipitation. Yet, as van Dijk (2014) noted in a study of multiple possible drivers of foredune conditions, "We still have a considerable distance to go in our understanding of how events combine to produce the cumulative effects that we see at longer time scales." With that in mind, other uniform controls may be at work, such as an ecogeomorphic lag from the LIA or CO_2 fertilization. We see the need for further specific research into the soil moisture and precipitation regimes of these dunefields, along with a regional quantification of vegetative growth associated with increased concentrations of atmospheric CO_2, possibly involving remote sensing, and controlled experiments investigating the response of native and invasive plant species to CO_2 fertilization. We would also encourage more conceptual research into the multiple steady state systems comprising inland coastal dunefields.

2.6 Conclusions

In this study, we demonstrated that vegetation has expanded at 20 sites in dunes along Lake Michigan's eastern shoreline through the use of repeat photography. These findings support recent research from White et al. (2019) that demonstrated expanding vegetation in state parks

along Lake Michigan since 1938. We used a semi-quantified process to describe the expansion of vegetation seen in these repeat photography pairs, then attempted to identify drivers of such a change through a statistical analysis of meteorological data and dune mobility indices for three stations – South Bend, Muskegon, and Traverse City. To learn if trends existed in these data, we first employed Durbin-Watson tests to detect serial correlation rather than use the pre-whitening process in a somewhat novel approach. Finding little evidence of serial correlation, we performed a series of Mann-Kendall tests designed to find trends in a time series, calculating the *Z*-statistic and Kendall's τ. Some weak-to-moderate trends were detected in our meteorological data and dune mobility indices, but the results were mixed. Still, an increase in annual total precipitation, which was represented by weak positive statistically significant trends at South Bend and Muskegon, stood out as a possible driver of dune vegetation expansion, a finding similar to White et al. (2019). Given the spatial consistency of vegetation expansion in our study, we considered the possibility that other uniform controls may be at work as drivers, including the increased concentrations of atmospheric CO_2 and a possible ecogeomorphic lag from the cooler and stormier conditions of the LIA. Regarding the effects of the LIA, the PLS notebooks from surveyors in the 1830s to 1850s that we examined showed signs of dune bare sand at most repeat photography sites, supporting the possibility that LIA conditions constrained vegetation growth on coastal dunes. Additionally, we discussed various local controls which could be contributing to dune behavior. Given the probable nonequilibrium of the coastal dune systems in our study area, we have concluded that a uniform control – possibly an increase in precipitation since the 1930s or an ecogeomorphic lag from the LIA – is primarily driving the expansion of vegetation in dunes along the eastern shore of Lake Michigan. We call for more research into how these potential drivers are interacting in a process-response manner with local internal dynamics, such as dune soil moisture thresholds and invasive species, to better understand the processes underway in Lake Michigan's coastal dunes.

2.7 Acknowledgments

Financial assistance for this research was provided, in part, by the Michigan Coastal Management Program, Water Resources Division; and the Michigan Department of Environment, Great Lakes, and Energy (EGLE), under the National Coastal Zone Management Program, through a grant from the National Oceanic and Atmospheric Administration (NOAA), U.S. Department of Commerce (Grant #RC109434). The project was managed by the Michigan Environmental Council (MEC) and Michigan State University (MSU). We would like to thank Tom Zimnicki, MEC project manager. Additionally, we appreciate the assistance provided by Jeffery A. Andresen and Morris Thomas, with MSU's Department of Geography, Environment, and Spatial Science. Andresen helped identify appropriate meteorological and reanalysis data, while Thomas provided advice on navigating the PLS collection at the Archives of Michigan. I would also like to thank members of my dissertation committee: Kyla Dahlin and Ethan J. Theuerkauf, with MSU's Department of Geography, Environment, and Spatial Science, and Robert B. Richardson, with MSU's Department of Community Sustainability.

APPENDICES

APPENDIX A:

Tables

Table 2.1: Repeat photographic pair details. New structure column refers to any new human-built structures on the dunes since the original photograph.

Photo Pair Site	Coast Location	Lat., Lon.	Original Photo Year	Re-Photo Year	Photo Interval (y)	New Struct.
Grand Beach (1)	South	41.782578, -86.778755	1987	2019	32	Y
Grand Beach (2)	South	41.782932, -86.779561	1987	2019	32	Y
Warren Dunes/ Painterville Drain	South	41.904067, -86.610062	1900	2019	119	N
Warren Dunes	South	41.903323, -86.603600	1946	2019	73	N
Saugatuck/ Oval Beach	Mid	42.662274, -86.216413	1947	2019	72	Y
Saugatuck/ Mt. Baldhead	Mid	42.661227, -86.207821	1890	2019	129	N
Laketown Beach	Mid	42.724575, -86.20641	1989	2019	30	N
Holland State Park Beach	Mid	42.777575, -86.2117	1958	2019	61	Y
Ottawa Beach	Mid	42.78062, -86.210398	1987	2019	32	Y
Grand Haven	Mid	43.063741, -86.230219	1935	2019	84	N
Muskegon Channel	Mid	43.220897, -86.330887	1915	2019	104	Y
Meinert Park	Mid	43.458357, -86.45728	1987	2019	32	N
Silver Creek (1)	Mid	43.657587, -86.529723	1915	2019	104	N
Silver Creek (2)	Mid	43.657858, -86.533719	1915	2019	104	N
Big Sable Point	Mid	44.062615, -86.509579	1915	2019	104	N
The Sleeping Bear	North	44.874237, -86.069461	1907	2019	112	N
Sleeping Bear Dune Climb	North	44.880368, -86.042494	1917	2019	102	Y
Sleeping Bear Day Farm	North	44.881866, -86.048518	1918	2019	101	N
Sleeping Bear Pt.	North	44.911859, -86.039546	1915	2019	104	N
N. Manitou Island	North	45.111807, -86.058765	1905	2019	114	N

Table 2.2: Bare sand/vegetation change analysis results.

ANY BARE SAND GAIN/ VEGETATION LOSS	SLIGHT BARE SAND LOSS/ VEGETATION GAIN	MORE BARE SAND LOSS/ VEGETATION GAIN	SIGNIFICANT BARE SAND LOSS/ VEGETATION GAIN	ALMOST COMPLETELY VEGETATED IN 2019
	Painterville Drain	Meinert Park	Warren Dunes	Grand Beach 1
	Big Sable Point	Sleeping Bear Day Farm	Ottawa Beach	Grand Beach 2
	The Sleeping Bear		Grand Haven	Oval Beach
			Sleeping Bear Point	Mt. Baldhead
			Sleeping Bear Dune Climb	Laketown Beach
			North Manitou Is.	Holland State Park Beach
				Muskegon Channel
				Silver Creek 1
				Silver Creek 2

Table 2.3: Phrases contained in U.S. Public Lands Survey (PLS) notebooks for each repeat photography site.

Photo Pair Site	Township/ Range + Sec.	Survey Year	Surveyor Name	Dunes/ Sand?	Veg.?	Surveyor Notes Selection
Grand Beach (1)	08S21W17	1829	Lucius Lyon	Y	Y	Section 8/17 boundary: No mention of sand dunes or vegetation. Section 17/18 boundary: "Land rolling and 3rd rate" "Timber dwarf oak" Meander 17/18: "Sandy beach with hills of loose sand"
Grand Beach (2)	08S21W17	1829	Lucius Lyon	Y	Y	Section 8/17 boundary: No mention of sand dunes or vegetation. Section 17/18 boundary: "Land rolling and 3rd rate" "Timber dwarf oak" Meander 17/18: "Sandy beach with hills of loose sand"
Warren Dunes/ Painterville Drain	06S20W34	1829	Lucius Lyon	N	N	Section 34/35 boundary: No mention of sand dunes or vegetation. Meander: "beach 2 chains wide"
Warren Dunes	06S20W35	1829	Lucius Lyon	N	N	Section 34/35 boundary: No mention of sand dunes or vegetation. Meander: "beach 2 chains wide"
Saugatuck/ Oval Beach	03N16W08	1831	Calvin Britain	Y	N	Section 8/17: "Land broken and soil the same".
Saugatuck/ Mt. Baldhead	03N16W09	1831	Calvin Britain	Y	Y	Section 8/9: "Indian fields", "hemlock", "sugar", "sand banks", "pine", "land broken", "soil thin".
Laketown Beach	04N16W21	1834	Calvin Britain	Y	N	Section 16/21: "Sand hills". Surveyor reported having difficulty finding a tree to use as a post.
Holland State Park Beach	05N16W33	1832	Noah Brookfield for Calvin Britain	Y	Y	Section 28/33: "Land very broken, 3rd rate", "Timber beech, pine, oak, and hemlock". According to map, camera location was likely the mouth of the Macatawa River.

Table 2.3 (Cont'd)

Ottawa Beach	05N16W33	1832	Noah Brookfield for Calvin Britain	Y	Y	Section 28/33: "Land very broken, 3rd rate", "Timber beech, pine, oak, and hemlock".
Grand Haven	08N16W20	1837	John Mullett	Y	N	For entire area: "Land high barren sand hills west of river".
Muskegon Channel	10N17W28	1837	John Mullett	Y	N	Section 28/33: "Land hilly 3rd rate", "Sand hills".
Meinert Park	12N18W09	1838	John Mullett	Y	N	Section 9/10: "Land hilly loose sand".
Silver Creek (1)	15N19W36	1838	John Mullett	Y	N	Section 25/36: "Land bald sand hills", "hilly", "poor sandy soil".
Silver Creek (2)	15N19W36	1838	John Mullett	Y	N	Section 35/36: "Loose drifting sand", "no trees", "Land hilly loose drifting sand". Corner post was driven into sand.
Big Sable Point	19N18W07	1838	Sylvester Sibley	Y	N	Section 6/7: "No trees", "Land sand hills".
The Sleeping Bear	29N15W36	1839	Sylvester Sibley	Y	N	Section 25/36: "No baring trees", "rolling and drifting sand hills", "no timber".
Sleeping Bear Dune Climb	29N14W30	1850	Orange Risdon			Section 30/31: "Sliding sand dune", "no bearings".
Sleeping Bear Day Farm	29N14W30	1850	Orange Risdon	Y	N	West boundary of 29N14: "No trees or timber", "land barren", "rolling sand drifts and ridges".
Sleeping Bear Pt.	29N14W18	1850	Orange Risdon	Y	Y	Section 18/19: "Cedar and fir to foot of sliding sand hill … from 100 to 150 ft high.", "Land barren", "rolling sand drifts", "cedar", "dry swamp"
N. Manitou Island	31N15W01	1847	Orange Risdon	Y	N	From survey maps parts 1 and 2: "Bare sand bluffs and hills".

Table 2.4: Results for the Durbin-Watson test by variable and meteorological station. Shown is the d-statistic with the acceptable serial correlation bounding range from Savin and White (1977) in smaller font and parentheses. The d-statistic range is 0-4 and is symmetrical with a value 2 denoting the absence of serial correlation. Values within the bounding range are assumed to lack serial correlation, while those that exceed the range might possess it. The one variable that violates the Durbin-Watson test is highlighted in dark gray.

Variable	South Bend	Muskegon	Traverse City
Mean annual temp.	1.887 (1.47 – 2.53)	1.506 (1.5 – 2.5)	1.452 (1.52 – 2.48)
Annual total precipitation	1.833 (1.47 – 2.53)	2.037 (1.47 – 2.53)	1.993 (1.52 – 2.48)
Annual total PET	2.025 (1.47 – 2.53)	1.777 (1.5 – 2.5)	1.708 (1.52 – 2.48)
Mean annual wind speed	2.036 (1.43 – 2.57)	2.213 (1.43 – 2.57)	1.857 (1.43 – 2.57)
Lancaster's *M*	2.123 (1.43 – 2.57)	2.439 (1.43 – 2.57)	2.175 (1.43 – 2.57)
Chepil's C	2.03 (1.43 – 2.57)	2.356 (1.43 – 2.57)	2.163 (1.43 – 2.57)
Drift potential	2.064 (1.43 – 2.57)	2.028 (1.43 – 2.57)	1.561 (1.43 – 2.57)

Table 2.5: Results from the Mann-Kendall test. Kendall's tau, the Z-statistic, and p-values (two-tailed) are reported. Results significant at P<0.05 are in bold. Z-statistic values designating any significant trend are underlined and italicized, as are tau values demonstrating a moderate or strong trend over time.

Variable	South Bend			Muskegon			Traverse City		
	Z	τ	P-value	Z	τ	P-value	Z	τ	P-value
Mean annual temp.	***2.49***	**0.191**	**0.013**	***2.69***	**0.192**	**0.007**	1.64	0.105	0.102
Annual total precip.	***2.36***	**0.181**	**0.018**	***3.09***	**0.233**	**0.002**	1.68	0.111	0.093
Annual total PET	***2.51***	**0.191**	**0.012**	***3.81***	***0.271***	**<0.001**	1.87	0.120	0.062
Mean annual wind spd.	***-3.75***	***-0.307***	**<0.001**	-1.46	-0.120	0.144	0.07	0.006	0.943
Lancaster's *M*	***-2.65***	**-0.217**	**0.008**	***-2.34***	**-0.192**	**0.019**	1.27	0.109	0.203
Chepil's C	*-1.95*	-0.159	0.052	***-2.27***	**-0.186**	**0.023**	1.53	0.131	0.125
Drift potential	-1.39	-0.114	0.165	0.02	0.002	0.984	1.19	0.097	0.236

APPENDIX B:

Figures

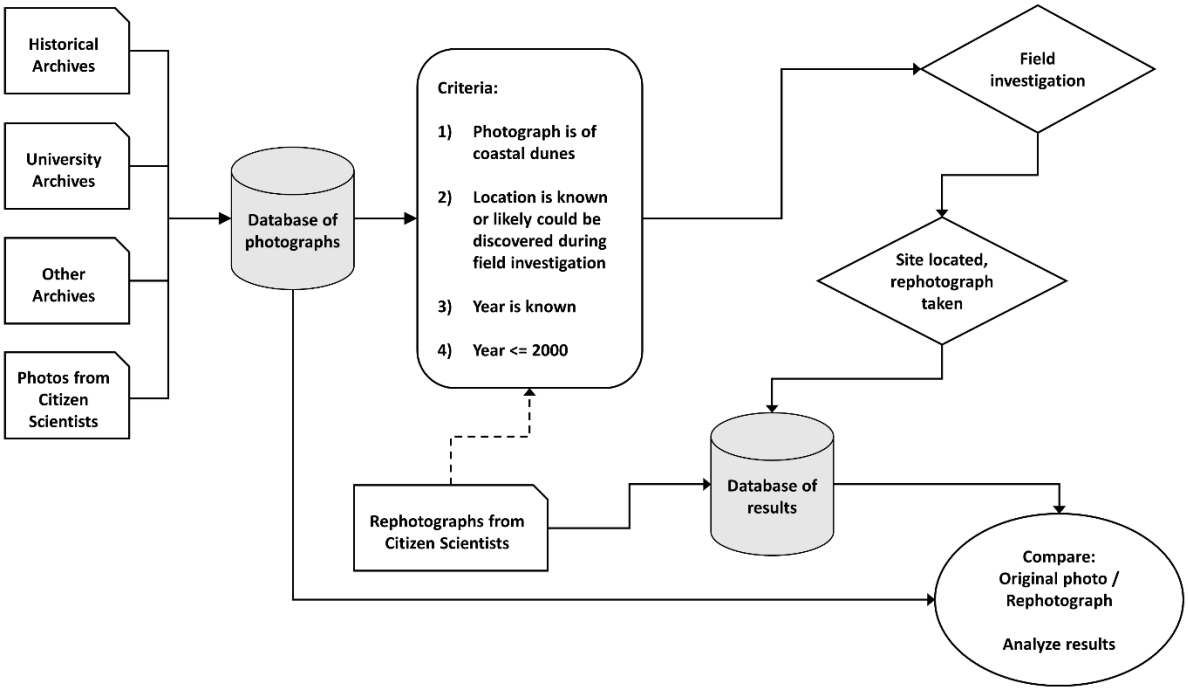

Figure 2.1: Repeat photography workflow process.

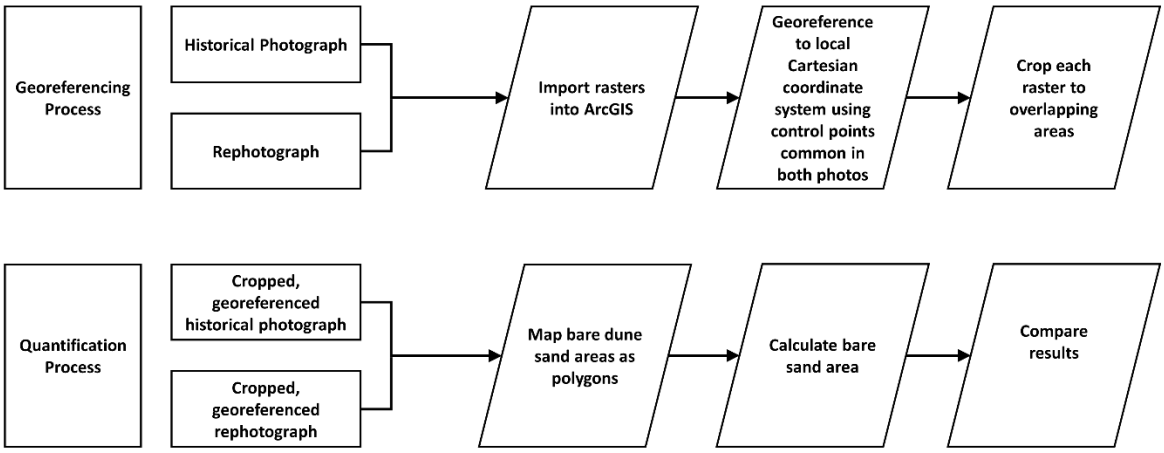

Figure 2.2: Photographic analysis workflow process. Adapted from Manier and Laven (2002, fig. 6).

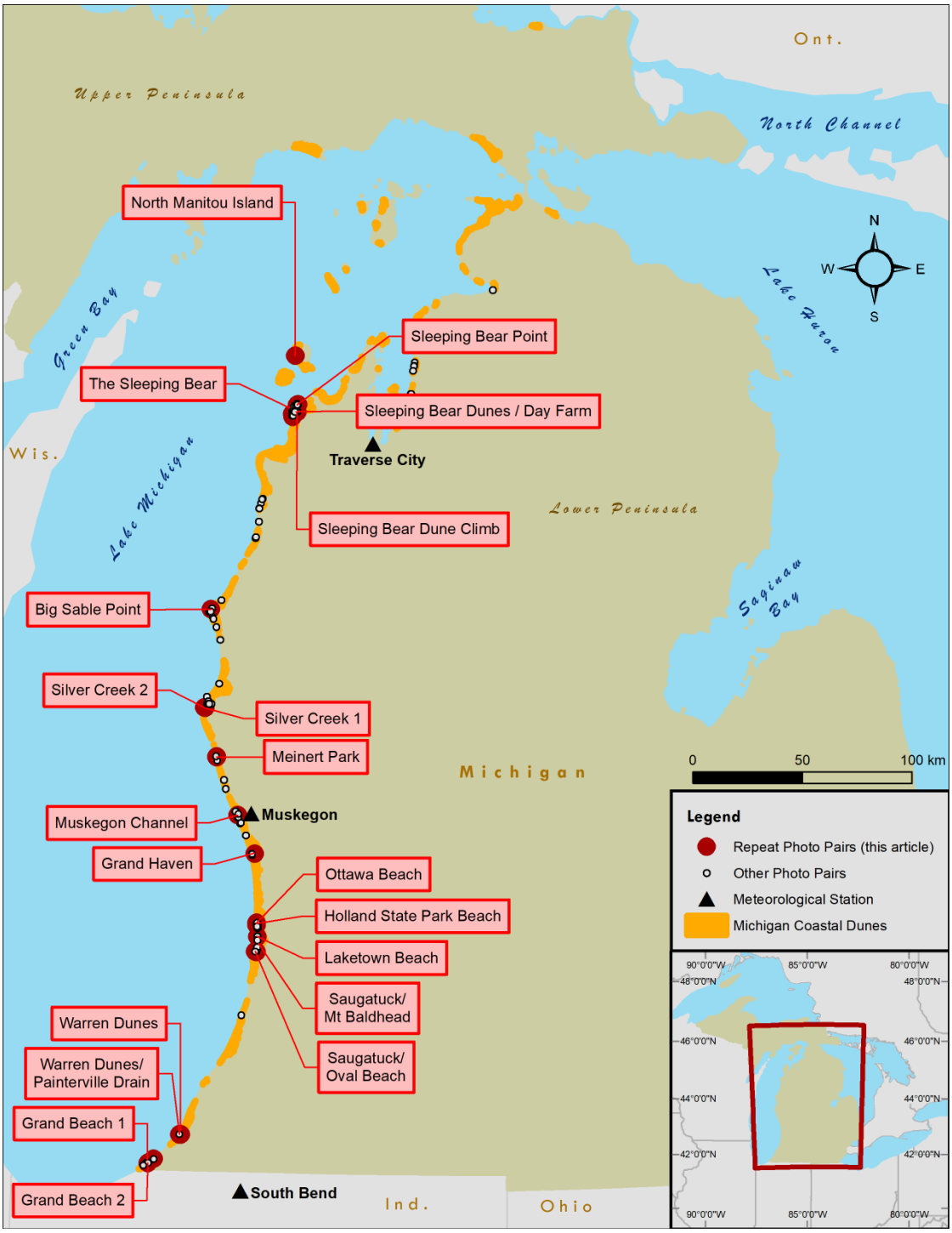

Figure 2.3: Location of repeat photographic pairs (ESRI) listed in Table 1. Coastal dune areas from Arbogast et al. (2018).

Figure 2.4: Grand Beach, looking WSW along Lake Park Drive. Original photo (left) is from 1987 courtesy of EGLE. Re-photo (right) is from 2019 by K. McKeehan. Note the expansion of vegetation and the built environment between the two photographs in the 32-year interval.

Figure 2.5: Laketown Beach, looking SSW. Original photo (left) is from 1989 courtesy of EGLE. Re-photo (right) is from 2019 by K. McKeehan. Note the expansion of vegetation between the two photographs and the establishment of trees in the 30-year interval.

Figure 2.6: Meinert Park, looking SSE. Original photo (left) is from 1987 courtesy of EGLE. Re-photo (right) is from 2019 by K. McKeehan. Note the expansion of vegetation between the two photographs, the changes in the Lake Michigan shoreline, and the new channel of Little Flower Creek in the 32-year interval.

Figure 2.7: Silver Creek at the south end of Silver Lake State Park, looking ESE. Original photo (left) is from 1915 from the Univ. of Chicago. Re-photo (right) is from 2019 by K. McKeehan. Note the expansion of vegetation at the expense of bare sand plus the growth of the forest on the dune slip face between the two photographs in the 104-year interval.

Figure 2.8: Taken from The Sleeping Bear, Sleeping Bear Dunes National Lakeshore, looking NNE. Original photo (left) is from 1907, Bentley Historical Library, Univ. of Michigan. Re-photo (right) is from 2019 by K. McKeehan. Exact location of original photograph had eroded and re-photograph was taken a few meters to the east and closer to base elevation. Note the expansion of vegetation, especially in the distance, between the two photographs in the 112-year interval.

Figure 2.9: Taken from below the Dune Climb at Sleeping Bear Dunes National Lakeshore, looking NNW. Original photo (left) is from 1917 from the Univ. of Chicago. Re-photo (right) is from 2019 by K. McKeehan. Note the expansion of vegetation at the expense of bare sand, with the exception of the location of the Dune Climb trail (center right), between the two photographs in the 112-year interval.

Figure 2.10: Quantification process example, from Silver Creek. Bare sand was mapped in hatched areas.

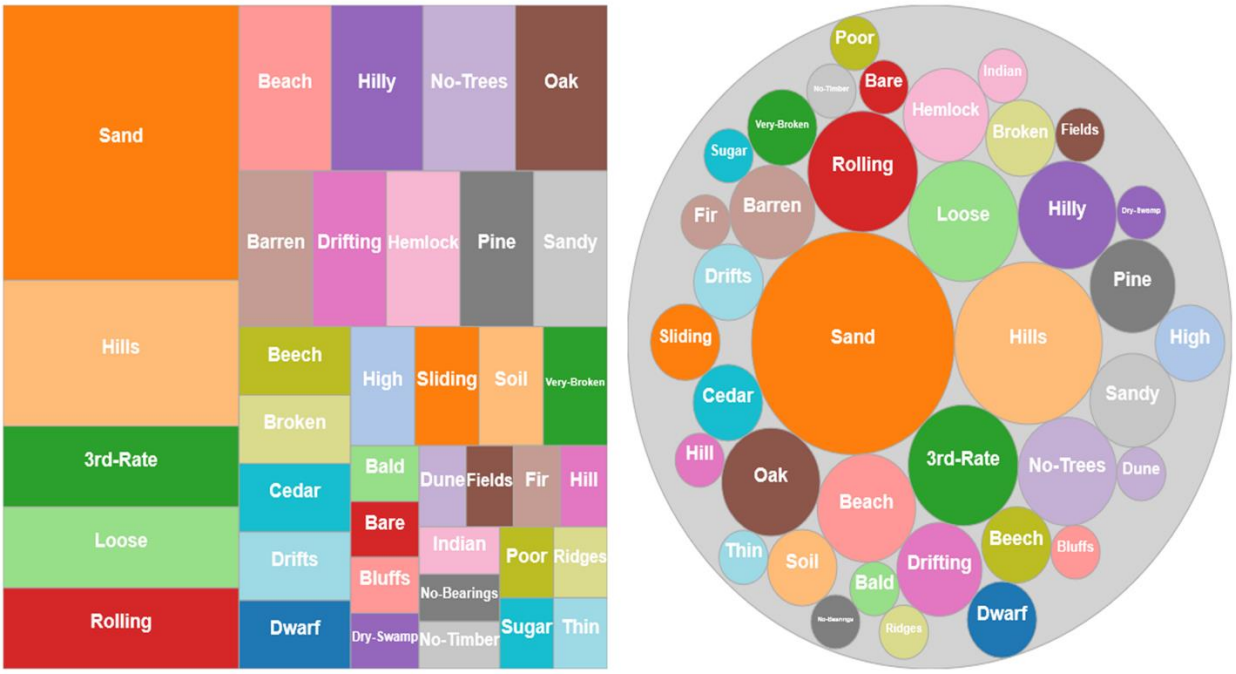

Figure 2.11: Word clouds for PLS notebook descriptions of repeat photography sites from 1829-1850 using Bjorn's Word Clouds software. Words evocative of bare sand dunes, such as "sand", "hills", "loose", and "rolling", are prominent, as is the term "3rd-rate", which is indicative of poor soil. The word sand was recorded 17 times out of 105 words or phrases in the PLS notebooks.

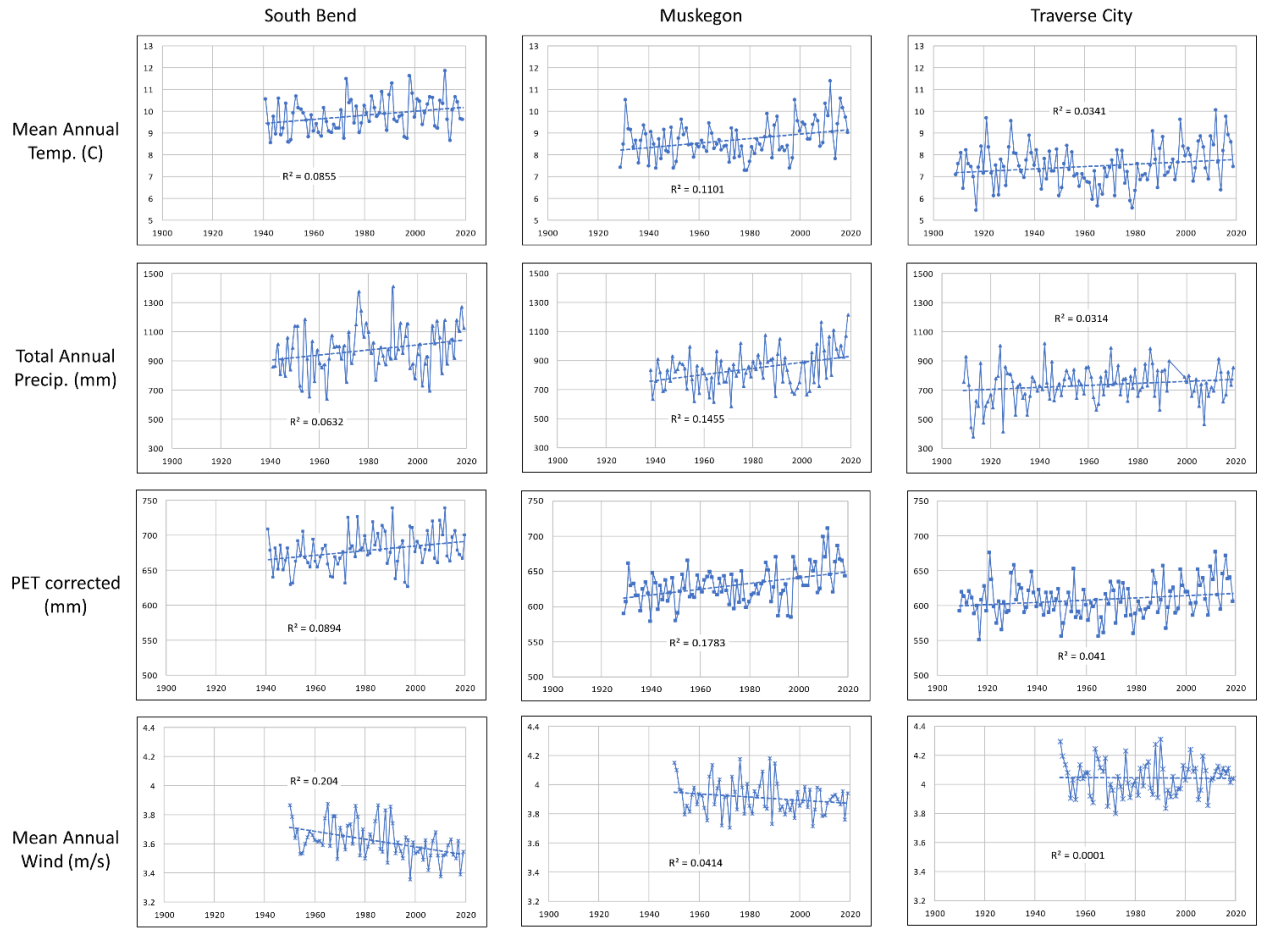

Figure 2.12: Meteorological data for South Bend, Muskegon, and Traverse City. Top row is mean annual temperature (C), followed by total annual precipitation (mm), corrected potential evapotranspiration (mm) using the Thornthwaite 1948 method, and the mean annual wind speed (m/s). Linear trend model lines are shown for each chart. All wind data is from 1950-2019. South Bend data is from 1941-2019 and Traverse City from 1909-2019, with a small gap in P data in the 1990s. Muskegon T and PET data is from 1929-2019, while precipitation data is from 1938-2019.

Figure 2.13: Dune mobility index results, 1950-2019.

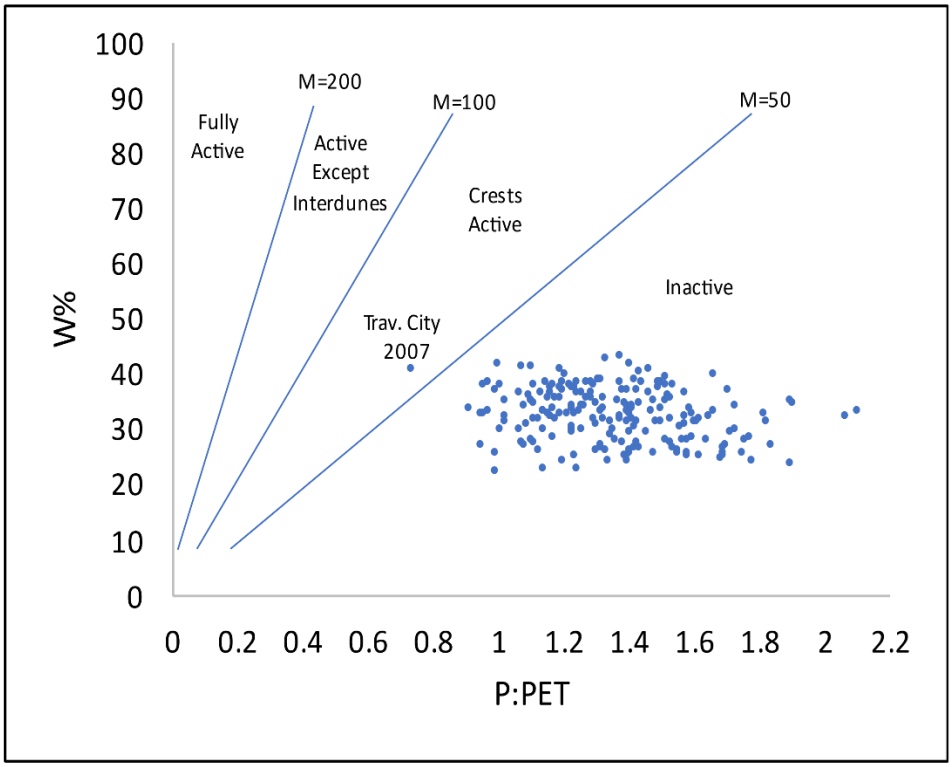

Figure 2.14: Lancaster's M for Lake Michigan coastal dunes using data from the three closest meteorological sites and the ECMWF. This statistic is plotted as the percentage of time wind speed exceeded 4.5 m/s in a year against the ratio of precipitation to potential evapotranspiration, which is the formula for M. All results were <50, with the exception of Traverse City in 2007, which would suggest inactive dunefields. From Lancaster (1988) and Muhs and Maat (1993).

APPENDIX C:

Additional Photograph Pairs

Figure 2A.1: GRAND BEACH (1). LAT: 41.782578, LON: -86.778755. This photograph, looking southwest, in 1987 captures a portion of a parabolic dune known as Eiffel Tower Dune. Photo Credit – 1987, EGLE; 2019, Kevin McKeehan, Michigan State University.

Figure 2A.2: GRAND BEACH (2). LAT: 41.782932, LON: -86.779561. This photograph, looking northeast, in 1987 captures a portion of a parabolic dune known as Eiffel Tower Dune. Photo Credit – 1987, EGLE; 2019, Kevin McKeehan, Michigan State University.

Figure 2A.3: WARREN DUNES / PAINTERSVILLE DRAIN. LAT: 41.904067, LON: -86.610062. These photographs are of Warren Dunes, where Painterville Drain enters Lake Michigan. The slopes of the dunes above the creek on the left show an expansion of grasses and tress over the last 119 years. Photo Credit – 1900, Archives of Michigan, Norman Asa Wood; 2019, Kevin McKeehan, Michigan State University.

Figure 2A.4: WARREN DUNES. LAT: 41.903323, LON: -86.6036. These photographs look WNW from the dunes in the vicinity of the south parking lot at Warren Dunes State Park. Photo Credit – 1946, Archives of Michigan; 2019, Kevin McKeehan, Michigan State University.

Figure 2A.5: SAUGATUCK, OVAL BEACH. LAT: 42.662274, LON: -86.216413. The original photograph is a postcard from 1947. The 2019 photograph from the same location shows that vegetation expanded over the bluff and stabilized it, which likely led to the aggradation and expansion lakeward of the bluff. Photo Credit – 1947, Saugatuck-Douglas Historical Society; 2019, Kevin McKeehan, Michigan State University.

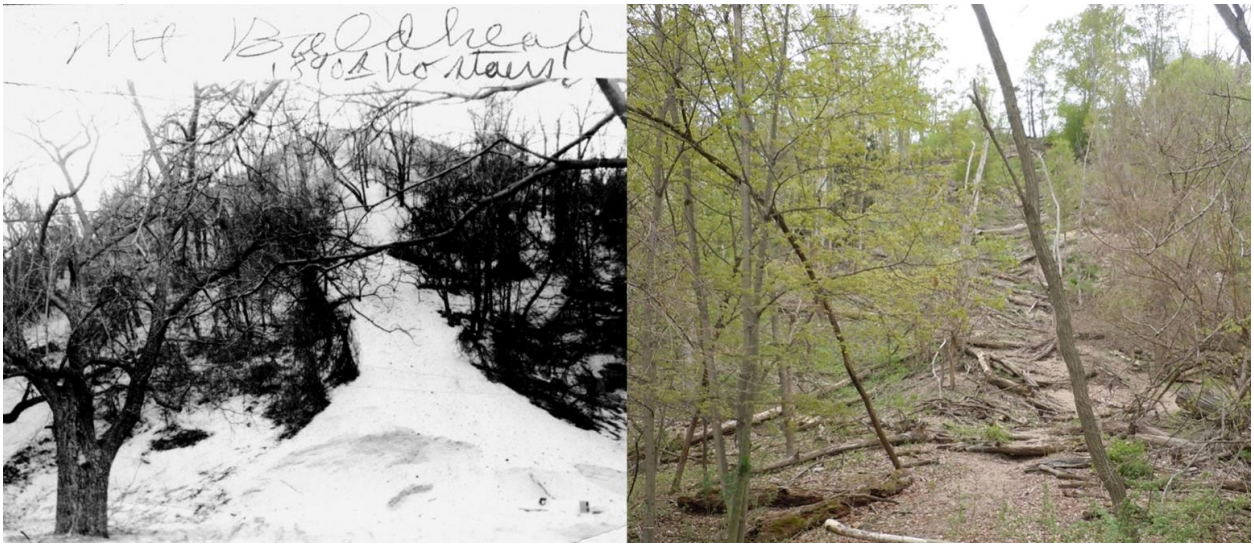

Figure 2A.6: SAUGATUCK, MT. BALDHEAD. LAT: 42.661227, LON: -86.207821. This historical photograph from 1890 from Mt. Baldhead near Saugatuck shows the large dune once was indeed "bald" with large amounts of bare sand atop its "head". Taken from the dune's eastern side. Photo Credit – 1890, Saugatuck-Douglas Historical Society; 2019, Kevin McKeehan, Michigan State University.

Figure 2A.7: LAKETOWN BEACH. LAT: 42.724575, LON: -86.20641. Laketown Beach, looking SSW. Note the expansion of vegetation between the two photographs and the establishment of trees in the 30-year interval. Photo Credit – 1989, Michigan EGLE; 2019, Kevin McKeehan, Michigan State University.

Figure 2A.8: HOLLAND STATE PARK BEACH. LAT: 42.777575, LON: -86.2117. This photo pair is looking north from Holland State Beach toward Ottawa Beach and the large sand dune in the distance that by 2019 has been covered by vegetation. The repeat photograph for this location by 2019 was taken 30 feet into Lake Michigan due to recent high lake levels. Photo Credit – 1958, Archives of Michigan; 2019, Kevin McKeehan, Michigan State University.

Figure 2A.9: OTTAWA BEACH. LAT: 42.78062, LON: -86.210398. These photographs are taken about 550m north-northeast of the Holland State Park Beach photographic pair (Figure 8). At the time of the original 1987 photograph, a planting effort was underway to stabilize the dune at the foot of a new housing development. Photo Credit – 1987, Michigan EGLE; 2019, Kevin McKeehan, Michigan State University.

Figure 2A.10: GRAND HAVEN, KITCHEL DUNE. LAT: 43.063741, LON: -86.230219. These photographs are taken down Grand Haven's Washington Street between Second and Third streets. In the distance, beyond downtown and across the Grand River, is Kitchel Dune. Photo Credit – 1935, Bentley Historical Library, Univ. of Michigan; 2019, Kevin McKeehan, Michigan State University.

Figure 2A.11: MUSKEGON CHANNEL. LAT: 43.220897, LON: -86.330887. The original photograph was taken in 1915 from a dune southeast of the entrance to the Muskegon Channel. A ghost forest amid bare sand populates the dune crest. By 2019, the entire dune has been overrun by woody vegetation and home construction. Through the trees in 2019, one can see the breakwater and lights for the channel, albeit barely. Photo Credit – 1915, Univ. of Chicago; 2019, Kevin McKeehan, Michigan State University.

Figure 2A.12: MEINERT PARK. LAT: 43.458357, LON: -86.45728. This photographic pair is from the Meinert Park area of Muskegon County. Since the original photograph was captured in 1987, vegetation has expanded, Little Flower Creek has cut a new channel to the lake, and the Lake Michigan shoreline is farther west in 2019. This is not to suggest that lake levels have fallen, but instead it appears large, vegetated, stable shoreline foredunes have formed in the last 30 years where the shore once was located. Photo Credit – 1987, Michigan EGLE; 2019, Kevin McKeehan, Michigan State University.

Figure 2A.13: SILVER CREEK (1), SILVER LAKE STATE PARK. LAT: 43.657587, LON: -86.529723. This photograph pair is from a location at the southern end of Silver Lake State Park on the north bank of Silver Creek. This spot is west of the Ruckel's Bridge area and west of a water control structure, which in 2019 photograph is obscured behind the trees. Note the expansion of vegetation at the expense of bare sand plus the growth of the forest on the dune slip face between the two photographs in the 104-year interval. Photo Credit – 1915, Univ. of Chicago; 2019, Kevin McKeehan, Michigan State University.

Figure 2A.14: SILVER CREEK (2), SILVER LAKE STATE PARK. LAT: 43.657858, LON: -86.533719. This photograph pair is from a location at the southern end of Silver Lake State Park on the north bank of Silver Creek, but is lakeward (west) from the other Silver Creek photographic pair. Lake Michigan is now obscured by woody vegetation. Photo Credit – 1915, Univ. of Chicago; 2019, Kevin McKeehan, Michigan State University.

Figure 2A.15: BIG SABLE POINT AND LIGHTHOUSE, LUDINGTON STATE PARK. LAT: 44.062615, LON: -86.509579. This photograph pair is of Big Sable Point looking southwest. The Big Sable Point Lighthouse, with its distinctive black and white stripes, is visible in both photographs. The 2019 photograph shows a somewhat transformed landscape, with less bare sand, more grasses, and much more water, possibly seeping from Lake Michigan, which is approximately 500m to the west. The modern dunes also appear larger and taller than in 1915. The research team would like to thank the staff at Ludington State Park for their assistance in recapturing this photograph. Photo Credit – 1915, Univ. of Chicago; 2019, Kevin McKeehan, Michigan State University.

Figure 2A.16: THE SLEEPING BEAR, SLEEPING BEAR DUNES NATIONAL LAKESHORE. LAT: 44.874237, LON: -86.069461. The original 1907 photograph was taken looking north toward South Manitou Island from the western flank of the vegetated dune feature known as The Sleeping Bear. Since that time, The Sleeping Bear has undergone changes, migrating inland and eroding in places. One place where erosion has taken place is the western slope where the original photograph was taken. Thus, the re-photograph was taken just east ~3m on the remaining slope and closer to base elevation. Note the expansion of vegetation, especially in the distance, between the two photographs in the 112-year interval. The research team would like to thank the staff at Sleeping Bear Dunes National Lakeshore for their assistance in recapturing this photograph. Photo Credit – 1907, Bentley Historical Library, Univ. of Michigan; 2019, Kevin McKeehan, Michigan State University.

Figure 2A.17: THE DUNE CLIMB, SLEEPING BEAR DUNES NATIONAL LAKESHORE. LAT: 44.880368, LON: -86.042494. The Dune Climb at Sleeping Bear Dunes National Lakeshore is one of the iconic places in Michigan. Many residents and tourists to the park hike up the side of this bare sand dune slipface in what some see at a Michigan bucket list experience. Despite a well-worn pathway up the Dune Climb, much of the dune slipface, crest, cornice, and flank in 2019 is covered with grasses. A comparison of the 2019 photograph to the 1917 image shows the Dune Climb area was almost exclusively bare sand except for an agricultural field and a forested area at the dune's toe. The research team would like to thank the staff at Sleeping Bear Dunes National Lakeshore for their assistance in recapturing this photograph. Photo Credit – 1917, Univ. of Chicago; 2019, Kevin McKeehan, Michigan State University.

Figure 2A.18: DUNE CLIMB BENCH AND DAY FARM, SLEEPING BEAR DUNES NATIONAL LAKESHORE. LAT: 44.881866, LON: -86.048518. The Dune Climb at Sleeping Bear Dunes National Lakeshore is one of the iconic places in Michigan. Many residents and tourists to the park trundle up the side of this bare sand dune slipface in what some see at a Michigan bucket list experience. At the crest of the Dune Climb from the parking lot, the pathway splits. If one follows the southern fork through bare sand and up the side of a larger dune, one will find a bench with a commanding view of the area to the northeast. This area includes the Day Farm and the far bluffs and perched dunes of Pyramid Point. The lowlands surrounding the Day Farm are not dunes and have been farmlands and pasturelands for some time, including in 1918, when the original photograph in this pair was taken. What is notable in the 1918 photograph is the extent of bare sand atop the Dune Climb from the crest to the east toward Lake Michigan to the west. The area west of the crest also appears to be relatively flat. By 2019, the shape of the land has changed and vegetation is extensive in the direction of Lake Michigan behind a second dune crest where bare sand once predominated. There are additional trees as well. The research team would like to thank the staff at Sleeping Bear Dunes National Lakeshore for their assistance in recapturing this photograph. Photo Credit – 1918, Univ. of Chicago; 2019, Kevin McKeehan, Michigan State University.

Figure 2A.19: NEAR SLEEPING BEAR POINT, SLEEPING BEAR DUNES NATIONAL LAKESHORE. LAT: 44.911859, LON: -86.039546. This photograph was taken near the Sleeping Bear Point Trail. In the original 1915 photograph, scientists from the University of Chicago study what appears to be a buried soil. By 2019, grasses, shrubs, and some trees have colonized and expanded over much of this area, except the trail itself. The research team would like to thank the staff at Sleeping Bear Dunes National Lakeshore for their assistance in recapturing this photograph. Photo Credit – 1915, Univ. of Chicago; 2019, Kevin McKeehan, Michigan State University.

Figure 2A.20: CRESCENT DOCK AREA, NORTH MANITOU ISLAND, SLEEPING BEAR DUNES NATIONAL LAKESHORE. LAT: 45.111807, LON: -86.058765. This photograph pair is of the west shore of North Manitou Island, specifically south of the Crescent Dock area. At the time of the original photograph, in approximately 1905, bare sand is noticeable along the dune slipfaces of the bluffs across the bay and among the foredunes up the shore. By 2019, grasses and trees have expanded across all these areas with the exception of the rocky beach. The research team would like to thank the staff at Sleeping Bear Dunes National Lakeshore for their assistance in recapturing this photograph. In particular, we'd like to thank Capt. David Schoeder and the National Park Service vessel Nahma for transportation across the Manitou Passage to the island. Photo Credit – 1905, National Park Service; 2019, Kevin McKeehan, Michigan State University.

REFERENCES

REFERENCES

Abbasi, H.R., Opp, C., Groll, M., Rohipour, H., Gohardoust, A., 2019. Assessment of the distribution and activity of dunes in Iran based on mobility indices and ground data. Aeolian Res. 41, 100539. https://doi.org/10.1016/j.aeolia.2019.07.005

Abhar, K.C., Walker, I.J., Hesp, P.A., Gares, P.A., 2015. Spatial-temporal evolution of aeolian blowout dunes at Cape Cod. Geomorphology 236, 148–162. https://doi.org/10.1016/j.geomorph.2015.02.015

Akoglu, H., 2018. User's guide to correlation coefficients. Turkish J. Emerg. Med. 18, 91–93. https://doi.org/10.1016/j.tjem.2018.08.001

Andersen, T., Carstensen, J., Hernández-García, E., Duarte, C.M., 2009. Ecological thresholds and regime shifts: approaches to identification. Trends Ecol. Evol. 24, 49–57. https://doi.org/10.1016/j.tree.2008.07.014

Anderton, J.B., Loope, W.L., 1995. Buried soils in a perched dunefield as indicators of late Holocene lake-level change in the Lake Superior basin. Quat. Res. 44, 190–199. https://doi.org/10.1006/qres.1995.1063

Arbogast, A.F., Hansen, E.C., Van Oort, M.D., 2002. Reconstructing the geomorphic evolution of large coastal dunes along the southeastern shore of Lake Michigan. Geomorphology 46, 241–255. https://doi.org/10.1016/S0169-555X(02)00076-4

Arbogast, A.F., Loope, W.L., 1999. Maximum-limiting ages of Lake Michigan coastal dunes: Their correlation with Holocene lake level history. J. Great Lakes Res. 25, 372–382. https://doi.org/10.1016/S0380-1330(99)70746-X

Arbogast, A.F., McKeehan, K.G., Richardson, R.B., Zimnicki, T., 2020. Learning to Live in Dynamic Dunes: Citizen Science and Participatory Modeling in the Service of Michigan Coastal Dune Decision-Making. Lansing, MI.

Arbogast, A.F., Schaetzl, R.J., Hupy, J.P., Hansen, E.C., 2004. The Holland Paleosol: An informal pedostratigraphic unit in the coastal dunes of southeastern Lake Michigan. Can. J. Earth Sci. 41, 1385–1400. https://doi.org/10.1139/E04-071

Argyilan, E.P., Lepper, K., Thompson, T.A., 2014. Late Holocene coastal development along the southern shore of Lake Michigan determined by strategic dating of stabilized parabolic dunes and wetlands of the Tolleston Beach, in: Coastline and Dune Evolution along the Great Lakes. Geological Society of America, pp. 31–46. https://doi.org/10.1130/2014.2508(03)

Baedke, S.J., Thompson, T.A., 2000. A 4,700-year record of lake level and isostasy for Lake Michigan. J. Great Lakes Res. 26, 416–426. https://doi.org/10.1016/S0380-1330(00)70705-2

Bagnold, R.A., 1941. The Physics of Blown Sand and Desert Dunes. Methuen, London.

Baldwin, K.A., Maun, M.A., 1983. Microenvironment of Lake Huron sand dunes. Can. J. Bot. 61, 241–255.

Baso, N.C., Coetzee, J.A., Ripley, B.S., Hill, M.P., 2021. The effects of elevated atmospheric CO2 concentration on the biological control of invasive aquatic weeds. Aquat. Bot. 170, 103348. https://doi.org/10.1016/j.aquabot.2020.103348

Bayazit, M., Önöz, B., 2007. To prewhiten or not to prewhiten in trend analysis? Hydrol. Sci. J. 52, 611–624. https://doi.org/10.1623/hysj.52.4.611

Bayr, U., 2021. Quantifying historical landscape change with repeat photography: an accuracy assessment of geospatial data obtained through monoplotting. Int. J. Geogr. Inf. Sci. 1–21. https://doi.org/10.1080/13658816.2021.1871910

Belford, A., Kenbeek, S.D., VanHorn, J., Van Dijk, D., 2014. Using remote sensing and geospatial analysis to understand changes to Lake Michigan dunes. Spec. Pap. Geol. Soc. Am. 508, 217–228. https://doi.org/10.1130/2014.2508(12)

Bell, B., Hersbach, H., Berrisford, P., Dahlgren, P., Horányi, A., Muñoz Sabater, J., Nicolas, J., Radu, R., Schepers, D., Simmons, A., Soci, C., Thépaut, J.-N., 2020. ERA5 hourly data on single levels from 1950 to 1978 (preliminary version), Copernicus Climate Change Service (C3S) Climate Data Store (CDS).

Bennett, S.B., Olyphant, G.A., 1998. Temporal and spatial variability in rates of eolian transport determined from automated sand traps: Indiana Dunes National Lakeshore, U.S.A. J. Coast. Res. 14, 283–290.

Bennett, S.B., Olyphant, G.A., 1993. Wind distribution and eolian sand transport on Mt. Baldy, Indiana Dunes National Lakeshore: Indiana Geological Survey Open-File Study 93-06.

Blain, G.C., Bardim-Camparotto, L., 2014. Detecting trends in 10-day rainfall amounts at five sites in the state ofSão Paulo, Brazil. Acta Sci. Technol. 36, 685–692. https://doi.org/10.4025/actascitechnol.v36i4.20513

Blumer, B.E., Arbogast, A.F., Forman, S.L., 2012. The OSL chronology of eolian sand deposition in a perched dune field along the northwestern shore of Lower Michigan. Quat. Res. 77, 445–455. https://doi.org/10.1016/j.yqres.2012.01.006

Botsch, R.E., 2011. Significance and Measures of Association [WWW Document]. URL http://polisci.usca.edu/apls301/Text/Chapter 12. Significance and Measures of Association.htm (accessed 3.12.21).

Bowman, D.M.J.S., Balch, J., Artaxo, P., Bond, W.J., Cochrane, M.A., D'Antonio, C.M., DeFries, R., Johnston, F.H., Keeley, J.E., Krawchuk, M.A., Kull, C.A., Mack, M., Moritz, M.A., Pyne, S., Roos,

C.I., Scott, A.C., Sodhi, N.S., Swetnam, T.W., 2011. The human dimension of fire regimes on Earth. J. Biogeogr. 38, 2223–2236.

Box, G.E.P., Jenkins, G.M., 1976. Time Series Analysis: Forecasting and Control, Revised Ed. ed. Holden-Day, San Francisco.

Chepil, W.S., Siddoway, F.H., Armbrust, D.V., 1963. Climatic index of wind erosion conditions in the Great Plains, in: Soil Science Society Proceedings. Division S-6 -- Soil and Water Management . pp. 449–452.

Clarke, M., Rendell, H., Tastet, J.-P., Clave, B., Masse, L., 2002. Late-Holocene sand invasion and North Atlantic storminess along the Aquitaine Coast, southwest France. The Holocene 12, 231–238. https://doi.org/10.1191/0959683602hl539rr

Clarke, M.L., Rendell, H.M., 2006. Effects of storminess, sand supply and the North Atlantic Oscillation on sand invasion and coastal dune accretion in western Portugal. The Holocene 16, 341–355. https://doi.org/10.1191/0959683606hl932rp

Clemmensen, L.B., Glad, A.C., Hansen, K.W.T., Murray, A.S., 2015. Episodes of aeolian sand movement on a large spit system (Skagen Odde, Denmark) and North Atlantic storminess during the Little Ice Age. Bull. Geol. Soc. Denmark 63, 17–28. https://doi.org/10.37570/bgsd-2015-63-03

Collaud Coen, M., Andrews, E., Bigi, A., Martucci, G., Romanens, G., Vogt, F.P.A., Vuilleumier, L., 2020. Effects of the prewhitening method, the time granularity, and the time segmentation on the Mann–Kendall trend detection and the associated Sen's slope. Atmos. Meas. Tech. 13, 6945–6964. https://doi.org/10.5194/amt-13-6945-2020

Colman, S.M., King, J.W., Jones, G.A., Reynolds, R.L., Bothner, M.H., 2000. Holocene and recent sediment accumulation rates in Southern Lake Michigan. Quat. Sci. Rev. 19, 1563–1580. https://doi.org/10.1016/S0277-3791(00)00007-X

Cook, B.I., Williams, A.P., Smerdon, J.E., Palmer, J.G., Cook, E.R., Stahle, D.W., Coats, S., 2018. Cold tropical Pacific sea surface temperatures during the late Sixteenth-Century North American Megadrought. J. Geophys. Res. Atmos. 123, 11,307-11,320. https://doi.org/10.1029/2018JD029323

Corbella, S., Stretch, D.D., 2013. Simulating a multivariate sea storm using Archimedean copulas. Coast. Eng. 76, 68–78. https://doi.org/10.1016/j.coastaleng.2013.01.011

Corder, G.W., Foreman, D.I., 2009. Nonparametric Statistics for Non-Statisticians. John Wiley & Sons, Inc., Hoboken, NJ, USA. https://doi.org/10.1002/9781118165881

Cordova, C.E., Porter, J.C., Lepper, K., Kalchgruber, R., Scott, G., 2005. Preliminary assessment of sand dune stability along a bioclimatic gradient, north-central and northwestern Oklahoma. Gt. Plains Res. 15, 227–49.

Cowles, H.C., 1899. The ecological relations of the vegetation on the sand dunes of Lake Michigan: Part I -Geographical relations of the dune floras. Bot. Gaz. 27, 95–117.

D'Antonio, C.M., Vitousek, P.M., 1992. Biological invasions by exotic grasses, the grass/fire cycle, and global change. Annu. Rev. Ecol. Syst. 63–87.

Davidson-Arnott, R., Hesp, P., Ollerhead, J., Walker, I., Bauer, B., Delgado-Fernandez, I., Smyth, T., 2018. Sediment budget controls on foredune height: Comparing simulation model results with field data. Earth Surf. Process. Landforms 43, 1798–1810. https://doi.org/10.1002/esp.4354

Dech, J.P., Maun, M.A., 2005. Zonation of vegetation along a burial gradient on the leeward slopes of Lake Huron sand dunes. Can. J. Bot. 83, 227–236. https://doi.org/10.1139/b04-163

Delcourt, H.R., Delcourt, P.A., 1996. Presettlement landscape heterogeneity: Evaluating grain of resolution using General Land Office Survey data. Landsc. Ecol. 11, 363–381.

Delgado-Fernandez, I., O'Keeffe, N., Davidson-Arnott, R.G.D., 2019. Natural and human controls on dune vegetation cover and disturbance. Sci. Total Environ. 672, 643–656. https://doi.org/10.1016/j.scitotenv.2019.03.494

Desai, A.R., Austin, J.A., Bennington, V., McKinley, G.A., 2009. Stronger winds over a large lake in response to weakening air-to-lake temperature gradient. Nat. Geosci. 2, 855–858. https://doi.org/10.1038/ngeo693

Dincer, T., Al-Mugrin, A., Zimmermann, U., 1974. Study of the infiltration and recharge through the sand dunes in arid zones with special reference to the stable isotopes and thermonuclear tritium. J. Hydrol. 23, 79–109. https://doi.org/10.1016/0022-1694(74)90025-0

Doing, H., 1985. Coastal fore-dune zonation and succession in various parts of the world. Vegetatio 61, 65–75.

Dow, K.W., 1937. The origin of perched dunes on the Manistee Moraine, Michigan. Mich. Acad. 23, 427–440.

Draper, N.R., Smith, H., 1998. Applied Regression Analysis, Third Edit. ed, Wiley Series in Probability and Statistics. John Wiley & Sons, New York. https://doi.org/10.1002/9781118625590

Duran, O., Moore, L.J., 2013. Vegetation controls on the maximum size of coastal dunes. Proc. Natl. Acad. Sci. 110, 17217–17222. https://doi.org/10.1073/pnas.1307580110

Durbin, J., Watson, G.S., 1951. Testing for Serial Correlation in Least Squares Regression. II. Biometrika 38, 159. https://doi.org/10.2307/2332325

Emery, S.M., Doran, P.J., Legge, J.T., Kleitch, M., Howard, S., 2013. Aboveground and belowground impacts following removal of the invasive species Baby's Breath (Gypsophila paniculata) on Lake Michigan sand dunes. Restor. Ecol. 21, 506–514. https://doi.org/10.1111/j.1526-100X.2012.00915.x

Emery, S.M., Gross, K.L., 2005. Effects of timing of prescribed fire on the demography of an invasive plant, spotted knapweed Centaurea maculosa. J. Appl. Ecol. 42, 60–69. https://doi.org/10.1111/j.1365-2664.2004.00990.x

Ezekiel, M., Fox, K.A., 1959. Methods of Correlation and Regression Analysis: Linear and Curvilinear, Third Edit. ed. John Wiley & Sons, New York.

Fryberger, S.G., Dean, G., 1979. Dune forms and wind regime. In: McKee, E. (Ed.), A Study of Global Sand Seas. USGS Professional Paper 1052. Washington, D.C.

Gardner, R., McLaren, S., 1999. Infiltration and moisture movement in coastal sand dunes, Studland, Dorset, U.K.: Preliminary results. J. Coast. Res. 15, 936–949.

Gates, F.C., 1950. The disappearing Sleeping Bear dune. Ecology 31, 386–392.

Gocic, M., Trajkovic, S., 2013. Analysis of changes in meteorological variables using Mann-Kendall and Sen's slope estimator statistical tests in Serbia. Glob. Planet. Change 100, 172–182. https://doi.org/10.1016/j.gloplacha.2012.10.014

Hall, F.C., 2001. Ground-based photographic monitoring. General Technical Report PNW-GTR-503. Portland, Ore.

Hansen, E., DeVries-Zimmerman, S., van Dijk, D., Yurk, B., 2009. Patterns of wind flow and aeolian deposition on a parabolic dune on the southeastern shore of Lake Michigan. Geomorphology 105, 147–157. https://doi.org/10.1016/j.geomorph.2007.12.012

Hansen, E.C., Arbogast, A.F., Yurk, B., 2004. The history of dune growth and migration along the southeastern shore of Lake Michigan: A perspective from Green Mountain Beach. Mich. Acad. 455–478.

Hansen, E.C., Fisher, T.G., Arbogast, A.F., Bateman, M.D., 2010. Geomorphic history of low-perched, transgressive dune complexes along the southeastern shore of Lake Michigan. Aeolian Res. 1, 111–127. https://doi.org/10.1016/j.aeolia.2009.08.001

Harley, M.D., Kinsela, M.A., Sánchez-García, E., Vos, K., 2019. Shoreline change mapping using crowd-sourced smartphone images. Coast. Eng. 150, 175–189. https://doi.org/10.1016/j.coastaleng.2019.04.003

Hattersley-Smith, G., 1966. The symposium on glacial mapping. Can. J. Earth Sci. 3, 737–741.

Hayes, L., Stocks, M., Blakers, A., 2021. Accurate long-term power generation model for offshore

wind farms in Europe using ERA5 reanalysis. Energy 229, 120603. https://doi.org/10.1016/j.energy.2021.120603

Helsel, D.R., Hirsch, R.M., 2002. Statistical methods in water resources. Techniques of water-resources investigations series 04-A3. Reston, Va. https://doi.org/10.3133/twri04A3

Hersbach, H., Bell, B., Berrisford, P., Biavati, G., Horányi, A., Muñoz Sabater, J., Nicolas, J., Peubey, C., Radu, R., Rozum, I., Schepers, D., Simmons, A., Soci, C., Dee, D., Thépaut, J.-N., 2018. ERA5 hourly data on single levels from 1979 to present, Copernicus Climate Change Service (C3S) Climate Data Store (CDS). https://doi.org/10.24381/cds.adbb2d47

Hesp, P., 2002. Foredunes and blowouts: Initiation, geomorphology and dynamics. Geomorphology 48, 245–268. https://doi.org/10.1016/S0169-555X(02)00184-8

Hesp, P.A., Hernández-Calvento, L., Gallego-Fernández, J.B., Miot da Silva, G., Hernández-Cordero, A.I., Ruz, M.-H., Romero, L.G., 2021. Nebkha or not? Climate control on foredune mode. J. Arid Environ. 187, 104444. https://doi.org/10.1016/j.jaridenv.2021.104444

Hugenholtz, C.H., Wolfe, S.A., 2005. Recent stabilization of active sand dunes on the Canadian prairies and relation to recent climate variations. Geomorphology 68, 131–147. https://doi.org/10.1016/j.geomorph.2004.04.009

Huggett, R., 2007. A history of the systems approach in geomorphology. Géomorphologie Reli. Process. Environ. 13, 145–158. https://doi.org/10.4000/geomorphologie.1031

Huggett, R.J., 2011. Fundamentals of Geomorphology, Third Edit. ed. Routledge, New York.

Hupy, C.M., Yansa, C.H., 2009. Late Holocene vegetation history of the forest tension zone in Central Lower Michigan, USA. Phys. Geogr. 30, 205–235. https://doi.org/10.2747/0272-3646.30.3.205

Indiana DNR, 2020. Great Lakes Water Level Table for Lake Michigan/Huron. Indianapolis, Ind.

Jackson, D.W.T., Costas, S., Guisado-Pintado, E., 2019. Large-scale transgressive coastal dune behaviour in Europe during the Little Ice Age. Glob. Planet. Change 175, 82–91. https://doi.org/10.1016/j.gloplacha.2019.02.003

Kendall, M.G., 1938. A new measure of rank correlation. Biometrika 30, 81–93.

Khamis, H., 2008. Measures of association: How to choose? J. Diagnostic Med. Sonogr. 24, 155–162. https://doi.org/10.1177/8756479308317006

Kilibarda, Z., Shillinglaw, C., 2015. A 70-year history of coastal dune migration and beach erosion along the southern shore of Lake Michigan. Aeolian Res. 17, 263–273. https://doi.org/10.1016/j.aeolia.2014.09.002

Kilibarda, Z., Venturelli, R., Goble, R., 2014. Late Holocene dune development and shift in dune-building winds along southern Lake Michigan, in: Coastline and Dune Evolution along the Great Lakes. Geological Society of America, pp. 47–64. https://doi.org/10.1130/2014.2508(04)

Kimball, B.A., 1983. Carbon dioxide and agricultural yield: An assemblage and analysis of 430 prior observations. Agron. J. 75, 779–788. https://doi.org/10.2134/agronj1983.00021962007500050014x

Klink, K., 2002. Trends and interannual variability of wind speed distributions in Minnesota. J. Clim. 15, 3311–3317. https://doi.org/10.1175/1520-0442(2002)015<3311:TAIVOW>2.0.CO;2

Kohek, Š., Strnad, D., Žalik, B., Kolmanič, S., 2017. Estimation of projection matrices from a sparse set of feature points for 3D tree reconstruction from multiple images. Period. Eng. Nat. Sci. 5. https://doi.org/10.21533/pen.v5i3.104

Kulkarni, A., von Storch, H., 1995. Monte Carlo experiments on the effect of serial correlation on the Mann-Kendall test of trend. Meteorol. Zeitschrift 4, 82–85.

Kull, C.A., 2005. Historical landscape repeat photography as a tool for land use change research. Nor. Geogr. Tidsskr. - Nor. J. Geogr. 59, 253–268. https://doi.org/10.1080/00291950500375443

Lancaster, N., 1988. Development of linear dunes in the southwestern Kalahari, Southern Africa. J. Arid Environ. 14, 233–244.

Lancaster, N., Helm, P., 2000. A test of a climatic index of dune mobility using measurements from the southwestern United States. Earth Surf. Process. Landforms 25, 197–207.

Lee, D.B., Ferdowsi, B., Jerolmack, D.J., 2019. The imprint of vegetation on desert dune dynamics. Geophys. Res. Lett. 46, 12041–12048. https://doi.org/10.1029/2019GL084177

Leege, L.M., Murphy, P.G., 2001. Ecological effects of the non-native Pinus nigra on sand dune communities. Can. J. Bot. 79, 429–437. https://doi.org/10.1139/cjb-79-4-429

Leege, L.M., Murphy, P.G., 2000. Growth of the non-native Pinus nigra in four habitats on the sand dunes of Lake Michigan. For. Ecol. Manage. 126, 191–200. https://doi.org/10.1016/S0378-1127(99)00085-7

Leimbach-Maus, H.B., McCluskey, E.M., Locher, A., Parks, S.R., Partridge, C.G., 2020. Genetic structure of invasive Baby's Breath (Gypsophila paniculata L.) populations in a Michigan dune system. Plants 9, 1123. https://doi.org/10.3390/plants9091123

Lepczyk, X.C., Arbogast, A.F., 2005. Geomorphic history of dunes at Petoskey State Park, Petoskey, Michigan. J. Coast. Res. 212, 231–241. https://doi.org/10.2112/02-043.1

Li, J., Liu, H., Su, Z., Fan, X., 2015. Changes in wind activity from 1957 to 2011 and their possible influence on aeolian desertification in northern China. J. Arid Land 7, 755–764. https://doi.org/10.1007/s40333-015-0050-z

Lichter, J., 2000. Colonization constraints during primary succession on coastal Lake Michigan sand dunes. J. Ecol. 88, 825–839.

Lichter, J., 1998. Primary succession and forest development on coastal Lake Michigan sand dunes. Ecol. Monogr. 68, 487. https://doi.org/10.2307/2657151

Loope, W.L., Arbogast, A.F., 2000. Dominance of an ~150-year cycle of sand-supply change in late Holocene dune-building along the eastern shore of Lake Michigan. Quat. Res. 54, 414–422. https://doi.org/10.1006/qres.2000.2168

Lovis, W.A., Arbogast, A.F., Monaghan, G.W., 2012. The Geoarchaeology of Lake Michigan Coastal Dunes. Michigan State University Press, East Lansing, Mich.

Manier, D.J., Laven, R.D., 2002. Changes in landscape patterns associated with the persistence of aspen (Populus tremuloides Michx.) on the western slope of the Rocky Mountains, Colorado. For. Ecol. Manage. 167, 263–284.

Manies, K.L., Mladenoff, D.., 2000. Testing methods to produce landscape-scale presettlement vegetation maps from the U.S. Public Land Survey records. Landsc. Ecol. 15, 741–754.

Mann, H.B., 1945. Nonparametric tests against trend. Econometrica 13, 245–259.

Mason, J.A., Swinehart, J.B., Lu, H., Miao, X., Cha, P., Zhou, Y., 2008. Limited change in dune mobility in response to a large decrease in wind power in semi-arid northern China since the 1970s. Geomorphology 102, 351–363. https://doi.org/10.1016/j.geomorph.2008.04.004

Mehta, B.K., Shiozawa, S., Nakano, M., 1994. Hydraulic properties of a sandy soil at low water contents. Soil Sci. 157, 208–214.

Millington, J.A., Booth, C.A., Fullen, M.A., Moore, G.M., Trueman, I.C., Worsley, A.T., Richardson, N., Baltrenaite, E., 2009. The role of long-term landscape photography as a tool in dune management. J. Environ. Eng. Landsc. Manag. 17, 253–260.

Muhs, D.R., Holliday, V.T., 1995. Evidence of active dune sand on the Great Plains in the 19th Century from accounts of early explorers. Quat. Res. 43, 198–208. https://doi.org/10.1006/qres.1995.1020

Muhs, D.R., Maat, P.B., 1993. The potential response of eolian sands to greenhouse warming and precipitation reduction on the Great Plains of the U.S.A. J. Arid Environ. 25, 351–361.

Nordstrom, K.F., 2015. Coastal dunes, in: Coastal Environments and Global Change. pp. 178–193. https://doi.org/10.1002/9781119117261.ch8

O'Geen, A.T., 2013. Soil water dynamics. Nat. Educ. Knowl. 4, 9.

Olson, J.S., 1958a. Lake Michigan dune development 1. Wind-velocity profiles. J. Geol. 66, 254–263.

Olson, J.S., 1958b. Lake Michigan dune development 2. Plants as agents and tools in geomorphology. J. Geol. 66, 345–351.

Olson, J.S., 1958c. Lake Michigan dune development 3. Lake-level, beach, and dune Oscillations. J. Geol. 66, 473–483.

PAGES 2k Consortium, 2013. Continental-scale temperature variability during the past two millennia. Nat. Geosci. 6, 339–346.

Pelletier, J.D., Mitasova, H., Harmon, R.S., Overton, M., 2009. The effects of interdune vegetation changes on eolian dune field evolution: a numerical-modeling case study at Jockey's Ridge, North Carolina, USA. Earth Surf. Process. Landforms 34, 1245–1254. https://doi.org/10.1002/esp.1809

Perry, G.L.W., 2002. Landscapes, space and equilibrium: Shifting viewpoints. Prog. Phys. Geogr. Earth Environ. 26, 339–359. https://doi.org/10.1191/0309133302pp341ra

Peterson, J., Dersch, E., 1981. guide to sand dune and coastal ecosystem functional relationships, Michigan State University Extension Bulletin EMICHU-SG-81-501. East Lansing, Mich.

Phillips, J.D., 2007. The perfect landscape. Geomorphology 84, 159–169. https://doi.org/10.1016/j.geomorph.2006.01.039

Pohlert, T., 2020a. Non-parametric trend tests and change-point detection [WWW Document]. URL https://cran.r-project.org/web/packages/trend/vignettes/trend.pdf (accessed 3.3.21).

Pohlert, T., 2020b. trend: Non-parametric trend tests and change-point detection.

Provoost, S., Jones, M.L.M., Edmondson, S.E., 2011. Changes in landscape and vegetation of coastal dunes in northwest Europe: a review. J. Coast. Conserv. 15, 207–226. https://doi.org/10.1007/s11852-009-0068-5

Puth, M.-T., Neuhäuser, M., Ruxton, G.D., 2015. Effective use of Spearman's and Kendall's correlation coefficients for association between two measured traits. Anim. Behav. 102, 77–84. https://doi.org/10.1016/j.anbehav.2015.01.010

Pye, K., Blott, S.J., Howe, M.A., 2014. Coastal dune stabilization in Wales and requirements for rejuvenation. J. Coast. Conserv. 18, 27–54.

Ratajczak, Z., Nippert, J.B., Ocheltree, T.W., 2014. Abrupt transition of mesic grassland to shrubland: evidence for thresholds, alternative attractors, and regime shifts. Ecology 95,

2633–2645.

Razavi, S., Vogel, R., 2018. Prewhitening of hydroclimatic time series? Implications for inferred change and variability across time scales. J. Hydrol. 557, 109–115. https://doi.org/10.1016/j.jhydrol.2017.11.053

Reyes, J., Elias, E., Haacker, E., Kremen, A., Parker, L., Rottler, C., 2020. Assessing agricultural risk management using historic crop insurance loss data over the ogallala aquifer. Agric. Water Manag. 232, 106000. https://doi.org/10.1016/j.agwat.2020.106000

Rodgers, S., O'Keeffe, N., Delgado-Fernandez, I., 2019. Factors affecting dune mobility in Newborough, Wales, in: Durán, R., Guillén, J., Simarro, G. (Eds.), X Jornadas de Geomorfología Litoral. pp. 129–132.

Rogers, G.F., Malde, H.E., Turner, R.M., 1984. Bibliography of Repeat Photography for Evaluating Landscape Change. University of Utah Press, Salt Lake City.

Ruggiero, P., Hacker, S., Seabloom, E., Zarnetske, P., 2018. The role of vegetation in determining dune morphology, exposure to sea-level rise, and storm-induced coastal hazards: A U.S. Pacific Northwest perspective, in: Barrier Dynamics and Response to Changing Climate. Springer International Publishing, Cham, pp. 337–361. https://doi.org/10.1007/978-3-319-68086-6_11

Salisbury, E., 1952. Downs & Dunes: Their Plant Life and Its Environment. G. Bell & Sons, Ltd., London.

Savin, N.E., White, K.J., 1977. The Durbin-Watson test for serial correlation with extreme sample sizes or many regressors. Econometrica 45, 1989. https://doi.org/10.2307/1914122

Schaetzl, R., Anderson, S., 2005. Soils: Genesis and Geomorphology. Cambridge University Press, New York.

Scheffer, M., Carpenter, Stephen R. Lenton, Timothy M. Bascompte, J., Brock, W., Dakos, V., van de Koppel, Johan van de Leemput, I.A., Levin, S.A., van Nes, E.H., Pascual, M., Vandermeer, J., 2012. Anticipating critical transitions. Science (80-.). 338, 344–348.

Schulte, L.A., Mladenoff, D.., 2001. The Original US Public Land Survey Records: Their Use and Limitations in Reconstructing Presettlement Vegetation. J. For. 99, 5–10.

Skidmore, E.L., 1974. A wind erosion equation: Development, application, and limitations, in: ERDA Symposi Urn Series 38, Atmosphere-Surface Exchange of Particul Ate and Gaseous Pollutants. pp. 452–465.

Smalley, I.J., 1970. Cohesion of soil particles and the intrinsic resistance of simple soil systems to wind erosion. J. Soil Sci. 21.

Smith, A.B., Jackson, D.W.T., Cooper, J.A.G., Hernández-Calvento, L., 2017. Quantifying the role of urbanization on airflow perturbations and dunefield evolution. Earth's Futur. 5, 520–539. https://doi.org/10.1002/2016EF000524

Somers, R.H., 1962. A similarity between Goodman and Kruskal's Tau and Kendall's Tau, with a partial interpretation of the latter. J. Am. Stat. Assoc. 57, 804–812.

Sperry, J.S., Venturas, M.D., Todd, H.N., Trugman, A.T., Anderegg, W.R.L., Wang, Y., Tai, X., 2019. The impact of rising CO 2 and acclimation on the response of US forests to global warming. Proc. Natl. Acad. Sci. 116, 25734–25744. https://doi.org/10.1073/pnas.1913072116

Szkornik, K., Gehrels, W.R., Murray, A.S., 2008. Aeolian sand movement and relative sea-level rise in Ho Bugt, western Denmark, during the `Little Ice Age'. The Holocene 18, 951–965. https://doi.org/10.1177/0959683608091800

Tabari, H., Hosseinzadeh Talaee, P., Shifteh Some'e, B., Willems, P., 2014. Possible influences of North Atlantic Oscillation on winter reference evapotranspiration in Iran. Glob. Planet. Change 117, 28–39. https://doi.org/10.1016/j.gloplacha.2014.03.006

Talbot, M.R., 1984. Late Pleistocene dune building and rainfall in the Sahel. Palaeoecol. Africa 16, 203–214.

Thompson, S.L., Govindasamy, B., Mirin, A., Caldeira, K., Delire, C., Milovich, J., Wickett, M., Erickson, D., 2004. Quantifying the effects of CO2-fertilized vegetation on future global climate and carbon dynamics. Geophys. Res. Lett. 31. https://doi.org/10.1029/2004GL021239

Thompson, T.A., Baedke, S.J., 1997. Strand-plain evidence for late Holocene lake-level variations in Lake Michigan. Geol. Soc. Am. Bull. 109, 666–682. https://doi.org/10.1130/0016-7606(1997)109<0666:SPEFLH>2.3.CO;2

Thompson, T.A., Lepper, K., Endres, A.L., Johnston, J.W., Baedke, S.J., Argyilan, E.P., Booth, R.K., Wilcox, D.A., 2011. Mid Holocene lake level and shoreline behavior during the Nipissing phase of the upper Great Lakes at Alpena, Michigan, USA. J. Great Lakes Res. 37, 567–576. https://doi.org/10.1016/j.jglr.2011.05.012

Thorn, C.E., Welford, M.R., 1994. The equilibrium concept in Geomorphology. Ann. Assoc. Am. Geogr. 84, 666–696.

Thornthwaite, C.W., 1948. An approach toward a rational classification of climate. Geogr. Rev. 38, 55–94.

Thornthwaite, C.W., 1931. The climates of North America: According to a new classification. Geogr. Rev. 21, 633–55.

Thornthwaite, C.W., Mather, J.R., 1957. Instructions and tables for computing potential evapotranspiration and the water balance. Publ. Climatol. X.

Tsoar, H., 2005. Sand dunes mobility and stability in relation to climate. Phys. A Stat. Mech. its Appl. 357, 50–56. https://doi.org/10.1016/j.physa.2005.05.067

Turner, M.G., Romme, W.H., Gardner, R.H., O'Neill, R. V., Kratz, T.K., 1993. A revised concept of landscape equilibrium: Disturbance and stability on scaled landscapes. Landsc. Ecol. 8, 213–227.

Vachaud, G., Passerat De Silans, A., Balabanis, P., Vauclin, M., 1985. Temporal stability of spatially measured soil water probability density function. Soil Sci. Soc. Am. J. 49, 822–828. https://doi.org/10.2136/sssaj1985.03615995004900040006x

van den Berg, L.J.L., Tomassen, H.B.M., Roelofs, J.G.M., Bobbink, R., 2005. Effects of nitrogen enrichment on coastal dune grassland: A mesocosm study. Environ. Pollut. 138, 77–85. https://doi.org/10.1016/j.envpol.2005.02.024

van den Berg, R.G., 2021. Kendall's Tau – Simple Introduction [WWW Document]. SPSS Tutorials. URL https://www.spss-tutorials.com/kendalls-tau/ (accessed 3.13.21).

van Dijk, D., 2014. Short- and long-term perspectives on the evolution of a Lake Michigan foredune, in: Coastline and Dune Evolution along the Great Lakes. Geological Society of America, pp. 195–216. https://doi.org/10.1130/2014.2508(11)

van Dijk, D., 2004. Contemporary geomorphic processes and change on Lake Michigan coastal dunes: an example from Hoffmaster State Park, Michigan. Mich. Acad. 35.

Van Oort, M.D., Arbogast, A.F., Hansen, E.C., Hansen, B., 2001. Geomorphological history of massive parabolic dunes, Van Buren State Park, Van Buren County, Michigan. Mich. Acad. 33.

Wang, T., Zlotnik, V.A., Wedin, D., Wally, K.D., 2008. Spatial trends in saturated hydraulic conductivity of vegetated dunes in the Nebraska Sand Hills: Effects of depth and topography. J. Hydrol. 349, 88–97. https://doi.org/10.1016/j.jhydrol.2007.10.027

Wang, Y., Zhang, J., Tong, S., Guo, E., 2017. Monitoring the trends of aeolian desertified lands based on time-series remote sensing data in the Horqin Sandy Land, China. Catena 157, 286–298. https://doi.org/10.1016/j.catena.2017.05.030

Warner, S., Jeffries, S., Lovis, W., Arbogast, A., Telewski, F., 2021. Tree ring-reconstructed late summer moisture conditions, 1546 to present, northern Lake Michigan, USA. Clim. Res. 83, 43–56. https://doi.org/10.3354/cr01637

White, R.A., Piraino, K., Shortridge, A., Arbogast, A.F., 2019. Measurement of vegetation change in critical dune sites along the eastern shores of Lake Michigan from 1938 to 2014 with

object-based image analysis. J. Coast. Res. 35, 842. https://doi.org/10.2112/jcoastres-d-17-00141.1

Wintle, A.G., Clarke, M.L., Musson, F.M., Orford, J.D., Devoy, R.J.N., 1998. Luminescence dating of recent dunes on Inch Spit, Dingle Bay, southwest Ireland. The Holocene 8, 331–339. https://doi.org/10.1191/095968398671791976

Yan, Z., Pang, L., Dong, S., 2020. Analysis of Extreme Wind Speed Estimates in the Northern South China Sea. J. Appl. Meteorol. Climatol. 59, 1625–1635. https://doi.org/10.1175/JAMC-D-20-0046.1

Yang, M.L., Rice, E., Leimbach-Maus, H., Partridge, C.G., 2019. Identification and characterization of Gypsophila paniculata color morphs in Sleeping Bear Dunes National Lakeshore, MI, USA. PeerJ 7, e7100. https://doi.org/10.7717/peerj.7100

Yizhaq, H., Ashkenazy, Y., Tsoar, H., 2007. Why do active and stabilized dunes coexist under the same climatic conditions? Phys. Rev. Lett. 98, 98–101. https://doi.org/10.1103/PhysRevLett.98.188001

Yue, S., Pilon, P., Cavadias, G., 2002a. Power of the Mann-Kendall and Spearman's rho tests for detecting monotonic trends in hydrological series. J. Hydrol. 259, 254–271.

Yue, S., Pilon, P., Phinney, B., Cavadias, G., 2002b. The influence of autocorrelation on the ability to detect trend in hydrological series. Hydrol. Process. 16, 1807–1829. https://doi.org/10.1002/hyp.1095

Zeileis, A., Hothorn, T., 2002. Diagnostic checking in regression relationships. R News 2, 7–10.

Zhu, Z., Piao, S., Myneni, R.B., Huang, M., Zeng, Z., Canadell, J.G., Ciais, P., Sitch, S., Friedlingstein, P., Arneth, A., Cao, C., Cheng, L., Kato, E., Koven, C., Li, Y., Lian, X., Liu, Y., Liu, R., Mao, J., Pan, Y., Peng, S., Peñuelas, J., Poulter, B., Pugh, T.A.M., Stocker, B.D., Viovy, N., Wang, X., Wang, Y., Xiao, Z., Yang, H., Zaehle, S., Zeng, N., 2016. Greening of the Earth and its drivers. Nat. Clim. Chang. 6, 791–795. https://doi.org/10.1038/nclimate3004

CHAPTER 3.
THE GEOGRAPHY AND PROGRESSION OF BLOWOUTS IN THE COASTAL DUNES ALONG THE EASTERN SHORE OF LAKE MICHIGAN SINCE 1938

Kevin G. McKeehan[a] and Alan F. Arbogast[a]

a: Department of Geography, Environment, and Spatial Sciences, Michigan State University, Geography Building, 673 Auditorium Rd, East Lansing, MI 48824, United States.
mckeeha2@msu.edu and dunes@msu.edu

3.1 Abstract

Coastal dunes are prominent features of the Lake Michigan shoreline, especially along the Lower Peninsula of Michigan. These dunes, perhaps the largest complex of freshwater coastal dunes in the world, comprise a unique coastal system because they developed under different conditions than marine dune systems elsewhere and without tectonic or tidal activity. Although the late-Holocene geomorphic evolution of Lake Michigan's dunes is well understood, less is known about the drivers of change in the modern period. For example, little is known about the evolution of blowouts in Lake Michigan's coastal dunes. These erosional features are common in coastal dunes elsewhere and are often key indicators of natural and anthropogenic disturbances. These disturbances, which can include changes in precipitation, temperature, or the introduction of a built environment, can destabilize existing dunes and cause blowout formation. The work we present here attempts to address this gap in knowledge. Here, we examine the blowouts of Lake Michigan's eastern shoreline and determine how they have evolved since the 1930s. We conducted a spatiotemporal analysis of ~200 blowouts by comparing repeat aerial images of the Lake Michigan coast beginning in 1938. Using an unsupervised classification known as iso-clustering, we mapped blowout morphologies from aerial images at three intervals – 1938, 1988, and 2018. We then compared the blowout geographies through a technique known as a spatial–temporal analysis of moving polygons (STAMP) model, which allowed us to analyze how

each individual blowout changes in time and space. Preliminary results show that since 1938 most blowouts are "healing" – or being stabilized through an expansion of vegetation. Moreover, we have not identified any new blowouts that have formed since 1938 along the ~500km shoreline or on any of the Lake Michigan islands. This suggests that the blowouts we have mapped could be artifacts of the drought conditions of the 1930s or perhaps the result of the stormier conditions during the Little Ice Age (1300–1900 CE) or earlier. Our preliminary findings comport with recent regional studies which showed an expansion of vegetation over the last ~100 years in Lake Michigan dunes, resulting in further stabilization of this sensitive landscape. Our findings also agree with studies in Europe that have shown a trend toward dune stabilization since the Little Ice Age.

Keywords: Coastal dunes, blowouts, dunes, Lake Michigan, geomorphology, aerial photography

3.2 Introduction

Coastal sand dunes adjoin much of the eastern shore of Lake Michigan and collectively comprise possibly the largest freshwater coastal dune system in the world (Peterson and Dersch, 1981) (Figure 1). A unique coastal system, dunefields line the shore for several kilometers along numerous parts of the coast and often extend up to a kilometer inland (Buckler, 1979). Some dunes exceed 50m in height and contain enormous volumes of sand (Arbogast et al., 2009). Unlike dune systems on marine coasts, Lake Michigan's coastal dunes developed without the influence of tectonic or tidal activity (Hansen et al., 2010). On the contrary, they are the product of many factors, but primarily are the result of the reworking of sandy glacial and lacustrine deposits in response to climatic and lake level variability (Hansen et al., 2010; Loope and Arbogast, 2000; Lovis et al., 2012; Thompson et al., 2011). The subsequent dune environments found in the eastern Lake Michigan basin are thus a subject of this variability, resulting in progradational or aggradational, regressive or transgressive aeolian landforms depending upon the geomorphological setting along the ~550km shoreline (Buckler, 1979; Kilibarda et al., 2014; Lepczyk and Arbogast, 2005; Lovis et al., 2012; Paskus and Enander, 2019; Wilson, 2001).

Dune building at many sites in the region, especially those toward the southern end of the lake basin, likely began ~5.5ka amidst an approximately 1,500-year period of elevated lake levels on ancestral Lake Michigan known collectively as the Nipissing transgressions (~6ka to 4.5ka) (Larsen, 1987; Lovis et al., 2012; Thompson et al., 2011). At the apex of the Nipissing transgressions was the Nipissing high stand, a period of maximum water height (Thompson et al., 2011). The high stand may have occurred as early as ~5.5ka (Lewis, 1969; Lovis et al., 2012; Petty et al., 1996) or as late as ~4.5ka (Baedke and Thompson, 2000; Fisher et al., 2012; Hansel and Mickelson, 1988; Larsen, 1987; Thompson et al., 2011; Thompson and Baedke, 1997). Regardless, the Nipissing high stand immediately proceeded a relatively sudden drop in lake levels, driven primarily by the effects of isostatic rebound on downstream lake outlets, after

which lake levels fluctuated near the modern mean (Baedke and Thompson, 2000; Bishop, 1990; Larsen, 1987; Lovis et al., 2012; Monaghan et al., 1986), although changes in regional climate may have played a role (Hansel and Mickelson, 1988; Petty et al., 1996).

Periods of aeolian activity on the eastern lakeshore continued thereafter, followed by brief intervals of dune stabilization (Arbogast et al., 2002; Blumer et al., 2012; Hansen et al., 2010, 2002; Kilibarda et al., 2014; Lepczyk and Arbogast, 2005; Lovis et al., 2012; Van Oort et al., 2001), although there exists some nonlinear spatiotemporal and geomorphological variability in dunefields between the northern and southern portions of the lakeshore (Fulop et al., 2019; Lovis et al., 2012). Several studies have identified periods of aeolian activity and stability since the embryonic stages of dune formation during the Nipissing transgressions. In their study of coastal dunes along the southern half of Lake Michigan's eastern shoreline, Hansen et al. (2010) identified six aeolian phases beginning from deglaciation through to present day, while Kilibarda et al. (2014) noted four phases of dune and coastal evolution on the southern reaches of Lake Michigan beginning at ~6ka. Lovis et al. (2012) detected a series of aeolian periods that varied in a spatiotemporal manner delineated primarily by the isostatic hinge line, north of which dunefields developed somewhat differently due to crustal rebound and other factors.

While different, all three studies also identified a pronounced late-Holocene episode of regional dune stability called the Holland Interlude, a period marked by vegetation expansion across the previously mobile coastal dunes. This period of stability resulted in the pedogenic formation of the Holland Paleosol, an Inceptisol present in dunes along Lake Michigan's southeastern coast (Arbogast et al., 2004; Hansen et al., 2006). The studies disagreed on the approximate dates of the so-called Holland Interlude, ranging ~3ka to ~0.5ka, but the studies overlapped for a period from ~1.6ka to 1ka (Hansen et al., 2010; Kilibarda et al., 2014; Lovis et al., 2012). Whatever the exact chronology, these distinct, identified aeolian phases were likely driven by a complex

system of climate and lake-level changes, which either increased or restricted the supply of sand. Recently, White et al. (2019) and McKeehan and Arbogast (2021) identified a modern trend toward dune stabilization along Lake Michigan's eastern shoreline by documenting the expansion of vegetation through an object-based analysis of aerial imagery and ground-level repeat photography, respectively. If true, these two findings could signal a new phase for the region's coastal dunefields (McKeehan and Arbogast, 2021; White et al., 2019), a phenomenon hinted at by Lovis et al. (2012, pg. 117), which notes a decreased sand supply in the regional coastal aeolian system over the last 500 years. Regional dune stabilization could also imply that a new regional mesoscale climate regime has begun to evolve across the Great Lakes (Yurk and Hansen, 2021). Thus, it is necessary to understand the trends and environments of Lake Michigan coastal dune systems, especially in regards to blowouts, which are aeolian landforms particularly attuned to climatic variability (Schwarz et al., 2018).

As Ritchie (1972, fig. 12) demonstrated, the aeolian conditions and landform morphologies in a given location are the product of a complex system at the nexus of interrelated terrestrial, atmospheric, and – in coastal areas – aquatic process (Schwarz et al., 2018). One of the "prime factors" controlling dune environments, according to Ritchie (1972), includes climate. An indicator of environmental and climatic conditions controlling aeolian landscapes – and thus the state of the complex geomorphic system outlined by Ritchie (1972) – are often the development, presence, and modes of dune blowouts (Hesp, 2002), possibly due to their "unique spatial and temporal patterns of change" (Dech et al., 2005). Blowouts are erosional depressions or troughs which have "blown out" through existing dunes due to natural or anthropogenic forcing (Bate and Ferguson, 1996; Hesp, 2002). The morphology of blowouts varies (Hesp and Hyde, 1996; Ritchie, 1972), as does the definition of the term "blowout" (Hesp and Hyde, 1996), but blowout landforms generally include a deflation basin from which sand is eroded, lateral erosional walls

which are often fixated at their crests by vegetation, and a downwind depositional lobe to which eroded sand is deposited (Adamson et al., 1988; Sloss et al., 2012).

Blowout initiation occurs due to an assortment of drivers, including wave and fluvial erosion, aeolian erosion from high velocity winds and the aerodynamic influences associated with the topographic acceleration of airflow over a dune crest, the density of dune vegetation and its effectiveness at geomorphic fixation, human and animal disturbance, storms, and changes in precipitation and temperature (Hesp, 2002; Hesp and Hyde, 1996; Jewell et al., 2017; Jungerius et al., 1981; Melton, 1940). Most of these blowout initiation factors are related to climate, although the mechanisms are likely more complex that a simple climate-blowout coupling, as coastal dunes are complex systems involving interrelated process-response relationships and evolutionary drivers operating at different spatiotemporal scales (Delgado-Fernandez, 2011; Walker et al., 2017). For example, coastal dunes along Lake Michigan are a function of the complicated interactions between lake levels, climate, wind, vegetation, and littoral and dune geomorphic processes (Cowles, 1899; Hansen et al., 2009; Loope and Arbogast, 2000; Olson, 1958a, 1958b, 1958c; van Dijk, 2014, 2004; Walker et al., 2017). Thus, changes in climate invariably affect the sensitive ecogeomorphic feedbacks and relationships determining dune behavior and blowout mode in any dunefield (Thom et al., 1994). This phenomenon potentially can be observed with Lake Michigan's coastal dunes, as the aforementioned White et al. (2019) and McKeehan and Arbogast (2021) papers suggest. Both studies observed an expansion in dune vegetation and, consequently, the geomorphic stabilization of some coastal dunes in the region, in the modern era (McKeehan and Arbogast, 2021; White et al., 2019), which roughly coincided with the end of the Little Ice Age (LIA). Both speculated that increases in precipitation in the last ~80 years was possibly driving the ecogeomorphic response observed across the landscape, although McKeehan and Arbogast (2021) also provided other process-response

explanations, including a non-linear ecogeomorphic lag from the drier conditions deeper back into the Holocene.

From a regional-scale perspective, dunefields might be considered a homogeneous environment consisting of similar sediment and mesoscale system process-responses, but dune features contain great variability in morphology, microenvironments, and vegetation (Carter, 1991; Loope and Arbogast, 2000; Mckenzie and Cooper, 2001). It is this variability, which Carter (1991) called the "natural heterogeneity" of dunes, which also contributes to blowout initiation. Dunes vary by height, width, steepness, sand grain size, vegetation coverage and diversity, pedogenic development, and geographic location within a dunefield (Cooper, 1958; Hack, 1941; Hesp et al., 2011; Mckenzie and Cooper, 2001; Melton, 1940). This results in what Phillips (2007) called the "heterogeneity of internal properties" which, when coupled with the "geographical and temporal variability of external forcings and controls" (Phillips, 2007), creates the conditions for blowout development in a dunefield, unless a uniform control is driving the response toward stabilization. Absent that control, concurrent blowout development, maintenance, and stabilization within a dunefield may be a natural condition (Dech et al., 2005). Ultimately, it is the ecogeomorphic interactions at the dune-scale, driven by climatic forcing, which create the impetus for blowout formation. In illustrating this point, blowouts and parabolic dunes were observed to be "wind in conflict with vegetation" by Melton (1940) in a seminal examination of Great Plains dunes, while Hack (1941) in describing coastal parabolic dunes described the geomorphic setting as "a contest between moving sand and vegetation". Aeolian and other erosional processes undertake at areas of vegetative and topographic vulnerability what Cooper (1958) called the "concentration of effective attack by wind at a point of weakness", resulting in the deflation of sand from the dune (Cooper, 1958; Schwarz et al., 2018), creating "wind-scoured gaps" (Bagnold, 1941; Hesp, 2002).

The effectiveness and consequence of the aeolian "attack" on a dune depends greatly upon the effective ecogeomorphic functionality of vegetation (Abhar et al., 2015; Cooper, 1958; Gares, 1992; Gares and Nordstrom, 1995; Lancaster and Baas, 1998; Lee et al., 2019; Miyanishi and Johnson, 2021; Nield and Baas, 2008; Ranwell, 1958; Schwarz et al., 2018). Weak, dead, or sparse vegetation may foster dune activation or blowouts (Schwarz et al., 2018). Moreover, the resultant blowout morphology post initiation is somewhat controlled by ecogeomorphic processes involving vegetation. For example, in Gares's (1992) study of two blowouts in coastal New Jersey, USA, vegetation coverage influenced blowout development and morphology by fostering downwind accretion along the stable rims of the blowout walls and constrained sand supply to the blowout basin by stabilizing a foredune at the throat of one blowout. Underscoring the interrelated ecogeomorphic processes at work in aeolian systems, the ample delivery of sand from the beach and foredune areas windward of blowout areas has many possible and varied outcomes (Laporte-Fauret et al., 2021; Miyanishi and Johnson, 2021; Schwarz et al., 2018).

This supply of sand could bury and destroy existing vegetation and hamper attempts by pioneering species to establish, or it could provide the conditions by which adaptive dune plant species can thrive, further fixating dunes (Brown and Zinnert, 2018; Cowles, 1899; Dech and Maun, 2005; Doing, 1985; Lane et al., 2008; Maun, 1998; Olson, 1958a). In general, sand supply is a key, dynamic variable controlling dunefield behavior and is related to beach width, active coastlines, dune morphology, and flow dynamics (Davidson-Arnott et al., 2018; Short and Hesp, 1982). Further, for several workers, sand supply is also key to blowout development, particularly how it is constrained or promulgated by interrelated ecogeomorphic and climatic factors at work in dune systems (e.g., Cooper, 1958). Ecogeomorphic feedback mechanisms also foster favorable edaphic conditions or hinder pedogenesis, thus either driving dune systems and blowouts toward stabilization regime or activation. Pioneering plant species on vegetated dunes,

for instance, are effective at deflecting and trapping airborne and saltating sediment, thus growing the foredune and enriching the soil in a positive ecogeomorphic feedback (Gardner and McLaren, 1999; Hesp, 1989, 1981; Maun, 1998; Ruggiero et al., 2018; Werner et al., 2011).

These interrelated ecogeomorphic processes, often in response to climatic and other disturbance forcings, also influence blowout morphology (Girardi and Davis, 2010; Schwarz et al., 2018), which influences and is influenced by subsequent flow dynamics within the blowout (Delgado-Fernandez et al., 2018; Fraser et al., 1998; Jungerius et al., 1981; Landsberg and Riley, 1943; Pease and Gares, 2013; Pluis, 1992; Smith et al., 2017). Schwarz et al. (2018) and Cooper (1958) both distilled blowout morphological types into the two primary forms: trough and saucer blowouts. Trough blowouts, as the name suggests, are characterized by a deep, elongated trench-like feature with high lateral walls, culminating in a depositional lope several meters high several meters downwind (Hesp, 2002). Melton (1940) stated that trough blowouts likely developed mostly in high-wind environments under unidirectional wind regimes. Additional geomorphic conditions for the development of trough blowouts include steep-sloped dunes and deep sandy substrata (Hesp, 2002; Luo et al., 2019). Unsurprisingly, trough morphologies have been associated with high-velocity aerodynamic jets (Hesp and Hyde, 1996). Lake Michigan's coastal dunes contain many trough blowouts, including several exceeding 100m in length. Saucer blowouts are perhaps less dramatic on the landscape, often occurring atop dunes or in environments with thin sand deposits and often appear as a "shallow dish" (Hesp, 2002). While trough blowouts often develop from strong onshore, unidirectional winds (Melton, 1940), saucer blowouts have been observed to be the product of winds perpendicular to blowout inception (Hails and Bennett, 1980). Hesp (2002) identified a third type of blowout morphology called cup blowouts, but noted that these often were saucer blowouts which evolved and deepened due to subsequent and continued erosion. In evaluating coastal dune blowouts in Scotland, Ritchie (1972)

identified five types of blowouts – cigar-shaped, V-shaped, scooped hollow, cauldron-and-corridor, and parabolic.

Ritchie's (1972) blowout classification schema might not be the most commonly utilized by aeolian workers, but it underscores Carter's (1991) "natural heterogeneity". The cigar- and V-shaped blowouts are variations on the trough blowout, distinguished by their topographic position and scale (Ritchie, 1972). Cigar-shaped blowouts were documented extending up the side of a dune ridge from its base, while V-shaped blowouts were slightly smaller and found adjacent to the beach perpendicular to the sea. Scooped hollows are similar to saucer blowouts, but the cauldron-and-corridor landform is a combination of both a trough and saucer, demonstrating the complexity and heterogeneity of the dunefield. Importantly for our study, Ritchie also classifies parabolic dunes as blowouts. Many workers prior to Ritchie (1972) and after have agreed that parabolic dunes, the classical U-shaped aeolian landform (Jennings, 1957; Landsberg, 1956), are either blowouts (Bagnold, 1941; Cooper, 1958; Hack, 1941; Hansen et al., 2009; Melton, 1940), inextricably related to blowouts (e.g., Girardi and Davis, 2010), or represent an evolutionary stage of a blowout (Jungerius et al., 1981; McCann and Byrne, 1994). A parabolic dune, Cooper (1958) stated, "is essentially a trough blowout." Bagnold (1941) viewed the entire parabola-blowout procession as a cycle in which a new dune was "born" downwind in the form a depositional lobe (Melton, 1940). We agree with these analyses and intend to include parabolic dune landforms in our assessment of Lake Michigan coastal blowouts.

In this paper, we attempt to identify all blowouts on the eastern shore of Lake Michigan with the USA state of Michigan, including those with parabolic morphologies in accordance with Cooper (1958) and others. We then conduct a series of spatiotemporal analyses to determine trends in blowout evolution. First, we utilized machine learning tools to map blowout extent using repeat aerial photography at separate timestamps – 1938, 1986-8, and 2018. Then, in a manner

similar to Abhar et al. (2015) in their study of coastal dune blowouts on Cape Cod, we employed an object-based image analysis technique known as a Spatial–Temporal Analysis of Moving Polygons (STAMP) model to assess whether blowouts expanded, migrated, stabilized, or fragmented. By examining the trends in blowout behavior since 1938, we can potentially determine if the dune stabilization trends observed by White et al. (2019) and McKeehan and Arbogast (2021) extend to these landforms, which are geomorphic markers born in response to climatic and ecogeomorphic forcing. In discussing our results, we also ascribe possible drivers of the observed blowout trends and the implications form Lake Michigan's dune systems.

3.3 Methodologies

3.3.1 Aerial Imagery

The time series geomorphic analysis of sand dunes often employs repeat aerial imagery (e.g., Abhar et al., 2015; Belford et al., 2014; Jungerius and van der Meulen, 1989; White et al., 2019) and remote sensing, which in general is an integral tool within the field of aeolian geomorphology (Bryant and Baddock, 2021). For our purposes, blowouts along Lake Michigan's eastern shore, including on islands in the northern part of the lake, were identified and their extent mapped by examining three sets of aerial imagery representing three distinct timestamps – 1938, 1986-8, and 2018 (Table 1). Aerial imagery from 1938 was captured by the U.S. Department of Agriculture (USDA) as part of New Deal efforts to develop scientifically-driven conservation and land use planning program and track their progress (Monmonier, 2002). Images from the same dataset were used by White et al. (2019) in their study of coastal dunes in Michigan state parks. A similar dataset was used recently to identify and interpret archaeological agricultural features in Wisconsin across Lake Michigan (McLeester and Casana, 2021). We obtained hundreds of 1938 aerial images of Lake Michigan coastal dune areas from

Michigan State University's Remote Sensing and GIS Aerial Imagery Archive. These images are black and white (BW) panchromatic with a scale of 1:20,000 and spatial resolution of ~0.8m after being georeferenced.

Aerial imagery for 1986-8 were obtained from the U.S. Geological Survey (USGS) from its National High Altitude Photography (NHAP) program dataset, a dataset sometimes used for mid-1980s landscape analyses (Rango et al., 2008). For areas along the southern portions of the lakeshore, NHAP BW images from 1988 with a scale of 1:80,000 were used (EROS, 2018a), while farther north, no suitable NHAP images for the year 1988 were available. Thus, we used NHAP images from 1986 for analysis of these areas, which included the Leelanau Peninsula. Occasionally, BW images were also not available and NHAP color infrared (CIR) aerial photographs with a 1:58,000 scale were used instead. The spatial resolution of all NHAP imagery post-georeferencing was ~6m. Studies have employed NHAP aerial imagery to conduct analysis of forest stand landscapes (e.g., Goldmann, 1990) and evaluate land use land cover (LULC) change over time (Drummond et al., 2019) amongst other analyses. For 2018 images, we used aerial photography from the National Agricultural Imagery Program (NAIP) dataset (EROS, 2018b). The NAIP dataset imagery is captured by the USDA during the growing season, with a spatial resolution of ~0.6m and three spectral natural color bands: red, green, and blue. In similar studies, he scale has been reported to be 1:20,000 (e.g., Abhar et al., 2015). The NAIP dataset, which was also obtained through the USGS, contains the highest spatial resolution amongst the three sets of imagery.

3.3.2 Blowout Mapping

All blowout mapping tasks, with the exception of STAMP model analyses, utilized ArcGIS 10.7 software (ESRI, Redlands, CA, 2021). Imagery from the 1938 USDA and NHAP datasets required georeferencing and the NAIP dataset was used a base reference in this task. Ground

control points (GCPs) visible on images at all three periods were used to effectuate the rubbersheeting during the georeferencing process. The establishment of GCPs was often challenging, as shorelines and dunefields in the Lake Michigan basin are dynamic environments subject to geomorphological changes (Theuerkauf et al., 2021). In more developed areas, landmarks, lighthouses, and static street intersections amongst other built environment infrastructure were used as GCPs, while in less developed areas GCPs were often sentinel trees, country crossroads, and old barns. Almost all georeferencing attempts required either second-order and third-order polynomial transformations. The target total Root Mean Square Error (RMSE) for each georectification was <5m and was often <1m (Table 1), especially for the 1938 aerial images as they covered smaller, though irregular, geographic areas (~4000m x 4000m). By contrast, each NHAP image comprises a 7.5-minute USGS quadrangle (EROS, 2018a).

The location of blowouts features were identified by examining the breadth of the shoreline within each aerial imagery dataset, informed by various Michigan dune databases and reports (e.g., Arbogast et al., 2020; Buckler, 1979; Paskus and Enander, 2019). However, the most influential guide to blowout identification was the Michigan Coastal Dune geodatabase created by Michigan State University researchers and managed by the Michigan Department of Natural Resources (DNR) (Arbogast et al., 2018). This GIS data resource contained the polygonal extent of 93,249 hectares (230,423 acres) of coastal dunes within the state of Michigan, although it did not delineate blowouts (Arbogast et al., 2018). Blowout-like features on aerial images well outside the spatial extent of the Michigan Coastal Dune GIS data were not flagged for mapping and were ignored in our workflow. By relying on these reports and datasets, it is possible that we have committed Type I (commission) and Type II (omission) errors during this identification process. When in conflict, however, we sought to lower the instances omission error rather than commission error. For example, as we stated in the Introduction section, we classified parabolic

dunes as blowouts for this analysis. Moreover, we feel the inclusion in this study of parabolic dunes and some other transgressive dune landforms which exhibit blowout behavior is geomorphically sound and follows the approaches taken by other studies (e.g., Cooper, 1958; Melton, 1940). This methodology also follows the approach of Buckler's 1979 mapping study of Lake Michigan's coastal dunes, which termed parabolic dunes "central extensions" of blowouts. While we counted parabolic dunes and other transgressive dune features as blowouts, each site needed to meet criteria in order for inclusion in the study. While Jungerius et al. (1981) noted that classic scour blowout morphology begins to manifest itself upon the landscape after initiation once the deflation basin reaches 5m in length, such an identification criterion for this study would be impossible give the spatial resolution and uncertainty of our data. Therefore, we employed a criterion noted in Hesp's (2002) survey, which noted that a 1:1 morphodynamic relationship between the length of a blowout's deflation basin and its depositional lobe begins at ~20m of deflation length. Smaller blowouts do not to appear share this morphodynamic relationship and, thus, call into question whether they could be accurately and consistently identified in air photos. Consequently, we adopted the 20m deflation basin length as an identification criterion, while allowing for some blowouts to be included which were slightly smaller if they could be positively deduced in our investigation.

The spatial extent of the blowouts we identified was then generated for each of the three timestamps of our spatiotemporal analysis. To accomplish this, we used machine learning (ML) techniques to map the blowout boundary by detecting bare sand in a way which minimized human bias. We first degraded the 1938 and 2018 aerial images to match the relatively coarser spatial resolution of the NHAP dataset by resampling those photographs in ArcGIS using the bilinear interpolation method. In a time series analysis of landscapes, it is considered best practice to resampling finer-resolution raster datasets to match the coarsest resolution dataset

(Campbell, 1996, p. 577). To not resample the higher-quality imagery would inject an additional vector of error into the time series analysis by comparing maps which "differ greatly in detail in accuracy" (Campbell, 1996, p. 577). After resampling, we selected an unsupervised ML algorithm known as the Iterative Self-Organizing Data Analysis Technique (ISODATA) method. The ISODATA classification method is often used in landscape analyses (e.g., Lemenkova, 2021), including in analyses of coastal environments (Tojo and Udo, 2018), due to its efficiency in processing large remote sensing datasets without the need for supervised training samples (Ma et al., 2020). Moreover, unsupervised ML methods, including the ISODATA algorithm, "offer the promise of objective anomaly assignment" (Kvamme et al., 2019), thus potentially reducing the bias of the authors to guide these procedures (Campbell, 1996, p. 318).

In a manner similar to Belford et al.'s (2014) time series analysis of three Lake Michigan coastal dunes using repeat aerial imagery, our process sought to leverage the contrast between the high albedo of bare dune sand with the relatively lower albedo of vegetated dunes. As the ISODATA ML algorithm effectuates its classification of an image by clustering pixels into statistically alike bins, we expected that a high-albedo bare sand cluster would naturally emerge separately amid a large lake, mid-latitude temperate forests, and other vegetation and built structures. The ISODATA method runs multiple iterations, regrouping pixels into possible bins, recalculating their means, and assessing the effects on pixel organization before statistically determining pixel classification (Abbas et al., 2016; Campbell, 1996, p. 337; Ma et al., 2020). After ArcGIS generated a rasterized pixel cluster of bare sand at a blowout location, we converted the blowout raster to a vector polygon. Some feature editing was necessary to separate the blowout throat (entrance) from Lake Michigan's beach foreshore, as this is usually not classified as part of a dune blowout. From this, we were able to create a geospatial inventory of Lake Michigan's eastern shore coastal dune blowouts at three timestamps since 1938. We also calculated each

blowout's physical area, upwind orientation, and calculated the amount of dune lost to human development, where applicable.

Assessing the accuracy and uncertainty of aerial image analyses of the environment is difficult given the numerous vectors for error and lack of uniform standards in aerial imagery analyses (Lunetta et al., 1991), especially in dynamic coastal areas (Moore, 2000). Within our workflow, potential sources of error included the horizonal accuracy of the original photographs, the georeferencing process for the 1938 and 1986-8 aerial images, the resampling of 1938 and 2018 aerial imagery, the ISODATA bare sand classification process, and the conversion of the ISODATA rasterized results to vector polygons (Abhar et al., 2015; Congalton, 1997; Lunetta et al., 1991; Mathew et al., 2010; Moore, 2000). In addition to calculating the RMSE associated with the georeferencing process (see above), we estimated uncertainty (Table 1). Somewhat similar to Mathew et al. (2010) and Abhar et al. (2015), we calculated uncertainty by adding the published horizonal error from each air photo dataset, the RMSE generated after georeferencing, and estimated delineation error from resampling and vectorization. Our uncertainty values are in line with those reported by Mathew et al. (2010) and Abhar et al. (2015) and in most cases are within 1m. This approach was undertaken as our focus was on bare sand identification and changes in blowout morphology. As this study did not seek to classify entire landscapes into land cover groups and sought only to identify bare sand, we did not calculate the error matrix typically associate with remote sensing classification analyses (Foody, 2002). As such, we did not assess classification accuracy or generate user and producer error statistics.

To determine if blowouts in 1938 differs statistically from blowouts in 2018, we used a Wilcoxon signed-ranks test. This test is the nonparametric equivalent of the paired samples *t*-test and was selected because we assumed the distribution of blowout size for both timestamps would be nonnormative (Corder and Foreman, 2009; Wilcoxon, 1945). The Wilcoxon signed-ranks test

was designed to compare a set of two paired samples of data to determine if significant differences exist between the sets. To do this, the absolute value in the difference between the values of each pair – in this case the blowout size in square meters for 1938 and 2018 – is calculated, then assigned ranks based upon the absolute value (Corder and Foreman, 2009). The sign difference is recorded, then all the number of positive ranks (ΣR_+) and negative ranks (ΣR_-) are summed separately (Corder and Foreman, 2009). The smaller of ΣR_+ and ΣR_- is the *T*-statistic, which is then fed into a formula to calculate the *Z*-statistic, a commonly used metric in trend analyses (Corder and Foreman, 2009; Gocic and Trajkovic, 2013):

$$Z = \frac{T - \bar{x}_T}{S_T} \tag{1}$$

where $\bar{x}_T$ is the mean of the *T*-statistic and S_T is its standard deviation. In terms of aeolian geomorphology research, the Wilcoxon signed-ranks test was used recently in a study of soil differences in coastal sand dunes, although the specific *Z*-statistic results were not divulged (Lopez et al., 2020). While the *Z*-statistic is also an output in the Mann-Kendall trend analysis tests, it is less frequently reported as an indicator of trend than Kendall's τ_b, even though it is easier to interpret (McKeehan and Arbogast, 2021). We calculated the *Z*-statistic from the Wilcoxon signed-ranks test for blowout sizes using the Two-Related Samples tool in IBM SPSS Statistics 27 (IBM Corp., 2020). In order than direct anthropogenic activity not influence the statistical analysis, we removed from the Wilcoxon signed-ranks test all blowouts where human development contributed to blowout loss. We also removed all blowouts from the test that had any missing data for either 1938, 1986-8, or 2018. Typically, the null hypothesis for a Wilcoxon signed-

ranks test is that no differences exist between the 1938 and 2018 blowout sizes; our research hypothesis, however, was otherwise.

3.3.3 STAMP Model

While time series analyses of dune behavior using repeat aerial imagery is relatively common in aeolian geomorphology, the manner in which landscape change is assessed often diverges amongst studies. Researchers used edge tracing over multiple images to study dune migration in Indiana on Lake Michigan southern shore (Kilibarda and Shillinglaw, 2015), GIS edge detection methods for three dunes near Holland in Michigan (Belford et al., 2014), remote sensing surface classifications in France (Rapinel et al., 2014), and an object-oriented approach at Cape Cod (Abhar et al., 2015), amongst other techniques. Here, we utilized an object-based image analysis technique advanced by Abhar et al. (2015) in their study of coastal dune blowouts on Cape Cod in Massachusetts (USA). They employed a STAMP model, or a spatial–temporal analysis of moving polygons, a process first proposed by Sadahiro and Umemura (2001) and codified into a model by Robertson et al. (2007). A STAMP model attempts to measure and classify the spatial changes in objects over time by quantifying their topologies and movements (Robertson et al., 2007; Sadahiro and Umemura, 2001). Changes are measured quantitatively as the difference between T_1 and T_2 timestamps and the change is then classified into categories, including "expansion", "stable", and "contraction" (Figure 2). From this, landform changes over time can be described. For our study, the STAMP model evaluated two types of time-transgressive events: 1) changes in 2-D blowout morphology between 1938 and 1986-8 and 2) changes in 2-D blowout morphology between 1986-8 and 2018, together of which we predict will yield possible mesoscale blowout behavioral trends, including possible blowout fragmentation. To run the STAMP model for all identified blowout locations, we utilized the R software package stampr (Long et al., 2018).

Alongside the STAMP analysis, we also evaluated a series of metrics often associated with fractal geography in an effort to determine blowout polygonal complexity as an additional indicator of fragmentation. We first calculated the area-to-perimeter ratio of Lake Michigan dune blowouts. Often used in ecological habitat studies (e.g., Helzer and Jelinski, 1999) and remote sensing analyses (e.g., Salas et al., 2003), the area-to-perimeter (*A:P*) ratio of polygons can also inform trends and complexity in geomorphic phenomena (Cheng, 1995; De Cola and Lam, 1993; Gao and Xia, 1996; Goodchild and Mark, 1987; Kent and Wong, 1982; Woronow, 1981). Here, we interpret a time-series analysis of the raw *A:P* ratios for regional blowouts can be an indication for trends in landscape complexity and geomorphic fragmentation, as an increasing perimeter length for features of similar area would constitute a higher fractal complexity. The calculation of a polygonal *A:P* ratio also can involve the determination of the natural logarithmic values for both *A* and *P* in an effort to analyze the fractal dimension of landscapes, a metric often used in geomorphic analyses (Gao and Xia, 1996; Phillips, 1993). While there is some evidence that fractal dimension comparisons offer limited geomorphic value (Gao and Xia, 1996), we calculated both the fractal dimension (*D*) and ratio of *ln(A):ln(P)*, which is required to determine the former per both Gao and Xia (1996) and Kent and Wong (1982).

3.4 Results

3.4.1 Blowout Identification and Characteristics

As the result of our analysis, we identified 435 blowout features along Lake Michigan's eastern shore and islands in 1938 (Figure 3, Table 2). Blowouts were located on six islands: South Manitou, North Manitou, South Fox, North Fox, High, and Beaver islands. Active blowouts accounted for at least ~19.1M m^2 or ~4,700 acres in 1938, according to our analysis. By 2018, that number dropped to ~12M m^2 or ~3,000 acres, consisting of a loss of >7.1M m^2 or 1,700 acres since 1938, a decline of ~37%. Dune blowouts, however, represent a tiny proportion of

the study area's total aeolian landscape. Blowouts in 2018 accounted for just 2.9% of the ~102,500 acres of dunes along the eastern shore of Lake Michigan, based upon overall dunefield totals from the statewide dune database compiled as part of the Arbogast et al. (2018) study.

Spatially, Lake Michigan's coastal dunes have been differentiated between dunefields north and south of the isostatic hinge line, which cuts across the lakeshore near Arcadia in northern Manistee County (Larsen, 1987; Lovis et al., 2012). Generally, north of the hinge line, large, perched dune complexes and progradational systems in embayments are more common as ongoing isostatic rebound has a great influence on coastal and aeolian processes, while south of the hinge line, coasts are isostatically stable and dunes are influenced more by lake level fluctuations (Lovis et al., 2012). Using this geomorphically-driven spatial division of the lakeshore, there are 166 blowouts south of the hinge line and 269 blowouts in the isostatically active north. According to a volumetric analysis of the dunefields in the study area, less than half of the shoreline's dune sand is north of the hinge line at Arcadia (Arbogast et al., 2009). Yet, the coastal regions north of Arcadia contain ~62% of the blowouts. Conversely, blowouts in the south lost more area overall (~1,300 acres) and per blowout (~8 acres/site) than blowouts in the north (~400 acres total, ~1.5 acres/site), despite having fewer blowouts. Spatially, Leelanau County, north of the hinge line and home to Sleeping Bear Dunes National Lakeshore, contains the largest number of blowouts with 116. Benzie County, just north of the hinge line and south of Leelanau County, has 90 blowouts, the second-highest total.

Some blowouts have disappeared. In 1938, Lake Michigan's eastern shore and islands had 435 blowouts, but 37 of those had disappeared completely by 2018. Of those 37 blowouts, 35 disappeared due to human development, the extend of which was measured as well. In all, 55 blowouts or 12.6% of all 1938 blowouts shrank in size partially or completely due to human

development, primarily the construction of residential structures. Development accounted for a decrease of ~1.4M m^2 or ~350 acres in blowout extent between 1938 and 2018. Ottawa County lost by far the largest amount of blowout areas to development since 1938, losing ~870,000 m^2 or ~215 acres along its ~40km long coast. This loss in Ottawa County is >50% of all blowout extent lost to human development in our study. While declines attributed to direct anthropogenic causes were an important component of blowout loss since 1938, most blowouts decreased in area due to the expansion of vegetation. In total, 368 blowouts, or 85% of all blowouts, contracted in size or disappeared from 1938 to 2018. Not all blowouts declined in size or disappeared, however; 53 blowouts expanded since 1938, some greatly. The largest expansion in blowout size occurred in a Benzie County blowout in Crystal Lake Township off George Street; it grew quadrupled in size over the 80-year time series analysis. There was insufficient data for 14 blowouts to determine whether they expanded or contracted in size during the period in question. Regarding our analysis of blowouts at the 1986-8 timestamp, we determined that blowouts had contracted at a higher rate over those ~50 years since 1938 (~25 acres/yr) than in the 30-year period between 1988 and 2018 (~16 acres/yr), although we lacked data for 35 sites for the 1986-8 timestamp.

These changes in blowout extend from 1938 to 2018 were significant. According to the results of the Wilcoxon signed-ranks test, the differences in blowout extent between 1938 and 2018 are statistically real (Table 3). The Z-statistic value of -13.526 well exceeded the critical threshold signifying differences between the two years. The Z-statistic is straightforward in its interpretation, as the null hypothesis is rejected if $Z > \pm 1.96$ at the 5% significance level (Gocic and Trajkovic, 2013). Moreover, the sum of the negative ranks exceeded the positive ranks by a factor of 10, a condition which could be interpreted as a strong negative trend in blowout extent (Corder and Foreman, 2009).

Also importantly, we found no new blowouts since 1938, except small anthropogenically driven blowout-like features at a handful of sites that occurred due to human attempts at landscaping. These were not mapped or analyzed. No relationship was found between magnitude of loss/gain in blowout extent and 1938 blowout size. Both saucer and trough blowouts were found along the shore, but trough blowouts were more prominent (Table 4). However, the distribution of blowout type may be explained by geomorphic position. For example, several saucer blowouts were located on embayments, especially in the north (e.g., Platte Bay area). Most dunes are oriented perpendicular to the shore, with westerly orientations most common (Figure 4, Table 2).

3.4.2 STAMP Model

Fragmenting blowouts, examples of which can be seen in Figures 5 and 6, were observed in all sections of the shoreline through our analysis of the aerial images. Furthermore, the STAMP model determined that most blowouts, except those which had disappeared, both contracted and expanded into new polygons, which can be interpreted per Robertson et al. (2007) partly as "fragmentation". Moreover, "contraction" as measured by the STAMP model was roughly twice the expansion of blowouts in 1986-8 and 2018 (Figure 7) (Long et al., 2018). Setting aside the photographic evidence from our aerial imagery analysis, it would be unlikely that blowout contraction as measured by the STAMP model took place merely at the polygonal boundaries of blowouts given the 2:1 ratio of contraction to expansion. Instead, blowout fragmentation must have taken place to some degree within the previous extent of blowout polygons. This interpretation is supported by the further analysis of area-to-perimeter ratios and fractal dimension metrics we calculated (Figure 8). An analysis of the area-to-perimeter ratio of blowout polygons shows the metric decreased from 1938 to 2018, as did the *lnA:lnP* ratio and fractal dimension (Figure 8) even as total blowout extent declined. However, area-to-perimeter ratios and the associated metrics did rise from 1938 to 1986-8 before declining, leading to similar questions of interpretation, scale, and methodology as raised by Gao and Xia (1996). In

addition to blowout extent, the STAMP model also calculated the direction of blowout expansion, if any occurred. The results showed some blowouts expanded downwind, even if the overall area of the blowout had decreased by 2018, while others prograded. There was no overall pattern of progression either leeward or windward.

3.5 Discussion

Our results show that blowouts along the eastern shore of Lake Michigan mostly have contracted in size since 1938, the starting point of our spatiotemporal analysis. Further, no new significant blowouts were detected at either the 1986-8 or 2018 timestamps, other than a handful of incidents tied directly to attempts at landscaping and terraforming windward of lakefront properties. This fits a broad, global trend toward dune stabilization as observed in other studies (e.g., Gao et al., 2020), including the trend of vegetation expansion in European coastal dunes since 1900 (Jackson et al., 2019; Provoost et al., 2011). Instead of expansion, most existing blowouts are not only contracting, but fragmenting, according to our analysis. Part of this broad reduction in blowout extent is the fragmentation of the bare sand areas of most blowouts, especially in the deflation basin, per the STAMP model results. Two questions emerge from these findings: First, what processes are driving this response by vegetation and blowouts? And second, if modern conditions are not conductive to blowout generation and expansion beyond the typical downwind expression of deflated sand onto the depositional lobe, then under what conditions did Lake Michigan's coastal dune blowouts form?

Regarding the process-response formulation that is driving blowout fragmentation, our findings suggest that either sand supply has diminished, vegetation growth has accelerated beyond the threshold at which incoming sand can suppress it, or some combination of both processes. Lovis et al. (2012) speculated that the sand supply for Lake Michigan's coastal dunes had decreased in

the last 500 years. Sand supply to coastal dunes can be fostered or constrained by several interrelated variables, including those related to lake levels and wind. High levels on Lake Michigan are related to dune activity and increased sand supply, according to several studies (Anderton and Loope, 1995; Dow, 1937; Loope and Arbogast, 2000; Lovis et al., 2012; Olson, 1958b). Mechanically, erosion of bluff sediment, beaches, and the amount of foredune sand increases during periods of high lake levels, according to this model. Increased erosion feeds more sand into the coastal system, making it available for entrainment downwind into the dune system once onto the foreshore (Pye, 1983). The active transport of deflating or saltating sand through the dune system hampers vegetative growth and stimulates additional aeolian activity through landscape destabilization. Under these conditions in this model, the rate and manner of shoreline and beach retreat often are coupled with the rate of inland active dune migration, a geomorphic system state termed "beach negative; dune steady" by Sherman and Bauer (1993).

Yet, evidence also suggests the contrary. Nearshore, foreshore, and dune zones are coupled in complex ways which vary spatially and temporally, creating multiple possible disequilibrium and steady states (Sherman and Bauer, 1993). Importantly for this study, foreshore morphology, which is influenced by nearshore processes such as waves, swash, and longshore action (Salisbury, 1952; Short, 2012; Short and Hesp, 1982), impacts the amount of sand supplied to the dune zone (Sherman and Bauer, 1993; van Dijk, 2004). Wide beaches, such as those possibly resulting from low levels on Lake Michigan, are associated with dissipative, yet high-energy environments (Short and Hesp, 1982). Wide beaches create the conditions for the increased deposition of sediment upon the foreshore and then the increased potential landward transport of sand due to the relatively longer fetch across the beach (Bauer and Davidson-Arnott, 2003; Davidson-Arnott, 1988; Delgado-Fernandez, 2010; Hesp and Smyth, 2016; Nordstrom, 2015; Sherman and Bauer, 1993; Short and Hesp, 1982). In an extensive study of coastal dunes at a state park in

Michigan, van Dijk (2004) found that foredune growth occurred between 2000-2003 during a period of low lake levels and wide beaches at the study area. Foredune growth did curtail sand supply to a dune rim downwind that was associated with a blowout (van Dijk, 2004), but such a circumstance seems to support the innate complexity of the process-response and ecogeomorphic mechanisms in coastal dune systems (Sherman and Bauer, 1993; Walker et al., 2017). Rather than drive all geomorphological components of the aeolian system at the state park into the same state, lower lake levels caused one response at the foredunes and another in the backdunes (van Dijk, 2004), underscoring Carter's (1991) "natural heterogeneity" in dunefields and the type of cycling dune churn or reworking described elsewhere (e.g., Black, 1951; Dech et al., 2005), or even a state of "bistability" (e.g., Yizhaq et al., 2007).

Therefore, lake levels on Lake Michigan seem unlikely to be the primary driver of blowout state as outlined in our study. Both dune activity models involving lake levels are likely correct at any given time, but neither is predominant now. Over the course of our 80-year spatiotemporal study, lake levels on Lake Michigan fluctuated a great deal at high frequency on roughly annual and decadal cycles around the modern mean (Baedke and Thompson, 2000; Bishop, 1990; Indiana DNR, 2020; Watras et al., 2014). There have been periods of both below- and above-average lake levels (Theuerkauf et al., 2021), reflecting the monthly, seasonal, annual, ~30-year, ~150-year, and other cycles observed by workers (Quinn, 2002; Thompson and Baedke, 1997; Watras et al., 2014). Moreover, since 2013, lake levels have been historically high (Indiana DNR, 2020; Theuerkauf et al., 2021). Yet, while lake levels fluctuate, no broad related trends exist that can explain blowout fragmentation or the lack of new blowouts. In other words, as Lake Michigan levels continues to cycle and change, albeit within a smaller range (Quinn, 2002), regional-scale blowout behavior has apparently decoupled – if it was ever coupled -- from lake

behavior and continued to trend toward fragmentation and stabilization at the impetus of vegetation expansion. Thus, other drivers must be more influential.

An additional possible driver of decreased sand supply is a reduction in wind power. Some studies place wind power, or wind energy, at the forefront of dune behavior (e.g., Tsoar, 2005), but other studies find it has less influence in aeolian landscapes than anticipated (e.g., Mason et al., 2008). Regardless, in coastal dunefields, a geomorphic function of wind includes transporting sand landward from the foreshore, a process involving a series of boundary layer adjustments (Walker et al., 2017). Deflating and saltating sand – and the winds compelling these aeolian processes – interact with foreshore and dune topography, developing complex steering patterns and affecting dune surfaces and vegetation, amongst other features (Arens, 1996; Bauer et al., 2012; Pluis, 1992). As stated earlier, winds also can induce dune blowouts and guide their morphology (Cooper, 1958; Hesp, 2002; Melton, 1940; Schwarz et al., 2018). There is some evidence that wind energy may have declined as much as 40% along the eastern shoreline since 1960 (Yurk and Hansen, 2021), although there is also evidence that mean annual wind speed, drift potential, and other dune mobility indices, such as Lancaster's *M* (Lancaster and Helm, 2000), remained relatively unchanged over a similar period of time or declined slightly (McKeehan and Arbogast, 2021). Likewise, there is evidence that winds over various decadal time periods have recently decreased globally (McVicar et al., 2012; Tian et al., 2019; Vautard et al., 2010), increased globally (Zeng et al., 2019), increased over oceans, but decreased terrestrially (Zeng et al., 2018), been mixed globally (Torralba et al., 2017), gotten stronger across Lake Superior to the north of our study area (Desai et al., 2009), gotten weaker across Minnesota to the northwest (Klink, 2002), and been mixed regionally (Torralba et al., 2017). In other words, no clear pattern with regards to wind energy has emerged yet in the Lake Michigan basin or anywhere else. Moreover, wind data, whether from reanalysis or observational datasets, are

often hampered by issues of completeness, error, and uncertainty (Julian, 1983; Morone, 1986; Torralba et al., 2017; Yin et al., 2021) and likely should employed with caution. Given this mixed bag of results, it is difficult to proclaim with certainty a loss of wind energy across the study area, or by extension a reduction in sand supply as a result, although it might be a factor.

A third factor in a potential regional reduction in sand supply is precipitation, which is identified in Delgado-Fernandez et al.'s (2019) dune vegetation model as a key driver, along with other related variables. Other dune behavior models have also identified the amount of precipitation in aeolian systems as important controls on dune vegetation (e.g., Ashkenazy et al., 2012). Precipitation performs several ecogeomorphic functions in aeolian systems. Moist dune sand surfaces can increase the shear wind velocity threshold by which sand deflates, dampening aeolian erosion (Cornelis and Gabriels, 2003; Han et al., 2011; Pluis, 1992). Precipitation in the form of ice and snow has a chilling effect on wind erosion, as well (Doing, 1985; van Dijk, 2014, 2004). On the other hand, falling precipitation can also stimulate additional sand supply through splash erosion, which is the process by which sediment grains are knocked loose from the dune crust and made available for later wind entrainment (Jungerius and van der Meulen, 1988; Riksen and Goossens, 2007). Like most dune processes, even the splash erosion process is entangled with other variables in feedback mechanisms and process-response frameworks. For instance, the effectiveness of splash erosion on dunefield sand supply depends upon the density of dune vegetation. If annual precipitation increases, effectiveness of splash erosion might increase temporarily until soil moisture reaches a threshold at which vegetation coverage might increase as well, which then in turn limits the effectiveness of splash erosion to affect sand supply.

Regardless, this description of splash erosion alludes to the main ecogeomorphic function of precipitation – the conduction of water into the sandy soil medium. As Tsoar (2005) noted about many aeolian environments, precipitation is not an important factor determining dune state due to

the high hydraulic conductivity of sand. This "singular physical characteristics of the sandy soil" is the rapid delivery of water through the soil profile to the water table (Tsoar, 2005). Sand lacks the cohesion to hold water within its pores, as the space between grains is relatively large (Dincer et al., 1974; Salisbury, 1952; Schaetzl and Anderson, 2005; Tsoar, 2005). Thus, gravimetric soil water content is <5% near the surface in both arid and humid sand dune soils (Bar Kutiel et al., 2016). In other words, sand in a desert environment responds in a similar fashion to water as coastal dune sand along Lake Michigan's eastern shoreline, a Udic soil moisture regime where precipitation is greater than potential evapotranspiration (PET) and dry conditions are rare (Schaetzl and Anderson, 2005).

Yet, if the amount of water supplied to a sand medium increases, pore spaces will become filled and moisture can be held, suggesting that each sandy soil may possess a threshold in the vadose zone by which water can made available to plants (Gardner and McLaren, 1999; Sala et al., 1988). Relatively large increases in precipitation over time can have an accompanying, rapid response in vegetative growth in sandy soils (Ashkenazy et al., 2012; Sala et al., 1988). This process potentially sets in motion a series of ecogeomorphic feedback mechanisms. For example, dune sand soils holding more soil moisture due to an increase in annual precipitation and the expansion of vegetation may demonstrate "temporal persistence" in soil moisture storage, according to the theory of the temporal stability of soil moisture (*TS SM*) (Vachaud et al., 1985; Wang et al., 2008). Persistently moist dune blowout soil may thus stay so, adjusted only for the needs of vegetation (Bar Kutiel et al., 2016). Further perpetuating these feedback mechanisms, organic matter and finer-grained particles are added to the soil as the consequence of the growth of vegetation (Shay et al., 2000). This phenomenon was observed in a study of Lake Huron dunes, where field capacity of water was higher on vegetated back dunes than on younger foredunes (Baldwin and Maun, 1983). Importantly, vegetation is a notable control of blowout

behavior. Upwind of the blowout and within the blowout itself, vegetation can constrain sand supply to the blowout, essentially denying it nourishment. This is the scenario described by Cooper (1958) and observed by Gares (1992). In a study of two dissimilar blowouts along New Jersey's coastline, Gares (1992) observed that vegetation had established itself in the throat of a blowout and had become the focal point for sand deposition, possibly growing into a foredune structure. This resulted in a "positive feedback that exists between vegetation growth and newly deposited sediment" (Gares, 1992). A similar observation was made at a blowout in our study area near Petosky, where a foredune vegetated with *Arctostaphylos uva-ursi* (bearberry) and *Prunus pumila* (sand cherry) starved a downwind blowout (Lepczyk and Arbogast, 2005).

Two recent studies have implied that vegetation growth in Lake Michigan's coastal dunes may be possibly ascribed to an increase in annual precipitation, amongst other possibilities (McKeehan and Arbogast, 2021; White et al., 2019). Annual precipitation increased ~180mm since 1940 at two regional weather stations – South Bend and Muskegon – along the southern and central portions of the lakeshore since 1940, but only modestly in the north at Traverse City (McKeehan and Arbogast, 2021). PET, too, increased since 1940, but was still less than precipitation (McKeehan and Arbogast, 2021). Yet, a statistical analysis found these precipitation trends to be only moderately positive with respect to the southern and central coast. Thus, while an increase in annual precipitation is a possible driver of blowout contraction and fragmentation, especially given the rapid response of sandy soils to a sustained increase in water, we cannot be certain it is the primary process causing stabilization in the dune system. Instead, it is likely that multiple factors are at work, likely enmeshed in complex process-response relationships and ecogeomorphic feedback mechanisms (Delgado-Fernandez et al., 2019; Schwarz et al., 2018). As we have mentioned, nearshore, beach, dune, and blowout processes in coastal systems are coupled through a number of interrelated variables that produce different state outcomes in

response to process stimuli, the results of which feedback recursively throughout the system, changing the process-response relationships across different spatiotemporal scales (Castelle et al., 2019; Delgado-Fernandez et al., 2019; Schwarz et al., 2018; Sherman and Bauer, 1993; Walker et al., 2017). A process-response framework of dune systems has been detailed previously in different ways in recent years (e.g., Ashkenazy et al., 2012; Delgado-Fernandez et al., 2019). Any understanding of the stabilization response by Lake Michigan coastal dunes must acknowledge a complex process-response framework, especially in the absence of a singular strong process driver trending toward obvious stabilization responses. After all, there are other potential drivers at work in the region, including increased atmospheric concentration of CO2 through anthropogenic means, atmospheric nitrogen deposition from anthropogenic means, land use changes, fire suppression, or the growth of invasive species, all of which are discussed in McKeehan and Arbogast (2021) and Yurk et al. (2021).

Given the regional scale of blowout response, the most likely driver or drivers of stabilization is uniform. Such drivers would likely be operating at the meso and macro spatiotemporal scales, influencing local controls and feedbacks throughout the dune system, resulting in variability and heterogeneity of dune conditions at landform and short temporal scales. When approaching questions of Lake Michigan coastal dune response, it may be helpful to think in terms of systems and states, despite some criticism of the ideas of landscape steady state or equilibrium (Huggett, 2007, 2011; Thorn and Welford, 1994). This theoretical approach does have merit if the landscape system process-response scales and components are understood (Turner et al., 1993). For example, Sherman and Bauer (1993) developed a scheme that sought to classification nine types of beach-dune coupling and their associated ecogeomorphic environments, a framework that has been examined in other studies (Davidson-Arnott et al., 2018; Walker et al., 2017).

Currently, much of our study area would be classified as "beach negative; dune positive" under this classification scheme, where high lake levels have encroached upon the beaches and made them less dissipative (Sherman and Bauer, 1993). At the same time, dune vegetation, which is expanding, is trapping sediment that would ordinarily be transported landward through the dune system, storing sediment, and creating a positive sediment budget. While compartmentalizing process-response environments might seem counterintuitive given the chaotic nature of outcomes in geomorphic systems (Phillips, 2007, 2006), these theoretic structures do provide the investigatory framework to begin detangling the complex ecogeomorphic feedbacks and mechanisms operating along Lake Michigan's eastern shoreline. As a start, we can state that Lake Michigan coastal dune systems might be 1) driven toward a steady, vegetated state since deeper in the Holocene, 2) driven between alternative states based upon which processes are dominant at a given scale, 3) in non-equilibrium due to a new process paradigm, or 4) responding chaotically to the same process stimuli (Huggett, 2011; Phillips, 2007). Next-step research needs to be designed with these geomorphic possibilities in mind.

One possible conceptual blowout model advanced here which incorporates this approach acknowledges three primary phenomenon – increased precipitation, fluctuating lake levels, and a trend toward "stillness", as Zeng et al. (2018) termed decreasing winds over land. Briefly, this model postulates that the moderate rise in annual precipitation has increased soil moisture across the study area and provided the pretext for the growth of pioneering plant species, specifically the species that do not require dune sand burial, but are adapted to aeolian landscapes, such as *Populus deltoides* (Eastern Cottonwood). Increased moisture also dampens aeolian transport of sediment and fosters vegetation on foredunes, a critical ecogeomorphic marker for this model. Concurrently, during high lake level periods, transgressive lake action erodes some foredunes and bluffs, making sand available to the coastal dune system upon its eventual deposition onto the

foreshore, if it is not lost offshore. Upon lower lake levels, the beach becomes dissipative, as under Short and Hesp's (1982) model. Longer fetch and higher energy allow for the more efficient transport of sand from the foreshore into the backshore areas, stimulating foredune growth through the ecogeomorphic capture of sediment, which creates a topographic barrier and blocks sand supply to downwind blowouts, especially in an environment of diminished wind power. Vegetation which has pioneered the blowout deflation basin thrives in the relatively high-precipitation, low-sand supply environment, enriching the soil through mutual feedback mechanisms and promoting additional vegetation growth. When transgressive lake behaviors return, the resultant high-stand foredune is somewhat eroded, partially removing the topographic barrier to the blowout and allowing for more sand to be supplied from the foreshore into the backdune areas. Any bare or patchy sand receives additional sand supply; species adapted to sand burial, such as *Ammophila arenaria* (marram grass) withstand this period and even bank seeds in the sand (Maun, 1998). Other fast-growing species, such as cottonwood trees, have grown fast enough to outpace the rate of sand burial and survive. As lake levels fluctuate, the cycle begins again. A myriad of variables at the landform-scale, such as topographic position, local dune geomorphology, and human disturbance, amongst other factors control some interactions and affect the overall state of blowouts in the dunefield.

If this represents a possible model to explain blowout contraction in the modern period, then under what conditions were blowouts along the eastern shore of Lake Michigan initiated and maintained, if current conditions largely are unfavorable for blowouts? There is some evidence that blowouts at the southern end of Lake Michigan at Indiana Dunes National Lakeshore originated during humid and cool periods (Kilibarda, 2018), although these observations were from foredune blowouts initiated by transgressive lake actions and storms. These blowouts then healed during subsequent low lake levels due to foredune growth, a similar mechanism observed

by van Dijk (2004), suggesting an ephemeral temporal aspect to the observed blowouts in that study (Kilibarda, 2018). Our study did not detect these transitory blowouts, likely due to the relatively longer temporal design of our study. Yet, it is worth noting that blowouts were observed forming at the southern end of the lake during a time of high water levels, relatively higher humidity, and cool temperatures (Kilibarda, 2018). The most recent global cooling event was the Little Ice Age (LIA), a period roughly dated from ~0.1ka to ~0.7ka (Nordstrom, 2015). The LIA was a period of episodic dune activity in Europe (Jackson et al., 2019; Provoost et al., 2011) and a period of cool, dry, and possibly erosive conditions around the Great Lakes (Colman et al., 2000; Hupy and Yansa, 2009; Warner et al., 2021), although lake levels appear to be at or slightly above modern levels (Baedke and Thompson, 2000).

Could large, transgressive blowouts seen across the eastern shore of Lake Michigan be artifacts from the LIA? It is possible, although it can be difficult to ascribe geomorphic events to specific climatic periods, especially since aeolian systems in general (Werner et al., 2011; Wright and Thom, 1977), and Lake Michigan's coastal systems in particular (Lovis et al., 2012; McKeehan and Arbogast, 2021), can exhibit lagged responses to forcing. Still, OSL dates taken specifically from parabolic dunes and blowouts along the eastern shore of Lake Michigan show some dates from the LIA. Fulop et al. (2019) reported one OSL date of 0.43ka $\pm$ 0.05 from a parabolic dune at Green Point, while Lovis et al. (2012) reported a date of 0.62–0.76ka at a blowout known as Mt. McSauba near Charlevoix. There is a scattering of other similar OSL dates associated with the LIA, but their association with parabolic dunes or blowouts is unclear.

More dates exist linking dune, and possible blowout, activity to the Medieval Climate Optimum (MCO) (1.2ka to 0.7ka), the Roman Climate Optimum (RCO) (~2.3ka to 1.6ka), and the Holocene Climate Optimum (HCO) (MIS 1). The oldest of these climatic intervals was the HCO, which in North America was the apogee of the mid-Holocene Northgrippian Age, a warm and dry period

defined as ~8.2ka to ~4.2ka (Schaney et al., 2021) and sometimes referred to as the Hypsithermal (Warner et al., 2021). Yet, the effects of the HCO were possibly regionally nonlinear, as some evidence suggests a cooling period commenced across portions of the continent at ~5.5ka (Shuman and Marsicek, 2016) and that Great Lakes snowbelts began forming around the region by ~5ka (Henne and Hu, 2010). The HCO, which coincided with the Nipissing transgressions, was the period of origin for Lake Michigan's coastal dunes (Hansen et al., 2010). As previously mentioned, periods of aeolian activity on the eastern lakeshore continued thereafter. For example, Hansen et al. (2010) identifies the Algoma period from 3.3ka to 1.6ka as an era of large parabolic dune formation; the latter half of the Algoma period aligns roughly with the RCO, an event associated with dune activity and fires in the western North America (Weppner et al., 2013), active dunes at Cape Cod (Forman, 2015), and drought on the Texas Gulf Coast (Livsey et al., 2016). Moreover, pollen-based reconstructions of annual precipitation found the Great Lakes region was likely drier than normal during portions of the RCO (Ladd et al., 2018), although, again, it is important to note that climate periods such as the RCO exhibit high geographic variability (Neukom et al., 2019).

Other evidence exists causally linking dune activity with the three drier warm periods since the mid-Holocene – the MCO, RCO, and HCO. Three studies representing spatial variation along the lakeshore reported dates each for the MCO, RCO, and HCO (Fulop et al., 2019; Hansen et al., 2010; Lepczyk and Arbogast, 2005), while two studies recorded parabolic dune and blowout OSL dates across the LIA, MCO, RCO, and HCO (Kilibarda et al., 2014; Lovis et al., 2012). Further, the findings by Lovis et al. (2012) and Kilibarda et al. (2014) seem to confirm that dunes were at least somewhat active during portions of the MCO, a global warming anomaly (Hunt, 2006) that was a time of megadroughts on the Great Plains and southwestern United States (Cook et al., 2016; Halfen and Johnson, 2013), dune activity at Cape Cod (Forman, 2015). Even

the Holland Interlude, a period of stabilization, can be roughly aligned with a climatic event. If we accept that despite the great variability in the dating of the Holland paleosol, we should acknowledge three important studies dating the event overlap for a period from ~1.6ka to 1ka (Hansen et al., 2010; Kilibarda et al., 2014; Lovis et al., 2012). These dating mostly coincide with the cool and wet period in North America known as the Dark Ages Cold Period (DACP) (~1.6ka to 1.2ka) (Helama et al., 2017), providing an additional potential data point linking Lake Michigan coastal dunes to climate variability.

Unfortunately, interpreting OSL dates from other studies and applying them to speculatory models of blowout behavior is difficult. Those studies were not designed with the goals of specifically establishing a theory of blowout development, nor do they provide a comprehensive picture of dunefield mode for the given time of activity or stability, keeping in mind Carter's (1991) "natural heterogeneity" and Yizhaq et al.'s (2007) "bistability". Yet, these studies provide a baseline for our knowledge. According to these OSL dates, there was dune activity at parabolic dune and blowout sites beginning at the HCO and in every other global warm period since then, including the RCO and MCO, with the exception of the current, anthropogenically-driven warming period, which began in the late 1800s (Ruddiman, 2014, p. 391). There is some, but less, evidence for blowout activity in the LIA. It is possible that large blowouts have formed, or at least been active and maintained, during all four climate events. Or it is possible that the ultimate spark for the large number of large, transgressive blowouts is the MCO, RCO, or HCO. Regardless, it is clear that many blowouts mapped in our study are relicts of the premodern environment and that some type of ecogeomorphic lag is underway in blowout response to late Holocene conditions.

To resolve these questions, we propose new research on two tracks. First, to better understand why blowouts are healing, we propose that efforts be made to discern which components of the

process-response mechanisms are driving stabilization. New research should involve longitudinal studies in the field of key indicator blowouts to understand geomorphic changes and drivers. Such research should attempt to determine regional blowout soil moisture thresholds, the process by which blowouts are vegetated, the impact on CO2 and N on dune plants, how foredune growth affects blowout sand supply and fragmentation, how blowouts respond to human activity, especially in their deflation basins, amongst other component processes in the Lake Michigan dunes. With regards to blowout geneses and the ecogeomorphic lag between initiation and fragmentation, we propose an intentional effort to date blowouts beginnings, perhaps by concentrating on the depositional lobes of large trough blowouts. The effort should feature spatial variability along the length of the lakeshore above and below the hinge line. Both research tracks are pertinent given the growing population of the region, economic value of the area, and the important dune ecosystems present (Arbogast et al., 2020, 2018; Harman and Arbogast, 2004; Schrotenboer and Arbogast, 2010). After all, while blowouts are currently stabilizing under vegetation, aeolian environments can experience rapid changes in short periods of time and are rarely stable for long (Delgado-Fernandez et al., 2018; Miyanishi and Johnson, 2021; Smith et al., 2017).

3.6 Conclusions

In this time-series study, we mapped 435 dune blowouts along the eastern shore of Lake Michigan using repeat aerial photography, machine learning tools, and a STAMP model to quantify blowout behavior at three temporal periods. From 1938 to 2018, no new blowouts formed along the entire lakeshore. In addition, blowout extent decreased ~37%, primarily due to an expansion of vegetation, although human development played a significant role, while the STAMP model suggested that blowouts were not merely shrinking, but fragmenting. This study confirmed the findings of White et al. (2019) and McKeehan and Arbogast (2021) that found coastal dunes

in the study area were stabilizing while vegetation was expanding over previous bare sand. The processes driving this response by blowouts are unclear, but could be a series of interrelated factors which stimulate ecogeomorphic feedbacks. An increase in annual precipitation, lake level fluctuations, and a decrease in wind power may be affecting dune blowouts in complex ways at different spatiotemporal scales to drive stabilization. Further, as no new blowouts were detected in our study, we speculated that the conditions which initiated blowout formation have apparently not occurred in the modern period and that blowouts in the study area may be geomorphic artifacts from climatic eras different than now, such as the Little Ice Age, Medieval Warm Period, Roman Climatic Optimum, and the Holocene Climatic Optimum. We also called for further research along two tracks to resolve these questions. Specifically, we proposed research into the process-response mechanisms which are driving blowout stabilization, while also exploring blowout origins.

APPENDIX

Figure 3.1: Overview map of eastern Lake Michigan dunefields.

Table 3.1: Spatial characteristics and uncertainty for aerial image datasets used in this study. Sources for this information include White et al. (2019), Abhar et al. (2015), EROS (2018a,b). Loosely based on Mathew et al. (2010) and Abhar et al. (2015), uncertainty is estimated as the sum of the published horizontal accuracy, average RMSE from georeferencing, and 1, which represents the potential error from resampling and vectorization.

Year	***Source***	***Scale***	***Spatial Extent***	***Pixel resolution (m)***	***Horizontal Accuracy (m)***	***Average Georeferencing RMSE (m)***	***Total Estimated Uncertainty (m)***
1938 (BW)	USDA	1:20,000	~4000m x 4000m	~0.8	-	~1m	~2m
1986-8 (BW)	NHAP	1:80,000	7.5-minute USGS quadrangle	~6	-	~3m	~4m
*1986-8 (CIR)**	NHAP	1:58,000	7.5-minute USGS quadrangle	~6	-	~2m	~3m
2018 (Color)	NAIP	1:20,000	3.75 x 3.75-minute USGS quarter quadrangle	~0.6	~1	-	~2m

Event type (stamp name)	Description	T_1	T_2	$T_1 U T_2$
Unchanged (stable)	Area of T_2 polygon that remains the same as T_1 polygon			
Contraction	Polygon contracts in area from T_1 to T_2			
Extension (expansion)	Polygon in extends in area from T_1 to T_2			

Figure 3.2: STAMP Model event types used in our analysis, modified from Abhar et al. (2015).

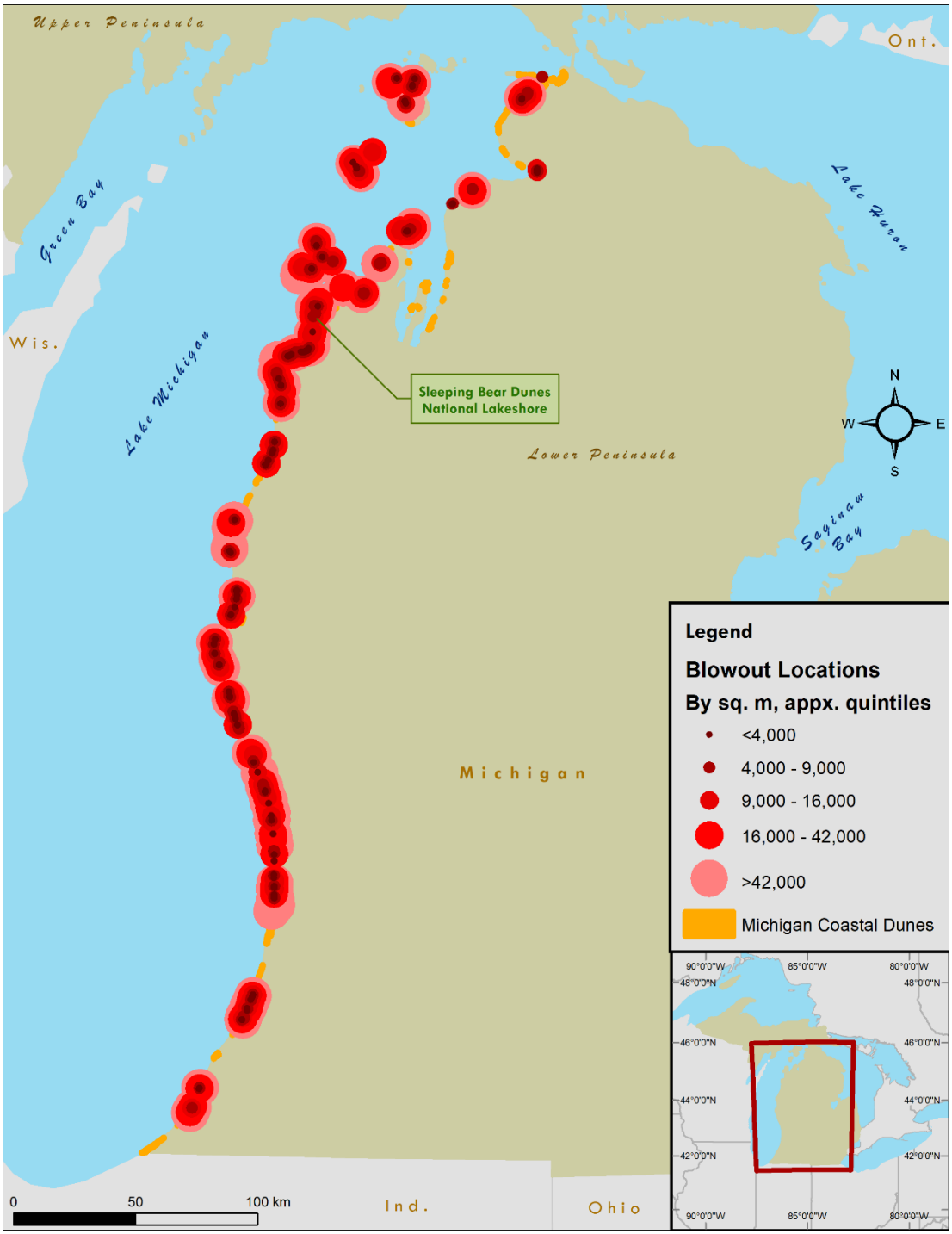

Figure 3.3: Blowout mapping results. Locations with 1938 spatial extent.

Table 3.2: Blowout mapping results, organized geographically north to south. Note – Some 1938 data are missing for Manistee County and, thus, the percentage change over time in blowout extent and the computation of the loss due to human development there cannot be calculated completely. Some scattered totals may be incomplete for 1986-8 for this reason, too.

County	Blowouts	Total Blowout Extent *(sq. m.) (x1000)*			Percentage Change in Extent			Blowout Loss Due to Human Development			Mean Orientation
		1938	1986-8	2018	1938 to 1986-8	1986-8 to 2018	1938 to 2018	Extent Loss *(sq. m.) (x1000)*	% of total loss	% of 1938 extent	
North of hinge line											
Emmet	31	616.2	472.2	353.6	-23.4%	-25.1%	-42.6%	61.7	23.4%	10.0%	W
Charlevoix	32	547.2	464.4	366.1	-15.1%	-21.2%	-33.1%	2.0	1.1%	0.4%	WSW
Leelanau	116	5,233.7	4,034.0	4,312.0	-22.9%	+ 6.9%	-17.6%	0	0%	0%	WSW
Benzie	90	1,778.5	1,096.6	1,445.2	-38.3%	+31.8%	-18.7%	0	0%	0%	W
South of hinge line											
Manistee	10	87.7	78.7	89.3	-10.3%	13.5%	+ 1.8%	18.0*	N/A*	N/A*	WNW
Mason	18	1,461.3	626.5	585.0	-57.1%	- 6.6%	-60.0%	329.2	37.6%	22.5%	W
Oceana	23	923.4	638.8	432.1	-30.8%	-32.4%	-53.2%	15.4	3.1%	1.7%	W
Muskegon	34	1,114.1	854.8	639.4	-23.3%	-25.2%	-42.6%	0	0%	0%	WSW
Ottawa	35	2,325.1	1,261.0	766.9	-45.8%	-39.2%	-67.0%	872.7	56.0%	37.5%	W
Allegan	16	3,290.3	3,048.1	1,890.4	- 7.4%	-38.0%	-42.5%	33.4	2.4%	1.0%	W
Van Buren	18	489.3	481.8	222.2	- 1.5%	-53.9%	-54.6%	12.9	4.8%	2.6%	WNW
Berrien	12	1,278.2	860.4	904.8	-32.7%	+5.2%	-29.2%	79.2	21.2%	6.2%	WNW
Total	435	19,145.0	13,917.4	12,007.0	-27.3%	-13.7%	-37.3%	1,424.5	20.0%	7.4%	WNW

Table 3.3: Results of the Wilcoxon signed-ranks test. The null hypothesis is rejected if $Z > \pm 1.96$ at the 5% significance level (Gocic and Trajkovic, 2013). Thus, significant differences exist in the blowout extent from 1938 to 2018.

	n	**Mean (m^2)**	**Std. Dev.**			**n**	**Sum of Ranks ΣR_+ or ΣR_-**		**T-statistic**	**Z-statistic**	**p-value (2-tailed)**
1938 Blowout Extent	366	42,874.8	116,442.4		Negative Ranks	314	60,977		6,184	-13.526	<0.001
2018 Blowout Extent	366	27,122.9	74,119.0		Positive Ranks	52	6,184				

Table 3.4: Blowout morphology by type and county. The complex category represents blowout sites exhibiting both trough and saucer morphologies or locations which transited between morphologies since 1938. Some of these "complex" sites could best be categorized as fitting Ritchie's (1972) "cauldron and corridor" morphology.

County	Total Blowouts	Trough	Saucer	Complex	Other / Undetermined
North of hinge line					
Emmet	31	18	7	4	2
Charlevoix	32	22	10	0	0
Leelanau	116	95	11	9	1
Benzie	90	54	27	7	2
South of hinge line					
Manistee	10	4	6	0	0
Mason	18	14	2	0	2
Oceana	23	12	9	2	0
Muskegon	34	24	8	0	2
Ottawa	35	22	8	5	0
Allegan	16	12	3	1	0
Van Buren	18	9	6	3	0
Berrien	12	7	3	2	0
Total	435	293	100	33	9

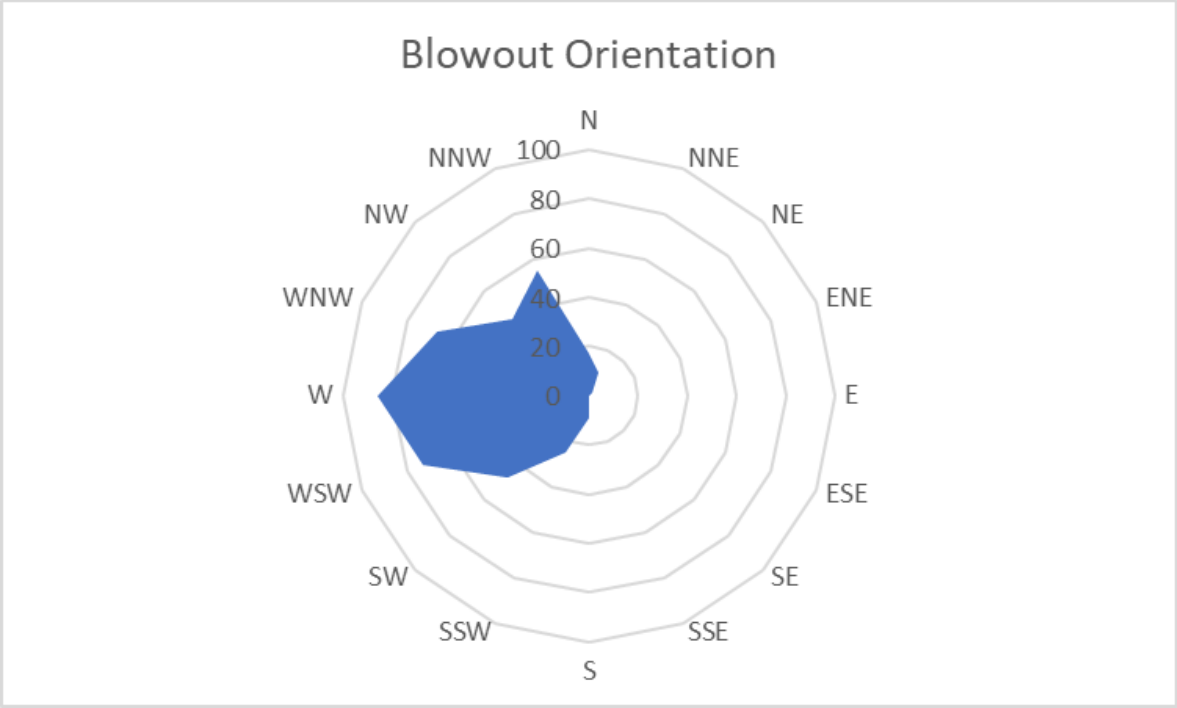

Figure 3.4: Blowout orientation, measured as the direction of the longitudinal axis of the blowout from its depositional lobe to its mouth. Thus, a blowout with a northerly orientation has its mouth north of its southerly depositional lobe.

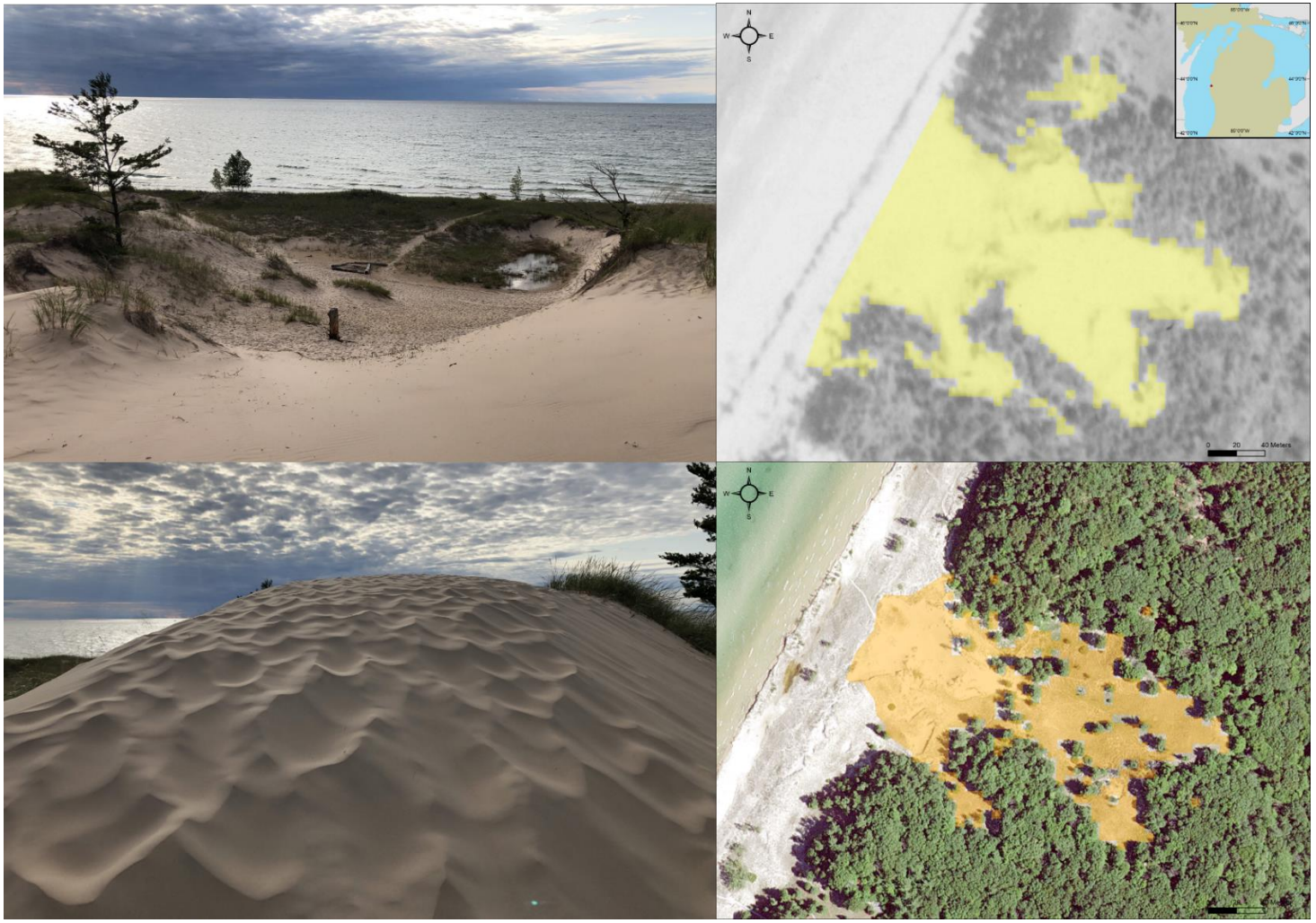

Figure 3.5: Blowout at Pentwater, Michigan, in Oceana County. On left, photographs from summer 2019 of the deflation basin (top) and depositional lobe (bottom). On right, blowout mapping results from 1938 (top) and 2018 (bottom). The 2018 results show fragmentation from sentinel trees and grasses.

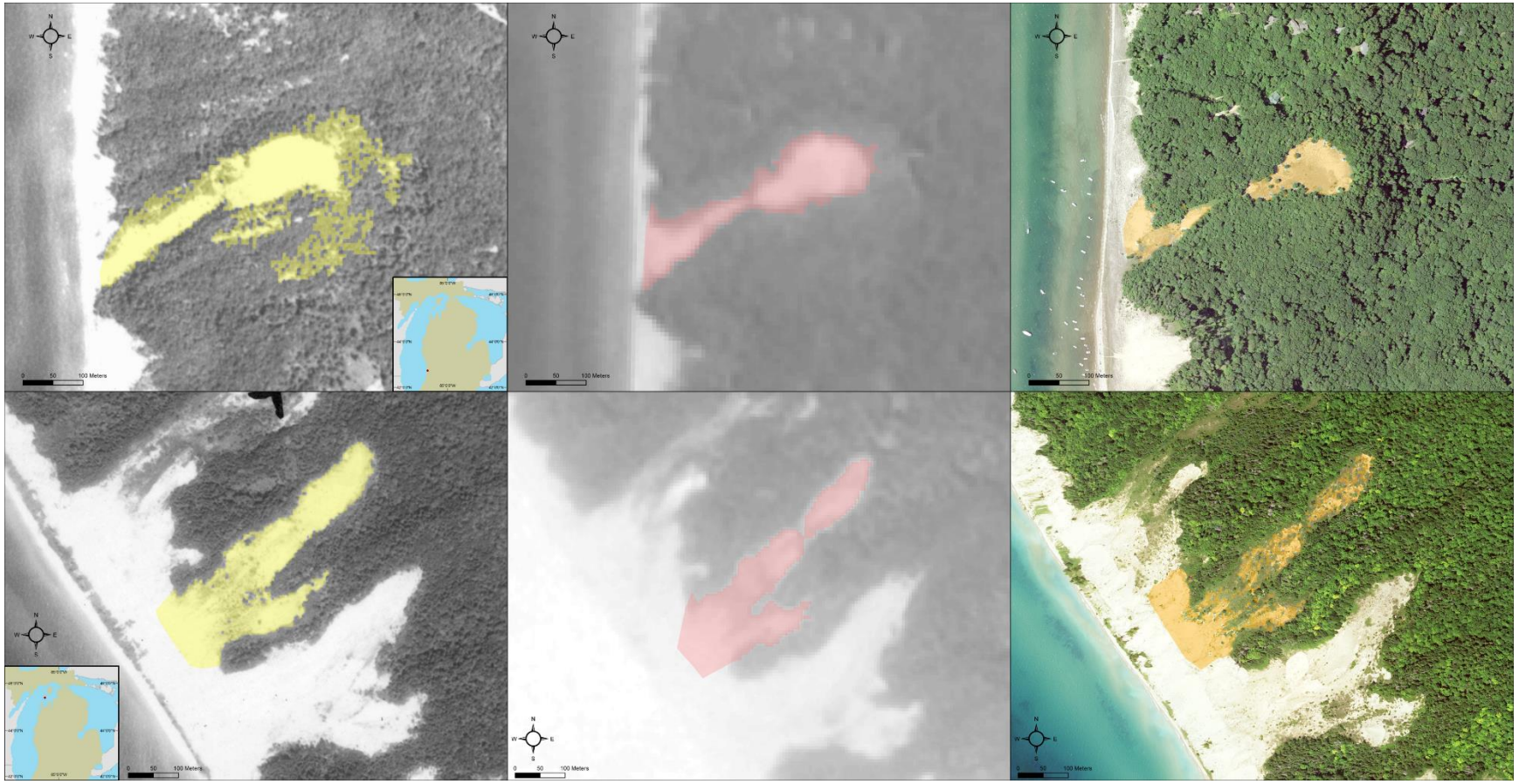

Figure 3.6: Examples of fragmentation of blowouts since 1938. Top row of images is from a blowout in Laketown Township, Michigan, while the bottom row of images is from South Fox Island in Lake Michigan. The images show the fragmentation of each blowout beginning at 1938 (left), at 1986 (center), and 2018 (right).

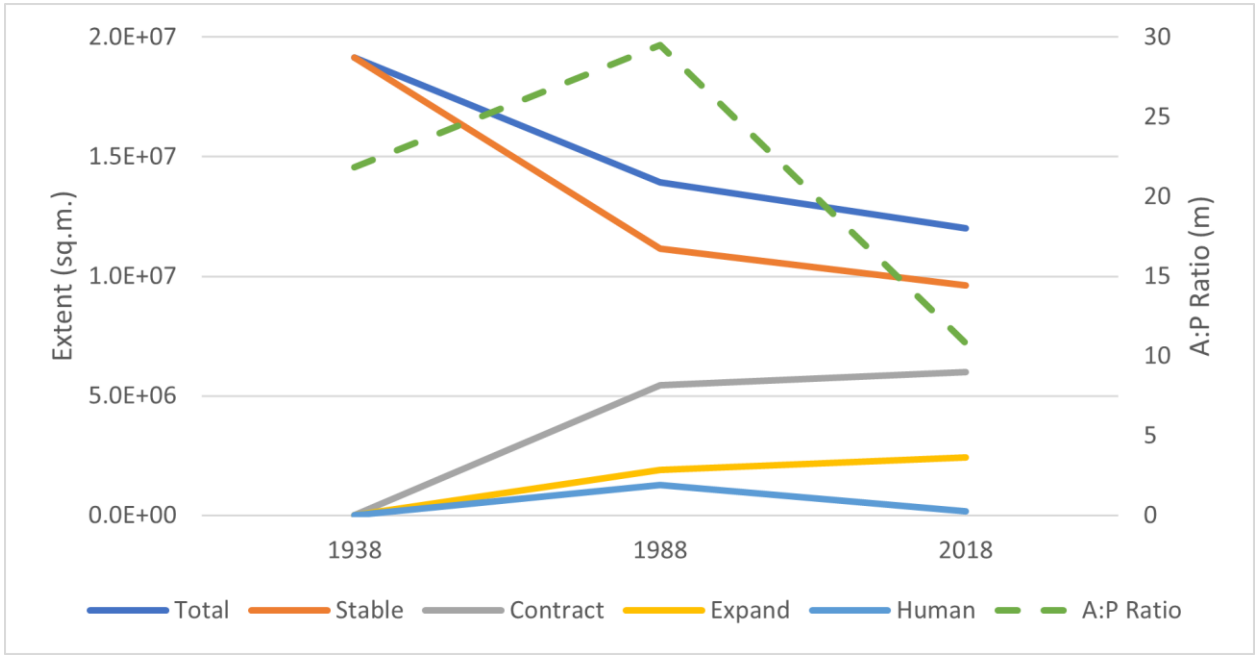

Figure 3.7: STAMP analysis results. Each line tracks the trends in various STAMP categories from 1938 to 2018, including the area in square meters determined to have remained within the blowout (Stable), the area lost within a blowout (Contract), and new blowout areas (Expand). Also added to the figure are the areas associated with human development, the total blowout area, and the area-to-perimeter ratio of each blowout polygon, which is interpreted as a measure of fragmentation, as is the outpacing of contracted areas from expanded areas.

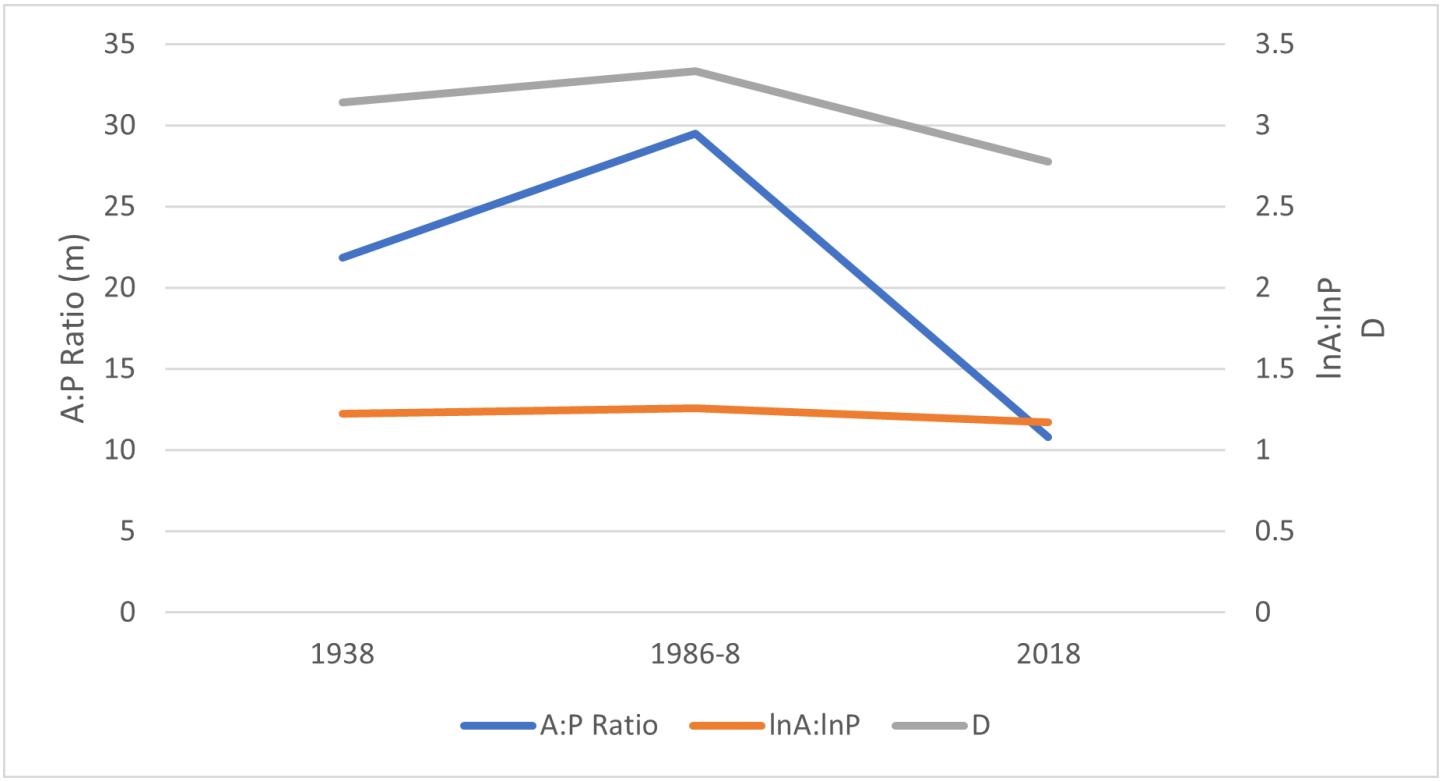

Figure 3.8: Results of the area-to-perimeter ratio and fractal dimensions analyses.

REFERENCES

REFERENCES

Abbas, A.W., Minallh, N., Ahmad, N., Abid, S.A.., Khan, M., 2016. K-Means and ISODATA Clustering Algorithms for Landcover Classification Using Remote Sensing. Sindh Univ. Res. J. (Science Ser. 48, 315–8.

Abhar, K.C., Walker, I.J., Hesp, P.A., Gares, P.A., 2015. Spatial-temporal evolution of aeolian blowout dunes at Cape Cod. Geomorphology 236, 148–162. https://doi.org/10.1016/j.geomorph.2015.02.015

Adamson, D., Selkirk, P., Colhoun, E., 1988. Landforms of aeolian, tectonic and marine origin in the Bauer Bay-Sandy Bay region of subantarctic Macquarie Island. Pap. Proc. R. Soc. Tasmania 122, 65–82. https://doi.org/10.26749/rstpp.122.1.65

Anderton, J.B., Loope, W.L., 1995. Buried soils in a perched dunefield as indicators of late Holocene lake-level change in the Lake Superior basin. Quat. Res. 44, 190–199. https://doi.org/10.1006/qres.1995.1063

Arbogast, A.F., Garmon, B., Sterrett Isely, E., Jarosz, J., Kreiger, A., Nicholls, S., Queen, C., Richardson, R.B., 2018. Valuing Michigan's Coastal Dunes: GIS Information and Economic Data to Support Management Partnerships.

Arbogast, A.F., Hansen, E.C., Van Oort, M.D., 2002. Reconstructing the geomorphic evolution of large coastal dunes along the southeastern shore of Lake Michigan. Geomorphology 46, 241–255. https://doi.org/10.1016/S0169-555X(02)00076-4

Arbogast, A.F., McKeehan, K.G., Richardson, R.B., Zimnicki, T., 2020. Learning to Live in Dynamic Dunes: Citizen Science and Participatory Modeling in the Service of Michigan Coastal Dune Decision-Making. Lansing, MI.

Arbogast, A.F., Schaetzl, R.J., Hupy, J.P., Hansen, E.C., 2004. The Holland Paleosol: An informal pedostratigraphic unit in the coastal dunes of southeastern Lake Michigan. Can. J. Earth Sci. 41, 1385–1400. https://doi.org/10.1139/E04-071

Arbogast, A.F., Shortridge, A.M., Bigsby, M.E., 2009. Volumetric Estimates of Coastal Sand Dunes in Lower Michigan: Explaining The Geography of Dune Fields. Phys. Geogr. 30, 479–500. https://doi.org/10.2747/0272-3646.30.6.479

Arens, S.M., 1996. Patterns of sand transport on vegetated foredunes. Geomorphology 17, 339–350. https://doi.org/10.1016/0169-555X(96)00016-5

Ashkenazy, Y., Yizhaq, H., Tsoar, H., 2012. Sand dune mobility under climate change in the Kalahari and Australian deserts. Clim. Change 112, 901–923. https://doi.org/10.1007/s10584-011-0264-9

Baedke, S.J., Thompson, T.A., 2000. A 4,700-year record of lake level and isostasy for Lake Michigan. J. Great Lakes Res. 26, 416–426. https://doi.org/10.1016/S0380-1330(00)70705-2

Bagnold, R.A., 1941. The Physics of Blown Sand and Desert Dunes. Methuen, London.

Bar Kutiel, P., Katz, O., Ziso-Cohen, V., Divinsky, I., Katra, I., 2016. Water availability in sand dunes and its implications for the distribution of Artemisia monosperma. CATENA 137, 144–151. https://doi.org/10.1016/j.catena.2015.09.007

Bate, G., Ferguson, M., 1996. Blowouts in coastal foredunes. Landsc. Urban Plan. 34, 215–224. https://doi.org/10.1016/0169-2046(95)00218-9

Bauer, B.O., Davidson-Arnott, R.G.D., 2003. A general framework for modeling sediment supply to coastal dunes including wind angle, beach geometry, and fetch effects. Geomorphology 49, 89–108. https://doi.org/10.1016/S0169-555X(02)00165-4

Bauer, B.O., Davidson-Arnott, R.G.D., Walker, I.J., Hesp, P.A., Ollerhead, J., 2012. Wind direction and complex sediment transport response across a beach-dune system. Earth Surf. Process. Landforms 37, 1661–1677. https://doi.org/10.1002/esp.3306

Belford, A., Kenbeek, S.D., VanHorn, J., Van Dijk, D., 2014. Using remote sensing and geospatial analysis to understand changes to Lake Michigan dunes. Spec. Pap. Geol. Soc. Am. 508, 217–228. https://doi.org/10.1130/2014.2508(12)

Bishop, C.T., 1990. Historical Variation of Water Levels in Lakes Erie and Michigan-Huron. J. Great Lakes Res. 16, 406–425. https://doi.org/10.1016/S0380-1330(90)71434-7

Black, R.F., 1951. Eolian Deposits of Alaska. ARCTIC 4. https://doi.org/10.14430/arctic3938

Blumer, B.E., Arbogast, A.F., Forman, S.L., 2012. The OSL chronology of eolian sand deposition in a perched dune field along the northwestern shore of Lower Michigan. Quat. Res. 77, 445–455. https://doi.org/10.1016/j.yqres.2012.01.006

Brown, J.K., Zinnert, J.C., 2018. Mechanisms of surviving burial: Dune grass interspecific differences drive resource allocation after sand deposition. Ecosphere 9. https://doi.org/10.1002/ecs2.2162

Bryant, R.G., Baddock, M.C., 2021. Remote Sensing of Aeolian Processes, in: Reference Module in Earth Systems and Environmental Sciences. Elsevier. https://doi.org/10.1016/B978-0-12-818234-5.00132-2

Buckler, W.R., 1979. Dune Type Inventory and Barrier Dune Classification Study of Michigan's Lake Michigan Shore: Report of Investigation 23. Lansing, MI.

Campbell, J.B., 1996. Introduction to Remote Sensing, 2nd ed. The Guilford Press, New York, NY.

Carter, R.W.G., 1991. Coastal Dunes, in: Coastal Environments: An Introduction to the Physical, Ecological, and Cultural Systems of the Coastlines. London, pp. 301–354.

Castelle, B., Marieu, V., Bujan, S., 2019. Alongshore-Variable Beach and Dune Changes on the Timescales from Days (Storms) toDecades Along the Rip-dominated Beaches of the Gironde Coast, SW France. J. Coast. Res. 157–171.

Cheng, Q., 1995. The perimeter-area fractal model and its application to geology. Math. Geol. 27, 69–82. https://doi.org/10.1007/BF02083568

Colman, S.M., King, J.W., Jones, G.A., Reynolds, R.L., Bothner, M.H., 2000. Holocene and recent sediment accumulation rates in Southern Lake Michigan. Quat. Sci. Rev. 19, 1563–1580. https://doi.org/10.1016/S0277-3791(00)00007-X

Congalton, R.G., 1997. Exploring and evaluation the consequences of vector-to-raster and raster-to-vector conversion. Photogramm. Eng. Remote Sensing 63, 425–34.

Cook, B.I., Cook, E.R., Smerdon, J.E., Seager, R., Williams, A.P., Coats, S., Stahle, D.W., Díaz, J.V., 2016. North American megadroughts in the Common Era: Reconstructions and simulations. Wiley Interdiscip. Rev. Clim. Chang. https://doi.org/10.1002/wcc.394

Cooper, W.S., 1958. Coastal Sand Dunes of Oregon and Washington. Geological Society of America - Memoir 72.

Corder, G.W., Foreman, D.I., 2009. Nonparametric Statistics for Non-Statisticians. John Wiley & Sons, Inc., Hoboken, NJ, USA. https://doi.org/10.1002/9781118165881

Cornelis, W.M., Gabriels, D., 2003. The effect of surface moisture on the entrainment of dune sand by wind: an evaluation of selected models. Sedimentology 50, 771–790. https://doi.org/10.1046/j.1365-3091.2003.00577.x

Cowles, H.C., 1899. The ecological relations of the vegetation on the sand dunes of Lake Michigan: Part I -Geographical relations of the dune floras. Bot. Gaz. 27, 95–117.

Davidson-Arnott, R., Hesp, P., Ollerhead, J., Walker, I., Bauer, B., Delgado-Fernandez, I., Smyth, T., 2018. Sediment budget controls on foredune height: Comparing simulation model results with field data. Earth Surf. Process. Landforms 43, 1798–1810. https://doi.org/10.1002/esp.4354

Davidson-Arnott, R.G.D., 1988. Temporal and spatial controls on beach/dune interaction, Long Point, Lake Erie. J. Coast. Res. 3, 131–136.

De Cola, L., Lam, N.S.-N., 1993. Introduction to Fractals in Geography, in: Lam, N.S.-N., De Cola, L. (Eds.), Fractals in Geography. Prentice Hall, Englewood Cliffs, N.J., pp. 3–22.

Dech, J.P., Maun, M.A., 2005. Zonation of vegetation along a burial gradient on the leeward

slopes of Lake Huron sand dunes. Can. J. Bot. 83, 227–236. https://doi.org/10.1139/b04-163

Dech, J.P., Maun, M.A., Pazner, M.I., 2005. Blowout dynamics on Lake Huron sand dunes: analysis of digital multispectral data from colour air photos. CATENA 60, 165–180. https://doi.org/10.1016/j.catena.2004.11.004

Delgado-Fernandez, I., 2011. Meso-scale modelling of aeolian sediment input to coastal dunes. Geomorphology 130, 230–243. https://doi.org/10.1016/j.geomorph.2011.04.001

Delgado-Fernandez, I., 2010. A review of the application of the fetch effect to modelling sand supply to coastal foredunes. Aeolian Res. 2, 61–70. https://doi.org/10.1016/j.aeolia.2010.04.001

Delgado-Fernandez, I., O'Keeffe, N., Davidson-Arnott, R.G.D., 2019. Natural and human controls on dune vegetation cover and disturbance. Sci. Total Environ. 672, 643–656. https://doi.org/10.1016/j.scitotenv.2019.03.494

Delgado-Fernandez, I., Smyth, T.A.G., Jackson, D.W.T., Smith, A.B., Davidson-Arnott, R.G.D., 2018. Event-Scale Dynamics of a Parabolic Dune and Its Relevance for Mesoscale Evolution. J. Geophys. Res. Earth Surf. 123, 3084–3100. https://doi.org/10.1029/2017JF004370

Desai, A.R., Austin, J.A., Bennington, V., McKinley, G.A., 2009. Stronger winds over a large lake in response to weakening air-to-lake temperature gradient. Nat. Geosci. 2, 855–858. https://doi.org/10.1038/ngeo693

Dincer, T., Al-Mugrin, A., Zimmermann, U., 1974. Study of the infiltration and recharge through the sand dunes in arid zones with special reference to the stable isotopes and thermonuclear tritium. J. Hydrol. 23, 79–109. https://doi.org/10.1016/0022-1694(74)90025-0

Doing, H., 1985. Coastal fore-dune zonation and succession in various parts of the world. Vegetatio 61, 65–75.

Dow, K.W., 1937. The origin of perched dunes on the Manistee Moraine, Michigan. Mich. Acad. 23, 427–440.

Drummond, M.A., Stier, M.P., Diffendorfer, J. (Jay) E., 2019. Historical land use and land cover for assessing the northern Colorado Front Range urban landscape. J. Maps 15, 89–93. https://doi.org/10.1080/17445647.2018.1548383

EROS, 2018a. USGS EROS Archive - Aerial Photography - National High Altitude Photography (NHAP).

EROS, 2018b. USGS EROS Archive - Aerial Photography - National Agriculture Imagery Program (NAIP). https://doi.org/10.5066/F7QN651G

Fisher, T.G., Weyer, K.A., Boudreau, A.M., Martin-Hayden, J.M., Krantz, D.E., Breckenridge, A., 2012. Constraining Holocene lake levels and coastal dune activity in the Lake Michigan basin. J. Paleolimnol. 47, 373–390. https://doi.org/10.1007/s10933-010-9460-2

Foody, G.M., 2002. <Foody.Pdf> 80, 185–201. https://doi.org/10.1016/S0034-4257(01)00295-4

Forman, S.L., 2015. Episodic eolian sand deposition in the past 4000 years in Cape Cod National Seashore, Massachusetts, USA in response to possible hurricane/storm and anthropogenic disturbances. Front. Earth Sci. 3. https://doi.org/10.3389/feart.2015.00003

Fraser, G.S., Bennett, S.W., Olyphant, G.A., Bauch, N.J., Ferguson, V., Gellasch, C.A., Millard, C.L., Mueller, B., O'Malley, P.J., Way, J.N., Woodfield, M.C., 1998. Windflow Circulation Patterns in a Coastal Dune Blowout, South Coast of Lake Michigan. J. Coast. Res. 14, 451–460.

Fulop, E.C.F., Johnson, B.G., Keen-Zebert, A., 2019. A geochronology-supported soil chronosequence for establishing the timing of shoreline parabolic dune stabilization. CATENA 178, 232–243. https://doi.org/10.1016/j.catena.2019.03.018

Gao, J., Kennedy, D.M., Konlechner, T.M., 2020. Coastal dune mobility over the past century: A global review. Prog. Phys. Geogr. Earth Environ. 44, 814–836. https://doi.org/10.1177/0309133320919612

Gao, J., Xia, Z., 1996. Fractals in physical geography. Prog. Phys. Geogr. Earth Environ. 20, 178–191. https://doi.org/10.1177/030913339602000204

Gardner, R., McLaren, S., 1999. Infiltration and moisture movement in coastal sand dunes, Studland, Dorset, U.K.: Preliminary results. J. Coast. Res. 15, 936–949.

Gares, P.A., 1992. Topographic changes associated with coastal dune blowouts at island beach state park, New Jersey. Earth Surf. Process. Landforms 17, 589–604. https://doi.org/10.1002/esp.3290170605

Gares, P.A., Nordstrom, K.F., 1995. A cyclic model of foredune blowout evolution for a leeward coast: Island Beach, New Jersey. Ann. Assoc. Am. Geogr. 85, 1–20.

Girardi, J.D., Davis, D.M., 2010. Parabolic dune reactivation and migration at Napeague, NY, USA: Insights from aerial and GPR imagery. Geomorphology 114, 530–541. https://doi.org/10.1016/j.geomorph.2009.08.011

Gocic, M., Trajkovic, S., 2013. Analysis of changes in meteorological variables using Mann-Kendall and Sen's slope estimator statistical tests in Serbia. Glob. Planet. Change 100, 172–182. https://doi.org/10.1016/j.gloplacha.2012.10.014

Goldmann, R.A., 1990. Using Multiresolution Remote Sensing Data and GIS Technology to Update

Forest Stand Compartment Maps Under Lake States Conditions. University of Wisconsin-Madison.

Goodchild, M.F., Mark, D.M., 1987. The Fractal Nature of Geographic Phenomena. Ann. Assoc. Am. Geogr. 77, 265–278. https://doi.org/10.1111/j.1467-8306.1987.tb00158.x

Hack, J.T., 1941. Dunes of the Western Navajo Country. Geogr. Rev. 31, 240. https://doi.org/10.2307/210206

Hails, J.R., Bennett, J., 1980. Wind and Sediment Movement in Coastal Dune Areas, in: Coastal Engineering 1980. American Society of Civil Engineers, New York, NY, pp. 1565–1575. https://doi.org/10.1061/9780872622647.094

Halfen, A.F., Johnson, W.C., 2013. A review of Great Plains dune field chronologies. Aeolian Res. https://doi.org/10.1016/j.aeolia.2013.03.001

Han, Q., Qu, J., Liao, K., Zhu, S., Zhang, K., Zu, R., Niu, Q., 2011. A wind tunnel study of aeolian sand transport on a wetted sand surface using sands from tropical humid coastal southern China. Environ. Earth Sci. 64, 1375–1385. https://doi.org/10.1007/s12665-011-0962-7

Hansel, A.K., Mickelson, D.M., 1988. A Reevaluation of the Timing and Causes of High Lake Phases in the Lake Michigan Basin. Quat. Res. 29, 113–128. https://doi.org/10.1016/0033-5894(88)90055-5

Hansen, E., DeVries-Zimmerman, S., van Dijk, D., Yurk, B., 2009. Patterns of wind flow and aeolian deposition on a parabolic dune on the southeastern shore of Lake Michigan. Geomorphology 105, 147–157. https://doi.org/10.1016/j.geomorph.2007.12.012

Hansen, E.C., Arbogast, a. F., Dijk, D. Van, Yurk, B., van Dijkco, D., 2006. Growth and migration of parabolic dunes along the southeastern coast of Lake Michigan. J. Coast. Res. - Spec. Issue 39 I, 209–214.

Hansen, E.C., Arbogast, A.F., Packman, S.C., Hansen, B., 2002. Post-Nipissing Origin of a Backdune Complex Along the Southeastern Shore of Lake Michigan. Phys. Geogr. 23, 233–244. https://doi.org/10.2747/0272-3646.23.3.233

Hansen, E.C., Fisher, T.G., Arbogast, A.F., Bateman, M.D., 2010. Geomorphic history of low-perched, transgressive dune complexes along the southeastern shore of Lake Michigan. Aeolian Res. 1, 111–127. https://doi.org/10.1016/j.aeolia.2009.08.001

Harman, J.R., Arbogast, A.F., 2004. Environmental ethics and coastal dunes in western Lower Michigan: Developing a rationale for ecosystem preservation. Ann. Assoc. Am. Geogr. 94, 23–36.

Helama, S., Jones, P.D., Briffa, K.R., 2017. Dark Ages Cold Period: A literature review and directions for future research. The Holocene 27, 1600–1606.

https://doi.org/10.1177/0959683617693898

Helzer, C.J., Jelinski, D.E., 1999. The Relative Importance of Patch Area and Perimeter-Area Ratio to Grassland Breeding Birds. Ecol. Appl. 9, 1448. https://doi.org/10.2307/2641409

Henne, P.D., Hu, F.S., 2010. Holocene climatic change and the development of the lake-effect snowbelt in Michigan, USA. Quat. Sci. Rev. 29, 940–951. https://doi.org/10.1016/j.quascirev.2009.12.014

Hesp, P., 2002. Foredunes and blowouts: Initiation, geomorphology and dynamics. Geomorphology 48, 245–268. https://doi.org/10.1016/S0169-555X(02)00184-8

Hesp, P., Martinez, M., da Silva, G.M., Rodríguez-Revelo, N., Gutierrez, E., Humanes, A., Laínez, D., Montaño, I., Palacios, V., Quesada, A., Storero, L., Trilla, G.G., Trochine, C., 2011. Transgressive dunefield landforms and vegetation associations, Doña Juana, Veracruz, Mexico. Earth Surf. Process. Landforms 36, 285–295. https://doi.org/10.1002/esp.2035

Hesp, P.A., 1989. A review of biological and geomorphological processes involved in the initiation and development of incipient foredunes. Proc. R. Soc. Edinburgh. Sect. B. Biol. Sci. 96, 181–201. https://doi.org/10.1017/S0269727000010927

Hesp, P.A., 1981. The Formation of Shadow Dunes. SEPM J. Sediment. Res. Vol. 51. https://doi.org/10.1306/212F7C1B-2B24-11D7-8648000102C1865D

Hesp, P.A., Hyde, R., 1996. Flow dynamics and geomorphology of a trough blowout. Sedimentology 43, 505–525. https://doi.org/10.1046/j.1365-3091.1996.d01-22.x

Hesp, P.A., Smyth, T.A.G., 2016. Surfzone-Beach-Dune interactions: Flow and Sediment Transport across the Intertidal Beach and Backshore. J. Coast. Res. 75, 8–12. https://doi.org/10.2112/SI75-002.1

Huggett, R., 2007. A history of the systems approach in geomorphology. Géomorphologie Reli. Process. Environ. 13, 145–158. https://doi.org/10.4000/geomorphologie.1031

Huggett, R.J., 2011. Fundamentals of Geomorphology, Third Edit. ed. Routledge, New York.

Hunt, B.G., 2006. The Medieval Warm Period, the Little Ice Age and simulated climatic variability. Clim. Dyn. 27, 677–694. https://doi.org/10.1007/s00382-006-0153-5

Hupy, C.M., Yansa, C.H., 2009. Late Holocene vegetation history of the forest tension zone in Central Lower Michigan, USA. Phys. Geogr. 30, 205–235. https://doi.org/10.2747/0272-3646.30.3.205

IBM Corp., 2020. IBM SPSS Statistics for Windows, Version 27.0.

Indiana DNR, 2020. Great Lakes Water Level Table for Lake Michigan/Huron. Indianapolis, Ind.

Jackson, D.W.T., Costas, S., Guisado-Pintado, E., 2019. Large-scale transgressive coastal dune behaviour in Europe during the Little Ice Age. Glob. Planet. Change 175, 82–91. https://doi.org/10.1016/j.gloplacha.2019.02.003

Jennings, J.N., 1957. On the Orientation of Parabolic or U-Dunes. Geogr. J. 123, 474. https://doi.org/10.2307/1790349

Jewell, M., Houser, C., Trimble, S., 2017. Phases of blowout initiation and stabilization on Padre Island revealed through ground-penetrating radar and remotely sensed imagery. Phys. Geogr. 38, 556–577. https://doi.org/10.1080/02723646.2017.1338042

Julian, P.R., 1983. On the Use of Observation Error Data in FGGE Main Level III-b Analysis, ECMWF Technical Memoranda #76. Shinfield Park, Reading, UK.

Jungerius, P.D., van der Meulen, F., 1989. The development of dune blowouts, as measured with erosion pins and sequential air photos. CATENA 16, 369–376. https://doi.org/10.1016/0341-8162(89)90021-0

Jungerius, P.D., van der Meulen, F., 1988. Erosion processes in a dune landscape along the Dutch coast. CATENA 15, 217–228. https://doi.org/10.1016/0341-8162(88)90046-X

Jungerius, P.D., Verheggen, A.J.T., Wiggers, A.J., 1981. The development of blowouts in 'de blink', a coastal dune area near Noordwijkerhout, The Netherlands. Earth Surf. Process. Landforms 6, 375–396. https://doi.org/10.1002/esp.3290060316

Kent, C., Wong, J., 1982. An Index of Littoral Zone Complexity and Its Measurement. Can. J. Fish. Aquat. Sci. 39, 847–853. https://doi.org/10.1139/f82-115

Kilibarda, Z., 2018. HUMID AND COOL CLIMATE RATHER THAN DROUGHTS LEAD TO COASTAL BLOWOUTS DEVELOPMENT IN THE GREAT LAKES REGION. https://doi.org/10.1130/abs/2018AM-320964

Kilibarda, Z., Shillinglaw, C., 2015. A 70-year history of coastal dune migration and beach erosion along the southern shore of Lake Michigan. Aeolian Res. 17, 263–273. https://doi.org/10.1016/j.aeolia.2014.09.002

Kilibarda, Z., Venturelli, R., Goble, R., 2014. Late Holocene dune development and shift in dune-building winds along southern Lake Michigan, in: Coastline and Dune Evolution along the Great Lakes. Geological Society of America, pp. 47–64. https://doi.org/10.1130/2014.2508(04)

Klink, K., 2002. Trends and interannual variability of wind speed distributions in Minnesota. J. Clim. 15, 3311–3317. https://doi.org/10.1175/1520-0442(2002)015<3311:TAIVOW>2.0.CO;2

Kvamme, K.L., Ernenwein, E.G., Menzer, J.G., 2019. Putting it all together: Geophysical data

integration, in: Innovation in Near-Surface Geophysics. Elsevier, pp. 287–339. https://doi.org/10.1016/B978-0-12-812429-1.00009-X

Ladd, M., Viau, A., Way, R., Gajewski, K., Sawada, M., 2018. Variations in precipitation in North America during the past 2000 years. The Holocene 28, 667–675. https://doi.org/10.1177/0959683617735583

Lancaster, N., Baas, A., 1998. Influence of vegetation cover on sand transport by wind: Field studies at Owens Lake, California. Earth Surf. Process. Landforms 23, 69–82. https://doi.org/10.1002/(SICI)1096-9837(199801)23:1<69::AID-ESP823>3.0.CO;2-G

Lancaster, N., Helm, P., 2000. A test of a climatic index of dune mobility using measurements from the southwestern United States. Earth Surf. Process. Landforms 25, 197–207.

Landsberg, H., Riley, N.A., 1943. Wind influences on the transportation of sand over a Michigan sand dune, in: Proceedings of the Second Hydraulics Conference, Bulletin No. 27, University of Iowa Studies in Engineering.

Landsberg, S.Y., 1956. The Orientation of Dunes in Britain and Denmark in Relation to Wind. Geogr. J. 122, 176. https://doi.org/10.2307/1790847

Lane, C., Wright, S.J., Roncal, J., Maschinski, J., 2008. Characterizing Environmental Gradients and Their Influence on Vegetation Zonation in a Subtropical Coastal Sand Dune System. J. Coast. Res. 4, 213–224. https://doi.org/10.2112/07-0853.1

Laporte-Fauret, Q., Castelle, B., Michalet, R., Marieu, V., Bujan, S., Rosebery, D., 2021. Morphological and ecological responses of a managed coastal sand dune to experimental notches. Sci. Total Environ. 782, 146813. https://doi.org/10.1016/j.scitotenv.2021.146813

Larsen, C.E., 1987. Geological History of Glacial Lake Algonquin and the Upper Great Lakes, U.S. Geological Survey Bulletin 1801. Denver, Colo.

Lee, D.B., Ferdowsi, B., Jerolmack, D.J., 2019. The imprint of vegetation on desert dune dynamics. Geophys. Res. Lett. 46, 12041–12048. https://doi.org/10.1029/2019GL084177

Lemenkova, P., 2021. ISO Cluster classifier by ArcGIS for unsupervised classification of the Landsat TM image of Reykjavík. Bull. Nat. Sci. Res. 11, 29–37. https://doi.org/10.5937/bnsr11-30488

Lepczyk, X.C., Arbogast, A.F., 2005. Geomorphic history of dunes at Petoskey State Park, Petoskey, Michigan. J. Coast. Res. 212, 231–241. https://doi.org/10.2112/02-043.1

Lewis, C.F.M., 1969. Late Quaternary history of lake levels in the Huron and Erie basins, in: Proceedings of the 12th Conference on Great Lakes Research. pp. 250–270.

Livsey, D., Simms, A.R., Hangsterfer, A., Nisbet, R.A., DeWitt, R., 2016. Drought modulated by

North Atlantic sea surface temperatures for the last 3,000 years along the northwestern Gulf of Mexico. Quat. Sci. Rev. 135, 54–64. https://doi.org/10.1016/j.quascirev.2016.01.010

Long, J., Robertson, C., Nelson, T., 2018. stampr: Spatial-Temporal Analysis of Moving Polygons in R. J. Stat. Softw. 84. https://doi.org/10.18637/jss.v084.c01

Loope, W.L., Arbogast, A.F., 2000. Dominance of an ~150-year cycle of sand-supply change in late Holocene dune-building along the eastern shore of Lake Michigan. Quat. Res. 54, 414–422. https://doi.org/10.1006/qres.2000.2168

Lopez, O.M., Hegy, M.C., Missimer, T.M., 2020. Statistical comparisons of grain size characteristics, hydraulic conductivity, and porosity of barchan desert dunes to coastal dunes. Aeolian Res. 43.

Lovis, W.A., Arbogast, A.F., Monaghan, G.W., 2012. The Geoarchaeology of Lake Michigan Coastal Dunes. Michigan State University Press, East Lansing, Mich.

Lunetta, R.S., Congalton, R.G., Fenstenmaker, L.K., Jensen, J.R., McGwire, K.C., Tinney, L.R., 1991. Remote sensing and Geographic Information System data integration: error sources and research issues. Photogramm. Eng. Remote Sensing 57, 677–87.

Luo, W., Wang, Z., Shao, M., Lu, J., Qian, G., Dong, Z., Hesp, P.A., Bateman, M.D., 2019. Historical evolution and controls on mega-blowouts in northeastern Qinghai-Tibetan Plateau, China. Geomorphology 329, 17–31. https://doi.org/10.1016/j.geomorph.2018.12.033

Ma, Z., Liu, Z., Zhao, Y., Zhang, L., Liu, D., Ren, T., Zhang, X., Li, S., 2020. An Unsupervised Crop Classification Method Based on Principal Components Isometric Binning. ISPRS Int. J. Geo-Information 9, 648. https://doi.org/10.3390/ijgi9110648

Mason, J.A., Swinehart, J.B., Lu, H., Miao, X., Cha, P., Zhou, Y., 2008. Limited change in dune mobility in response to a large decrease in wind power in semi-arid northern China since the 1970s. Geomorphology 102, 351–363. https://doi.org/10.1016/j.geomorph.2008.04.004

Mathew, S., Davidson-Arnott, R.G.D., Ollerhead, J., 2010. Evolution of a beach–dune system following a catastrophic storm overwash event: Greenwich Dunes, Prince Edward Island, 1936–2005. Can. J. Earth Sci. 47, 273–290. https://doi.org/10.1139/E09-078

Maun, M.A., 1998. Adaptations of plants to burial in coastal sand dunes. Can. J. Bot. 76, 713–738.

McCann, S.B., Byrne, M.L., 1994. DUNE MORPHOLOGY AND THE EVOLUTION OF SABLE ISLAND, NOVA SCOTIA, IN HISTORIC TIMES. Phys. Geogr. 15, 342–357. https://doi.org/10.1080/02723646.1994.10642521

McKeehan, KG, and Arbogast, AF, 2021. Repeat photography of Lake Michigan coastal dunes: Expansion of vegetation since 1900 and possible drivers. Journal of Great Lakes Research

47(6), 1518-1537. doi.org/10.1016/j.jglr.2021.09.016

Mckenzie, G., Cooper, A.G., 2001. Post emplacement dune evolution of Atlantic coastal dunes, Northwest Ireland. J. Coast. Res. - Spec. Issue 34 ICS 2000 N.

McLeester, M., Casana, J., 2021. Finding Fields: Locating Archaeological Agricultural Landscapes Using Historical Aerial Photographs. Am. Antiq. 86, 283–304. https://doi.org/10.1017/aaq.2020.102

McVicar, T.R., Roderick, M.L., Donohue, R.J., Li, L.T., Van Niel, T.G., Thomas, A., Grieser, J., Jhajharia, D., Himri, Y., Mahowald, N.M., Mescherskaya, A. V., Kruger, A.C., Rehman, S., Dinpashoh, Y., 2012. Global review and synthesis of trends in observed terrestrial near-surface wind speeds: Implications for evaporation. J. Hydrol. 416–417, 182–205. https://doi.org/10.1016/j.jhydrol.2011.10.024

Melton, F.A., 1940. A Tentative Classification of Sand Dunes Its Application to Dune History in the Southern High Plains. J. Geol. 48, 113–174. https://doi.org/10.1086/624871

Miyanishi, K., Johnson, E.A., 2021. Coastal dune succession and the reality of dune processes, in: Plant Disturbance Ecology. Elsevier, pp. 253–290. https://doi.org/10.1016/B978-0-12-818813-2.00007-1

Monaghan, G.W., Lovis, W.A., Fay, L., 1986. The Lake Nipissing transgression in the Saginaw Bay region, Michigan. Can. J. Earth Sci. 23, 1851–1854. https://doi.org/10.1139/e86-169

Monmonier, M., 2002. Aerial Photography at the Agricultural Adjustment Administration: Acreage Controls, Conservation Benefits, and Overhead Surveillance in the 1930s. Photogramm. Eng. Remote Sens. 68, 1257–1261.

Moore, L.J., 2000. Shoreline Mapping Techniques. J. Coast. Res. 16, 111–24.

Morone, L.L., 1986. The Observational Error of Automated Wind Reports from Aircraft. Bull. Am. Meteorol. Soc. 67, 177–185. https://doi.org/10.1175/1520-0477-67.2.177

Neukom, R., Steiger, N., Gómez-Navarro, J.J., Wang, J., Werner, J.P., 2019. No evidence for globally coherent warm and cold periods over the preindustrial Common Era. Nature 571, 550–554. https://doi.org/10.1038/s41586-019-1401-2

Nield, J.M., Baas, A.C.W., 2008. The influence of different environmental and climatic conditions on vegetated aeolian dune landscape development and response. Glob. Planet. Change 64, 76–92. https://doi.org/10.1016/j.gloplacha.2008.10.002

Nordstrom, K.F., 2015. Coastal dunes, in: Coastal Environments and Global Change. pp. 178–193. https://doi.org/10.1002/9781119117261.ch8

Olson, J.S., 1958a. Lake Michigan dune development 2. Plants as agents and tools in

geomorphology. J. Geol. 66, 345–351.

Olson, J.S., 1958b. Lake Michigan dune development 3. Lake-level, beach, and dune Oscillations. J. Geol. 66, 473–483.

Paskus, J.J., Enander, H., 2019. Spatial Data to Improve Coastal Resiliency and Better Inform Local Decision-Making. Lansing, MI.

Pease, P., Gares, P., 2013. The influence of topography and approach angles on local deflections of airflow within a coastal blowout. Earth Surf. Process. Landforms 38, 1160–1169. https://doi.org/10.1002/esp.3407

Peterson, J., Dersch, E., 1981. guide to sand dune and coastal ecosystem functional relationships, Michigan State University Extension Bulletin EMICHU-SG-81-501. East Lansing, Mich.

Petty, W., Delcourt, P., Delcourt, H., 1996. Holocene lake-level fluctuations and beach-ridge development along the northern shore of Lake Michigan, USA. J. Paleolimnol. 15. https://doi.org/10.1007/BF00196778

Phillips, J.D., 2007. The perfect landscape. Geomorphology 84, 159–169. https://doi.org/10.1016/j.geomorph.2006.01.039

Phillips, J.D., 2006. Deterministic chaos and historical geomorphology: A review and look forward. Geomorphology 76, 109–121. https://doi.org/10.1016/j.geomorph.2005.10.004

Phillips, J.D., 1993. Interpreting the Fractal Dimension of River Networks, in: Lam, N.S.-N., De Cola, L. (Eds.), Fractals in Geography. Prentice Hall, Englewood Cliffs, N.J., pp. 142–153.

Pluis, J.L.A., 1992. Relationships between deflation and near surface wind velocity in a coastal dune blowout. Earth Surf. Process. Landforms 17, 663–673. https://doi.org/10.1002/esp.3290170703

Provoost, S., Jones, M.L.M., Edmondson, S.E., 2011. Changes in landscape and vegetation of coastal dunes in northwest Europe: a review. J. Coast. Conserv. 15, 207–226. https://doi.org/10.1007/s11852-009-0068-5

Pye, K., 1983. Coastal dunes. Prog. Phys. Geogr. Earth Environ. 7, 531–557. https://doi.org/10.1177/030913338300700403

Quinn, F.H., 2002. Secular Changes in Great Lakes Water Level Seasonal Cycles. J. Great Lakes Res. 28, 451–465. https://doi.org/10.1016/S0380-1330(02)70597-2

Rango, A., Laliberte, A., Winters, C., 2008. Role of aerial photos in compiling a long-term remote sensing data set. J. Appl. Remote Sens. 2, 023541. https://doi.org/10.1117/1.3009225

Ranwell, D., 1958. Movement of Vegetated Sand Dunes at Newborough Warren, Anglesey. J.

Ecol. 46, 83. https://doi.org/10.2307/2256905

Rapinel, S., Clément, B., Magnanon, S., Sellin, V., Hubert-Moy, L., 2014. Identification and mapping of natural vegetation on a coastal site using a Worldview-2 satellite image. J. Environ. Manage. 144, 236–246. https://doi.org/10.1016/j.jenvman.2014.05.027

Riksen, M.J.P.M., Goossens, D., 2007. The role of wind and splash erosion in inland drift-sand areas in the Netherlands. Geomorphology 88, 179–192. https://doi.org/10.1016/j.geomorph.2006.11.002

Ritchie, W., 1972. The evolution of coastal sand dunes. Scott. Geogr. Mag. 88, 19–35. https://doi.org/10.1080/00369227208736205

Robertson, C., Nelson, T.A., Boots, B., Wulder, M.A., 2007. STAMP: spatial–temporal analysis of moving polygons. J. Geogr. Syst. 9, 207–227. https://doi.org/10.1007/s10109-007-0044-2

Ruddiman, W.F., 2014. Earth's Climate, Past and Future, Third Edit. ed. W.H. Freeman and Company, New York, NY.

Ruggiero, P., Hacker, S., Seabloom, E., Zarnetske, P., 2018. The role of vegetation in determining dune morphology, exposure to sea-level rise, and storm-induced coastal hazards: A U.S. Pacific Northwest perspective, in: Barrier Dynamics and Response to Changing Climate. Springer International Publishing, Cham, pp. 337–361. https://doi.org/10.1007/978-3-319-68086-6_11

Sadahiro, Y., Umemura, M., 2001. A computational approach for the analysis of changes in polygon distributions. J. Geogr. Syst. 3, 137–154. https://doi.org/10.1007/PL00011471

Sala, O.E., Parton, W.J., Joyce, L.A., Lauenroth, W.K., 1988. Primary Production of the Central Grassland Region of the United States. Ecology 69, 40–45. https://doi.org/10.2307/1943158

Salas, W.A., Boles, S.H., Frolking, S., Xiao, X., Li, C., 2003. The perimeter/area ratio as an index of misregistration bias in land cover change estimates. Int. J. Remote Sens. 24, 1165–1170. https://doi.org/10.1080/0143116021000044841

Salisbury, E., 1952. Downs & Dunes: Their Plant Life and Its Environment. G. Bell & Sons, Ltd., London.

Schaetzl, R., Anderson, S., 2005. Soils: Genesis and Geomorphology. Cambridge University Press, New York.

Schaney, M.L., Kite, J.S., Schaney, C.R., Thompson, J.A., 2021. Evidence of Mid-Holocene (Northgrippian Age) Dry Climate Recorded in Organic Soil Profiles in the Central Appalachian Mountains of the Eastern United States. Geosciences 11, 477.

https://doi.org/10.3390/geosciences11110477

Schrotenboer, B.R., Arbogast, A.F., 2010. Locating alternative sand sources for Michigan's foundry industry: A geographical approach. Appl. Geogr. 30, 697–719. https://doi.org/10.1016/j.apgeog.2010.02.001

Schwarz, C., Brinkkemper, J., Ruessink, G., 2018. Feedbacks between Biotic and Abiotic Processes Governing the Development of Foredune Blowouts: A Review. J. Mar. Sci. Eng. 7, 2. https://doi.org/10.3390/jmse7010002

Shay, J.M., Herring, M., Dyck, B.S., 2000. Dune colonization in the Bald Head Hills, southwestern Manitoba. Can. Field-Naturalist 114, 612–627.

Sherman, D.J., Bauer, B.O., 1993. Dynamics of beach-dune systems. Prog. Phys. Geogr. Earth Environ. 17, 413–447. https://doi.org/10.1177/030913339301700402

Short, A.D., Hesp, P.A., 1982. Wave, beach and dune interactions in southeastern Australia. Mar. Geol. 48, 259–284. https://doi.org/10.1016/0025-3227(82)90100-1

Shuman, B.N., Marsicek, J., 2016. The structure of Holocene climate change in mid-latitude North America. Quat. Sci. Rev. 141, 38–51. https://doi.org/10.1016/j.quascirev.2016.03.009

Sloss, C.R., Shepherd, M., Hesp, P.A., 2012. Coastal Dunes: Geomorphology. Nat. Educ. Knowl. 3, 2.

Smith, A.B., Jackson, D.W.T., Cooper, J.A.G., Hernández-Calvento, L., 2017. Quantifying the role of urbanization on airflow perturbations and dunefield evolution. Earth's Futur. 5, 520–539. https://doi.org/10.1002/2016EF000524

Theuerkauf, E., Mattheus, C.R., Braun, K., Bueno, J., 2021. Patterns and processes of beach and foredune geomorphic change along a Great Lakes shoreline: Insights from a year-long drone mapping study along Lake Michigan. Shore & Beach 46–55. https://doi.org/10.34237/1008926

Thom, B., Hesp, P., Bryant, E., 1994. Last glacial "coastal" dunes in Eastern Australia and implications for landscape stability during the Last Glacial Maximum. Palaeogeogr. Palaeoclimatol. Palaeoecol. 111, 229–248. https://doi.org/10.1016/0031-0182(94)90065-5

Thompson, T.A., Baedke, S.J., 1997. Strand-plain evidence for late Holocene lake-level variations in Lake Michigan. Geol. Soc. Am. Bull. 109, 666–682. https://doi.org/10.1130/0016-7606(1997)109<0666:SPEFLH>2.3.CO;2

Thompson, T.A., Lepper, K., Endres, A.L., Johnston, J.W., Baedke, S.J., Argyilan, E.P., Booth, R.K., Wilcox, D.A., 2011. Mid Holocene lake level and shoreline behavior during the Nipissing phase of the upper Great Lakes at Alpena, Michigan, USA. J. Great Lakes Res. 37, 567–

576. https://doi.org/10.1016/j.jglr.2011.05.012

Thorn, C.E., Welford, M.R., 1994. The equilibrium concept in Geomorphology. Ann. Assoc. Am. Geogr. 84, 666–696.

Tian, Q., Huang, G., Hu, K., Niyogi, D., 2019. Observed and global climate model based changes in wind power potential over the Northern Hemisphere during 1979–2016. Energy 167, 1224–1235. https://doi.org/10.1016/j.energy.2018.11.027

Tojo, K., Udo, K., 2018. Analysis of Beach Recovery After the 2011 Tohoku Earthquake Tsunami Based on Shoreline Extraction by ISODATA. J. Coast. Res. 85, 171–175. https://doi.org/10.2112/SI85-035.1

Torralba, V., Doblas-Reyes, F.J., Gonzalez-Reviriego, N., 2017. Uncertainty in recent near-surface wind speed trends: a global reanalysis intercomparison. Environ. Res. Lett. 12, 114019. https://doi.org/10.1088/1748-9326/aa8a58

Tsoar, H., 2005. Sand dunes mobility and stability in relation to climate. Phys. A Stat. Mech. its Appl. 357, 50–56. https://doi.org/10.1016/j.physa.2005.05.067

Turner, M.G., Romme, W.H., Gardner, R.H., O'Neill, R. V., Kratz, T.K., 1993. A revised concept of landscape equilibrium: Disturbance and stability on scaled landscapes. Landsc. Ecol. 8, 213–227.

Vachaud, G., Passerat De Silans, A., Balabanis, P., Vauclin, M., 1985. Temporal stability of spatially measured soil water probability density function. Soil Sci. Soc. Am. J. 49, 822–828. https://doi.org/10.2136/sssaj1985.03615995004900040006x

van Dijk, D., 2014. Short- and long-term perspectives on the evolution of a Lake Michigan foredune, in: Coastline and Dune Evolution along the Great Lakes. Geological Society of America, pp. 195–216. https://doi.org/10.1130/2014.2508(11)

van Dijk, D., 2004. Contemporary geomorphic processes and change on Lake Michigan coastal dunes: an example from Hoffmaster State Park, Michigan. Mich. Acad. 35.

Van Oort, M.D., Arbogast, A.F., Hansen, E.C., Hansen, B., 2001. Geomorphological history of massive parabolic dunes, Van Buren State Park, Van Buren County, Michigan. Mich. Acad. 33.

Vautard, R., Cattiaux, J., Yiou, P., Thépaut, J.-N., Ciais, P., 2010. Northern Hemisphere atmospheric stilling partly attributed to an increase in surface roughness. Nat. Geosci. 3, 756–761. https://doi.org/10.1038/ngeo979

Walker, I.J., Davidson-Arnott, R.G.D., Bauer, B.O., Hesp, P.A., Delgado-Fernandez, I., Ollerhead, J., Smyth, T.A.G., 2017. Scale-dependent perspectives on the geomorphology and evolution of beach-dune systems. Earth-Science Rev. 171, 220–253.

https://doi.org/10.1016/j.earscirev.2017.04.011

Wang, T., Zlotnik, V.A., Wedin, D., Wally, K.D., 2008. Spatial trends in saturated hydraulic conductivity of vegetated dunes in the Nebraska Sand Hills: Effects of depth and topography. J. Hydrol. 349, 88–97. https://doi.org/10.1016/j.jhydrol.2007.10.027

Warner, S., Jeffries, S., Lovis, W., Arbogast, A., Telewski, F., 2021. Tree ring-reconstructed late summer moisture conditions, 1546 to present, northern Lake Michigan, USA. Clim. Res. 83, 43–56. https://doi.org/10.3354/cr01637

Watras, C.J., Read, J.S., Holman, K.D., Liu, Z., Song, Y.-Y., Watras, A.J., Morgan, S., Stanley, E.H., 2014. Decadal oscillation of lakes and aquifers in the upper Great Lakes region of North America: Hydroclimatic implications. Geophys. Res. Lett. 41, 456–462. https://doi.org/10.1002/2013GL058679

Weppner, K.N., Pierce, J.L., Betancourt, J.L., 2013. Holocene fire occurrence and alluvial responses at the leading edge of pinyon–juniper migration in the Northern Great Basin, USA. Quat. Res. 80, 143–157. https://doi.org/10.1016/j.yqres.2013.06.004

Werner, C.M., Mason, J.A., Hanson, P.R., 2011. Non-linear connections between dune activity and climate in the High Plains, Kansas and Oklahoma, USA. Quat. Res. 75, 267–277. https://doi.org/10.1016/j.yqres.2010.08.001

White, R.A., Piraino, K., Shortridge, A., Arbogast, A.F., 2019. Measurement of vegetation change in critical dune sites along the eastern shores of Lake Michigan from 1938 to 2014 with object-based image analysis. J. Coast. Res. 35, 842. https://doi.org/10.2112/jcoastres-d-17-00141.1

Wilcoxon, F., 1945. Individual Comparisons by Ranking Methods. Biometrics Bull. 1, 80. https://doi.org/10.2307/3001968

Wilson, S.E., 2001. Michigan's Sand Dunes: An Michigan's Study of Coastal Sand Dune Mining in Michigan. Pamplet 7. Geological Survey Division, Michigan Department of Environmental Quality, Lansing. http://www.michigan.gov/documents/deq/ PA07_304669_7.pdf.

Woronow, A., 1981. Morphometric consistency with the Hausdorff-Besicovich dimension. J. Int. Assoc. Math. Geol. 13, 201–216. https://doi.org/10.1007/BF01029798

Wright, L.D., Thom, B.G., 1977. Coastal depositional landforms. Prog. Phys. Geogr. Earth Environ. 1, 412–459. https://doi.org/10.1177/030913337700100302

Yin, J., Han, W., Gao, Z., Chen, H., 2021. Assimilation of Doppler radar radial wind data in the GRAPES mesoscale model with observation error covariances tuning. Q. J. R. Meteorol. Soc. 147, 2087–2102. https://doi.org/10.1002/qj.4036

Yizhaq, H., Ashkenazy, Y., Tsoar, H., 2007. Why do active and stabilized dunes coexist under the

same climatic conditions? Phys. Rev. Lett. 98, 98–101. https://doi.org/10.1103/PhysRevLett.98.188001

Yurk, B., Bodenbender, B., Hansen, E.C., Harlow, B., Schaetzl, R., Devries-Zimmerman, S., 2021. AEOLIAN TRANSPORT OF SAND ACROSS A FOREST CANOPY IN THE LEE OF A LARGE PARABOLIC DUNE. https://doi.org/10.1130/abs/2021AM-368207

Yurk, B., Hansen, E., 2021. Effects of wind patterns and changing wind velocities on aeolian drift potential along the Lake Michigan shore. J. Great Lakes Res. 47, 1504–1517. https://doi.org/10.1016/j.jglr.2021.09.006

Zeng, Z., Piao, S., Li, L.Z.X., Ciais, P., Li, Y., Cai, X., Yang, L., Liu, M., Wood, E.F., 2018. Global terrestrial stilling: does Earth's greening play a role? Environ. Res. Lett. 13, 124013. https://doi.org/10.1088/1748-9326/aaea84

Zeng, Z., Ziegler, A.D., Searchinger, T., Yang, L., Chen, A., Ju, K., Piao, S., Li, L.Z.X., Ciais, P., Chen, D., Liu, J., Azorin-Molina, C., Chappell, A., Medvigy, D., Wood, E.F., 2019. A reversal in global terrestrial stilling and its implications for wind energy production. Nat. Clim. Chang. 9, 979–985. https://doi.org/10.1038/s41558-019-0622-6

CHAPTER 4.
THE INFLUENCE OF TERRAIN RUGGEDNESS AND VEGETATION IN AN INLAND FRESHWATER COASTAL DUNEFIELD ON LAKE MICHIGAN

Kevin G. McKeehan[a], Alan F. Arbogast[a], and Kyla M. Dahlin[a]

a: Department of Geography, Environment, and Spatial Sciences, Michigan State University, Geography Building, 673 Auditorium Rd, East Lansing, MI 48824, United States.
mckeeha2@msu.edu and dunes@msu.edu

4.1 Abstract

Vegetation and terrain are linked in important ways, but in aeolian systems this relationship is understudied and poorly quantified. Here, we explored the relationship between terrain ruggedness and vegetation in a coastal dunefield along Lake Michigan's eastern shore. To quantify ruggedness at the dunefield at Ludington State Park, we calculated two terrain indices – Riley's Terrain Ruggedness Index (TRI) and Sappington's Vector Ruggedness Measure (VRM) – from 10m DEMs. To measure vegetation, we computed the Soil-Adjusted Vegetation Index (SAVI), also from 10m resolution data. We employed a land systems framework, which identified four land systems for analysis, specifically: foredunes, dune barrens, active inland linear dunes, and mature woodland dunes. Using this land systems approach, we found that ruggedness and SAVI were strongly-to-moderately negatively correlated in one land system – the dune barrens environment midway along the ecogeomorphic gradient between the foredunes and mature wooded backdunes. Within the dune barrens land system, we found that ruggedness decreased with increasing SAVI, which was interpreted as an increasing incidence of woody vegetation along with density. Likewise, with grassy or patchy vegetation, terrain ruggedness increased within the dune barrens land system, which is characterized as by mixed vegetation and hummocky landforms. In other land systems where one type of vegetation is dominant, no relationship was found between terrain ruggedness and vegetation. These finding suggest that, based upon the concepts of ecogeomorphic hysteresis, bistability, and deterministic chaos, vegetation is perhaps

exerting an overwhelming influence upon the landscape in the foredune and mature woodland dune land systems. By contrast, the dune barrens represent a land system where the feedback mechanisms amongst the dune system variables have not yet produced results that exceed the system's thresholds and drive a particularly dominant response. Thus, in the dune barrens, terrain ruggedness and vegetation still exert influence upon the other, producing more rugged grassy dunes and less rugged wooded dunes.

Keywords: Coastal dunes, terrain ruggedness, dunes, Lake Michigan, VRM, TRI, SAVI

4.2 Introduction

Vegetation and terrain are linked in important ways and form the basis of ecogeomorphic feedback mechanisms within dune systems (Dietrich and Perron, 2006; Schwarz et al., 2018; Wheaton et al., 2011). In dunefields in all climates, there are clear ecogeomorphic process-response mechanisms tied to the relationship between vegetation and terrain heterogeneity (Cowie et al., 2013; Schwarz et al., 2018), a concept which has many terminologies and definitions, including the word "ruggedness" (Lane, 2005; Smith, 2014). Amongst other ecogeomorphic functions, vegetation has the ability to stabilize dune landforms and deflect and trap airborne sand, integrating the deflated eolian material into the dune soil (Ruggiero et al., 2018; Zarnetske et al., 2012). These functions shape the dune landscape and directly affect its morphology (Salisbury, 1952; Sankey et al., 2010). In the geosciences, several methods exist for measuring terrain heterogeneity or ruggedness (Drummond and Dennis, 1968; Lane, 2005; Moore et al., 1991; Olaya, 2009; Smith, 2014). Additionally, there exists a well-documented and commonly-used method – the soil-adjusted vegetation index, known as SAVI – for quantifying vegetation on landscapes with high reflectance, such as those often found in dunefields (Huete, 1988). So, too, do the tools and data exist to quantify both ruggedness and vegetation (Bryant and Baddock, 2021). Still, a research gap exists in understanding how these concepts are quantitatively linked in dune landscapes, although some studies have advanced our knowledge in this regard (e.g., Stallins and Parker, 2003).

The purpose of this study is to learn more about the relationship between terrain ruggedness and vegetation in dunefields by specifically examining both variables at Ludington State Park on the eastern shoreline of Lake Michigan. Broadly, we intend to ascertain whether measures of ruggedness and vegetation from remotely-sensed data can be used to discern dune morphology, if differences in ruggedness and vegetation exists between different ecogeomorphic areas of the dunefield, and it a geostatistical relationship exists between terrain ruggedness and vegetation.

The answers to these questions could improve concepts regarding the ecogeomorphic processes and responses within dunefields, enhance coastal dunefield models, and help inform dune landscape management practices.

4.3 Literature Review and Justification

Dunefields, and the sand dunes contained within them, have great ecogeomorphic variability at multiple spatiotemporal scales (Carter, 1991; Walker et al., 2017). Dunes vary across time and space by morphology, height, width, steepness, soil and sand composition, and vegetation coverage and diversity (Cooper, 1958; Hack, 1941; Hesp et al., 2011; Hesp and Smyth, 2016; Mckenzie and Cooper, 2001; Melton, 1940), resulting in a "natural heterogeneity", according to Carter (1991). Driving this geomorphic variability is the nature of dune environments, which are subjected to the forces of wind and climate and can experience rapid changes in short periods of time (Miyanishi and Johnson, 2021; Smith et al., 2017). This is especially true for coastal dunefields (e.g., Davidson et al., 2021; Jackson et al., 2019), where changes can occur of hourly, daily, weekly, monthly, seasonal, annual, decadal scales or longer (Davidson-Arnott and Law, 1996; Hesp, 2002; van Dijk, 2014). Given this geomorphic variability and the associated potential instability of coastal dunefields, coastal dune management is of active concern (Arbogast et al., 2020; Bar et al., 2016; Barbier et al., 2011; Doody, 2013a; Harman and Arbogast, 2004; Laporte-Fauret et al., 2021; Millington et al., 2009; Pye et al., 2014; Weymer et al., 2015), especially considering the possible damage caused by migrating eolian sands (Loope et al., 1999).

Coastal dune systems are complex, multivariate process-response systems (Delgado-Fernandez et al., 2019; Walker et al., 2017). These systems, which govern dune and dunefield mode, often contain considerable stochasticity, which results in nonlinear geomorphic and ecogeomorphic

outcomes (Chorley, 1962; Hesp, 2002; Lichter, 2000; Miyanishi and Johnson, 2021; Phillips, 2007; Schwarz et al., 2018; Sherman and Bauer, 1993; Stallins and Parker, 2003; Walker et al., 2017; Werner, 1999; Wright and Thom, 1977). Some evidence suggests dune systems begin in equilibrium and are then driven toward complex, yet self-organizing patterns, behaviors, and states by the external energy inflicted upon them (Baas, 2002; Ewing et al., 2006; Horton, 1945; Kocurek and Ewing, 2005; Werner, 1999). By contrast, evidence also suggests that landform response in geomorphic systems in general (Baas, 2002; Leopold and Langbein, 1962; Phillips, 2006), and dune systems in particular (Baas, 2002; Forey et al., 2008; Phillips, 2007; Phillips et al., 1996), are partially, though not necessarily always, subject to entropy and stochasticity through the interactions of multiple, related variables. The variables determining landscape form and behavior, which include terrestrial, atmospheric, and – in coastal areas – marine and littoral processes, often influence each other and are intertwined in feedback mechanisms (Cooper, 1958; Delgado-Fernandez et al., 2019; Hesp, 2002; Ritchie, 1972; Schwarz et al., 2018; Stallins and Parker, 2003; Wright and Thom, 1977). For example, it has been observed that sand supply to dune blowouts can be constrained by the inception of vegetation downwind in the mouth of the blowout, fostering the growth of a foredune, which consequently further impedes the sand supply to the blowout (Cooper, 1958; Gares, 1992; Jewell et al., 2017; Lepczyk and Arbogast, 2005; van Dijk, 2004). Such a scenario may be related to climate or other factors, but, regardless, the ecogeomorphic consequences of the emergence of a vegetated foredune at the downwind mouth of a dune blowout are many, affecting blowout sand supply, vegetation type, foredune and blowout morphology, dune soil pedogenesis, and the potential stabilization of the blowout itself. And this is but one process-response mechanism amongst many in dune systems (Kim and Yu, 2009; Ruggiero et al., 2018; Walker et al., 2017; Wright and Thom, 1977).

Various studies have attempted to model the process-response mechanisms of coastal dunes at different scales to best explain dune behavior and form. Delgado-Fernandez et al. (2019) proposed a dune model that distilled through an ecogeomorphic lens the complex process-response interactions and human disturbances into the following formula: $V + D = V_O$, where V represents expected vegetation cover, D represents total natural and anthropogenic disturbance, and V_O represents observed vegetation cover. Within this formula are nested sub-routine formulae which feed the V and D parameters. For example, the D parameter is an estimated summation of all disturbance forcings in relation to vegetation coverage and bare sand extent; some disturbances, such as storm surge and visitor pressure, suppress vegetation and promote bare sand ($+D$), while other disturbances, such as planting and certain land use policies, fosters vegetation at the expense of bare sand ($-D$). For the V parameter, Delgado-Fernandez et al. (2019) calculate the dune-mobility index known as Lancaster's M (Lancaster, 1988; Lancaster and Helm, 2000), which attempts to determine dune behavior from a suite of climate variables. Specifically, Lancaster's M evaluates wind, annual precipitation and adjusted potential evapotranspiration as calculated using the Thornthwaite method in determining dune mobility potential (Lancaster, 1988; Lancaster and Helm, 2000; Thornthwaite, 1948; Thornthwaite and Mather, 1957). Thus, the V parameter in Delgado-Fernandez et al.'s (2019) formula is an attempt to estimate dune landscape response to some, often related, climate processes, without modeling all complex processes responsible for driving dune behavior and form.

The ecogeomorphic aspects of dune systems in particular exhibit such complexity, as vegetation exerts considerable control on dune morphology and behavior, including the physical fixation of dunes and the trapping of deflated and saltated sand flux (Cowles, 1899; Dech and Maun, 2005; Durán and Herrmann, 2006; Durán and Moore, 2013; Lee et al., 2019; McKeehan and Arbogast, 2021; Melton, 1940; Miller et al., 2001; Nordstrom, 2015; Olson, 1958; Ruggiero et

al., 2018; Schwarz et al., 2018; Wolfe and Nickling, 1993; Xu et al., 2015). For instance, Walker et al. (2017) compiled a list of 17 variables critical to determining coastal dune morphology and behavior and assigned each the role of dependent variable, independent variable, parameter, or indeterminate role at the spatiotemporal scales of landscape, landform, and plot. These three scalar categories span the breadth of the physical and temporal frameworks for dune systems, as scale is central to understanding dune behavior. The landscape category roughly operates at the spatial scale of a dunefield and the temporal scale of decades and more, while the landform category encompasses the approximate spatial scale of a dune and the temporal scale of months and years (Walker et al., 2017). The plot spatiotemporal scale is, therefore, the smallest spatial and shortest temporal scales of all. Underscoring the intricacy of dune systems, most of the variables change roles depending upon the spatiotemporal scale. For example, vegetation cover is a dependent variable at the landscape scale, working in response to the independent variables of time, geological context, sea/lake transgressions, climate, and coastal and littoral geomorphology (Walker et al., 2017). Yet, at the landform or dune scale, vegetation cover is both a dependent and independent variable, working in concert with 15 of the 16 other variables.

Other models emphasize other key variables to explain dune morphology and behavior, including several which focus on wind processes, which is a component of both Delgado-Fernandez's et al. (2019) and Walker et al.'s (2017) frameworks. Many models build upon the aeolian sediment transport model developed by Bagnold (1941), which primarily considers the relationship of wind shear velocity to threshold shear velocity, which is similar to shear stress (τ), and sometimes communicated as friction velocity. In many ways, Bagnold's work has formed the basis of the wind parameter, which is key in many dune models (Belly, 1962; Delgado-Fernandez, 2011; Durán et al., 2011; Hsu, 1971; Kawamura, 1951; Strypsteen et al., 2021). Often at issue in

these models was the need to parameterize the boundary-layer conditions that impacted threshold shear velocity, including most importantly mean dune sand grain size, the degree of surface roughness, dune vegetation coverage, and dune sand moisture content (Bagnold, 1941; Chepil et al., 1963; Fryberger and Dean, 1979). For example, the type of soil and the amount of disturbance in dune sands can affect the threshold shear velocity (Gillette et al., 1980). To solve this model parameterization problem, Fryberger and Dean (1979) proposed to calculate *potential* sand drift by estimating these related boundary layer and dune variables. In their classic paper, Fryberger and Dean (1979) detailed the drift potential (*DP*) model, which calculates the potential for sand transport by focusing solely on wind power (Fryberger and Dean, 1979; Yizhaq et al., 2007). The aforementioned Lancaster's *M* addresses the same issue from a more climatologically wholistic approach (Lancaster, 1988). In addition to wind power, Lancaster's *M* incorporates rainfall effectiveness, which could be related to both dune vegetation coverage potential and dune sand moisture content.

Parameterizing the variables central to aeolian sediment transport models remains a challenge, as Fryberger and Dean (1979) noted, as these variables are difficult to observe in the field, especially at smaller scales (Bauer and Davidson-Arnott, 2003; Davidson-Arnott et al., 2018). Two of these variables – surface roughness and vegetation – which affect aeolian sand transport and determine dune form and behavior are likely related (Levin et al., 2008; Wolfe and Nickling, 1993) and possibly exhibit interrelated feedback processes (Schwarz et al., 2018). In meteorology, engineering, and some aeolian studies, surface roughness, which is sometimes called aerodynamic roughness or surface roughness length (z_0), most often refers to height above the surface at which the wind speed theoretically would be negligible due to the physical biotic and abiotic ground objects (Durán et al., 2011; Lane, 2005; Raupach, 1992; Shao and Yang, 2005). Some studies have established a relationship between z_0 and the frontal windward area of

ground objects, also known as roughness density (λ) (Durán et al., 2011; Okin et al., 2006; Shao and Yang, 2005). Yet, z_0 as a measure of wind flow and a roughness numerical modeling parameter is different from the physical roughness of the surface, which is sometimes called geometrical roughness (Durán et al., 2011; Smith, 2014) or terrain ruggedness (Riley et al., 1999; Sappington et al., 2007).

Terrain ruggedness and z_0 share a similar terminology, but have different meanings (Lane, 2005). Yet, z_0 and terrain ruggedness are related (Sherman and Bauer, 1993; Smith, 2014). Clearly, a mountainous landscape with a high terrain ruggedness would also exhibit high roughness density through an extensive exposed windward frontal area (λ), resulting in a large z_0 value. In fact, efforts have been made to link z_0 values to landscape features and classifications (e.g., Wiernga, 1993, 1986). Yet, such correlations are only somewhat useful in geomorphology, as their applications often assume a homogenous landscape, such as agroecosystems, and consider the built environment (Brown and Hugenholtz, 2012). The application of z_0 values to aeolian properties in complex process-response landscapes with multiple feedback mechanisms, rather than homogeneous settings, is "still rather rudimentary" (Sherman and Bauer, 1993). Still, conceptually, it is important to note the geomorphic link between z_0 and terrain ruggedness, as the latter exerts influence in several geophysical systems (Grohmann et al., 2011; Moore et al., 1991). For example, terrain is a fundamental driver in the development of soils (Jenny, 1941), including coastal dune soils (Kim et al., 2008). Terrain ruggedness also influences soil erosion from rainfall and fluvial forcings, as erosion increases with increased ruggedness (Römkens et al., 2002). Further, ruggedness is a key metric in assessing landslide risk in physical hazards geography and engineering (Althuwaynee et al., 2014; e.g., McKean and Roering, 2004; Różycka et al., 2017). There is also research into how terrain ruggedness affects fluvial and

glacial processes, including the development of erosional and depositional events (Lane, 2005; Smith, 2014).

Specifically, terrain ruggedness is a metric of "terrain complexity" (Olaya, 2009), an attempt to express the landscape variability at scale (Grohmann et al., 2011; Moore et al., 1991; Sankey et al., 2010). In aeolian geomorphology, terrain ruggedness is acknowledged to influence or be influenced by process-response systems in dune environments, often as part of feedback mechanisms (Smith, 2014), although this acknowledgment has been advanced whether measured directly or inferred indirectly through landscape interpretation. In other words, some aeolian studies have measured terrain ruggedness intentionally and quantitatively (e.g., Sankey et al., 2010), but far more have inferred a relationship between dune systems and terrain ruggedness, without directly measuring it as such. For example, workers have studied the possible relationship between aeolian sand budgets and the form, height, and volume of coastal foredunes (Davidson-Arnott et al., 2018; Durán and Moore, 2013; Walker et al., 2017). These three coastal foredune metrics, when taken together, possibly could be interpreted as a quantification of terrain ruggedness by other means. In this suite of foredune studies, it was proposed that foredune height had a maximum limit controlled by the growth of vegetation, rather than sand supply from the foreshore (Durán and Moore, 2013). A later study found no maximum control imposed by vegetation on foredune height and instead found that ample sand supply could contribute to vertical dune accretion for decades if conditions were unchanged (Davidson-Arnott et al., 2018).

Rugged terrain in dunefields also influences how eolian sand is transported through the system, thus affecting dune form. This effect can be observed with dune blowouts, which are erosional features which have "blown out" through existing dunes due to natural or anthropogenic means (Adamson et al., 1988; Bate and Ferguson, 1996; Hesp, 2002). The morphology of blowouts makes their form and progression uniquely susceptible to changes in airflow and sand transport

due to terrain characteristics, including ruggedness. The high lateral walls of blowouts – very often fixated by vegetation – that bracket the erosional deflation basin are excellent conduits for airflow and the transport of sand, which both follow the morphology of the blowout and shape it, too (Hesp and Hyde, 1996; Pease and Gares, 2013). Additionally, topographically vulnerable dunes and dune crests – which could be interpreted as having higher ruggedness than the surrounding landforms – often are the point of "attack" for aeolian forcing, resulting in erosion and blowout inception (Cooper, 1958). This is often due to the aerodynamic forces associated with the topographic acceleration of airflow over the rugged point of vulnerability, often an elevated dune crest (Hesp, 2002). Beyond blowouts, studies have found terrain slope, "geometry", and other important topographic elements drive dune morphology and other characteristics (Bauer and Davidson-Arnott, 2003; Howard et al., 1978; Jerolmack et al., 2012; Zhao et al., 2019). All these terrain elements and others could be construed as indirect, informal measurements of terrain ruggedness.

The most conceptually straightforward measurements of terrain complexity involve slope (Chrisman, 2002, p. 170), defined simply as the change in elevation over a surface (Bolstad, 2008, p. 417). In calculus and geometry, the first-order derivative of a function can be expressed as the slope of the line representing the function's rate of change. Thus, it should be unsurprising that in geomorphology the terrain metric of slope is the first-order derivative measurement of a landscape, given a set of gridded z values representing the landscape's surface as a scalar field (Chrisman, 2002, pp. 170–179). Consequently, slope is an oft-used landscape metric due to its simple linkages to geomorphic principles, mathematical concepts, and its ability to be analyzed statistically (Olaya, 2009). In fact, a statistical assessment of slope – its standard deviation – is also a common terrain ruggedness metric (Grohmann et al., 2011; Olaya,

2009). Grohmann et al. (2011) utilized the standard deviation of slope amongst other metrics in their study of a varied landscape in Scotland.

The second-order deviation of slope, known as curvature, is also a commonly-used surrogate of terrain ruggedness and can be calculated using specific terrain functions in many geographic information systems (GIS) software packages (Grohmann et al., 2011; Olaya, 2009; Schmidt et al., 2003). Curvature is the "concavity and convexity" of the surface and is comprised of three components – profile, planform, and tangential curvature (Grohmann et al., 2011; Olaya, 2009; Schmidt et al., 2003). Profile measures the curvature parallel to the slope aspect, while planform considers the curvature of the surface perpendicular to the slope. Schmidt et al. (2003) employed curvature in their assessment of terrain ruggedness in a varied landscape in Germany, as did Grohmann et al. (2011) in their aforementioned study in Scotland. Importantly, as a second-order derivative, curvature assesses the manner of change of slope, which itself is a derivative of the actual surface. Geomorphologists have considered using a third-order derivative of slope – the rate of change in curvature – in further landscape studies, but, this, thus far, has remained mostly theoretical and it has yet to be widely evaluated quantitatively (Minár et al., 2013). Fractal geographers also have proposed the computation of various fractal metrics, including the fractal dimension of a landscape, as a method of determining terrain ruggedness (Lam and De Cola, 1993; Moore et al., 1991; Olaya, 2009; Smith, 2014).

Clearly, a multitude of methods have been advanced for the calculation of terrain ruggedness (Drummond and Dennis, 1968; Grohmann et al., 2011; Moore et al., 1991; Olaya, 2009; Smith, 2014), but a different approach exists separate from the calculation of slope derivatives, its statistics, and fractal geography. Several workers have developed or used existing indices which assess terrain ruggedness. Many of these indices were developed in the field of wildlife ecology and have been used to explore habitat suitability for species (e.g., Beasom et al., 1983; Riley et

al., 1999; Sappington et al., 2007), although the effectiveness of such analyses, like all assessments of terrain ruggedness, depend upon choosing the appropriate landscape scale (Wilson et al., 2007). Ecologists have used surficial roughness to assess habitats for bobcats (*Felis rufus*) in Idaho (Koehler and Hornocker, 1989), for antelope in Africa (Coetzee and Fabricius, 1992), for bighorn sheep (*Ovis Canadensis nelsoni*) in the Mojave Desert of North America (Sappington et al., 2007), and even for marine species in oceanic environments (Wilson et al., 2007).

In the geosciences, various terrain ruggedness indices have been used to identify landforms and geologic attributes (e.g., Caruso et al., 2018; De Reu et al., 2013; Mokarram et al., 2015; Tagil and Jenness, 2008), delineate the confines of watersheds (e.g., Pike and Wilson, 1971), determine soil erosion potential (e.g., Kreznor et al., 1989), and analyze landscape susceptibility to landslides and mass wasting (e.g., Claessens et al., 2006), where extensive use of indices have been deployed (Różycka et al., 2017). In aeolian geomorphology, terrain ruggedness indices were used to determine landscape heterogeneity in China's Loess Plateau (Dong and Shortridge, 2019), amongst other studies. Some reviews in geoscience literature even place the mathematical models of fluvial network irregularity, such as Horton's Laws (Horton, 1945) and Schumm's drainage basin area index (Schumm, 1956), as terrain ruggedness index methods (Beasom et al., 1983; Drummond and Dennis, 1968; Kirchner, 1993; Melton, 1956). The goal of developing and deploying indices in geomorphology is to capture statistically any correlation between interrelated geophysical processes and resultant phenomena, such as landforms, at a particular scale (Melton, 1956; Weiss, 2001). Generally, indices, including most terrain ruggedness indices, are composite indicators often built from other statistics and designed to be mathematical measures of change (Ralph et al., 2015, pp. 1–8). Most indices are referenced to benchmarks (Ralph et al., 2015, pp. 1–8), such as landform classifications. For example, the values from

Riley's Terrain Ruggedness Index (TRI) are pegged to corresponding landscape classes, from "Level" to "Extremely Rugged" (Riley et al., 1999).

As there are many methods of determining terrain ruggedness (Moore et al., 1991), so, too, are terrain ruggedness indices, each unique in scope and approach (Drummond and Dennis, 1968; Olaya, 2009). An early index of note is Melton's HD, or "ruggedness number" (Beasom et al., 1983; Drummond and Dennis, 1968; Melton, 1956). Melton's HD was devised to capture the effects of interrelated climatological and geomorphological processes on fluvial system morphology and behavior at the scale of the drainage basin (Melton, 1956). Yet, Melton condensed these complex process-response relationships into a simple formula which could be easily computed; for Melton, ruggedness (HD) could be expressed as the product of total relief (H) and drainage density (D), or total length of all streams per unit of area (Beasom et al., 1983; Drummond and Dennis, 1968; Melton, 1956; Olaya, 2009). Melton acknowledged that the HD number was a synthesis of Horton's Laws, but also aimed to develop an index that was firmly affixed to the geomorphic concept of terrain ruggedness (Melton, 1956).

Other important indices followed, including Salisbury-McConnell's relief-slope relationship index (McConnell, 1966), Hobson's surface roughness factor (Hobson, 1972), and Beason et al.'s (1983) Land Surface Ruggedness Index (LSRI), which measured the density of contour lines to determine terrain complexity. Two of the most frequently used indices – the Topographic Position Index (TPI) and the Topographic Wetness Index (TWI) – were mostly developed later. The TPI, which built upon the ideas of Fels and Zobel's Landscape Position Index (Tagil and Jenness, 2008), evaluates the relative elevation difference of a pixel in a digital elevation model (DEM) to its neighborhood pixels (Weiss, 2001), whereas the TWI emerged from Beven and Kirkby's (1979) and O'Loughlin's (1986) work and was codified into a common index to estimate soil water

characteristics across a landscape (Beven and Kirkby, 1979; Moore et al., 1991; O'Loughlin, 1986; Różycka et al., 2017).

In light of recent advances in quantitative computing power and the increased availability of digital terrain data, these indices and others not noted could be the subject of a comprehensive geomorphometric review paper, as previously reviews of ruggedness research tended to focus more on derivative methods rather than indices (e.g., Smith, 2014). Yet, for our purposes, we will concentrate on Riley's Terrain Ruggedness Index (TRI) and Sappington's Vector Ruggedness Measure (VRM) (Riley et al., 1999; Sappington et al., 2007). These two indices, which are detailed in our Methodologies section, both are designed solely to discern terrain heterogeneity, which given Carter's (1991) "natural heterogeneity" of aeolian landscapes, seems appropriate for dunefield analyses. Further, Sappington's VRM was developed specifically in response to perceived issues with Riley's TRI (Sappington et al., 2007). Thus, our analysis of terrain ruggedness will utilize these two indices.

A key factor in shaping the ruggedness of terrain is the presence of vegetation. For example, recent studies have shown a global expansion of vegetation since the 1980s (Cowie et al., 2013; Zhu et al., 2016). A possible consequence of this expansion is that while observed wind speeds over ocean expanses have increased, terrestrial wind speeds have decreased, an effect likely due to increased terrain ruggedness associated with a more vegetated surface (Zeng et al., 2018). This terrestrial "stillness", as Zeng et al. (2018) termed it, has ecogeomorphic consequences in aeolian systems. Increased vegetation in dunefields reduces aeolian erosion and sediment flux (Lancaster and Baas, 1998; Lee et al., 2019), which in turn reduces dunefield dust production (Cowie et al., 2013; Sweeney et al., 2016; Werner et al., 2011). The opposite is also true, as decreased vegetation in dunefields sets in motion feedback mechanisms fosters more dust production (Lee and Gill, 2015). Vegetation can also deflect and trap airborne dust and

saltating sand, contributing to changes in dune morphology and elevation through accretion (Cohn et al., 2018; Gardner and McLaren, 1999; Maun, 1998; Suter-Burri et al., 2013; Werner et al., 2011; Wolfe and Nickling, 1993). This action often enriches the soil, which fosters the embryonic soil development already underway, enhancing vegetative growth through a positive feedback mechanism (Hesp, 1981).

Through these ecogeomorphic mechanisms, vegetation fixates dunes, stabilizing and shaping their morphology (Cowles, 1899; Doing, 1985; Durán and Herrmann, 2006; Lee et al., 2019; Olson, 1958; Pelletier et al., 2009; Xu et al., 2015). For some workers, the presence of vegetation is the pretext for the development of a sand medium into a more advanced dune landform (e.g., Doing, 1985; Salisbury, 1952), usually beginning as nebkha dunes (Charbonneau et al., 2021), as some grass and shrub species possess ecogeomorphic qualities inherent to "dune-building" (van Denack, 1961). Cowles (1899) used several terms to describe plants possessing this capability. To Cowles, such a plant, including the Eastern Cottonwood (*Populus deltoides*), which could be found as a sentinel plant amongst a bare sand dune or blowout, was a "sand-binder", a "dune-holder", and a "dune-former". Durán and Moore (2013) called these types of plants "dune-building grasses," although the differences in morphology, growth form, tillers, and other characteristics result in dissimilar effectiveness in these ecogeomorphic capabilities amongst species (Ruggiero et al., 2018; Stallins and Parker, 2003; Wolfe and Nickling, 1993; Zarnetske et al., 2012).

The ecogeomorphic function of vegetation is mostly well-established (Lee et al., 2019), although many mechanisms are unclear, especially with regards to dune ruggedness. Durán and Moore (2013) found a "coevolution" – a term echoed by Miyanishi and Johnson (2021) – between terrain and vegetation, while Juergens et al. (2013) used terrain ruggedness as a determining factor in crafting a vegetation classification map of the central Namib Desert. Stallins and Parker

(2003) found that vegetation "mediated" the systemic organization of dune morphology and biogeographic gradients in coastal barrier island systems along the North American Atlantic shore. Still, the broader details of results of the process-response ecogeomorphic mechanisms remain unclear. The signatures of biotic processes have imprinted the terrestrial world in comprehensive ways, leading to new ideas about ecogeomorphic process-response relationships (Dietrich and Perron, 2006; Reinhardt et al., 2010; Ruggiero et al., 2018; Wheaton et al., 2011; Zarnetske et al., 2012). Yet, in some aeolian landscapes, these signatures with regards to ruggedness are difficult to discern. Some research has focused on dune height and its relationship to vegetation coverage. Although imperfect, the metric of dune height could be assumed as a proxy for the ruggedness of an aeolian terrain. For example, Xu et al. (2015) found that vegetating dunes in western China became "elongated" with lower dune heights, an effect that lowered their aerodynamic roughness (z_0) and, presumably, lowered their terrain ruggedness. Other studies found similar results (e.g., Cowles, 1899; Durán and Herrmann, 2006; Durán and Moore, 2013; Levin et al., 2006; Pelletier et al., 2009; Roskin et al., 2014a, 2014b). Two studies from Israel found vegetated dunes had "elongated" over time (Roskin et al., 2014a, 2014b), possibly becoming less rugged. Also in Israel, Levin et al. (2006) generally found dunes with higher elevation to have a correlation to higher Soil-Adjusted Vegetation Index (SAVI) values. Cowles (1899) noted qualitatively in his survey of Lake Michigan coastal dunes that active, bare sand dunes were "rough and uneven" compared to vegetated dunes nearby. Pelletier et al. (2009) found that unvegetated coastal dunes in North Carolina were higher and more topographically complex than vegetated dunes, which had lower elevations. Two related studies emerging from work in White Sands, New Mexico, developed and expanded upon a model which proposed that vegetation imposed a maximum dune height (Durán and Herrmann, 2006; Durán and Moore, 2013), suggesting that vegetated dunes would shed their rugged profile over time and become smoother landforms. Durán and Moore (2013, fig. 6) also

proposed a model scenario in which a coastal dunefield with a short, reflective beach could transition to a smooth, vegetated, mostly homogeneous sand sheet over time, again linking vegetation to a reduction in terrain ruggedness.

Other studies reached different conclusions regarding vegetation and various proxies for ruggedness (e.g., Davidson-Arnott et al., 2018; Ruggiero et al., 2018; Sankey et al., 2010; Zarnetske et al., 2015). Davidson-Arnott et al. (2018) directly refuted Durán and Moore's (2013) model assumptions and conclusions. According to Davidson-Arnott et al. (2018), there is no theoretical dune height maximum related to vegetation growth. Instead, the ecogeomorphic functions of vegetation would continue to act upon the dune based upon conditions, allowing plants to deflect and trap more and more airborne dust and saltating sand. Thus, vegetated dunes could continue to accrete and grow vertically and horizontally (Davidson-Arnott et al., 2018), theoretically maintaining a relatively rugged profile. The possibility of relatively rugged, vegetated dunes is supported by other studies. In a series of studies of Pacific coastal dunes, foredune elevation increased with vegetation cover (Ruggiero et al., 2018; Zarnetske et al., 2015). The observed vegetated foredunes in these studies increased in height and became adept at trapping sand downwind of the foreshore, becoming more rugged against the wind. This effect was also observed in an inland dune environment in Idaho, where more rugged terrain expanded vertically through aeolian depositional processes, while smoother dunes lost surface elevation through erosion (Sankey et al., 2010).

Somewhat equidistant to these studies, Jerolmack et al. (2012) proposed a model based upon an empirical study of dunes at White Sands. In the model, a large unvegetated foredune at the most windward point in a dunefield creates an internal boundary layer (IBL) based on the relative sudden increase in z_0, resulting in a first-order pattern of smaller dunes downwind that become more vegetated with distance from the roughness of the IBL contact (Jerolmack et al., 2012, fig.

2). The effect would be similar to what transpired in several dune blowout studies, where an observed foredune at the throat of a blowout grew continuously until it choked off sand supply upwind to the deflation basin, resulting an expansion of vegetation there (e.g., Gares, 1992). This pattern has also been observed elsewhere in coastal dunes (e.g., Otvos, 2000). Moreover, a study of foredunes at the southern end of Lake Michigan concurred with this model, noting a "steepness" to the initial foredunes that contrasted to vegetated "low" backdune areas (Poulson, 1995). Salisbury (1952) described a similar, but slightly different pattern along a representative transect of coastal dunes in Britain. For Salisbury, it was typical to find a vegetated foredune to be the largest dune in a coastal dunefield, with backdune areas densely vegetated and topographically smooth. Thus, Salisbury's representative transect is part Jerolmack et al. (2012), part Davidson-Arnott et al. (2018), and part Durán and Moore (2013). Further, while Salisbury's (1952) dunefield description was rather spatially delineated, such a description recalls Carter's "natural heterogeneity" of dunes and Phillips' (2007) randomness of geomorphic systems. Both Doing (1985) in temperate coastal dunefields and Suter-Burri et al. (2013) in laboratory experiments documented heterogeneity and non-linear responses in dune morphology with respect to terrain and vegetation. Suter-Burri et al. (2013) even paraphrased Okin et al. (2006) by noting that vegetation growth leads to dunefield heterogeneity in which a "small-scale mosaic of depositional and erosional sediment transport regimes" develop geomorphologically throughout the landscape.

This paper does not intent to resolve the differences between these studies. Instead, the purpose of this study is to determine more about the relationship between terrain ruggedness and vegetation in dunefields – and hopefully illuminate which, if any, of these models is valid for our study area. As we've demonstrated, terrain ruggedness – not z_0 – has been explored mostly indirectly in aeolian system research, leaving the concept broadly understudied. Moreover,

ruggedness appears related to one of the most important variables driving dune morphology and behavior – vegetation. For this work, we intended to answer a series of related questions by calculating Riley's TRI and Sappington's VRM through an ecogeomorphic land-systems approach in a coastal dunefield along Lake Michigan's eastern shoreline. To determine vegetation coverage in the study area, we calculated SAVI and then related the results to the ruggedness metrics within these ecogeomorphic land systems. We aim to answer 1) if TRI, VRM, and SAVI can detect dune morphology and ecosystems; 2) if different dunefield land systems are more rugged than others; 3) if TRI, VRM, and SAVI can be a proxy for time since dune activity in landforms, with the more mature vegetation suggesting long-stabilized mature dunes; 4) and, finally, if there is a relationship between terrain ruggedness and vegetation? Our hypotheses to these questions are that a relationship between vegetation type and terrain type exists and that these metrics can enlighten our knowledge of terrain ruggedness and vegetation in dunes. Specifically, we hypothesize that grassy vegetation is either related to more rugged terrain or less rugged terrain than woody vegetation.

4.4 Study Area

Lake Michigan's eastern shore contains a distinctive coastal dune system, comprising of ~3.5M acres of dunes (Arbogast et al., 2018) (Figure 1). The coastal dunes here are possibly the largest freshwater dune system in the world (Peterson and Dersch, 1981) and developed under conditions unique from most other coastal dune systems elsewhere (Hansen et al., 2010). Specifically, the Lake Michigan coastal dune systems developed without the influence of tectonic or tidal activity (Hansen et al., 2010). Instead, Lake Michigan's coastal dunes formed mostly due to reworking of sandy glacial and lacustrine deposits by forces related to climatic and lake level variability (Hansen et al., 2010; Loope and Arbogast, 2000; Lovis et al., 2012; Thompson et al., 2011). According to reconstructed lake level chronologies and the dating of aeolian sands and buried

soils at many dune sites (e.g., Arbogast and Loope, 1999; Baedke and Thompson, 2000; Fulop et al., 2019; Kilibarda et al., 2014; Loope and Arbogast, 2000), coastal dunes began forming during ancestral Lake Michigan's Nipissing high phase (~5.5ka) (Arbogast et al., 2002; Lovis et al., 2012). Some dune sites, especially along the lake's southern shore, may have begun forming somewhat later (e.g., Argyilan et al., 2014; Kilibarda et al., 2014), but since then periods of dune activity and stability followed (Lovis et al., 2012).

During the last ~2k years, the general state of dunes along the Lake Michigan shore has roughly oscillated between mostly stable, mostly active, and mixed, although the transitions to these states has been spatially and temporally non-linear. From ~2ka to ~1ka, dunes in some areas here were largely stabilized by vegetation, a condition which resulted in the formation in dunes along Lake Michigan's southeastern coast of an Inceptisol informally known as the Holland Paleosol (Arbogast et al., 2004; Lovis et al., 2012). Dunes subsequently reactivated and remained so throughout the Little Ice Age (LIA) and into the modern period until very recently (Lovis et al., 2012; McKeehan and Arbogast, 2021). Beginning sometime in mid-to-late 20th Century, dunes along the Lake Michigan coast began stabilizing due to an expansion of vegetation, according to repeat photographic analyses (McKeehan and Arbogast, 2021; White et al., 2019).

To better understand the relationship of terrain ruggedness to vegetation in dune systems, we selected as a study area the coastal dunefield of Ludington State Park in the USA state of Michigan (Figure 2). The northern portion of the state park was the subject of Brown and Arbogast's (1999) digital photogrammetric study of dune sediment transport over a 22-year period from 1965 to 1987. Using aerial imagery to build DEMs, that paper found an increase in sand sedimentation, especially in vegetated areas (Brown and Arbogast, 1999), an effect likely due to the ecogeomorphic function of vegetation, which can trap aeolian sand and aggrade the landscape (Olson, 1958; van Denack, 1961; Zarnetske et al., 2015). In many ways, Big Sable

Point, at the mouth of the Big Sable River, is the pivot point for the park, the lakeshore, and Lake Michigan's coastal dune systems. Ludington State Park sits astride the Big Sable River, which bifurcates the park roughly into two sections. Big Sable Point is also the approximate midway point between the southern end of Lake Michigan and the Straits of Mackinac at the northern tip of the Lower Michigan, where Lake Michigan transitions into Lake Huron. Ludington State Park also sits just south of a isostatic hinge line, north of which the earth's crust is still isostatically rebounding from the presence of continental glaciers (Larsen, 1987; Lovis et al., 2012), which exited Lower Michigan at ~11.8ka (Larson and Schaetzl, 2001). Relatedly, north of Ludington State Park and Big Sable Point, the coastal dunes are geomorphically more isolated landforms, with dunefields perched high on prominent headlands, tucked into embayments, and at the mouths of rivers, such as the Platte River, while within the park and south of Big Sable Point the dunes are mostly low-perched systems (Lovis et al., 2012).

While there have been no known studies dating dunes at Ludington State Park, studies from nearby dunefields can illuminate the park's likely aeolian geochronology. The dunes at Ludington State Park likely began forming ~4.5ka during the Nipissing high lake stand (Blumer et al., 2012; Hansen et al., 2010), which coincided with the end of the Holocene Climatic Optimum in North America (Schaney et al., 2021). A period of dune building across the immediate region followed at ~3.5ka (Blumer et al., 2012; Lovis et al., 2012), when a dune ridge probably formed ~0.5km east of the modern shoreline atop lacustrine sediment along the archaic coast (Lovis et al., 2012). To the north ~50km at Arcadia Dunes, the large, high-perched dunes there were active ~1.7ka and again intermittently beginning ~1.0ka until ~0.5ka (Blumer et al., 2012). Photographic evidence suggests large parts of Ludington State Park were bare sand until recently (Brown and Arbogast, 1999; McKeehan and Arbogast, 2021; White et al., 2019). According to ground-level photographs, the area surrounding Big Sable Lighthouse on Big Sable Point was mostly bare sand

~100 years ago (McKeehan and Arbogast, 2021) (Figure 3). In 1938, only ~20% of the park was vegetated, according to aerial photographs; by 2014, nearly half the park's sand dunes had become vegetated (White et al., 2019, fig. 6).

As a result of these episodic periods of dune activity and stability, much of the aeolian geomorphology of the park consists of low-perched transgressive dunes, linear and parabolic in nature, that mantle a baymouth bar complex (Brown and Arbogast, 1999; Hansen et al., 2010). Impounded behind Ludington State Park's relatively wide bar complex is Hamlin Lake, which developed through the Big Sable River's interaction with the bar dune formation at the river's mouth. Barrier bar complexes such as Big Sable Point often occur on the Great Lakes where longshore sediment transport fosters the formation of a barrier across a coastal embayment (Hansen et al., 2010). Where these baymouth bar complexes are wide, the Great Lakes dunefield morphologies are often more complex (Hansen et al., 2010), in a manner similar to a wide, dissipative beach described by Short and Hesp (1982). Ultimately, the resulting dunefield landscape at Ludington State Park is an ordered geomorphic gradient, where younger dunes lakeward transition to older dunes downwind and inland.

In addition to functioning as a geographic and geomorphic pivot point, the area also serves as an ecological transition point. The park is situated within a climatic transition zone between the northern hardwood forest zone to the south and the boreal forest zone to the north (Dister, 2017). As such, the park contains species of both zones (Dister, 2017). Ludington State Park exhibits a *Dfb* climate, which is classified as cold and without a dry season, but possessing a warm summer, according to the revised Köppen-Geiger climate classification scheme (Peel et al., 2007) and meteorological data from the Michigan State Climatologist for the nearest weather station at Manistee. Specifically, Manistee experiences an average of ~1,200mm of precipitation annually, cold winters with a mean January temperature of -4.6°C and warm summers with a

mean July temperature of 21.3°C. The prevailing wind regime at the Muskegon meteorological station ~90km on the coast to the south is bimodal from the southwest and northwest, resulting in mostly onshore sand transport, according to Brown and Arbogast (1999).

There are 8 areas of analysis within this study area, representing four different ecogeomorphic land systems (Figure 2). The land systems approach to geomorphic analysis was advanced by Christian and Steward (1964) as a landscape categorization methodology which emphasized *observed* patterns of landforms, soils, and vegetation (Wilson, 1997). According to the land systems theory, locations within a study area which exhibit similar of landforms, soils, and vegetation could be assumed to experience similar ecogeomorphic processes and could, therefore, be grouped into the same land system for the purpose of analysis (Christian and Stewart, 1964; Wilson, 1997). The land systems analytical framework is most commonly employed in the study of complex glacial landscapes (e.g., Schaetzl et al., 2020), but given the geomorphic gradient often inherent in coastal dune environments (e.g., Chen et al., 2015; Lepczyk and Arbogast, 2005) a land systems approach to coastal dunefield analysis is appropriate. The land systems concept differs from a chronosequence classification, as the latter is concerned with temporally-driven clustering (Schmid, 2013). Further, the aim of chronosequence analysis is to make assertions about the geomorphic age of the landscape, vegetation, and soils, using what we know about a space as a substitute for what we don't know about time (Phillips, 2021). Additionally, the "natural communities" botanical framework, while helpful from a biogeographical perspective, clusters ecogeomorphic regimes through the use of botanical surveys and collections (e.g., Dister, 2017) and may not consider geomorphic setting as extensively for our purposes. By contrast, the lands systems approach is an analytical framework that classifies landscape regions based upon observations often from aerial photographs and pattern analysis (Christian and Stewart, 1964). For example, Christian and Stewart (1964) distilled a ~100,000

km^2 sandy region of central Australia into four categories based upon predominant landforms, soils, and vegetation as observed by images taken from an airplane. The resulting four land systems were 1) sand plains, 2) swales, 3) linear dunes, and 4) alluvial flats (Christian and Stewart, 1964).

Within our study area, the land systems approach led us to select areas of analyses based upon an observed clustering of dune landforms and vegetation type. As a guide in constructing a land systems framework, we used several sources, including the coastal dune land systems schema proposed by Salisbury (1952) and modified by Doody (2013b), plus a natural communities and flora inventory undertaken by Dister (2017) at Ludington State Park, in addition to institutional knowledge of the study area. We did not adhere strictly to any particular system, however, and crafted a land systems approach from all these sources. From the lakeshore inland, our land systems for this research analysis included 1) foredunes, which are "young dunes" and sometimes "yellow dunes" in Salisbury's (1952) and Doody's (2013b) methodology, 2) dune barrens, which were identified by Dister (2017), 3) active upland linear dunes, and 4) mature woodland dunes (Figure 2 and Figure 4). Foredunes and yellow dunes are mostly associated with dune-fixating grasses along the coast, while the mature woodland dunes here are often the oldest dunes in the dunefield and are characterized by mature forests (Doody, 2013b; Salisbury, 1952). Between these two poles in the dunefield ecogeomorphic gradient is an interdunal region with swales – mostly unvegetated and periodically wet areas immediately downwind of the foredunes where scour has driven the land surface to the water table – and, then, sequentially dune barrens (Cohen et al., 2015; Dister, 2017; Doody, 2013b). Between the dune barrens and the mature woodland dunes at Ludington State Park is an area of mostly active upland linear dunes characterized by bare sand, some grasses, and relatively high elevation. There is no topographic

impediment windward of these linear ridges, which represent some of the highest points in the study area.

Midway along the gradient from the lakeshore to the mature woodland dunes is a key area for the purposes of this study – the dune barrens land system. Dune barrens usually contains patchy vegetation of a mixed variety, including woody vegetation and grasses, in an irregular pattern (Doody, 2013b). In the Lake Michigan region, Cohen et al. (2015) described the dune barrens natural community as a "savanna" of "scattered and clumped trees and an often dense, low or creeping shrub layer". Often, plants here are also fire- and drought-resistant (Doody, 2013b; Salisbury, 1952). The precise definition – and name – of this land system is not established and definitions often blur into other dunefield land system categories. To some, this area is called interdunal "barrens" (e.g., Cohen et al., 2015; Dister, 2017) or "dune shrubland" (e.g., Hop et al., 2011), especially in the Lake Michigan basin. In other sources, "grey dunes" seem to refer to dune barrens (e.g., Riksen et al., 2016; Salisbury, 1952), while "dune scrub" is used elsewhere (e.g., Doody, 2013b; Holton and Johnson, 1979). In Salisbury's (1952) system, this landscape beyond the foredune and swale regions and lakeward of the mature woodland dunes could also be described as a late yellow dune stage or a transition to grey dunes ecogeomorphology.

For our analysis, two sites from four land systems – foredunes, dune barrens, active upland linear dunes, and mature woodland dunes – were examined, one each north and south of the Big Sable River. The swales land system was not selected for analysis due to concerns that ponded water would alter the detection of both ruggedness and vegetation. The south foredune and dune barrens sites overlap slightly with a study site from McKeehan and Theuerkauf (*in prep.*). Additionally, the southern land systems are arrayed in a transect from the lake inland. Unfortunately, this was not possible north of the Big Sable River due to erosion of some foredunes on the north shore. Consequently, we could not select a series of land system areas that

resembled a transect, but instead selected the areas which best represented each land system north of the river.

4.5 Methodologies

4.5.1 Digital Elevation Models

The foundational dataset for measuring many land surface characteristics, including ruggedness, is the digital elevation model (DEM) (Olaya, 2009). A DEM is a raster dataset which stores elevation values for a location in a matrix of similar-sized cells and is often derived from the raw *z*-value points of LiDAR data (Bolstad, 2008, pp. 265–270). For our study, we chose DEMs from the United States Geological Survey (USGS) with a spatial resolution of ~10m. Finer-scale DEMs (<2m) have been used to assess ruggedness at the plot scale level in other studies (e.g., Sankey et al., 2010) and were available. However, the finest resolution at which SAVI values could be obtained remotely was 10m (see below). Thus, we chose to utilize the 1/3 arc-second resolution (~10m) DEMs from the USGS's 3D Elevation Program (3DEP) dataset (USGS, 2019). Temporally, the DEMs were created from "diverse source data" collected between 2015 and 2019 (USGS, 2019), but appears to be from 2019 in our case.

4.5.2 Terrain Ruggedness Indices

From these DEMs, ruggedness can be calculated. We employed two indices – Riley's TRI and Sappington's VRM – to determine the ruggedness at various scales at Ludington State Park. Both indices were developed to assess the appropriateness of terrain for purposes of wildlife ecology (Riley et al., 1999; Sappington et al., 2007). A review of the relevant literature shows that both the papers proposing the original TRI and VRM indices have cited repeatedly by studies, including one paper where the indices were combined to aid in the classification of landscape terrain (Gruber et al., 2019). Both Riley et al. (1999) and Sappington et al. (2007) were described briefly by Smith (2014) in one of the most recent reviews of ruggedness methods and, according to Sappington et al. (2007), Riley's TRI is the most used terrain ruggedness index. Still,

the two indices have key differences. Riley's TRI is rooted somewhat philosophically in Beasom et al.'s (1983) work on the LSRI index (Riley et al., 1999), while Sappington's VRM is anchored to Hobson's surface roughness factor (Gruber et al., 2019; Hobson, 1972; Sappington et al., 2007); thus, while their goals are similar, their approaches to the question of terrain ruggedness are different mathematically.

Computationally, Riley's TRI mirrors somewhat an Analysis of Variance (ANOVA) with its emphasis on the square root of the sum of the squared differences for a central pixel *z*-value within a designated neighborhood window, which is then normalized onto a binned unitless scale that runs from 0 (level) to >959 (extremely rugged) (Gruber et al., 2019; Riley et al., 1999). Riley's TRI was one of the first ruggedness indices specifically designed to incorporate DEM datasets as an input into its calculations (Riley et al., 1999). The usage of a DEM, with its grid format, allowed for a focus on and inclusion of the central neighborhood pixel, which was somewhat unique and not a feature in all previous ruggedness methods (Shortridge, 2019 personal communication). The 1999 paper documenting the TRI presented computer code written in the ARC Macro Language (AML), an Arc/Info-specific language at the time. Riley's original code also contained a typo (Riley et al., 1999; Wilson et al., 2007). Modifications were made to Riley's TRI so that it could be calculated in subsequent versions of ArcGIS (Wilson et al., 2007), which we modified further into an ArcGIS 10.x-specific workflow (Figure 5).

Alternatively, Sappington's VRM was developed partly in reaction to the computational approach of Riley's TRI (Sappington et al., 2007). As the TRI considers *z*-value differences within a designated neighborhood moving window to be the cornerstone of its metric, its follows that the TRI would be closely linked to the slope geometry of a DEM. Sappington et al. (2007) documented the strong positive correlation between TRI and slope at three field sites. Spearman's ρ coefficients between slope and TRI values (and LSRI) were all $\rho>0.9$, while the

correlation values between slope and VRM for two of the same sites in Nevada were $\rho<0.5$, while a third was $\rho<0.75$ (Sappington et al., 2007, fig. 3). The correlation of TRI to slope could pose issues for analyses of low-relief, yet heterogeneous, terrain (Sappington et al., 2007), such as dunefields. Thus, as slope is essentially a measurement in two dimensions when aspect is absent, VRM attempts to detrend TRI's ruggedness from slope rate by considering the DEM in three dimensions – the geometric *x,y,z* orthogonal vectors. The orientation of these three vectors to the surface is then considered trigonometrically and the results indexed to scale between 0 (flat) and 1 (most rugged) (Gruber et al., 2019; Sappington et al., 2007).

Although neither index appears to have been applied widely in aeolian environments, VRM was used to develop plant zonation classifications in the Namib Desert (Juergens et al., 2013), although only some of the study area is a dunefield. Yet, the Juergens et al. (2013) study is notable for linking the terrain index, along with other variables, to vegetation characteristics. A different study used VRM to classify dune landforms in a desert in Iran, employing a 90m resolution DEM (Nazari Samani et al., 2016). The study found that the most complex dune landforms – compound dunes – returned the most rugged VRM values compared to other dune morphologies, while VRM values for vegetated "fixed" dunes were neither the smoothest nor the most rugged (Nazari Samani et al., 2016, fig. 5). Barrows (2011) employed Sappington's VRM to assess habitat suitability for two reptiles in the Mojave Desert. That study used a large 18x18 neighborhood window and ~10m DEMs (Barrows, 2011), although the Mojave Desert, like the study areas of the other two VRM papers, is not solely a dunefield environment. For this study, we calculated TRI based upon the workflow detailed in Figure 4, which was based upon moderations made by Wilson et al. (2007), for each of the 8 sites representing four land systems. We did the same for VRM, except we used computer code which had been codified into an

ArcGIS 10.x toolbox that was downloaded from the ESRI website (Sappington, 2012). In each calculation, we employed a 3x3 neighborhood window.

4.5.3 Soil-Adjusted Vegetation Index (SAVI)

Vegetation in our study area was measured by calculating the soil-adjusted vegetation index (SAVI) from remote sensing data using Google Earth Engine (GEE). Specifically, we processed high-resolution data in two bands from the Sentinel-2 MSI: MultiSpectral Instrument, Level-1C, which is collected by twin polar-orbiting satellites in low-Earth orbit (Bryant and Baddock, 2021; European Space Agency, 2015). Sentinel-2 data was chosen over remote sensing data from other satellites due to its relatively fine ground resolution of 10m in the key spectral bands, its relatively frequent revisit time over the study area (~5 days), and its public availability (Bryant and Baddock, 2021; Ding et al., 2020). Sentinel-2 data has been used in aeolian environments to spatiotemporally track dunefield migration in China (Ding et al., 2020), but for our study, we used two bands of the Sentinel-2 dataset to focus on vegetation in coastal dunes. Sentinel-2 data was obtained for the month of July 2017 and the median values were taken from the multiple, cloudless scenes over that period.

SAVI is an adjustment to the commonly-used Normalized Difference Vegetation Index (NDVI), which attempts to quantify vegetation by measuring the green leaf area and plant biomass (Tucker, 1979). NDVI quantifies vegetative concentration by evaluating the differences and ratios between photosynthesis activity and leaf density, the former of which absorbs red-wavelength light and the latter of which reflects near-infrared (NIR) wavelengths (Tucker, 1979). The red wavelength and NIR wavelength capacity of a vegetated ground surface can be detected by sensors from satellites and other aerial devices, such as unpiloted aerial vehicles (UAV) (Bryant and Baddock, 2021).

After a study found NDVI was sensitive to soil "brightness" – a common albedo characteristic of bare sand (Cowles, 1899; Salisbury, 1952) – and a "spectral effect" in areas of patchy vegetation cover (Huete et al., 1985), the SAVI was developed to account for these influences by introducing a corrective constant (*L*) (Huete, 1988). Huete (1988) proposed the following formula for SAVI:

$$SAVI = \left[\frac{(NIR - red)}{(NIR + red + L)}\right] \times (1 + L) \quad (1)$$

The *L* constant is adjusted per the discretion of the analyst between a range of 0 to 1 based upon a sense of a study area's leaf area index (Huete, 1988). The goal of the *L* constant is to reduce "soil noise inherent in the NDVI" (Jensen, 2007) and the declaration of a suitable *L* constant value seems crucial to the successful implementation of SAVI in many studies (Ren et al., 2018). Levin et al. (2006), working in a semi-vegetated coastal dunefield lacking trees, used trial and error to select $L = 0.25$ for their computation of SAVI, while a different study of dunes in the Kalahari Desert affixed $L = 0.5$, but gave no indication why (Kong et al., 2015). For our study of dunes in a *Dfb* climate where bare sand, grasses, and woody vegetation, sometimes ample, coexist, we chose the midpoint $L = 0.5$ as our corrective constant. With this, SAVI was then calculated using JavaScript code within GEE's coding environment and a mask employed to extract the processed section of the Sentinel-2 tiles for use in our analyses. Our interpretation of the SAVI results will be somewhat similar to Ibrahim (2018) and Munyati (2022), both of which were concerned with the grass and woody vegetation factions in their study areas. We will interpret any SAVI value ~>0.45 as having a signal indicative of significant aboveground biomass similar to dense and/or woody vegetation (Munyati, 2022). SAVI values ~<0.45 will be assumed to have less dense vegetation indicative of grasses or mixed vegetation (Ibrahim, 2018; Munyati, 2022).

4.5.4 Statistical Analyses

Beyond computing basic descriptive statistics for each metric at the various site locations within the study area, we calculated other statistics and tests using IBM SPSS Statistics 27 (IBM Corp., 2020) to assess the hypotheses posed in this paper. To understand the shape of the distributions of all three primary metrics – TRI, VRM, and SAVI – we calculated skewness and kurtosis, in addition to constructing histograms. Skewness is a measure of the x-axis distribution of a data variable against frequency, or its "horizontal symmetry", while kurtosis is a measure of its frequency and is tied to a variable's standard deviation (Corder and Foreman, 2009, pp. 12–37). Taken together with other descriptive statistics and the aforementioned histograms, the skewness and kurtosis statistics helped define whether the data are parametric or nonparametric. Further, these statistics also help determine how to approach tests of correlation, regression, the null hypothesis, and whether any data transformations will be necessary to convert the variables into a more normal distribution. We anticipated the TRI and VRM distributions at all sites would be skewed right somewhat, resulting in positive skewness values, as the study area terrain is relatively more flat than rugged, even in the upland backdune areas. In other words, TRI values close to 1 and VRM values close to 0 should be more common within most land systems. This positive skewness necessitated the use of nonparametric statistical analysis methods and possible data transformations.

Differences in terrain ruggedness between sites and land systems for the same metric would reveal relevant details about aeolian geomorphic processes and the ability of indices to detect them. For example, significant differences for terrain ruggedness and vegetation between the northern and southern sites or foredune and dune barrens sites at Ludington State Park potentially could establish whether certain foredune models are correct and which aeolian process-response regimes dominate. Interpretations of terrain ruggedness and SAVI, however, should be tempered by an understanding that many of our results are scale-dependent and could change based upon

the use of DEMs with different spatial resolutions or implementing a different neighborhood window. Analyses at different scales could yield different results. Indeed, questions of scale are "fundamental" in any geographic analysis (Atkinson and Tate, 2000) and must be considered in any evaluation of experimental results. When observed from different geospatial scales, landscape patterns for the same area can be perceived to change (Turner et al., 1989), while interrelated geomorphic processes and responses can appear unrelated or become unrelated as scale changes (Phillips, 1988). Confronting such problems of spatial perception, an entire subdiscipline of geography emerged partly based on the posit that the length of the coastline of Britain is longer at finer scales of observation (De Cola and Lam, 1993; Mandelbrot, 1967). For this study, our analyses will be conducted with a spatial resolution of 10m, but we rightly acknowledge that any effects we report could be different under different experiment settings.

To determine if differences exist between dunefield land systems, we conducted a series of Mann-Whitney *U*-tests. This test is used to determine if differences exist between two independent, nonparametric data samples (Corder and Foreman, 2009, pp. 57–78; Helsel and Hirsch, 2002, pp. 117–136; Mann and Whitney, 1947). The Mann-Whitney *U*-test, also called the Wilcoxon rank-sum test, assesses if a clustering exists in the ranking distribution of values in each independent group (Corder and Foreman, 2009, pp. 57–78). Such a clustering in either group would mean the probability of a value x in one group would be less or more than the value of y in the other group. The null hypothesis for the Mann-Whitney *U*-test states that no such probability difference exists in values between the groups and that they are largely similar. A multiple-step process is involved in performing the Mann-Whitney *U*-test, beginning with the computation of the *U*-statistic for each sample group i amongst samples n_1 and n_2 (Corder and Foreman, 2009, pp. 57–78):

$$U_i = n_1 n_2 + \frac{n_i(n_i + 1)}{2} - \sum R_i \quad (2)$$

Where n_1 and n_2 are the number of values in independent samples 1 and 2, n_i is the sample of interest, and R_i is the sum of ranks for that sample. The *U*-Statistic then is the smaller of U_1 and U_2. Once the *U*-statistic is calculated, it must be tested for magnitude through the computation of the *Z*-statistic (Corder and Foreman, 2009, pp. *57–78*):

$$Z = \frac{U - \bar{x}_U}{S_U} \quad (3)$$

Where $\bar{x}_u$ and S_U are the mean and standard deviation of *U,* respectively. This operation standardizes *U* by transforming it to the *Z*-statistic, which is then indexed to a critical value threshold based on the size of the data and selected level of significance (Corder and Foreman, 2009, pp. *57–78*). The *Z*-statistic is a commonly used metric in trend analyses (Corder and Foreman, 2009; Gocic and Trajkovic, 2013) and is easily interpreted. Since our *U*-statistic scores are likely to be very high given the large size of the sample data, we reported the standardized test statistic – the *Z*-statistic. If the *Z*-statistic is less than the critical value, then significant differences exist between the datasets and the null hypothesis is rejected.

To understand the relationship between terrain ruggedness and SAVI, we examined the possible relationship in two different ways. First, we tested the relationship directly at each site between both ruggedness metrics and SAVI by measuring their correlation through Spearman's rank correlation coefficient, also known as Spearman's ρ. Then, we tested at each site if the independent explanatory variable of vegetation can predict the dependent response variable of

ruggedness through linear regression analysis. Spearman's ρ is designed to test the correlation of two nonparametric variables by separately ranking their values ordinally and indexing the relationship on a scale between +1 and -1, with ρ=0 signifying no correlation between the variables (Corder and Foreman, 2009, pp. 122–133; Helsel and Hirsch, 2002, pp. 217–218; Spearman, 1904). Thus, Spearman's ρ is calculated as (Helsel and Hirsch, 2002, pp. 217–218):

$$\rho = \frac{\sum_{i=1}^{n}(Rx_i Ry_i) - n\left(\frac{n+1}{2}\right)^2}{n(n^2-1)/12} \tag{4}$$

Where Rx_i and Ry_i represent the ranks of the x and y variables, respectively.

Establishing a moderate or strong correlation between our ruggedness and vegetation measures would be a significant finding for our study. However, in the geosciences it is common to further test any correlation by attempting to quantify the relationship and possibly develop a predictive model explaining the two supposedly related geophysical phenomena (Helsel and Hirsch, 2002, pp. 221–263). We did this at each site by performing a simple linear regression analysis, which is calculated through the following formula (Helsel and Hirsch, 2002, pp. 221–263):

$$y_i = \beta_0 + \beta_1 x_i + \varepsilon_i \tag{5}$$

Where y_i is the dependent variable, x_i is the independent variable, β_0 is the y-intercept, β_1 is the slope, and ε_i is the random error or residual observation, and n is the sample size. From this equation – and through a series of subsequent equations too long to list here – we can calculate the percentage of variance in the dependent variable possibly explained by our "model". The ratio of the sum of the squares regression (SSR) to the sum of the squared residuals (SSE), which,

respectively, are a measure of the observed values and predicted values, is known as the coefficient of determination or R^2. This ratio (R^2) can be interpreted as the percentage of the variance explained by the relationship between the dependent and independent variables (Gerber and Voelkl Finn, 2005, pp. 139–161).

Yet, a simple linear regression analysis is not necessarily appropriate for nonparametric data. In the likely event that our data for ruggedness and vegetation are nonnormative and a simple linear regression analysis is uninformative, we will attempt to transform either the y-variable space, the x-variable space, or both to achieve a more parametric distribution for regression analysis. The data transformation of the y and x variables that we use may depend upon the skewness of the distribution of the variables (Draper and Smith, 1998; Malik et al., 2018). For instance, a right or positively skewed distribution often requires a log(10) transformation of variable values (Malik et al., 2018). A common suite of data transformation procedures often applied to nonparametric data is codified in a process called the Box-Cox method (Box and Cox, 1964; Draper and Smith, 1998). In the Box-Cox methodology, the analyst declares a constant λ, which prescribes a particular transformation of the variable of interest, usually the y variable. Common λ declarations and associated Box-Cox transformations are (From Box and Cox, 1964; Malik et al., 2018):

- $\lambda = 1$ (No transformation needed; produces results identical to original data)
- $\lambda = 0.5$ (square root transformation)
- $\lambda = 0.33$ (cube root transformation)
- $\lambda = 0.25$ (fourth root transformation)
- $\lambda = 0$ (natural log transformation)
- $\lambda = -0.5$ (reciprocal square root transformation)
- $\lambda = -1$ (reciprocal or inverse transformation)

We anticipated that some type of data transformation would be necessary with regards to the terrain ruggedness data, especially given the low-relief terrain of the coastal dunefields in the study area. We also anticipated that once the proper data transformation was selected, that a simple linear regression analysis could show a more significant relationship between ruggedness and vegetation.

4.6 Results

4.6.1 Digital Elevation Models

The 10m DEMs for the Ludington State Park dunefield offered unique visual (Figure 6) and statistical (Table 1) insights to the study area and provided a good justification for the use of the land systems analytical framework. The maximum elevation (~229m), minimum elevation (~175m), mean elevation (~189m), and standard deviation of elevation (~9m) roughly correspond to expected values for a Lake Michigan coastal dunefield. Statistically, it would be expected that the study area would contain large parabolic dunes amid a landscape with a mean dune height that is relatively close to the minimum elevation and in which most variance can be explained by the propensity of ~10m dune landforms. Visually, the DEM results identify other facets of coastal dunefield geomorphology. Much like geomorphology at Silver Lake State Park on Little Sable Point ~40km along the coast to the south (Hansen et al., 2010), a large dunefield comprised of long, sinuous dune ridges has emerged at Ludington State Park on a baymouth bar. These dune ridges, interspersed with occasional parabolic structures which result in the sinuosity, run roughly parallel to the lakeshore. South of the Big Sable River, the ridges are oriented to the southwest, while north of the river, the ridges pivot to the west-northwest, nearly, but not completely, parallel to that portion of the shoreline.

Generally, the elevation of the crests of the dune ridges increases with distance from the foreshore. While no geochronological dates exist for these ridges, it is speculated that these

backdune ridges are relic foredunes from the Algoma period of Lake Michigan dune-building, which coincided with a modest rise in lake levels (Hansen et al., 2010). Since that time, the shoreline and dunefield has prograded westward into the lake. In some areas at Ludington State Park, these dune ridges in the backdune regions exceed ~35m in height. At the backshore, foredunes are visible, but at most represent ~5-8m of relief over the foreshore and are not topographically as prominent as the backdune ridges. Swales ~100-500m in length exist between the foredunes and backdune ridges and just lakeward from the dune barrens land system. According to aerial images, the swales here occasionally contain water, but are also often dry, resulting in a playa-like structure with a dry, dusty surface. A graph of elevation along a transect from the south foreshore to the edge of the backdune area confirms the presence of the high backdune ridges, lower foredunes, shallow swales, and hummocky dune barrens that seem typical of this study area (Figure 7). Additionally, the active upland linear dune land system, between the dune barrens and mature woodland dunes, have a prominence of ~35m above the downwind dune barrens area and is exposed to the winds off the lake.

Taken together, the geomorphic landscape revealed by the DEMs resembles Arbogast's (2009) "Low-Perched Transgressive Dunes: Baymouth Bar Complex" classification. In that classification, a coastal dunefield is characterized by sinuous, but low-slung foredune ridge, while the backdune region contains large dune ridges with imbedded parabolic structures (Arbogast, 2009), some of which may be active or wooded. The backdune morphology is not necessarily a product of current processes, but relic processes during conditions conducive to widespread aeolian activity, resulting in transgressive morphologies (Lovis et al., 2012). Yet, conditions changed and longshore sediment deposition and other processes eventually prograded the shoreline westward and new foredunes formed in near-linear fashion downwind of the current backdune ridges. A visual inspection of the DEM seems to confirm the possibility of this dune-construction model.

4.6.2 Terrain Ruggedness Indices

Like the DEM results, a visualization of the terrain ruggedness metrics produced reasonable and expected outcomes (Figures 8-9). However, variability between the two metrics exist (Table 2). Overall, both TRI and VRM identified many of the same prominent dune geomorphic features observed in the visualization of the DEM. However, visually, it appears TRI is detecting more terrain heterogeneity than the VRM index, especially around dune landform ridges. Statistically, for the TRI when viewed through the lens of the land systems framework, areas in the backdunes farther from Lake Michigan were more rugged overall, while the foredunes and dune barrens closer to lake were smoother topographically (Table 3). For the VRM index, that pattern is less clear (Table 4). Still, both indices identified the dune barrens land systems as being less rugged than other land systems. Overall, the TRI finds a ruggedness gradient that increases with distance from Lake Michigan, while the VRM index does not detect such a gradient. Possibly, the VRM index is more sensitive to localized landform heterogeneity, while the TRI is more attuned to land system heterogeneity.

4.6.3 Soil-Adjusted Vegetation Index (SAVI)

The interpretation of the results from a remote sensing vegetation index analysis, including those using SAVI, is subject a number of factors (Gu et al., 2007; Guo et al., 2000; Piao et al., 2006), including drought, seasonality, and various input parameters, such as the aforementioned *L* constant. Thus, there is no consistent interpretation of SAVI values that always denote bare sand from grasses and grasses from woody vegetation. As stated in the Methodologies section, we were guided by – but did not adopt wholly – the interpretation of SAVI by Ibrahim (2018) and Munyati (2022). We also used empirical knowledge of the study area, a visual inspection of the results overlain atop aerial images, the land systems framework of Christian and Stewart (1964), and classification schemes garnered from other aeolian-influenced landscapes (e.g., Lu et al., 2015). According to our analysis, forest comprises the largest vegetation group in the study

area, encompassing about half of Ludington State Park's dune areas, followed by grasses and mixed vegetation. Bare sand accounts for ~10% of the dunefield.

When examined from a land systems perspective, the ecogeomorphic gradient in the study area is evident (Table 5). Foredunes have the lowest mean SAVI, while mature woodland dunes have the highest; the mean SAVI values for the dune barrens and upland linear dune land systems are in between. Figures 10 and 11 illustrate this point further by demonstrating the geographic and geomorphic distribution of bare sand, grasses, and forest. Foredune areas and the swales behind those foredunes contain more bare sand and grasses; older backdune areas are more forested. Grasses track closely along some dune crests in the backdunes, but atop other crests, likely along older dunes, forests dominate. A DEM hillshade map of the dunefield with SAVI values coded atop the terrain illustrates this effect (Figure 12). It appears less dense vegetation and grasses are found windward toward the lake presumably on younger dunes and atop newer portions of the relic barrier bar, while woody vegetation inhabits older, larger relic dunes that possibly date to the Algoma period. Thus, we could conclude that vegetation type may be closely linked to dune age at Ludington State Park.

4.6.4. Statistical Analyses

A series of statistical analyses provided the ability to understand more about terrain ruggedness and vegetation in our study area. As expected, for all of the 8 analysis sites, the distribution of the ruggedness results was right or positively skewed (Figures 13-14, Tables 3-4). The distribution of SAVI, however, shows more variability (Figure 15). Most SAVI distributions are skewed right, but the distributions for the mature woodland dunes land system are skewed left. Additionally, for both for the entire dunefield and at north Dune Barrens site, SAVI values are bimodal. The overall dunefield distribution for SAVI contains a peak at ~0.2, the boundary for bare sand and grasses, and within the range of woody vegetation (~>0.45). The consequence of

all these nonnormal distributions for the TRI, VRM, and SAVI variables necessitates the use of nonparametric tests, including, as anticipated, the Mann-Whitney *U*-test for differences and Spearman's ρ for correlation, as opposed to their parametric counterparts.

The Mann-Whitney *U*-test results demonstrate that, despite similarities within metrics for particular land systems, significant differences exist between almost all sites (Tables 6-8). The null hypothesis for these tests, which declared that the distribution of TRI, VRM, and SAVI are roughly the same between the 8 different analysis sites, is rejected almost completely. For SAVI between all sites, the null hypothesis was rejected, while we rejected the null hypothesis for all but one test for TRI and two tests for VRM. All three tests for which we failed to reject the null hypothesis involved the north foredunes land system. For every other land systems combination regarding ruggedness, the Mann-Whitney *U*-test found significant differences between the TRI and VRM results. Roughly, the medians for TRI and SAVI increase significantly between the lakeward land systems and the mature woodland dune land system, while the VRM index has no discernible geographic pattern. Yet, when compared in Mann-Whitney *U*-tests, the *Z*-statistic results for almost each analysis site pair comparison exceeded ± 1.96, which is the test of significance for the *Z*-statistic. Generally, very large *Z*-statistic scores between sites exist for SAVI, while relatively smaller, but still significant, *Z*-statistic scores were returned for TRI and VRM between sites. These results suggest widespread dunefield variability with regards to terrain ruggedness and vegetation density.

If widespread ecogeomorphic heterogeneity exists within our study site and between sites within the same land system, there are many possible relationship modes between ruggedness and vegetation. Thus, it is unsurprising that our correlation analyses found the relationship between terrain ruggedness and vegetation was not consistent across different land systems and diverged depending upon dunefield position (Table 9). According to our correlation analyses, terrain

ruggedness and vegetation are only related in the dune barrens, which also happens to be the land system with the least rugged profile. Using Corder and Foreman's (2009) interpretation of Spearman's ρ values, the correlation between both terrain ruggedness indices and SAVI are strongly or moderately negatively correlated (ρ <-0.45, p-value <0.001). These results suggest that as vegetation density declines in the dune barrens land systems, ruggedness increases. This correlation pattern does not hold for any other land systems. When grouped by land systems, the other sites either fail to demonstrate a correlation pattern or presently only a weak correlation, as was the case with the active upland linear dunes land systems, where there is a weak positive correlation only (+0.08 < ρ <+0.16, p-value <0.001). In other words, amongst the upland active linear dunes, vegetation and terrain ruggedness loosely increase and decrease together, although this correlation, while statistically significant, is also statistically weak.

Yet, whatever correlation between terrain ruggedness and vegetation detected through the calculation of Spearman's ρ, the relationship is not strong enough to be predictive in any land system. While a correlation exists in the dune barrens, according to our simple linear regression analyses, vegetation density cannot explain any response in terrain ruggedness at any site (Table 10). A typical scatter plot and regression line result can be seen in Figure 16. Only four R^2 values out of 16 simple linear regression analyses exceeds 0.1. Two of those R^2 results >0.1 (α = 0.05, p-value <0.001) were obtained for the south dune barrens site for both TRI and VRM. Many of the remaining 12 R^2 values approach 0. Consequently, SAVI cannot explain much variability with the two terrain ruggedness indices in our predictive model, except only weakly at one dune barrens site and at two other locations. From all these statistical results, it may be possible to state two things: 1) These results suggest, together with the Spearman's ρ results, that some type of relationship may occur between vegetation and terrain ruggedness where the dune barrens land system exists. 2) Yet, beyond the dune barrens land system, a considerable amount

of stochasticity exists in the relationship between vegetation and terrain ruggedness at Ludington State Park for the spatial grain and neighborhood extent examined.

4.7 Discussion

There are three primary findings revealed by the results of our analyses: 1) Both TRI and VRM can detect dune landforms, while SAVI can detect vegetation differences in dunefield land systems, with mature woodland dunes in the backdune regions and grassy foredunes well-distinguished in the SAVI values. 2) An ecogeomorphic gradient exists at the Ludington State Park dunefield from the foreshore to the far backdune reaches, in which the landscape transitions through distinct landforms, elevation, and vegetation. From the foreshore, the landscape transitions inland through low-elevation foredunes, wet-dry swales, then dune barrens with mixed grasses and woody vegetation into upland active linear dunes, and, finally, mature woodland dunes farthest from the shoreline, the latter two land systems inhabiting some of the tallest portions of the park. The landscape transitions temporally along this gradient as well, as younger foredunes and "yellow dunes" inhabit the backshore and the area near the lake, while "grey dunes" occupy the aeolian environment farthest from the water, much as Salisbury (1952) modeled. 3) Terrain ruggedness and vegetation are apparently unrelated or weakly related, except in the dune barrens land system, where decreasing ruggedness is associated with dense vegetation. Elsewhere along the aforementioned ecogeomorphic gradient, there exists in the other land systems much heterogeneity and, likely, stochasticity in the process-response regime governing dune terrain and vegetation. While the former two findings are of interest, they confirm fundamentally obvious hypotheses; ruggedness indices were designed to detect terrain heterogeneity, while the ecogeomorphic gradient present in Lake Michigan coastal dune systems has been mostly well-established since the work of Cowles (1899). The latter finding, however, is potentially important. It suggests two ideas, stated briefly at the end of the Results section: That

terrain ruggedness and vegetation are related in the dune barrens land system, while the rest of the dunefield is the product of ecogeomorphic random walks. While these findings may seem contradictory, they fit together with certain ecogeomorphic ideas.

The dune barrens land system, as identified and analyzed here, is a unique ecogeomorphic unit (Figure 17). It is characterized by patchy, yet diverse vegetation. Species growing in this land system include grasses, such as marram grass (*Ammophila breviligulata*), and forbs, including common milkweed (*Asclepias syriaca*) (Cohen et al., 2015). Woody vegetation in the dune barrens includes common juniper (*Juniperus communis*) and jack pine (*Pinus banksiana*). On the DEM and ruggedness maps, the variability in dune barrens elevation is relatively slight, yet the landscape is hummocky and pockmarked with bare sand and small dunes. It is a land system marked by transitions, as can be seen in a comparison between aerial imagery from 1938 and 2018 (Figure 18). In 1938, much of the area we designated as the dune barrens land system in the southern half of Ludington State Park was bare sand; by 2018, most of the bare sand had transitioned to vegetation. Woody vegetation, primarily juniper, jack pine, and shrubs appears to have migrated lakeward through the now-dune barrens land system, although the mature woodland dunes to the east contain pine or pine-hardwood forests (Dister, 2017).

Understanding the cause – and the implications – of this transition in the now-barrens from open dunes to vegetation is important for comprehending the relationship between terrain ruggedness and vegetation. In 1938, the dune barrens area primarily appears to be ecogeomorphically similar to the swale land system just lakeward and upwind to the west. In fact, currently, some wet swale areas still exist within the dune barrens, landforms at Ludington State Park which Dister (2017) termed "interdunal wetlands", but that others elsewhere name "dune slack" (e.g., Baldwin and Maun, 1983). The moisture content in the swales and these interdunal wetlands is roughly synchronous with lake levels (Dister, 2017), which fluctuate seasonally and annually and have

known cycles spanning decades to 150-years (Baedke and Thompson, 2000; Loope and Arbogast, 2000; Theuerkauf et al., 2021). These cycles are possibly driven by climatic variability (Petty et al., 1996) and they likely affect the water table elevation, which in turn affect dune swale characteristics (Dott and Mickelson, 1995). Further, since the mid-20th Century, there has been an increase in annual precipitation regionally (McKeehan and Arbogast, 2021; White et al., 2019). It is possible this modest, but somewhat significant, increase in annual precipitation has increased soil moisture levels in Lake Michigan dunefields. Other factors may be acting upon the study area's dune landscape as well, such a waning sand supply due to diminishing wind power (Lovis et al., 2012; Yurk and Hansen, 2021), and increased CO_2 and N fertilization, fire suppression, and other anthropogenic forcing (McKeehan and Arbogast, 2021). All these factors may have provided the pretextual conditions necessary to affect the transition of this portion of the Ludington dunefield from mostly bare sand to a heterogenic environment of low, hummocky dune landforms and mixed vegetation.

As always, however, scale is important. When viewing the dunefield from a regional geomorphic perspective, Ludington State Park – and many dunefields – exemplifies Carter's (1991) "natural heterogeneity" principle. At the dunefield system scale, landform morphology, vegetation, edaphic conditions, and other variables exhibit a relatively high degree of heterogeneity (Carter, 1991; Cooper, 1958; Melton, 1940). However, when viewed from the perspective of land systems or another classification framework, much of the chaotic heterogeneity gives way to zonation, with less variability within zones than between zones (Dech and Maun, 2005; Lichter, 1998). For example, in our study, the grassy foredunes comprise a land systems zone parallel to the lakeshore from the backshore to the lee slope swales. The terrain and vegetation there, according to our analyses, are mostly consistent. Yet, there was no statistical relationship between terrain ruggedness and vegetation in this land system that we could detect. Therefore, it seems

paradoxical that an inherently heterogenic land system, such as the dune barrens, with mixed vegetation type may contain correlated patterns of terrain and vegetation. In dunefield land systems where one vegetation type is more dominant, such as the mature woodland dune land system, no relationship existed between terrain ruggedness and vegetation. In other words, dominant vegetation regimes tended to overcome any terrain constraints that might exist. Once established, the northern hardwood forest species in the mature upland dunes had no topographic barrier to becoming the dominant type of vegetation in that land system. This, along with research detailing the expansion of vegetation in dune systems regionally (e.g., McKeehan and Arbogast, 2021; White et al., 2019) and elsewhere in the world (e.g., Jackson et al., 2019; Provoost et al., 2011), suggest that the controls constraining the positive feedback mechanisms forcing vegetation expansion are possibly no longer effective.

The dune barrens land system is somewhat equidistant between the lakeshore and the last backdune ridge, but is morphodynamically dependent on the aeolian processes linked to the foredune land system. Winds off Lake Michigan encounter the internal boundary layer (IBL) created by the foredunes fronting the backshore. The effects of the IBL and the aerodynamic roughness of the foredune cause drag near the surface, but acceleration higher in the wind profile as the winds crest the stoss slopes (Walker and Hesp, 2013). As the winds encounter the lee of the foredune land system, the flow diverges into and an upper and lower wake (Frank and Kocurek, 1996), the latter of which descends the lee slopes into a series of flows and vortexes (Walker and Hesp, 2013). In the lower wake, the flow remains aloft, but slowly descends, reencountering the surface at a distance of ~4-10x the height of the foredune (Frank and Kocurek, 1996; Walker and Hesp, 2013). The foredune crests in our study area are ~15m above the elevation of the swales of the backdunes, meaning that the point of "reattachment" – where the flow again encounters the dunefield surface – is ~60-150m leeward of the foredune

crest. At Ludington State Park, the swale land system indeed begins within this range inland from the foredune crest, confirming the various leeward dune wind models described by Walker and Hesp (2013). The swale land system – where post-foredune point of reattachment is located – is a landscape of erosional scours, dry-wet playa, grassy vegetation, and some open dunes, a pattern intimated by some dune models which incorporate the effects of a foredune IBL (e.g., Jerolmack et al., 2012). At Ludington State Park, the swale land system is ~300m wide in some places from the edge of the foredune land system to the dune barrens; in other areas, it has transitioned completely to dune barrens.

There are possibly two explanations, neither mutually exclusive, for expansion of dune barrens vegetation across the mostly bare sand swales since 1938. First, as mentioned previously, climatic and anthropogenic forcings provided the pretextual conditions to support vegetation in the swale land system. Second, a change in the aeolian sand transport regime occurred in the study area, altering the amount of sand delivered from the foreshore beach to the park's backdune regions, including the swale and dune barrens land systems. Lovis et al. (2012) noted a possible reduction in sand supply since the Little Ice Age (LIA) in their geochronological study of Lake Michigan coastal dunes. Such a reduction in sand supply could be explained by a corresponding reduction in wind power regionally (Yurk and Hansen, 2021) or with changes in foredune height. Increasing foredune height can diminish downwind sand supply and transform downwind land systems as a result (Konlechner et al., 2016). Often, increasing foredune prominence is related to the expansion of vegetation on the foredune (Konlechner et al., 2016; Ruggiero et al., 2018; Zarnetske et al., 2015), creating a feedback mechanism in which increasing vegetation density increases the ecogeomorphic ability of species to deflect aeolian sediment from the foreshore, integrating the new material into the soil and increasing foredune height further (Davidson-Arnott et al., 2018).

Downwind in the backdune land systems, increasing foredune height limits the supply of new aeolian sand (Konlechner et al., 2016). While some dune species respond well to sand burial in the Great Lakes basin (Maun, 1998), the diminishing supply of sand to the backdune land systems, particularly those of the swales and dune barrens, may invoke ecogeomorphic changes there (Dech and Maun, 2005). In Australia, the process of increasing foredune height and vegetation provoked an erosional response downwind, as deflation surfaces increased significantly (Konlechner et al., 2016). Along Lake Huron, increasing foredune height led to an expansion of vegetation downwind in the swales, where deflation erosion lowered the dune surface closer to the water table (Dech and Maun, 2005). If sand supply was constrained due to increased foredune height and/or vegetation, there may have been an expansion of deflation surfaces leeward of the reattachment point in the swale area, which then became the dune barrens land system. This condition, along with favorable climatic changes, potentially set in motion a positive feedback mechanism which propelled vegetation to expand in the dune barrens area. Species, such as juniper, which benefits from a shallow water table and decreased sand burial, may have been able to establish itself under these conditions. At this stage, the ability of a species to grow faster than the rate of sand burial would be the key to changing the ecogeomorphic conditions in the backdunes (Okin, 2013). Then, as grasses and vegetation changed the surface roughness (z_o) of the land system, the resulting IBL pushed windward, effectively sheltering the new vegetation assemblages. Thus, formed the dune barrens land system evident in repeat aerial images of Ludington State Park.

Yet, how did this process-response mechanism between the foredune and dune barrens affect the correlation between terrain ruggedness and vegetation? Elsewhere in the dunefield, terrain ruggedness and vegetation are unrelated seemingly, especially in land systems where one type of vegetation is dominant. In the dune barrens, however, rugged terrain is moderately to strongly

related to grasses and bare sand, while smooth terrain is related to woody vegetation. The growth of dunefield vegetation, at least initially, leads to what Suter-Burri et al. (2013) and Okin et al. (2006) called the "small-scale mosaic of depositional and erosional sediment transport regimes". As Okin (2013) notes, any such transition in the dune barrens as outlined here would result in the formation of nebkhas, also called coppice dunes, where woody vegetation might have established itself. These would not be large dune landforms, perhaps only a few meters high (Kidron and Zohar, 2016). However, any grasses would likely form convex dunes surfaces similar to foredunes, due to the ability of grasses to deflect and integrate airborne sediment (Ruggiero et al., 2018; Zarnetske et al., 2012). These processes would result in a terrain response closely related to vegetation type, which would explain the moderate-to-strong negative correlation between SAVI and the two terrain ruggedness indices in our study at the scale of this analysis. Clearly, scale is an important consideration when interpreting these results, as mentioned in both the Literature Review and Methodologies sections; both the results and interpretation should be tempered by uncertainty of scale. Not only is the pixel size of the DEM inputs important, but the research design and the configuration of the index computations depends upon a clear understanding of scale. Should dunefield ruggedness be measured at the landform scale, as was attempted here, or at the plot or areal scale? The answer to this question affects not only the scale of the analysis, but also the configuration of the neighborhood index computation window.

Nevertheless, if the drivers of the current ecogeomorphic process-response regimes remain roughly analogous to current condition, however, it can be expected that more swale and dune slack areas would transition to dune barrens. Several concepts of landscape evolution make this outcome likely. First, is the concept of Tsoar's (2005) hysteresis curve of dune vegetation coverage. This concept posits that the reduction in wind power necessary to prompt vegetation

expansion in dunes is far smaller than the wind power necessary to dislodge and reduce vegetation coverage once it has been established (Tsoar, 2005). Yizhaq et al. (2009) expanded upon Tsoar's hysteresis curve concept by incorporating precipitation and other climatic and anthropogenic factors into the hysteresis model of dune activity. In their model of bistability, climate and anthropogenic conditions can permit heterogeneity amongst dune vegetation regimes, effectively allowing vegetated, fixed dunes to coexist with open bare sand dunes within the same land system (Yizhaq et al., 2009). This condition could be interpreted as reflecting Carter's "natural heterogeneity" (1991) and the product of unpredictable interactions amongst countless variables across geologic time (Melton, 1958; Scheidegger and Langbein, 1966). Yet, once the interrelated variables drive dune landscape response toward one stable bistability state or the other, rather than permit both simultaneously, the energy necessary from within the system or from outside of it (e.g., human intervention) to reverse the response is difficult to generate (Yizhaq et al., 2009). Thus, the transition from swale to dune barrens may be, as Yizhaq et al. (2009) termed it, "irreversible", unless extraordinary changes with the variables within the process-response system occur.

These related concepts of dune-vegetation hysteresis and bistability invokes somewhat a further geomorphic theory known as "deterministic chaos" (Phillips, 2006). Under the concept of deterministic chaos, the state of any geomorphic system at a given spatiotemporal point and at a given scale is the result of the interactions of several interrelated variables responding to accumulating processes in the manner of a random walk (Leopold and Langbein, 1962). A random walk is a probability concept in which all outcomes within a process-response system have an equal probability due to the inherent chaos within that system (Leopold and Langbein, 1962). Thus, the geomorphic system exhibits a stochasticity amongst its processes and responses, resulting in a heterogeneity of outcomes at that point. Yet, the ultimate sum of outcomes at the macroscale

of the geomorphic system is deterministic. This explains why a dunefield exhibits great ecogeomorphic heterogeneity, but still contains rational ecogeomorphic gradients, zonation, and land systems. The theory of deterministic chaos can, then, explain the existence of an aeolian systems gradient extending along a transect from the foreshore to the backdunes at Ludington State Park that generally increases in dune formation age and elevation with distance from the lake and progresses from grasses to mature woodland. Simultaneously, the theory of deterministic chaos can also explain why some constituent parts of the dunefield exhibit a bistability state of vegetation along the gradient and nonequilibrium and nonlinearity elsewhere. This is the chaos obscuring the order in the ecogeomorphic system (Huggett, 2011; Malanson et al., 1992). The stochasticity embedded within the ecogeomorphic systems of Lake Michigan's dunefields is well-established (e.g., Lichter, 2000), but so too is the macroscale, time-transgressive response toward stable states of ecogeomorphic mode in the region's coastal dunes (e.g., Cowles, 1899; Lovis et al., 2012).

Ultimately, we feel these concepts explain our findings. Theories of ecogeomorphic hysteresis, bistability, and deterministic chaos can explain why land systems with dominant modes of vegetation lack a relationship between vegetation type and terrain ruggedness. Once a dominant mode of vegetation establishes itself, all other constraining factors – such as climate and terrain – become nearly irrelevant in affecting ecogeomorphic outcomes absent a significant amount of forcing. Recall that the Holland paleosol persisted as a pedogenic phenomenon for ~1k years (Lovis et al., 2012), although some uncertainty exists within the dating of that informal paleosol. Given Tsoar's hysteresis curve, it is unlikely that the conditions favorable for vegetation expansion and soil developed aligned perfectly with the Holland paleosol's existence, but instead ceased earlier than the paleosol's demise and burial, the dunes becoming reactivated only once enough geophysical forcing dislodged the vegetation from the dune system. In other words,

sustained, relatively significant climate change likely occurred to close this period of dunefield stability on the eastern shore of Lake Michigan. Conversely, within certain land systems, such as the dune barrens, the relationship between terrain ruggedness and vegetation type exists because the ecogeomorphic system there remains within the influence of the bistability model, where the complex feedback mechanisms amongst the system variables have not yet produced results that exceed the system's thresholds and drive a particular variable toward dominating influence. In the dune barrens land system within our study area, the influences of a number of interrelated variables – wind power, foredune morphology, climate, water table level, interdunal wetland geographic, vegetation type, amongst many – are still relevant to ecogeomorphic outcomes. Not only that, but these land systems exhibit the capacity to change rapidly (Delgado-Fernandez et al., 2018; Smith et al., 2017), as a comparison of aerial images from 1938 and 2018 of the dune barrens suggests.

These findings are relevant for several reasons. First, it suggests that the direct relationship between terrain ruggedness and vegetation is only evident in land systems where no vegetation type is dominant. In other land systems, vegetation maybe exerting an overwhelming influence upon the landscape. The findings also suggest that more research needs to be conducted at the land systems scale to better understand this relationship, especially in heterogeneous landscapes. Further, it is clear from a review of the relevant literature that other indices of ruggedness and vegetation, calculated at different scales with different neighborhood parameters in other dune systems could produce different results. After all, scale is fundamental to geographic analysis and must be accounted for (Atkinson and Tate, 2000). We believe the data and tools exist to test in a dune landscape all relevant ruggedness and vegetation index methods at various scales and parameters to find the optimal methodological approach to quantifying terrain and vegetation characteristics in dunefields. Such efforts could prove helpful to parameterizing

ruggedness and vegetation in dunefield models. Based upon our results, which show important correlations between ruggedness and vegetation in some landscape and a reasonable lack of such elsewhere, dunefield models likely should exhibit elasticity when parameterizing the two variables. Delgado-Fernandez's et al. (2019) dune vegetation cover model exhibits the flexibility necessary to incorporate the fluctuating correlation between terrain ruggedness and vegetation, where ruggedness and land system could be included as elastic disturbance (*D*) parameters. Otherwise, developing the perfect parameterization of the transitory ruggedness-vegetation relationship for models may prove difficult and impractical, as increased parameterization does not necessarily lead to a better model or an understanding of geophysical processes (Phillips, 2007) and prove impossible (Melton, 1958).

4.8 Conclusions

This study explored the relationship between terrain ruggedness and vegetation in a coastal dunefield along Lake Michigan's eastern shore. To quantify ruggedness for the dunefield at Ludington State Park, we calculated two terrain indices – Riley's Terrain Ruggedness Index (TRI) and Sappington's Vector Ruggedness Measure (VRM) – from 10m DEMs. To measure vegetation, we computed the Soil-Adjusted Vegetation Index (SAVI), also from 10m resolution remote sensing data. Using a land systems approach, we found that ruggedness and SAVI were strongly-to-moderately negatively correlated in one land system – the dune barrens environment midway along the ecogeomorphic gradient between the foredunes and mature wooded backdunes. Within the dune barrens land system, we found that ruggedness decreased with increasing SAVI, which was interpreted as an increasing incidence of woody vegetation and plant density. Likewise, with grassy or patchy vegetation, terrain ruggedness increased within the dune barrens land system, which is characterized as by mixed vegetation and hummocky landforms. In other land systems where one type of vegetation is dominant, no relationship existed between terrain

ruggedness and vegetation. These finding suggest that, based upon the concepts of ecogeomorphic hysteresis, bistability, and deterministic chaos, that vegetation maybe exerting an overwhelming influence upon the landscape in the foredune and mature woodland dune land systems. By contrast, the dune barrens represent a land system where the feedback mechanisms amongst the system variables have not yet produced results that exceed the system's thresholds and drive a particularly dominant response. We also found that TRI and VRM performed reasonably well in identifying dune landforms, while SAVI was successful in detecting dunefield vegetation zonation. These findings are useful in the continued quest to understand the relationship between terrain and vegetation in coastal dune systems. As vegetation and terrain are important variables in determining dune behavior, such as sand supply and foredune growth, we call for more research in this important area and in the indices employed in their measurement.

APPENDIX

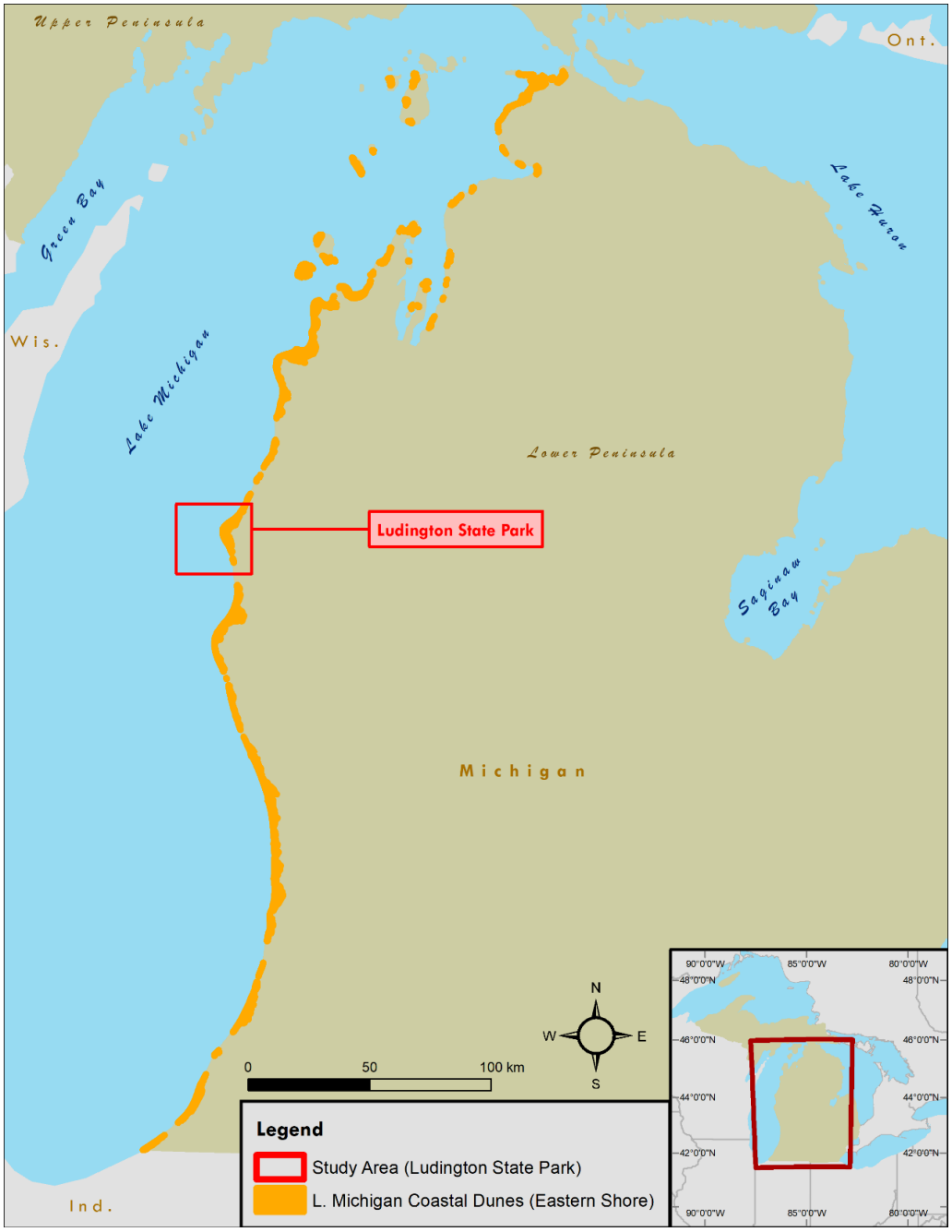

Figure 4.1: The coastal dunes of Lake Michigan's eastern shore, with the location of Ludington State Park. Coastal dune extent is from Arbogast et al. (2018).

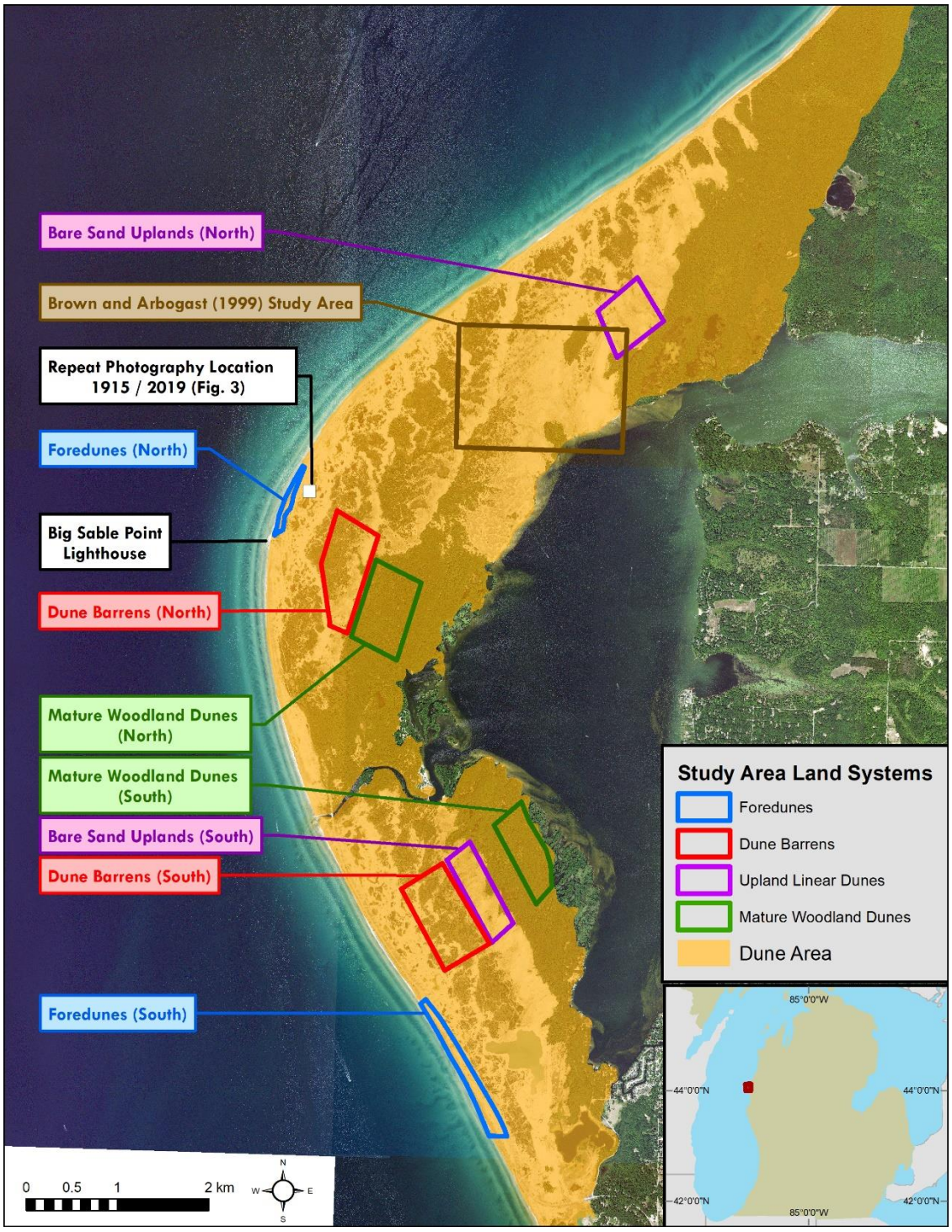

Figure 4.2: Map of study area Land Systems, a framework for geographic analyses. Aerial images are from July 2018 from the National Agriculture Imagery Program (NAIP) and were obtained from U.S. Geological Survey. Dune area is from Arbogast et al. (2018).

Figure 4.3: Big Sable Point and Lighthouse, Ludington State Park, LAT: 44.062615, LON: -86.509579. This repeat photograph pair is of Big Sable Point and Lighthouse. The 2019 photograph shows a somewhat transformed landscape, with less bare sand, more grasses, and much more water, possibly due to a change in the water table due to interaction with Lake Michigan, which is approximately 480m to the west. The modern dunes also appear larger and taller than in 1915. While lake level records prior to the mid-20th Century are problematic, it appears water levels on Lake Michigan were ~1m higher in 2019 at the time of the later picture than in 1915 (Indiana DNR, 2020; NOAA, 1992). *From McKeehan and Arbogast (2021). Photo Credit – 1915, Univ. of Chicago; 2019, Kevin McKeehan, Michigan State University.*

Figure 4.4: Land systems examples. From left to right and along an ecogeomorphic gradient from the foreshore to far backdunes: 1) Foredunes, 2) swales, 3) dune barrens, 4) mature woodland dunes. Upland bare sand land system not shown. All photographs except the mature woodland dunes photo were taken in September 2019 at Ludington State Park along the south transect analysis area. The mature woodland dunes photograph was taken in May 2019 at Mt. Baldhead near Saguatuck to the south of the study area. Notice that grasses are dominant at the foredunes, but some trees appear in the distance. Likewise, hardwood trees are dominant in the mature woodland dunes, which exhibit characteristics consistent with Salisbury's (1952) grey dunes. The swales are characterized by water, while the dune barrens mostly lack water and contain more woody vegetation.

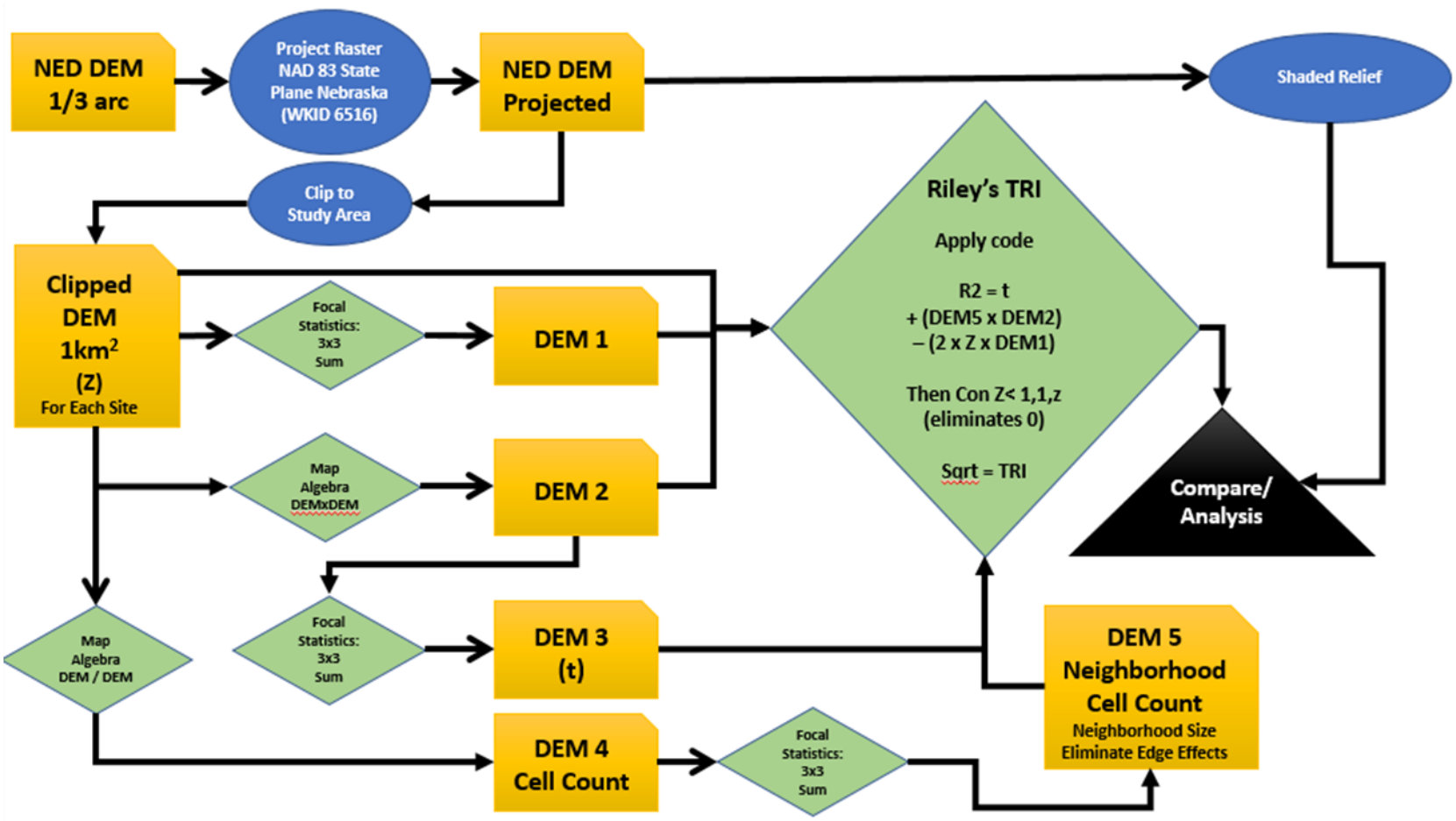

Figure 4.5: Workflow used to calculate Riley's Terrain Ruggedness Index. Created after interpreting Riley et al. (1999) and Wilson et al. (2007).

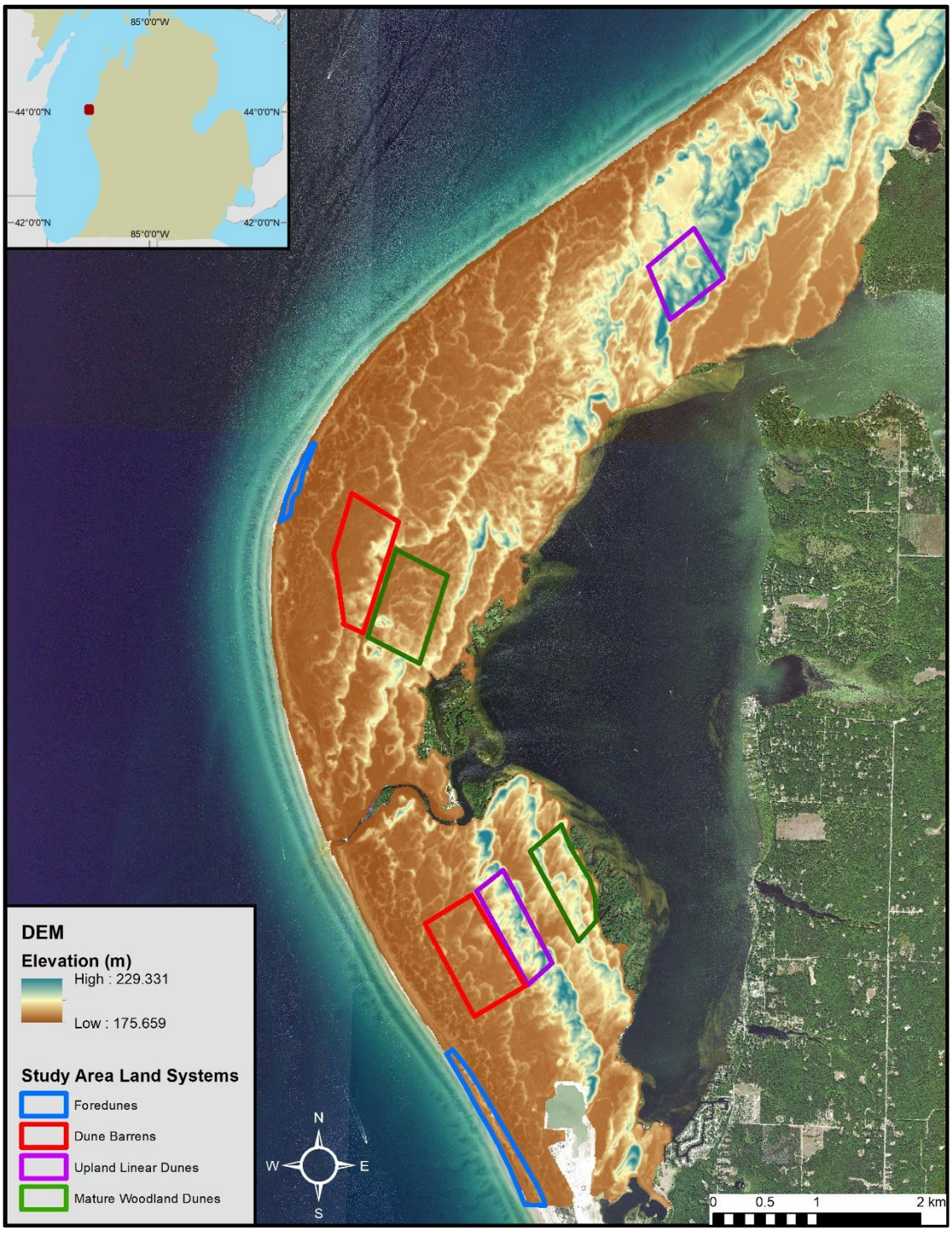

Figure 4.6: Digital Elevation Model (DEM) of Ludington State Park dunefield area from USGS 2019 ~10m spatial resolution DEM dataset.

Table 4.1: Digital Elevation Model (DEM) characteristics for the study area.

DEM	Resolution	Max. (m)	Min. (m)	Mean (m)	SD (m)	Area (km^2)
USGS 3D Elevation Program (3DEP) dataset 2019	~10m (1/3 arc-second)	229.33	175.66	188.56	9.18	~30.3

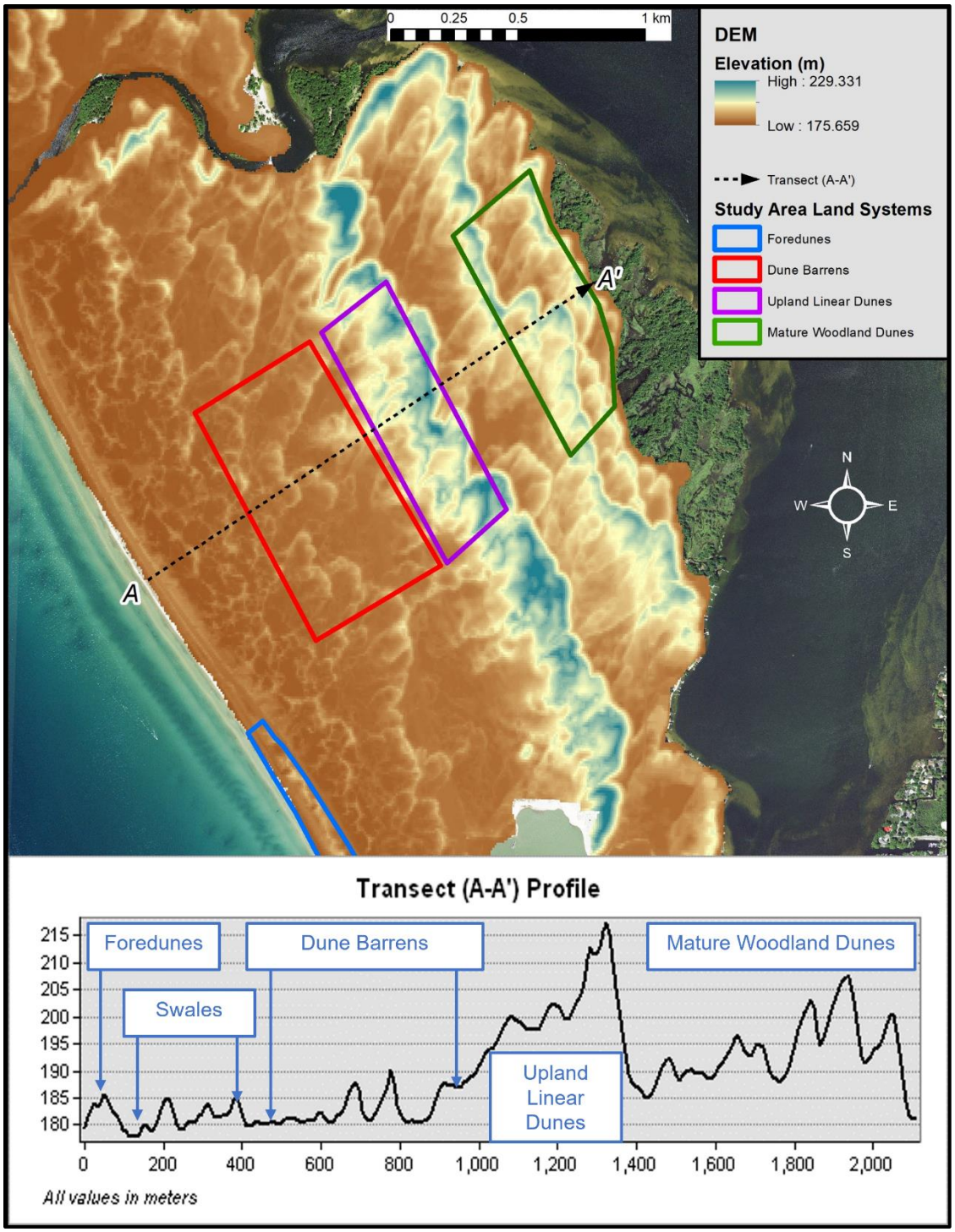

Figure 4.7: Transect A-A' profile, which traverses an area in the southern portion of the study area, including the dune barrens, upland linear dunes, and mature woodland dunes land systems. Additionally, the transect moves across foredunes and swales, although not the foredune area used for land systems analysis due to the presence of a road.

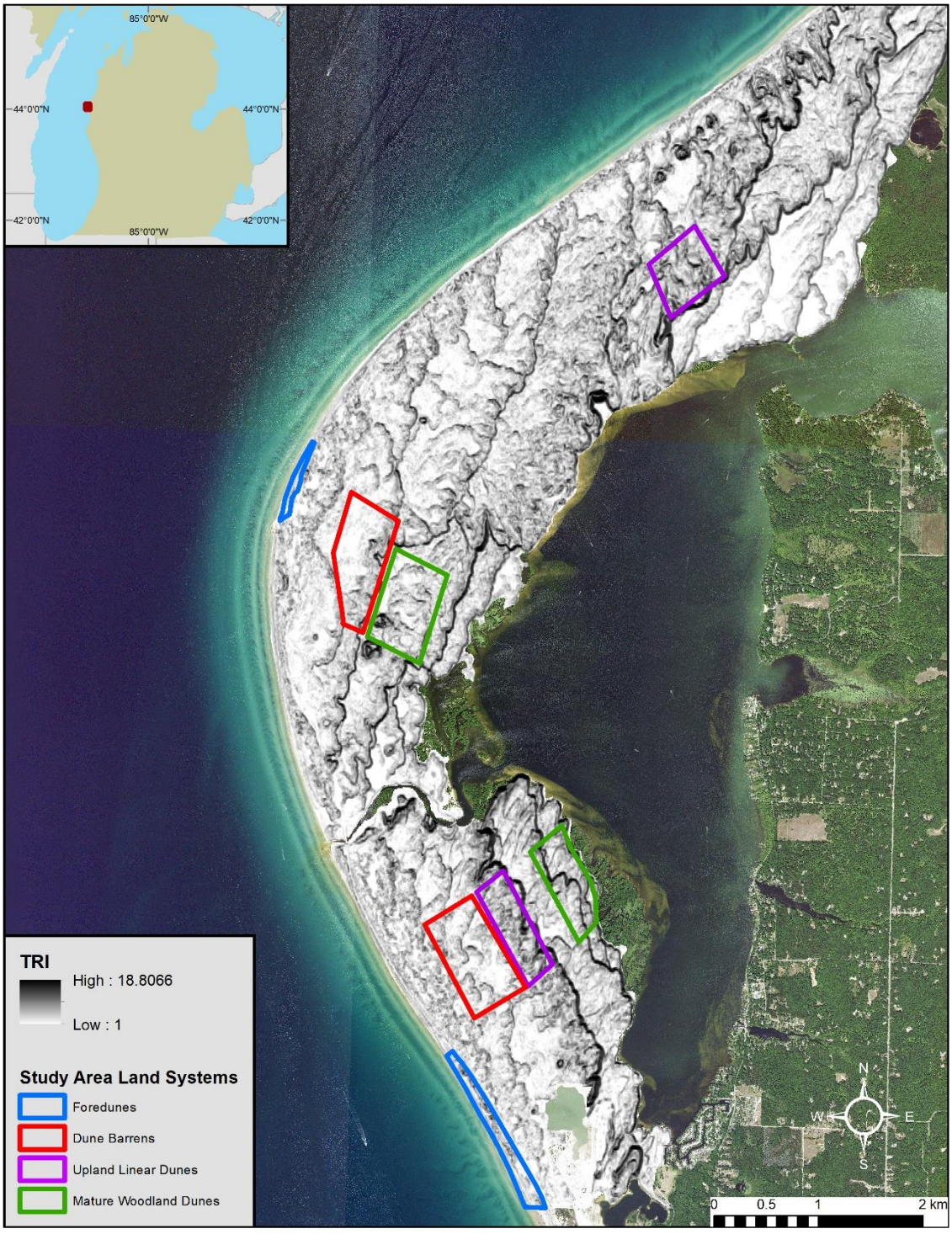

Figure 4.8: Map of Terrain Ruggedness Index (TRI) values for the study area.

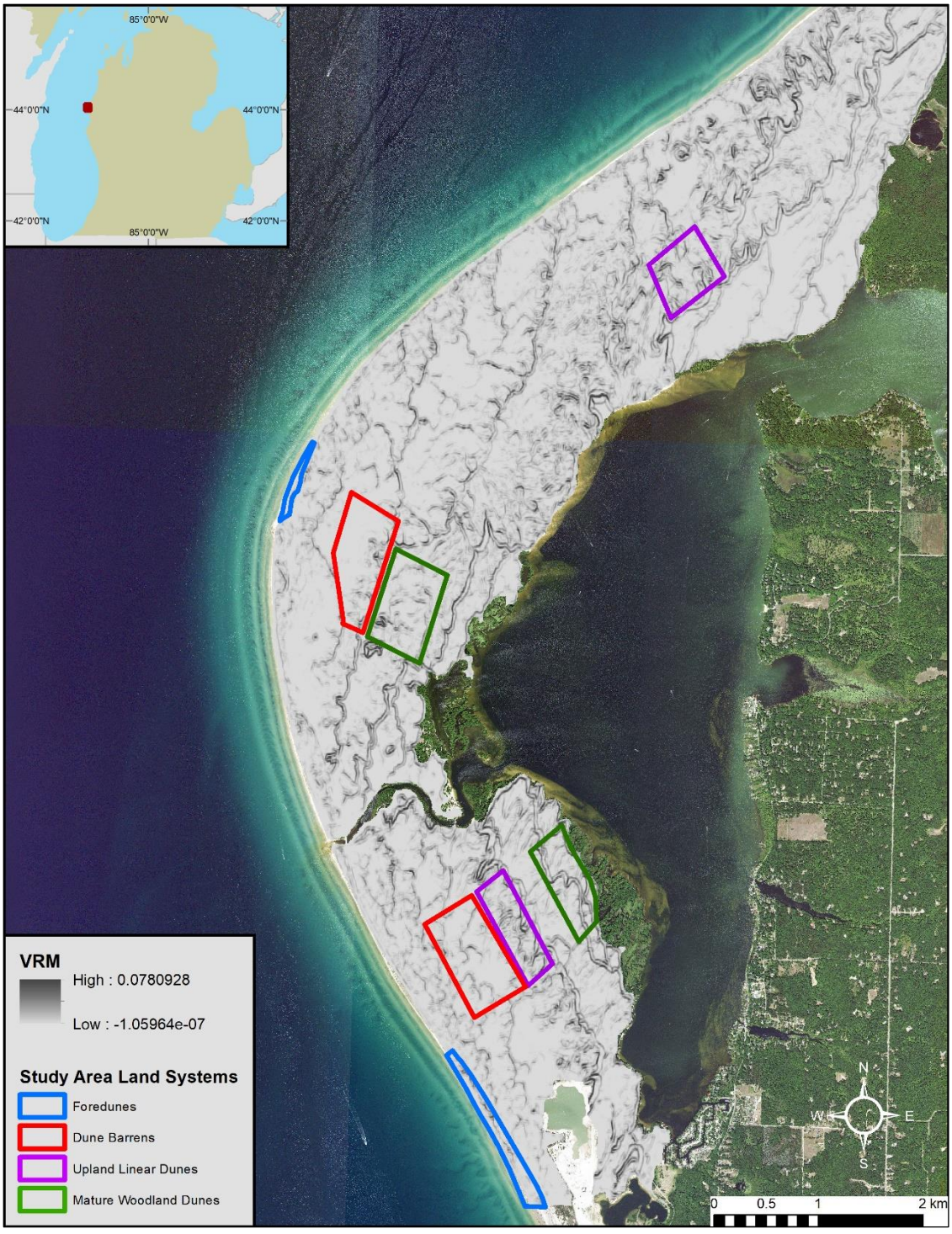

Figure 4.9: Vector Ruggedness Measure (VRM) index values for the study area.

Table 4.2: Descriptive statistics for TRI, VRM, and SAVI calculation results.

Index	Resolution	Max. (m)	Min. (m)	Mean (m)	SD (m)
TRI	~10m (1/3 arc-second)	18.81	1.0	3.99	2.78
VRM	~10m (1/3 arc-second)	0.0781	-1.05e-07	0.004	0.005
SAVI	10m	1.16	-0.45	0.55	0.3

Table 4.3: Descriptive statistics for TRI by land system.

TRI by Land System		Mean	Median	Mode	Max.	St. Dev.	Skewness	Kurtosis	n
Foredunes	North	3.20	3.18	2.51	8.43	1.15	0.72	1.1	625
	South	3.77	3.36	1	12.54	1.96	1.2	1.56	2932
Swale	*Not Analyzed*								
Dune Barrens	North	3.14	2.29	1	15.0	2.45	1.62	2.55	6501
	South	3.04	2.59	1	13.2	1.94	1.19	1.31	7334
Upland Linear Dunes	North	5.19	4.74	1	15.58	2.49	0.75	0.20	4332
	South	5.59	5.15	1	16.25	2.76	0.88	0.68	4177
Mature Woodland Dunes	North	3.58	3	1	16.89	2.42	1.61	3.17	6491
	South	5.58	4.77	1	15.32	3.1	0.83	-0.08	4422

Table 4.4: Descriptive statistics for VRM by land system.

VRM by Land System		Mean	Median	Mode	Max.	St. Dev.	Skewness	Kurtosis	n
Foredunes	North	0.0043	0.0041	0.0022	0.0093	0.0021	0.57	-0.61	625
	South	0.0062	0.0043	0.0010	0.0260	0.0051	1.36	1.42	2932
Swale	*Not Analyzed*								
Dune Barrens	North	0.0026	0.0010	0.0001	0.0527	0.0042	3.38	17.01	6501
	South	0.0026	0.0014	0.0001	0.0291	0.0033	2.84	11.54	7334
Upland Linear Dunes	North	0.0052	0.0033	0.0014	0.0541	0.0056	2.45	8.77	4332
	South	0.0063	0.0041	0.0002	0.0650	0.0066	2.42	8.42	4177
Mature Woodland Dunes	North	0.0036	0.0020	~0	0.0613	0.0051	4.45	29.99	6491
	South	0.0064	0.0036	0.0030	0.0452	0.0068	1.73	3.23	4422

Table 4.5: Descriptive statistics for SAVI by land system.

SAVI by Land System		Mean	Median	Mode	Max.	St. Dev.	Skewness	Kurtosis	n
Foredunes	North	0.25	0.24	0.16	0.45	0.06	0.39	0.61	625
	South	0.22	0.22	0.31	0.53	0.07	-1.08	7.23	2932
Swale	*Not Analyzed*								
Dune Barrens	North	0.44	0.46	0.37	0.91	0.13	0.03	-0.16	6501
	South	0.40	0.41	0.33	0.72	0.11	-0.24	-0.37	7334
Upland Linear Dunes	North	0.29	0.27	0.25	0.88	0.08	1.68	8.32	4332
	South	0.37	0.34	0.35	0.93	0.14	1.81	3.47	4177
Mature Woodland Dunes	North	0.86	0.89	0.86	0.99	0.10	-2.42	6.46	6491
	South	0.91	0.92	0.90	1.05	0.06	-0.58	0.06	4422

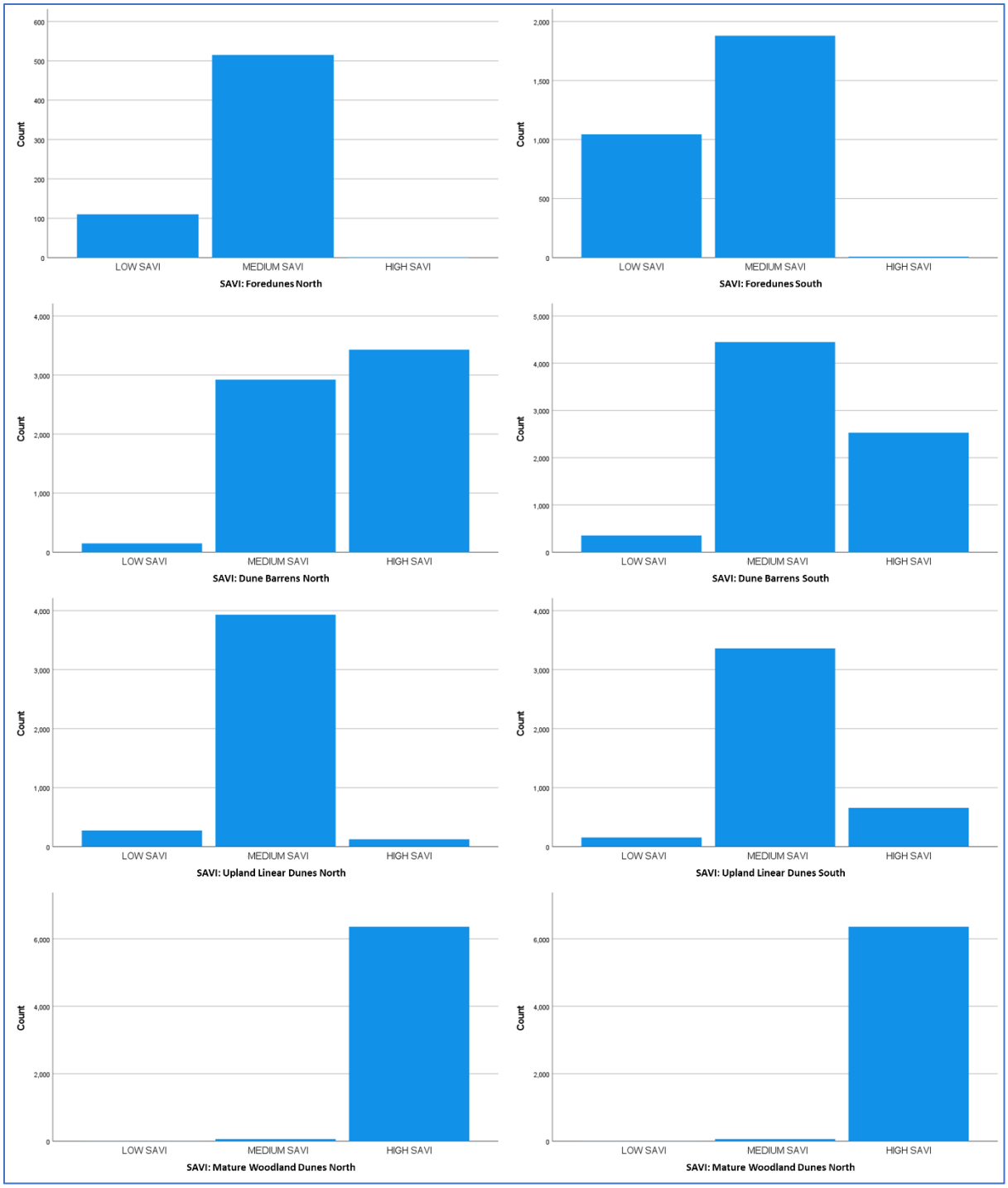

Figure 4.10: Bar charts of SAVI category by land system. The left and right columns compare SAVI values for the north and south study areas, respectively. Each row represents the same land system. For our study, we interpreted SAVI <=0.25 as low, possibly bare sand and patchy grasses. For pixels where 0.25<SAVI<=0.45, we interpreted this as medium SAVI, or possibly grasses and mixed vegetation. SAVI >0.45 was interpreted as high value, most likely woody vegetation and forests.

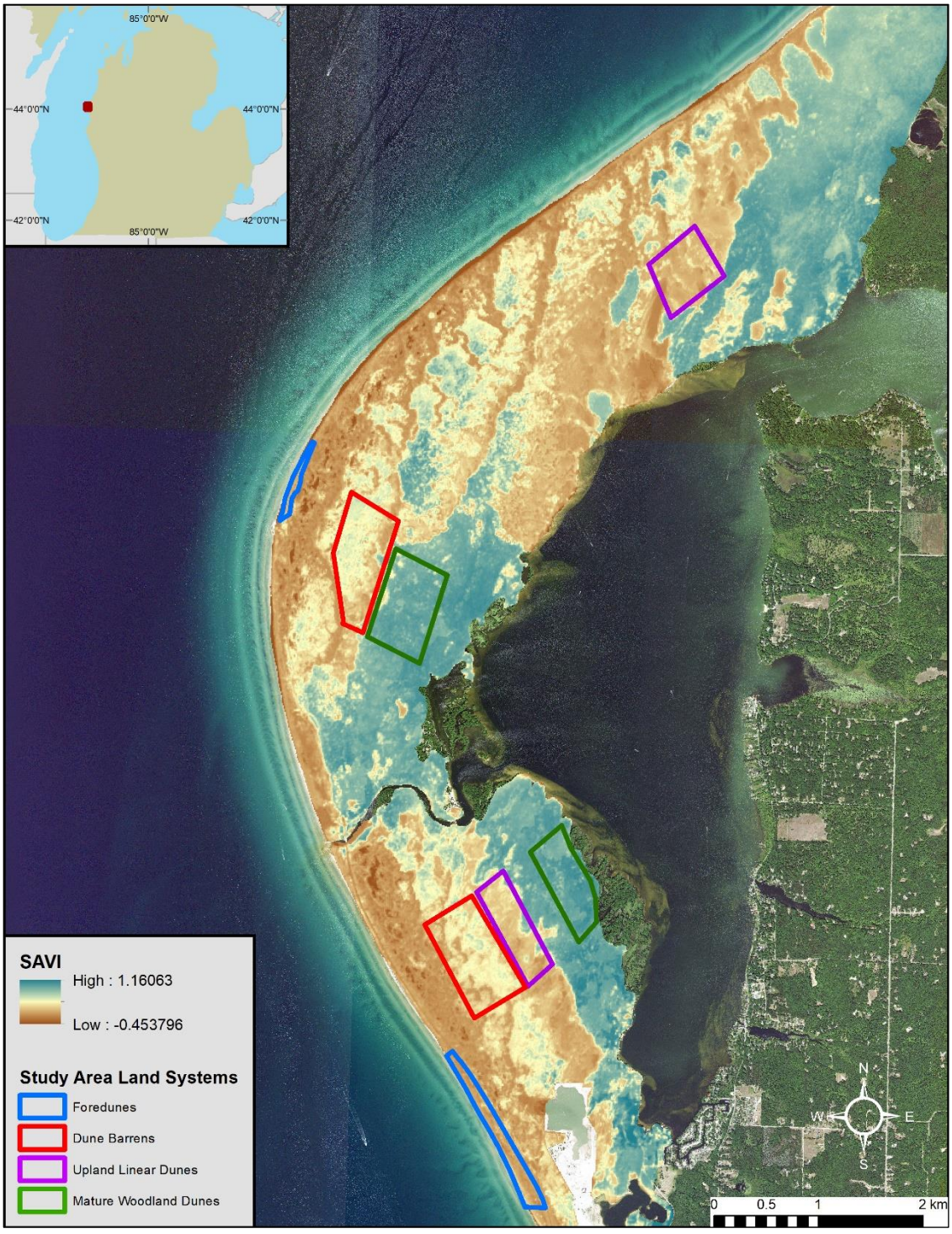

Figure 4.11: SAVI map for the Ludington State Park dunefield.

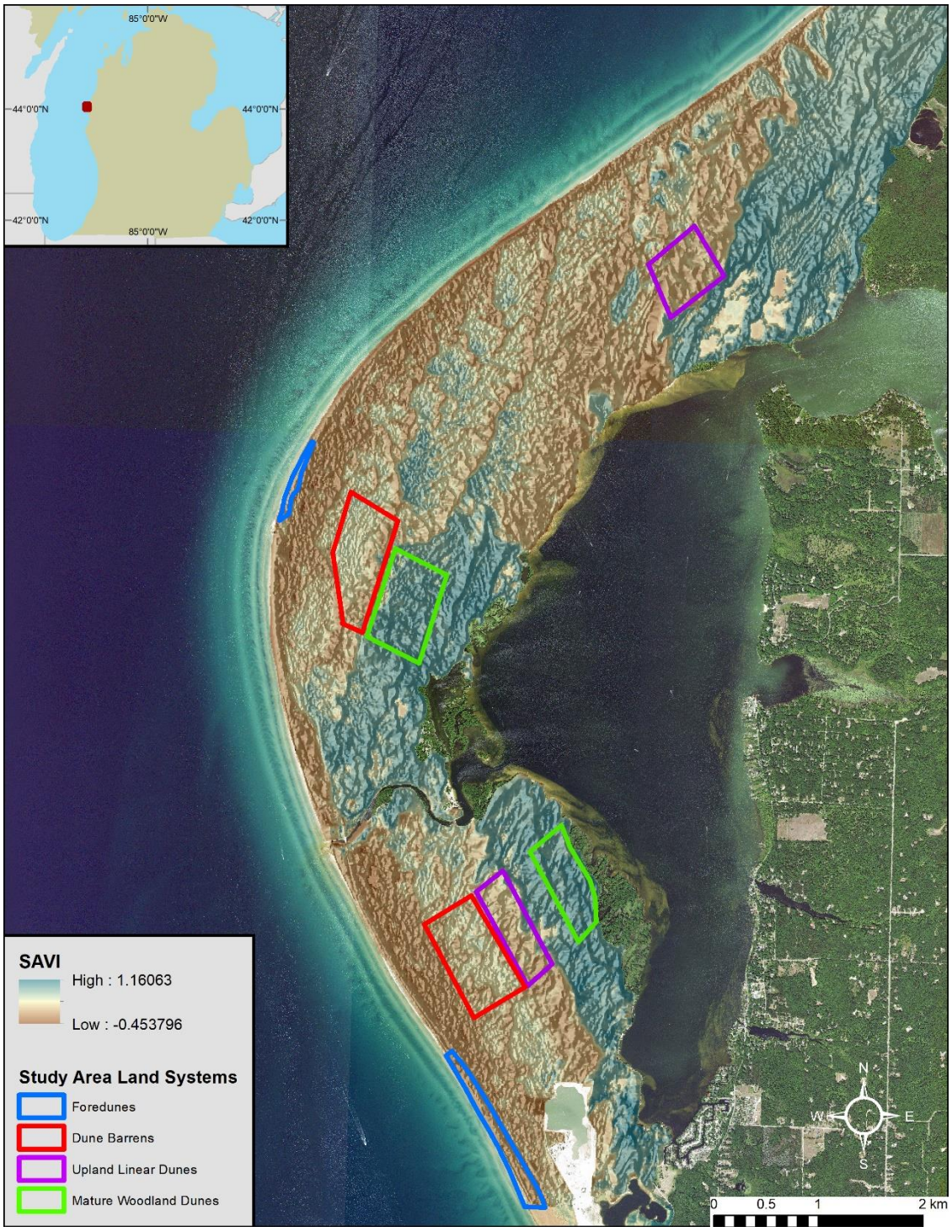

Figure 4.12: SAVI values draped over DEM-derived hillshade model, with a 270-degree azimuth and 45-degree sun angle. Generated in ArcGIS 10.7.1.

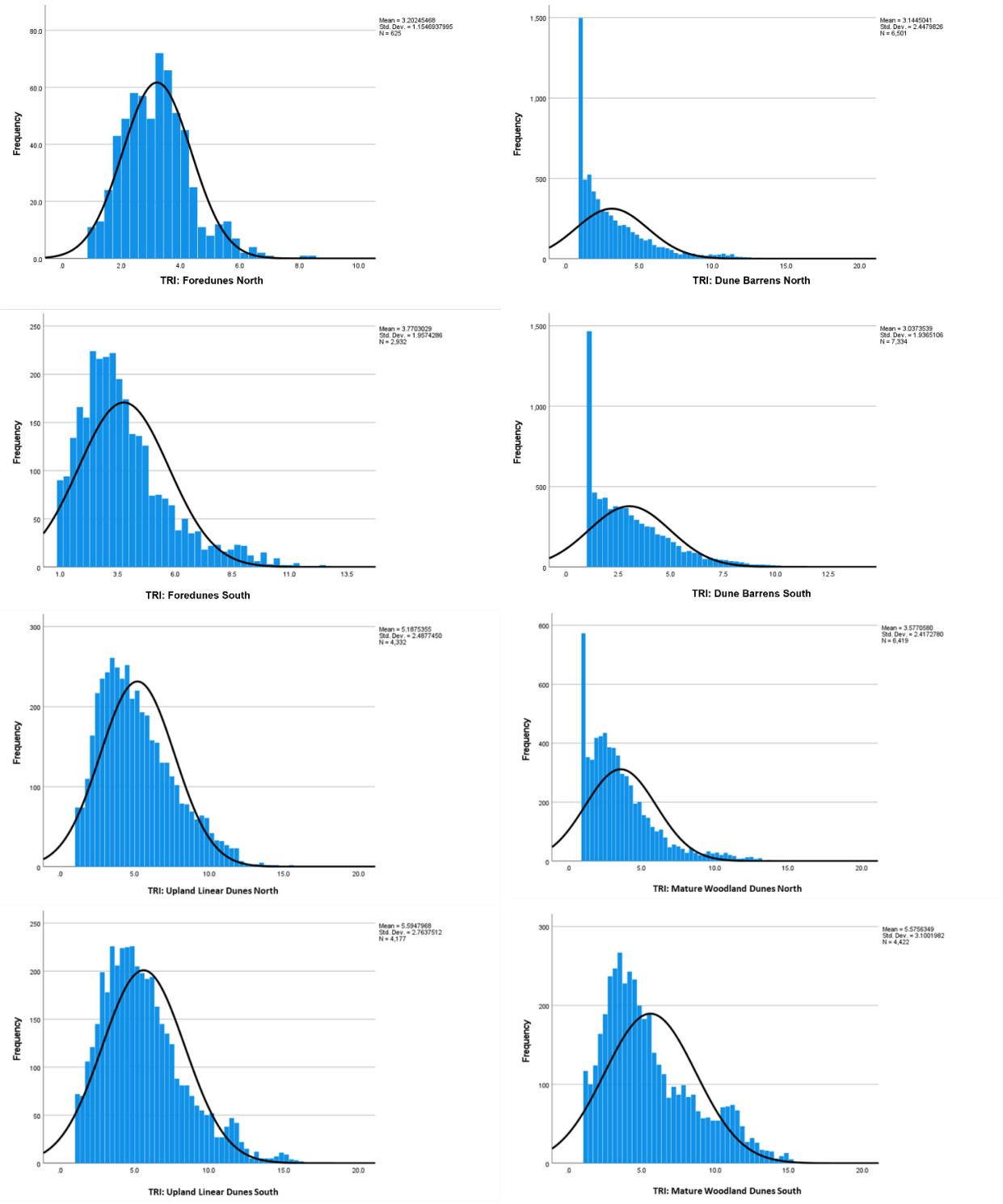

Figure 4.13: Histograms for TRI values by land system.

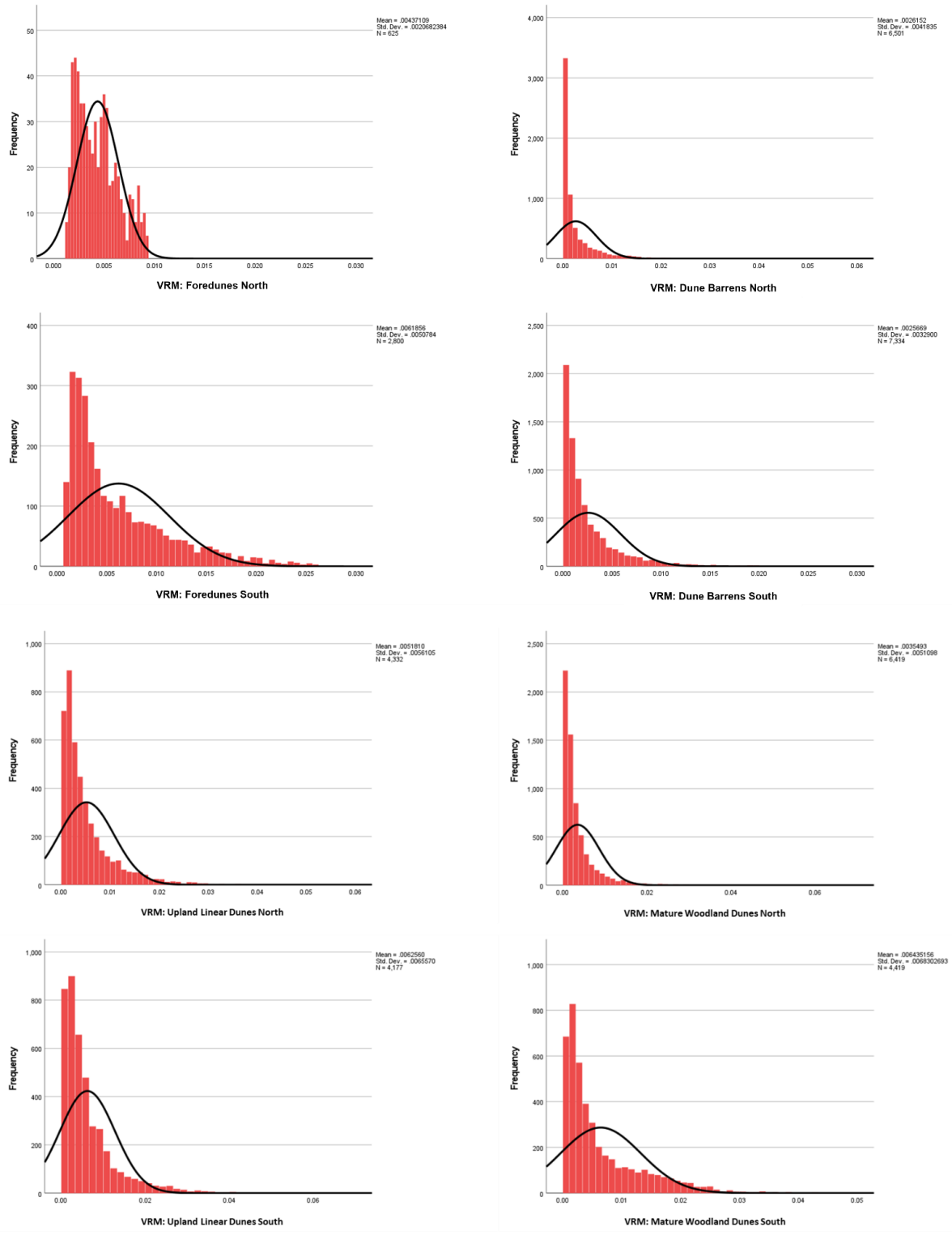

Figure 4.14: Histograms for VRM values by land system.

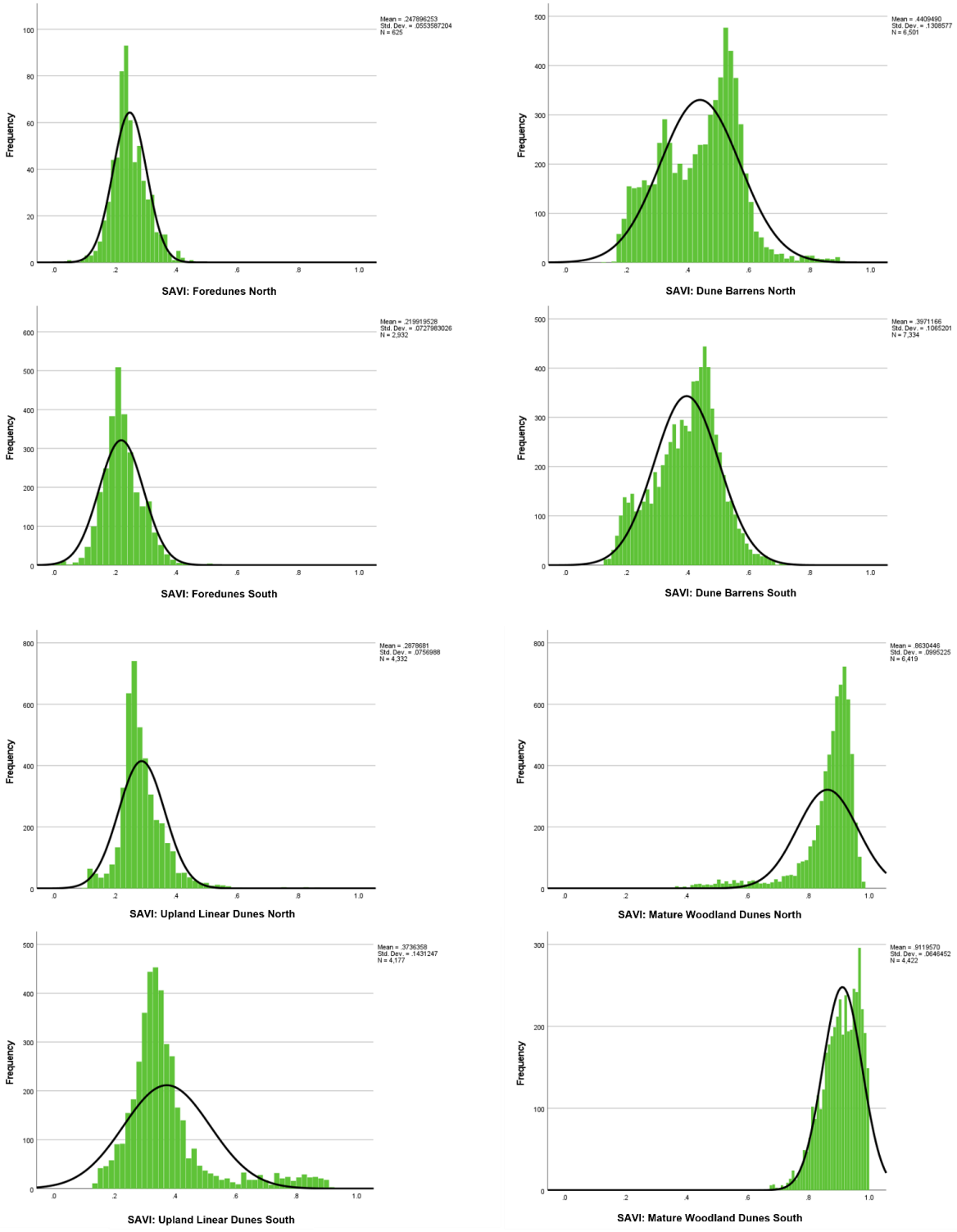

Figure 4.15: Histograms for SAVI values by land system.

Table 4.6: Mann-Whitney U-test results for TRI by land system. The Z-statistic for each test is shown. All U-tests were calculated for an assumed significance level of 0.05 and a confidence interval of 95%. For all tests, the null hypothesis was rejected with P-value of <0.001, with a few exceptions. For the U-test between the North Mature Woodland Dunes and the North Foredune land systems (shaded in gold), the null hypothesis was retained with a P-value=0.31. For three results, the null hypothesis was rejected, but the P-values were either <0.005 (in italics and underlined). Blue-shaded cells are where the lowest Mann-Whitney U-test results would be expected, as these would be between sites of the same land system.

	North Foredune	**South Foredune**	**North Dune Barrens**	**South Dune Barrens**	**North Upland Linear Dunes**	**South Upland Linear Dunes**	**North Mature Woodland Dunes**	**South Mature Woodland Dunes**
North Foredune	X	4.96	8.86	-7.17	-20.54	23.14	-1.01	19.99
South Foredune	4.96	X	21.89	20.33	-25.69	-30.30	9.41	-26.04
North Dune Barrens	8.86	21.89	X	3.88	-45.82	49.03	15.64	46.32
South Dune Barrens	-7.17	20.33	3.88	X	-48.00	-51.76	-12.94	48.14
North Upland Linear Dunes	-20.54	-25.69	-45.82	-48.00	X	6.36	-36.84	*2.82*
South Upland Linear Dunes	23.14	-30.30	49.03	-51.76	6.36	X	41.21	*-3.19*
North Mature Woodland Dunes	-1.01	9.41	15.64	-12.94	-36.84	41.21	X	37.35
South Mature Woodland Dunes	19.99	-26.04	46.32	48.14	*2.82*	*-3.19*	37.35	X

Table 4.7: Mann-Whitney U-test results for VRM by land system. The Z-statistic for each test is shown. All U-tests were calculated for an assumed significance level of 0.05 and a confidence interval of 95%. For all tests, null hypothesis was rejected with a P-value of <0.001, with a few exceptions. For two Mann-Whitney U-tests (shaded in gold), the null hypothesis was retained with P-values =~0.25. For one result, the null hypothesis was rejected, but the P-value =0.009 (in italics and underlined). Blue-shaded cells are where the lowest Mann-Whitney U-test results would be expected, as these would be between sites of the same land system.

	North Foredune	**South Foredune**	**North Dune Barrens**	**South Dune Barrens**	**North Upland Linear Dunes**	**South Upland Linear Dunes**	**North Mature Woodland Dunes**	**South Mature Woodland Dunes**
North Foredune	X	3.76	24.31	-23.28	5.07	1.15	-17.64	-1.17
South Foredune	3.76	X	46.76	44.71	13.74	4.52	34.16	-6.95
North Dune Barrens	24.31	46.76	X	10.98	-40.54	47.03	24.35	44.86
South Dune Barrens	-23.28	44.71	10.98	X	-35.60	-43.93	-15.44	40.48
North Upland Linear Dunes	5.07	13.74	-40.54	-35.60	X	9.50	-22.32	6.42
South Upland Linear Dunes	1.15	4.52	47.03	-43.93	9.50	X	31.69	*-2.62*
North Mature Woodland Dunes	-17.64	34.16	24.35	-15.44	-22.32	31.69	X	27.74
South Mature Woodland Dunes	-1.17	-6.95	44.86	40.48	6.42	*-2.62*	27.74	X

Table 4.8: Mann-Whitney U-test results for SAVI by land system. The Z-statistic for each test is shown. All U-tests were calculated for an assumed significance level of 0.05 and a confidence interval of 95%. For all tests, the null hypothesis was rejected with a P-value of <0.001, with no exceptions.

	North Foredune	**South Foredune**	**North Dune Barrens**	**South Dune Barrens**	**North Upland Linear Dunes**	**South Upland Linear Dunes**	**North Mature Woodland Dunes**	**South Mature Woodland Dunes**
North Foredune	X	-10.26	-33.00	31.19	-14.76	28.02	41.33	40.53
South Foredune	-10.26	X	-66.52	-64.46	-39.39	-55.96	-77.69	72.72
North Dune Barrens	-33.00	-66.52	X	-22.02	58.55	-30.82	94.83	88.49
South Dune Barrens	31.19	-64.46	-22.02	X	54.08	22.90	-99.63	90.97
North Upland Linear Dunes	-14.76	-39.39	58.55	54.08	X	37.31	87.82	80.96
South Upland Linear Dunes	28.02	-55.96	-30.82	22.90	37.31	X	-84.21	79.08
North Mature Woodland Dunes	41.33	-77.69	94.83	-99.63	87.82	-84.21	X	27.98
South Mature Woodland Dunes	40.53	72.72	88.49	90.97	80.96	79.08	27.98	X

Table 4.9: Correlation analysis results for TRI-SAVI and VRM-SAVI. Spearman's ρ and P-values shown. Results demonstrating a moderate or strong correlation (>±0.45) are in italics, bold, and underlined.

		TRI-SAVI		VRM-SAVI	
		Spearman's *ρ*	***P*-value**	**Spearman's *ρ***	***P*-value**
Foredunes	North	-0.01	0.94	0.44	<0.001
	South	-0.11	<0.001	-0.17	<0.001
Dune Barrens	North	***-0.53***	<0.001	***-0.50***	<0.001
	South	***-0.45***	<0.001	***-0.45***	<0.001
Upland Linear Dunes	North	0.11	<0.001	0.08	<0.001
	South	0.16	<0.001	0.09	<0.001
Mature Woodland Dunes	North	0.31	<0.001	0.29	<0.001
	South	-0.04	0.005	-0.03	0.027

Table 4.10: Simple linear regression analysis results for the TRI-SAVI and the VRM-SAVI relationship by land system.

		TRI-SAVI		VRM-SAVI	
		R^2	*P*-value	R^2	*P*-value
Foredunes	North	0.00	0.854	0.10	<0.001
	South	0.01	<0.001	0.00	<0.001
Dune Barrens	North	0.08	<0.001	0.04	<0.001
	South	0.14	<0.001	0.10	<0.001
Upland Linear Dunes	North	0.04	<0.001	0.02	<0.001
	South	0.15	<0.001	0.05	<0.001
Mature Woodland Dunes	North	0.09	<0.001	0.04	<0.001
	South	0.02	0.003	0.02	0.002

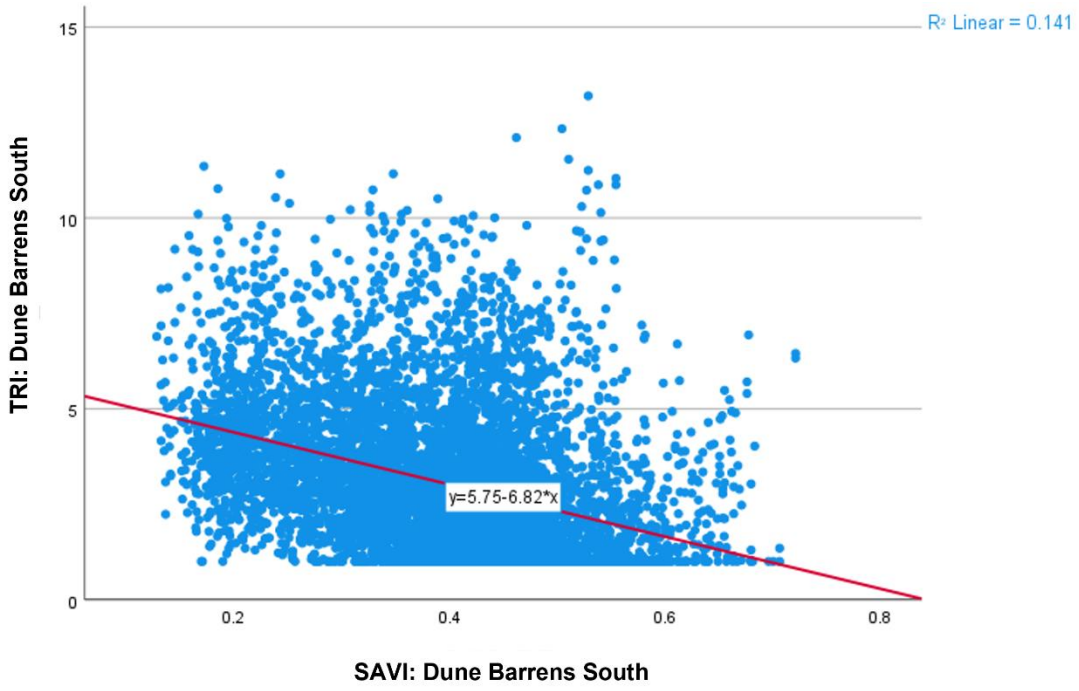

Figure 4.16: Simple Linear Regression scatter plot example for the TRI-SAVI relationship at the Dune Barrens South land system.

Figure 4.17: An additional example of the Dune Barrens land system at Ludington State Park. Photo from July 2016 by David C. Dister from Dister (2017).

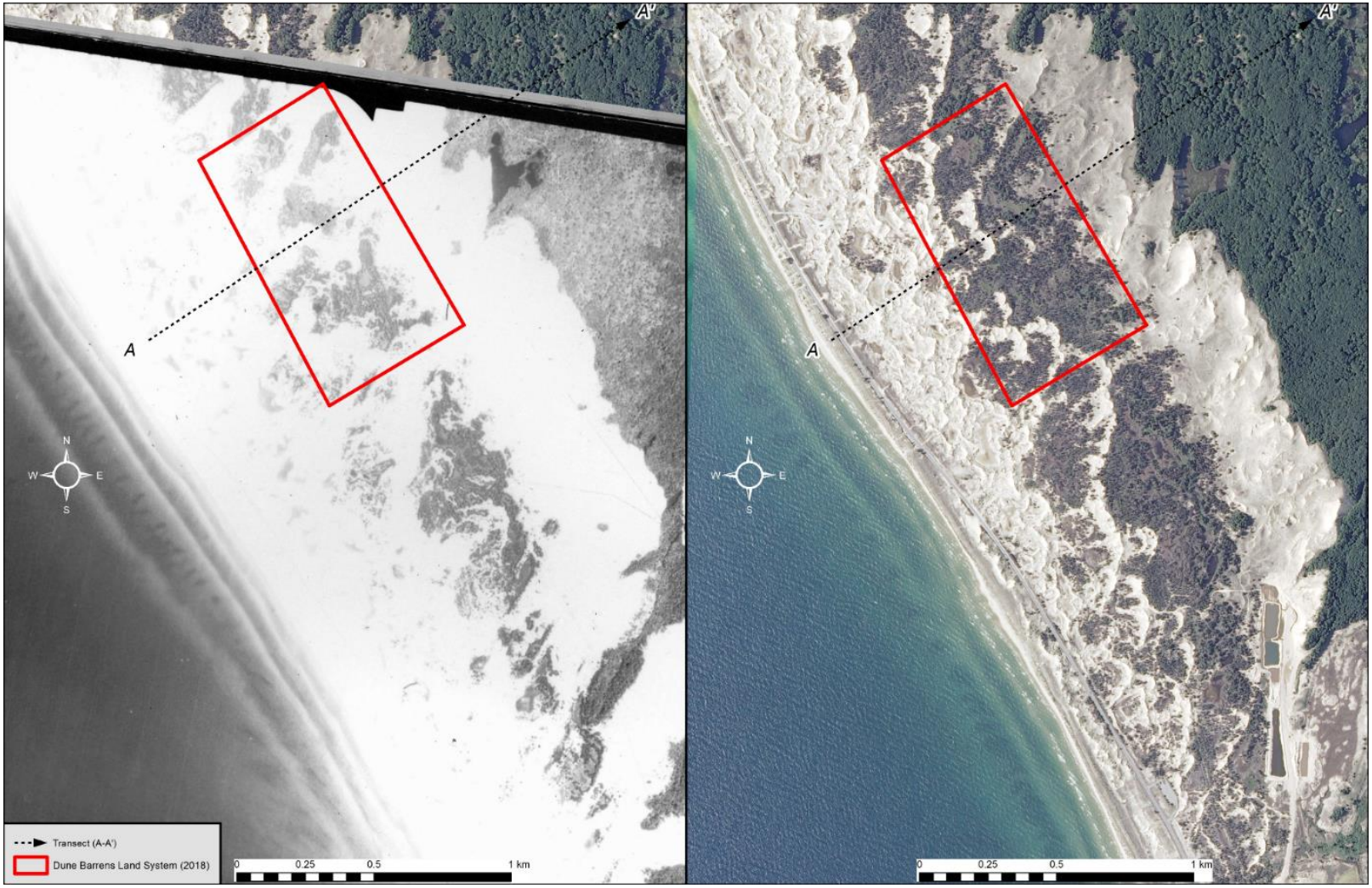

Figure 4.18: Comparison of the Dune Barrens land system area in the southern part of Ludington State Park between 1938 and 2018. Vegetation has expanded in the 80-year temporal interval in the Dune Barrens. The 1938 aerial image was obtained from Michigan State University's Remote Sensing and GIS Aerial Imagery Archive, whereas the 2019 image is from the National Agricultural Imagery Program (NAIP) dataset and was obtained from the USGS.

REFERENCES

REFERENCES

Adamson, D., Selkirk, P., Colhoun, E., 1988. Landforms of aeolian, tectonic and marine origin in the Bauer Bay-Sandy Bay region of subantarctic Macquarie Island. Pap. Proc. R. Soc. Tasmania 122, 65–82. https://doi.org/10.26749/rstpp.122.1.65

Althuwaynee, O.F., Pradhan, B., Park, H.-J., Lee, J.H., 2014. A novel ensemble bivariate statistical evidential belief function with knowledge-based analytical hierarchy process and multivariate statistical logistic regression for landslide susceptibility mapping. CATENA 114, 21–36. https://doi.org/10.1016/j.catena.2013.10.011

Arbogast, A.F., 2009. Sand dunes, in: Schaetzl, R.J., Darden, J.T., Brandt, D. (Eds.), Michigan Geography and Geology. Pearson Custom Publishing, Boston, pp. 274–287.

Arbogast, A.F., Garmon, B., Sterrett Isely, E., Jarosz, J., Kreiger, A., Nicholls, S., Queen, C., Richardson, R.B., 2018. Valuing Michigan's Coastal Dunes: GIS Information and Economic Data to Support Management Partnerships.

Arbogast, A.F., Hansen, E.C., Van Oort, M.D., 2002. Reconstructing the geomorphic evolution of large coastal dunes along the southeastern shore of Lake Michigan. Geomorphology 46, 241–255. https://doi.org/10.1016/S0169-555X(02)00076-4

Arbogast, A.F., Loope, W.L., 1999. Maximum-limiting ages of Lake Michigan coastal dunes: Their correlation with Holocene lake level history. J. Great Lakes Res. 25, 372–382. https://doi.org/10.1016/S0380-1330(99)70746-X

Arbogast, A.F., McKeehan, K.G., Richardson, R.B., Zimnicki, T., 2020. Learning to Live in Dynamic Dunes: Citizen Science and Participatory Modeling in the Service of Michigan Coastal Dune Decision-Making. Lansing, MI.

Arbogast, A.F., Schaetzl, R.J., Hupy, J.P., Hansen, E.C., 2004. The Holland Paleosol: An informal pedostratigraphic unit in the coastal dunes of southeastern Lake Michigan. Can. J. Earth Sci. 41, 1385–1400. https://doi.org/10.1139/E04-071

Argyilan, E.P., Lepper, K., Thompson, T.A., 2014. Late Holocene coastal development along the southern shore of Lake Michigan determined by strategic dating of stabilized parabolic dunes and wetlands of the Tolleston Beach, in: Coastline and Dune Evolution along the Great Lakes. Geological Society of America, pp. 31–46. https://doi.org/10.1130/2014.2508(03)

Atkinson, P.M., Tate, N.J., 2000. Spatial scale problems and geostatistical solutions: A review. Prof. Geogr. 52, 607–623.

Baas, A.C.W., 2002. Chaos, fractals and self-organization in coastal geomorphology: Simulating dune landscapes in vegetated environments. Geomorphology 48, 309–328.

Baedke, S.J., Thompson, T.A., 2000. A 4,700-year record of lake level and isostasy for Lake Michigan. J. Great Lakes Res. 26, 416–426. https://doi.org/10.1016/S0380-1330(00)70705-2

Bagnold, R.A., 1941. The Physics of Blown Sand and Desert Dunes. Methuen, London.

Baldwin, K.A., Maun, M.A., 1983. Microenvironment of Lake Huron sand dunes. Can. J. Bot. 61, 241–255.

Bar, P., Becker, N., Segev, M., 2016. Sand dunes management: a comparative analysis of ecological versus economic valuations applied to the Coastal region in Israel. Reg. Environ. Chang. 16, 941–950. https://doi.org/10.1007/s10113-015-0808-z

Barbier, E.B., Hacker, S.D., Kennedy, C., Koch, E.W., Stier, A.C., Silliman, B.R., 2011. The value of estuarine and coastal ecosystem services. Ecol. Monogr. 81, 169–193. https://doi.org/10.1890/10-1510.1

Barrows, C.W., 2011. Sensitivity to climate change for two reptiles at the Mojave–Sonoran Desert interface. J. Arid Environ. 75, 629–635. https://doi.org/10.1016/j.jaridenv.2011.01.018

Bate, G., Ferguson, M., 1996. Blowouts in coastal foredunes. Landsc. Urban Plan. 34, 215–224. https://doi.org/10.1016/0169-2046(95)00218-9

Bauer, B.O., Davidson-Arnott, R.G.D., 2003. A general framework for modeling sediment supply to coastal dunes including wind angle, beach geometry, and fetch effects. Geomorphology 49, 89–108. https://doi.org/10.1016/S0169-555X(02)00165-4

Beasom, S.L., Wiggers, E.P., Giardino, J.R., 1983. A Technique for Assessing Land Surface Ruggedness. J. Wildl. Manage. 47, 1163. https://doi.org/10.2307/3808184

Belly, P.-Y., 1962. Sand Movement by Wind. Beach Erosion Board, Corps of Engineers, U.S. Army, Institute of Engineering Research Technical Report Series 72, Issue 7.

Beven, K.J., Kirkby, M.J., 1979. A physically based, variable contributing area model of basin hydrology / Un modèle à base physique de zone d'appel variable de l'hydrologie du bassin versant. Hydrol. Sci. Bull. 24, 43–69. https://doi.org/10.1080/02626667909491834

Blumer, B.E., Arbogast, A.F., Forman, S.L., 2012. The OSL chronology of eolian sand deposition in a perched dune field along the northwestern shore of Lower Michigan. Quat. Res. 77, 445–455. https://doi.org/10.1016/j.yqres.2012.01.006

Bolstad, P., 2008. GIS Fundamentals: A First Text on Geographic Information Systems, 3rd ed. Eider Press, White Bear Lake, MN.

Box, G.E.P., Cox, D.R., 1964. An Analysis of Transformations. J. R. Stat. Soc. 26, 211–52.

Brown, D.G., Arbogast, A.F., 1999. Digital photogrammetric change analysis as applied to active coastal dunes in Michigan. Photogramm. Eng. Remote Sens. 65, 467–474.

Brown, O.W., Hugenholtz, C.H., 2012. Estimating aerodynamic roughness (zo) in mixed grassland prairie with airborne LiDAR. Can. J. Remote Sens. 37, 422–428. https://doi.org/10.5589/m11-051

Bryant, R.G., Baddock, M.C., 2021. Remote Sensing of Aeolian Processes, in: Reference Module in Earth Systems and Environmental Sciences. Elsevier. https://doi.org/10.1016/B978-0-12-818234-5.00132-2

Carter, R.W.G., 1991. Coastal Dunes, in: Coastal Environments: An Introduction to the Physical, Ecological, and Cultural Systems of the Coastlines. London, pp. 301–354.

Caruso, A.S., Clarke, K.D., Tiddy, C.J., Delean, S., Lewis, M.M., 2018. Objective Regolith-Landform Mapping in a Regolith Dominated Terrain to Inform Mineral Exploration. Geosciences 8, 318. https://doi.org/10.3390/geosciences8090318

Charbonneau, B.R., Dohner, S.M., Wnek, J.P., Barber, D., Zarnetske, P., Casper, B.B., 2021. Vegetation effects on coastal foredune initiation: Wind tunnel experiments and field validation for three dune-building plants. Geomorphology 378, 107594. https://doi.org/10.1016/j.geomorph.2021.107594

Chen, C.R., Hou, E.Q., Condron, L.M., Bacon, G., Esfandbod, M., Olley, J., Turner, B.L., 2015. Soil phosphorus fractionation and nutrient dynamics along the Cooloola coastal dune chronosequence, southern Queensland, Australia. Geoderma 257–258, 4–13. https://doi.org/10.1016/j.geoderma.2015.04.027

Chepil, W.S., Siddoway, F.H., Armbrust, D.V., 1963. Climatic index of wind erosion conditions in the Great Plains, in: Soil Science Society Proceedings. Division S-6 -- Soil and Water Management . pp. 449–452.

Chorley, R.J., 1962. Geomorphology and General Systems Theory, Professional Paper 500-B. https://doi.org/10.3133/pp500B

Chrisman, N., 2002. Exploring Geographic Information Systems, 2nd ed. John Wiley & Sons, Inc., New York, NY.

Christian, C.A., Stewart, G.A., 1964. Methodology of integrated surveys, in: Conference on Principles and Methods of Integrating Aerial Survey Studies of Natural Resources for Potential Development, U.N.E.S.C.O., Toulouse, France. p. 145.

Claessens, L., Verburg, P.H., Schoorl, J.M., Veldkamp, A., 2006. Contribution of Topographically Based Landslide Hazard Modelling to the Analysis of the Spatial Distribution and Ecology of Kauri (Agathis australis). Landsc. Ecol. 21, 63–76. https://doi.org/10.1007/s10980-005-5769-z

Coetzee, K., Fabricius, C., 1992. Geographic information systems and artificial intelligence for predicting the presence or absence of mountain reedbuck. South African J. Wildl. Res. 22, 80–86.

Cohen, J.G., Kost, M.A., Slaughter, B.S., Albert, D.A., 2015. A Field Guide to the Natural Communities of Michigan. Michigan State University Press, East Lansing, Mich. https://doi.org/10.14321/j.ctt14bs117

Cohn, N., Ruggiero, P., Vries, S., Kaminsky, G.M., 2018. New Insights on Coastal Foredune Growth: The Relative Contributions of Marine and Aeolian Processes. Geophys. Res. Lett. 45, 4965–4973. https://doi.org/10.1029/2018GL077836

Cooper, W.S., 1958. Coastal Sand Dunes of Oregon and Washington. Geological Society of America - Memoir 72.

Corder, G.W., Foreman, D.I., 2009. Nonparametric Statistics for Non-Statisticians. John Wiley & Sons, Inc., Hoboken, NJ, USA. https://doi.org/10.1002/9781118165881

Cowie, S.M., Knippertz, P., Marsham, J.H., 2013. Are vegetation-related roughness changes the cause of the recent decrease in dust emission from the Sahel? Geophys. Res. Lett. 40, 1868–1872. https://doi.org/10.1002/grl.50273

Cowles, H.C., 1899. The ecological relations of the vegetation on the sand dunes of Lake Michigan: Part I -Geographical relations of the dune floras. Bot. Gaz. 27, 95–117.

Davidson-Arnott, R., Hesp, P., Ollerhead, J., Walker, I., Bauer, B., Delgado-Fernandez, I., Smyth, T., 2018. Sediment budget controls on foredune height: Comparing simulation model results with field data. Earth Surf. Process. Landforms 43, 1798–1810. https://doi.org/10.1002/esp.4354

Davidson-Arnott, R.G.D., Law, M.N., 1996. Measurement and Prediction of Long-Term Sediment Supply to Coastal Foredunes. J. Coast. Res. 12, 654–663.

Davidson, S.G., Hesp, P., Miot da Silva, G., 2021. Rapid shoreline erosion and dunefield change, Salmon Hole, South Australia. Sci. Total Environ. 767, 145406. https://doi.org/10.1016/j.scitotenv.2021.145406

De Cola, L., Lam, N.S.-N., 1993. Introduction to Fractals in Geography, in: Lam, N.S.-N., De Cola, L. (Eds.), Fractals in Geography. Prentice Hall, Englewood Cliffs, N.J., pp. 3–22.

De Reu, J., Bourgeois, J., Bats, M., Zwertvaegher, A., Gelorini, V., De Smedt, P., Chu, W., Antrop, M., De Maeyer, P., Finke, P., Van Meirvenne, M., Verniers, J., Crombé, P., 2013. Application of the topographic position index to heterogeneous landscapes. Geomorphology 186, 39–49. https://doi.org/10.1016/j.geomorph.2012.12.015

Dech, J.P., Maun, M.A., 2005. Zonation of vegetation along a burial gradient on the leeward

slopes of Lake Huron sand dunes. Can. J. Bot. 83, 227–236. https://doi.org/10.1139/b04-163

Delgado-Fernandez, I., 2011. Meso-scale modelling of aeolian sediment input to coastal dunes. Geomorphology 130, 230–243. https://doi.org/10.1016/j.geomorph.2011.04.001

Delgado-Fernandez, I., O'Keeffe, N., Davidson-Arnott, R.G.D., 2019. Natural and human controls on dune vegetation cover and disturbance. Sci. Total Environ. 672, 643–656. https://doi.org/10.1016/j.scitotenv.2019.03.494

Delgado-Fernandez, I., Smyth, T.A.G., Jackson, D.W.T., Smith, A.B., Davidson-Arnott, R.G.D., 2018. Event-Scale Dynamics of a Parabolic Dune and Its Relevance for Mesoscale Evolution. J. Geophys. Res. Earth Surf. 123, 3084–3100. https://doi.org/10.1029/2017JF004370

Dietrich, W.E., Perron, J.T., 2006. The search for a topographic signature of life. Nature 439, 411–418. https://doi.org/10.1038/nature04452

Ding, C., Zhang, L., Liao, M., Feng, G., Dong, J., Ao, M., Yu, Y., 2020. Quantifying the spatio-temporal patterns of dune migration near Minqin Oasis in northwestern China with time series of Landsat-8 and Sentinel-2 observations. Remote Sens. Environ. 236, 111498. https://doi.org/10.1016/j.rse.2019.111498

Dister, D.C., 2017. The Vascular Flora of Ludington State Park, Mason County, Michigan. Gt. Lakes Bot. 56, 52–90.

Doing, H., 1985. Coastal fore-dune zonation and succession in various parts of the world. Vegetatio 61, 65–75.

Dong, Y., Shortridge, A.M., 2019. A regional ASTER GDEM error model for the Chinese Loess Plateau. Int. J. Remote Sens. 40, 1048–1065. https://doi.org/10.1080/01431161.2018.1524171

Doody, J.P., 2013a. Sand Dune Conservation, Management and Restoration. Coastal Research Library, vol. 4. Springer Science+Business Media, Inc., Dordrecht.

Doody, J.P., 2013b. Introduction, in: Sand Dune Conservation, Management and Restoration. Coastal Research Library, Vol 4. Springer, Dordrecht, pp. 1–36. https://doi.org/10.1007/978-94-007-4731-9_1

Dott, E.R., Mickelson, D., 1995. Lake Michigan water levels and the development of Holocene beach-ridge complexes at Two Rivers, Wisconsin: Stratigraphic, geomorphic, and radiocarbon evidence. Geol. Soc. Am. Bull. 107, 286–0296. https://doi.org/10.1130/0016-7606(1995)107<0286:LMWLAT>2.3.CO;2

Draper, N.R., Smith, H., 1998. Applied Regression Analysis, Third Edit. ed, Wiley Series in Probability and Statistics. John Wiley & Sons, New York.

https://doi.org/10.1002/9781118625590

Drummond, R.R., Dennis, H.W., 1968. QUALIFYING RELIEF TERMS. Prof. Geogr. 20, 326–332. https://doi.org/10.1111/j.0033-0124.1968.00326.x

Durán, O., Claudin, P., Andreotti, B., 2011. On aeolian transport: Grain-scale interactions, dynamical mechanisms and scaling laws. Aeolian Res. 3, 243–270. https://doi.org/10.1016/j.aeolia.2011.07.006

Durán, O., Herrmann, H.J., 2006. Vegetation Against Dune Mobility. Phys. Rev. Lett. 97, 188001. https://doi.org/10.1103/PhysRevLett.97.188001

Durán, O., Moore, L.J., 2013. Vegetation controls on the maximum size of coastal dunes. Proc. Natl. Acad. Sci. 110, 17217–17222. https://doi.org/10.1073/pnas.1307580110

European Space Agency, 2015. Sentinel-2 User Handbook.

Ewing, R.C., Kocurek, G., Lake, L.W., 2006. Pattern analysis of dune-field parameters. Earth Surf. Process. Landforms 31, 1176–1191. https://doi.org/10.1002/esp.1312

Forey, E., Chapelet, B., Vitasse, Y., Tilquin, M., Touzard, B., Michalet, R., 2008. The relative importance of disturbance and environmental stress at local and regional scales in French coastal sand dunes. J. Veg. Sci. 19, 493–502. https://doi.org/10.3170/2008-8-18392

Frank, A., Kocurek, G., 1996. Toward a model for airflow on the lee side of aeolian dunes. Sedimentology 43, 451–458. https://doi.org/10.1046/j.1365-3091.1996.d01-20.x

Fryberger, S.G., Dean, G., 1979. Dune forms and wind regime. In: McKee, E. (Ed.), A Study of Global Sand Seas. USGS Professional Paper 1052. Washington, D.C.

Fulop, E.C.F., Johnson, B.G., Keen-Zebert, A., 2019. A geochronology-supported soil chronosequence for establishing the timing of shoreline parabolic dune stabilization. CATENA 178, 232–243. https://doi.org/10.1016/j.catena.2019.03.018

Gardner, R., McLaren, S., 1999. Infiltration and moisture movement in coastal sand dunes, Studland, Dorset, U.K.: Preliminary results. J. Coast. Res. 15, 936–949.

Gares, P.A., 1992. Topographic changes associated with coastal dune blowouts at island beach state park, New Jersey. Earth Surf. Process. Landforms 17, 589–604. https://doi.org/10.1002/esp.3290170605

Gerber, S.B., Voelkl Finn, K., 2005. Using SPSS for Windows: Data Analysis and Graphics, 2nd Editio. ed. Springer Science+Business Media, Inc., New York, NY.

Gillette, D.A., Adams, J., Endo, A., Smith, D., Kihl, R., 1980. Threshold velocities for input of soil particles into the air by desert soils. J. Geophys. Res. 85, 5621.

https://doi.org/10.1029/JC085iC10p05621

Gocic, M., Trajkovic, S., 2013. Analysis of changes in meteorological variables using Mann-Kendall and Sen's slope estimator statistical tests in Serbia. Glob. Planet. Change 100, 172–182. https://doi.org/10.1016/j.gloplacha.2012.10.014

Grohmann, C.H., Smith, M.J., Riccomini, C., 2011. Multiscale analysis of topographic surface roughness in the Midland Valley, Scotland. IEEE Trans. Geosci. Remote Sens. 49, 1200–1213. https://doi.org/10.1109/TGRS.2010.2053546

Gruber, F.E., Baruck, J., Mair, V., Geitner, C., 2019. From geological to soil parent material maps - A random forest-supported analysis of geological map units and topography to support soil survey in South Tyrol. Geoderma 354. https://doi.org/10.1016/j.geoderma.2019.113884

Gu, Y., Brown, J.F., Verdin, J.P., Wardlow, B., 2007. A five-year analysis of MODIS NDVI and NDWI for grassland drought assessment over the central Great Plains of the United States. Geophys. Res. Lett. 34, L06407. https://doi.org/10.1029/2006GL029127

Guo, X., Price, K.P., Stiles, J.M., 2000. Modeling Biophysical Factors for Grasslands in Eastern Kansas Using Landsat TM Data. Trans. Kansas Acad. Sci. 103, 122. https://doi.org/10.2307/3628261

Hack, J.T., 1941. Dunes of the Western Navajo Country. Geogr. Rev. 31, 240. https://doi.org/10.2307/210206

Hansen, E.C., Fisher, T.G., Arbogast, A.F., Bateman, M.D., 2010. Geomorphic history of low-perched, transgressive dune complexes along the southeastern shore of Lake Michigan. Aeolian Res. 1, 111–127. https://doi.org/10.1016/j.aeolia.2009.08.001

Harman, J.R., Arbogast, A.F., 2004. Environmental ethics and coastal dunes in western Lower Michigan: Developing a rationale for ecosystem preservation. Ann. Assoc. Am. Geogr. 94, 23–36.

Helsel, D.R., Hirsch, R.M., 2002. Statistical methods in water resources. Techniques of water-resources investigations series 04-A3. Reston, Va. https://doi.org/10.3133/twri04A3

Hesp, P., 2002. Foredunes and blowouts: Initiation, geomorphology and dynamics. Geomorphology 48, 245–268. https://doi.org/10.1016/S0169-555X(02)00184-8

Hesp, P., Martinez, M., da Silva, G.M., Rodríguez-Revelo, N., Gutierrez, E., Humanes, A., Laínez, D., Montaño, I., Palacios, V., Quesada, A., Storero, L., Trilla, G.G., Trochine, C., 2011. Transgressive dunefield landforms and vegetation associations, Doña Juana, Veracruz, Mexico. Earth Surf. Process. Landforms 36, 285–295. https://doi.org/10.1002/esp.2035

Hesp, P.A., 1981. The Formation of Shadow Dunes. SEPM J. Sediment. Res. Vol. 51.

https://doi.org/10.1306/212F7C1B-2B24-11D7-8648000102C1865D

Hesp, P.A., Hyde, R., 1996. Flow dynamics and geomorphology of a trough blowout. Sedimentology 43, 505–525. https://doi.org/10.1046/j.1365-3091.1996.d01-22.x

Hesp, P.A., Smyth, T.A.G., 2016. Surfzone-Beach-Dune interactions: Flow and Sediment Transport across the Intertidal Beach and Backshore. J. Coast. Res. 75, 8–12. https://doi.org/10.2112/SI75-002.1

Hobson, R.D., 1972. Surface Roughness in Topography: A Quantitative Approach, in: Chorley, R.J. (Ed.), Spatial Analysis in Geomorphology. Methuen, London, pp. 221–245.

Holton, B., Johnson, A.F., 1979. Dune Scrub Communities and Their Correlation with Environmental Factors at Point Reyes National Seashore, California. J. Biogeogr. 6, 317. https://doi.org/10.2307/3038084

Hop, K., Drake, J., Lubinski, S., Menard, S., Dieck, J., 2011. National Park Service Vegetation Inventory Program: Sleeping Bear Dunes National Lakeshore, Michigan, Natural Resource Report, NPS/GLKN/NRR—2011/395. Fort Collins, Colo.

Horton, R.E., 1945. Erosional Development of Streams and Their Drainage Basins; Hydrophysical Approach to Quantitative Morphology. Geol. Soc. Am. Bull. 56, 275–370.

Howard, A.D., Morton, J.B., Gad-El-Hak, M., Pierce, D.B., 1978. Sand transport model of barchan dune equilibrium. Sedimentology 25, 307–338. https://doi.org/10.1111/j.1365-3091.1978.tb00316.x

Hsu, S.-A., 1971. Wind stress criteria in eolian sand transport. J. Geophys. Res. 76, 8684–8686. https://doi.org/10.1029/JC076i036p08684

Huete, A.., 1988. A soil-adjusted vegetation index (SAVI). Remote Sens. Environ. 25, 295–309. https://doi.org/10.1016/0034-4257(88)90106-X

Huete, A.R., Jackson, R.D., Post, D.F., 1985. Spectral response of a plant canopy with different soil backgrounds. Remote Sens. Environ. 17, 37–53. https://doi.org/10.1016/0034-4257(85)90111-7

Huggett, R.J., 2011. Fundamentals of Geomorphology, Third Edit. ed. Routledge, New York.

IBM Corp., 2020. IBM SPSS Statistics for Windows, Version 27.0.

Ibrahim, S., 2018. Remote sensing of tree/grass fractional cover using phenological signal decomposition of MODIS time series data. University of Leicester.

Jackson, D.W.T., Costas, S., González-Villanueva, R., Cooper, A., 2019. A global 'greening' of coastal dunes: An integrated consequence of climate change? Glob. Planet. Change 182,

103026. https://doi.org/10.1016/j.gloplacha.2019.103026

Jenny, H., 1941. Factors of Soil Formation: A System of Quantitative Pedology, First edit. ed. McGraw-Hill, New York.

Jensen, J.R., 2007. Remote Sensing of the Environment: An Earth Resource Perspective, Second Edi. ed. Pearson Prentice Hall.

Jerolmack, D.J., Ewing, R.C., Falcini, F., Martin, R.L., Masteller, C., Phillips, C., Reitz, M.D., Buynevich, I., 2012. Internal boundary layer model for the evolution of desert dune fields. Nat. Geosci. 5, 206–209. https://doi.org/10.1038/ngeo1381

Jewell, M., Houser, C., Trimble, S., 2017. Phases of blowout initiation and stabilization on Padre Island revealed through ground-penetrating radar and remotely sensed imagery. Phys. Geogr. 38, 556–577. https://doi.org/10.1080/02723646.2017.1338042

Juergens, N., Oldeland, J., Hachfeld, B., Erb, E., Schultz, C., 2013. Ecology and spatial patterns of large-scale vegetation units within the central Namib Desert. J. Arid Environ. 93, 59–79. https://doi.org/10.1016/j.jaridenv.2012.09.009

Kawamura, R., 1951. Study on Sand Movement by Wind. The Report of the Institute of Science and Technology.

Kidron, G.J., Zohar, M., 2016. Factors controlling the formation of coppice dunes (nebkhas) in the Negev Desert. Earth Surf. Process. Landforms 41, 918–927. https://doi.org/10.1002/esp.3875

Kilibarda, Z., Venturelli, R., Goble, R., 2014. Late Holocene dune development and shift in dune-building winds along southern Lake Michigan, in: Coastline and Dune Evolution along the Great Lakes. Geological Society of America, pp. 47–64. https://doi.org/10.1130/2014.2508(04)

Kim, D., Bae Yu, K., Jin Park, S., 2008. Identification and Visualization of Complex Spatial Pattern of Coastal Dune Soil Properties Using GIS-Based Terrain Analysis and Geostatistics. J. Coast. Res. 4, 50–60. https://doi.org/10.2112/06-0721.1

Kim, D., Yu, K.B., 2009. A conceptual model of coastal dune ecology synthesizing spatial gradients of vegetation, soil, and geomorphology. Plant Ecol. 202, 135–148. https://doi.org/10.1007/s11258-008-9456-4

Kirchner, J.W., 1993. Statistical inevitability of Horton's laws and the apparent randomness of stream channel networks. Geology 21, 591–594.

Kocurek, G., Ewing, R.C., 2005. Aeolian dune field self-organization – implications for the formation of simple versus complex dune-field patterns. Geomorphology 72, 94–105. https://doi.org/10.1016/j.geomorph.2005.05.005

Koehler, G.M., Hornocker, M.G., 1989. Influences of Seasons on Bobcats in Idaho. J. Wildl. Manage. 53, 197. https://doi.org/10.2307/3801331

Kong, T.M., Marsh, S.E., van Rooyen, A.F., Kellner, K., Orr, B.J., 2015. Assessing rangeland condition in the Kalahari Duneveld through local ecological knowledge of livestock farmers and remotely sensed data. J. Arid Environ. 113, 77–86. https://doi.org/10.1016/j.jaridenv.2014.10.003

Konlechner, T.M., Buckley, E.E.C.., Hilton, M.J., Wakes, S.J., 2016. Downwind dune dynamics following Ammophila arenaria invasion. J. Coast. Res. 75, 298–302. https://doi.org/10.2112/SI75-60.1

Kreznor, W.R., Olson, K.R., Banwart, W.L., Johnson, D.L., 1989. Soil, Landscape, and Erosion Relationships in a Northwest Illinois Watershed. Soil Sci. Soc. Am. J. 53, 1763–1771. https://doi.org/10.2136/sssaj1989.03615995005300060026x

Lam, N.S.-N., De Cola, L., 1993. Fractal Measurement, in: Fractals in Geography. Prentice Hall, Englewood Cliffs, N.J., p. 308.

Lancaster, N., 1988. Development of linear dunes in the southwestern Kalahari, Southern Africa. J. Arid Environ. 14, 233–244.

Lancaster, N., Baas, A., 1998. Influence of vegetation cover on sand transport by wind: Field studies at Owens Lake, California. Earth Surf. Process. Landforms 23, 69–82. https://doi.org/10.1002/(SICI)1096-9837(199801)23:1<69::AID-ESP823>3.0.CO;2-G

Lancaster, N., Helm, P., 2000. A test of a climatic index of dune mobility using measurements from the southwestern United States. Earth Surf. Process. Landforms 25, 197–207.

Lane, S.N., 2005. Roughness - time for a re-evaluation? Earth Surf. Process. Landforms 30, 251–253. https://doi.org/10.1002/esp.1208

Laporte-Fauret, Q., Castelle, B., Michalet, R., Marieu, V., Bujan, S., Rosebery, D., 2021. Morphological and ecological responses of a managed coastal sand dune to experimental notches. Sci. Total Environ. 782, 146813. https://doi.org/10.1016/j.scitotenv.2021.146813

Larsen, C.E., 1987. Geological History of Glacial Lake Algonquin and the Upper Great Lakes, U.S. Geological Survey Bulletin 1801. Denver, Colo.

Larson, G.J., Schaetzl, R.J., 2001. Origin and Evolution of the Great Lakes. J. Great Lakes Res. 27, 518–546.

Lee, D.B., Ferdowsi, B., Jerolmack, D.J., 2019. The imprint of vegetation on desert dune dynamics. Geophys. Res. Lett. 46, 12041–12048. https://doi.org/10.1029/2019GL084177

Lee, J.A., Gill, T.E., 2015. Multiple causes of wind erosion in the Dust Bowl. Aeolian Res. 19, 15–

36. https://doi.org/10.1016/j.aeolia.2015.09.002

Leopold, L.B., Langbein, W.B., 1962. The Concept of Entropy in Landscape Evolution, Professional Paper 500-A. https://doi.org/10.3133/pp500A

Lepczyk, X.C., Arbogast, A.F., 2005. Geomorphic history of dunes at Petoskey State Park, Petoskey, Michigan. J. Coast. Res. 212, 231–241. https://doi.org/10.2112/02-043.1

Levin, N., Ben-Dor, E., Kidron, G.J., Yaakov, Y., 2008. Estimation of surface roughness (z 0) over a stabilizing coastal dune field based on vegetation and topography. Earth Surf. Process. Landforms 33, 1520–1541. https://doi.org/10.1002/esp.1621

Levin, N., Kidron, G.J., Ben-Dor, E., 2006. The spatial and temporal variability of sand erosion across a stabilizing coastal dune field. Sedimentology 53, 697–715. https://doi.org/10.1111/j.1365-3091.2006.00787.x

Lichter, J., 2000. Colonization constraints during primary succession on coastal Lake Michigan sand dunes. J. Ecol. 88, 825–839.

Lichter, J., 1998. Primary succession and forest development on coastal Lake Michigan sand dunes. Ecol. Monogr. 68, 487. https://doi.org/10.2307/2657151

Loope, D.B., Mason, J.A., Dingus, L., 1999. Lethal sandslides from eolian dunes. J. Geol. 107, 707–713.

Loope, W.L., Arbogast, A.F., 2000. Dominance of an ~150-year cycle of sand-supply change in late Holocene dune-building along the eastern shore of Lake Michigan. Quat. Res. 54, 414–422. https://doi.org/10.1006/qres.2000.2168

Lovis, W.A., Arbogast, A.F., Monaghan, G.W., 2012. The Geoarchaeology of Lake Michigan Coastal Dunes. Michigan State University Press, East Lansing, Mich.

Lu, L., Kuenzer, C., Wang, C., Guo, H., Li, Q., 2015. Evaluation of Three MODIS-Derived Vegetation Index Time Series for Dryland Vegetation Dynamics Monitoring. Remote Sens. 7, 7597–7614. https://doi.org/10.3390/rs70607597

Malanson, G.P., Butler, D.R., Georgakakos, K.P., 1992. Nonequilibrium geomorphic processes and deterministic chaos. Geomorphology 5, 311–322. https://doi.org/10.1016/0169-555X(92)90011-C

Malik, F., Khan, A.W., Tahir Ali Shah, M., 2018. Box-Cox Transformation Approach for Data Normalization: A Study of New Product Development in the Manufacturing Sector of Pakistan. IBT J. Bus. Stud. 14, 110–119. https://doi.org/10.46745/ilma.jbs.2018.14.01.09

Mandelbrot, B., 1967. How Long Is the Coast of Britain? Statistical Self-Similarity and Fractional Dimension. Science (80-.). 156, 636–638. https://doi.org/10.1126/science.156.3775.636

Mann, H.B., Whitney, D.R., 1947. On a Test of Whether one of Two Random Variables is Stochastically Larger than the Other. Ann. Math. Stat. 18, 50–60. https://doi.org/10.1214/aoms/1177730491

Maun, M.A., 1998. Adaptations of plants to burial in coastal sand dunes. Can. J. Bot. 76, 713–738.

McConnell, H., 1966. A STATISTICAL ANALYSIS OF SPATIAL VARIABILITY OF MEAN TOPOGRAPHIC SLOPE ON STREAM DISSECTED GLACIAL MATERIALS. Ann. Assoc. Am. Geogr. 56, 712–728. https://doi.org/10.1111/j.1467-8306.1966.tb00587.x

McKean, J., Roering, J., 2004. Objective landslide detection and surface morphology mapping using high-resolution airborne laser altimetry. Geomorphology 57, 331–351. https://doi.org/10.1016/S0169-555X(03)00164-8

McKeehan, KG, and Arbogast, AF, 2021. Repeat photography of Lake Michigan coastal dunes: Expansion of vegetation since 1900 and possible drivers. Journal of Great Lakes Research 47(6), 1518-1537. doi.org/10.1016/j.jglr.2021.09.016Mckenzie, G., Cooper, A.G., 2001. Post emplacement dune evolution of Atlantic coastal dunes, Northwest Ireland. J. Coast. Res. - Spec. Issue 34 ICS 2000 N.

Melton, F.A., 1956. An analysis of the relations among elements of climate, surface properties, and geomorphology. Columbia Univ., Dept. of Geology, Proj. NR 389-042, Tech. Rep. 11, New York, N.Y.

Melton, F.A., 1940. A Tentative Classification of Sand Dunes Its Application to Dune History in the Southern High Plains. J. Geol. 48, 113–174. https://doi.org/10.1086/624871

Melton, M.A., 1958. Correlation Structure of Morphometric Properties of Drainage Systems and Their Controlling Agents. J. Geol. 66, 442–460. https://doi.org/10.1086/626527

Miller, D.L., Thetford, M., Yager, L., 2001. Evaluation of Sand Fence and Vegetation for Dune Building Following Overwash by Hurricane Opal on Santa Rosa Island, Florida. J. Coast. Res. 17, 936–948.

Millington, J.A., Booth, C.A., Fullen, M.A., Moore, G.M., Trueman, I.C., Worsley, A.T., Richardson, N., Baltrenaite, E., 2009. The role of long-term landscape photography as a tool in dune management. J. Environ. Eng. Landsc. Manag. 17, 253–260.

Minár, J., Jenčo, M., Evans, I.S., Minár, J., Kadlec, M., Krcho, J., Pacina, J., Burian, L., Benová, A., 2013. Third-order geomorphometric variables (derivatives): definition, computation and utilization of changes of curvatures. Int. J. Geogr. Inf. Sci. 27, 1381–1402. https://doi.org/10.1080/13658816.2013.792113

Miyanishi, K., Johnson, E.A., 2021. Coastal dune succession and the reality of dune processes, in: Plant Disturbance Ecology. Elsevier, pp. 253–290. https://doi.org/10.1016/B978-0-12-818813-2.00007-1

Mokarram, M., Roshan, G., Negahban, S., 2015. Landform classification using topography position index (case study: salt dome of Korsia-Darab plain, Iran). Model. Earth Syst. Environ. 1, 40. https://doi.org/10.1007/s40808-015-0055-9

Moore, I.D., Grayson, R.B., Ladson, A.R., 1991. Digital terrain modelling: A review of hydrological, geomorphological, and biological applications. Hydrol. Process. 5, 3–30. https://doi.org/10.1002/hyp.3360050103

Munyati, C., 2022. Detecting the distribution of grass aboveground biomass on a rangeland using Sentinel-2 MSI vegetation indices. Adv. Sp. Res. 69, 1130–1145. https://doi.org/10.1016/j.asr.2021.10.048

Nazari Samani, A., Khosravi, H., Mesbahzadeh, T., Azarakhshi, M., Rahdari, M.R., 2016. Determination of sand dune characteristics through geomorphometry and wind data analysis in central Iran (Kashan Erg). Arab. J. Geosci. 9, 716. https://doi.org/10.1007/s12517-016-2746-6

Nordstrom, K.F., 2015. Coastal dunes, in: Coastal Environments and Global Change. pp. 178–193. https://doi.org/10.1002/9781119117261.ch8

O'Loughlin, E.M., 1986. Prediction of Surface Saturation Zones in Natural Catchments by Topographic Analysis. Water Resour. Res. 22, 794–804. https://doi.org/10.1029/WR022i005p00794

Okin, G.S., 2013. 11.22 Linked Aeolian-Vegetation Systems, in: Treatise on Geomorphology. Elsevier, pp. 428–439. https://doi.org/10.1016/B978-0-12-374739-6.00315-8

Okin, G.S., Gillette, D.A., Herrick, J.E., 2006. Multi-scale controls on and consequences of aeolian processes in landscape change in arid and semi-arid environments. J. Arid Environ. 65, 253–275. https://doi.org/10.1016/j.jaridenv.2005.06.029

Olaya, V., 2009. Chapter 6 Basic Land-Surface Parameters. pp. 141–169. https://doi.org/10.1016/S0166-2481(08)00006-8

Olson, J.S., 1958. Lake Michigan dune development 2. Plants as agents and tools in geomorphology. J. Geol. 66, 345–351.

Otvos, E.G., 2000. Beach ridges — definitions and significance. Geomorphology 32, 83–108.

Pease, P., Gares, P., 2013. The influence of topography and approach angles on local deflections of airflow within a coastal blowout. Earth Surf. Process. Landforms 38, 1160–1169. https://doi.org/10.1002/esp.3407

Peel, M.C., Finlayson, B.., McMahon, T.A., 2007. Updated world map of the K¨oppen-Geiger climate classification. Hydrol. Earth Syst. Sci.

Pelletier, J.D., Mitasova, H., Harmon, R.S., Overton, M., 2009. The effects of interdune vegetation changes on eolian dune field evolution: a numerical-modeling case study at Jockey's Ridge, North Carolina, USA. Earth Surf. Process. Landforms 34, 1245–1254. https://doi.org/10.1002/esp.1809

Peterson, J., Dersch, E., 1981. guide to sand dune and coastal ecosystem functional relationships, Michigan State University Extension Bulletin EMICHU-SG-81-501. East Lansing, Mich.

Petty, W., Delcourt, P., Delcourt, H., 1996. Holocene lake-level fluctuations and beach-ridge development along the northern shore of Lake Michigan, USA. J. Paleolimnol. 15. https://doi.org/10.1007/BF00196778

Phillips, J.D., 2021. Historical contingency in landscape evolution, in: Landscape Evolution. Elsevier, pp. 117–157. https://doi.org/10.1016/B978-0-12-821725-2.00005-3

Phillips, J.D., 2007. The perfect landscape. Geomorphology 84, 159–169. https://doi.org/10.1016/j.geomorph.2006.01.039

Phillips, J.D., 2006. Deterministic chaos and historical geomorphology: A review and look forward. Geomorphology 76, 109–121. https://doi.org/10.1016/j.geomorph.2005.10.004

Phillips, J.D., 1988. The Role of Spatial Scale in Geomorphic Systems. Geogr. Anal. 20, 308–317. https://doi.org/10.1111/j.1538-4632.1988.tb00185.x

Phillips, J.D., Perry, D., Garbee, A.R., Carey, K., Stein, D., Morde, M.B., Sheehy, J.A., 1996. Deterministic uncertainty and complex pedogenesis in some Pleistocene dune soils. Geoderma 73, 147–164. https://doi.org/10.1016/0016-7061(96)00038-9

Piao, S., Mohammat, A., Fang, J., Cai, Q., Feng, J., 2006. NDVI-based increase in growth of temperate grasslands and its responses to climate changes in China. Glob. Environ. Chang. 16, 340–348. https://doi.org/10.1016/j.gloenvcha.2006.02.002

Pike, R.J., Wilson, S.E., 1971. Elevation-Relief Ratio, Hypsometric Integral, and Geomorphic Area-Altitude Analysis. Bull. Geol. Soc. Am. 82, 1079–1084.

Poulson, T.L., 1995. The role of allogenic and autogenic processes in dune succession at Miller, Indiana. Am. J. Bot. 82, 34.

Provoost, S., Jones, M.L.M., Edmondson, S.E., 2011. Changes in landscape and vegetation of coastal dunes in northwest Europe: a review. J. Coast. Conserv. 15, 207–226. https://doi.org/10.1007/s11852-009-0068-5

Pye, K., Blott, S.J., Howe, M.A., 2014. Coastal dune stabilization in Wales and requirements for rejuvenation. J. Coast. Conserv. 18, 27–54.

Ralph, J., O'Neill, R., Winton, J., 2015. A Practical Introduction to Index Numbers. John Wiley &

Sons, Ltd, Chichester, UK. https://doi.org/10.1002/9781118977781

Raupach, M.R., 1992. Drag and drag partition on rough surfaces. Boundary-Layer Meteorol. 60, 375–395. https://doi.org/10.1007/BF00155203

Reinhardt, L., Jerolmack, D., Cardinale, B.J., Vanacker, V., Wright, J., 2010. Dynamic interactions of life and its landscape: feedbacks at the interface of geomorphology and ecology. Earth Surf. Process. Landforms 35, 78–101. https://doi.org/10.1002/esp.1912

Ren, H., Zhou, G., Zhang, F., 2018. Using negative soil adjustment factor in soil-adjusted vegetation index (SAVI) for aboveground living biomass estimation in arid grasslands. Remote Sens. Environ. 209, 439–445. https://doi.org/10.1016/j.rse.2018.02.068

Riksen, M.J.P.M., Goossens, D., Huiskes, H.P.J., Krol, J., Slim, P.A., 2016. Constructing notches in foredunes: Effect on sediment dynamics in the dune hinterland. Geomorphology 253, 340–352. https://doi.org/10.1016/j.geomorph.2015.10.021

Riley, S.J., DeGloria, S.D., Elliot, R., 1999. A terrain ruggedness index that quantifies topographic heterogeneity. Intermt. J. Sci. 5, 23–27.

Ritchie, W., 1972. The evolution of coastal sand dunes. Scott. Geogr. Mag. 88, 19–35. https://doi.org/10.1080/00369227208736205

Römkens, M.J.., Helming, K., Prasad, S.., 2002. Soil erosion under different rainfall intensities, surface roughness, and soil water regimes. CATENA 46, 103–123. https://doi.org/10.1016/S0341-8162(01)00161-8

Roskin, J., Blumberg, D.G., Katra, I., 2014a. Last millennium development and dynamics of vegetated linear dunes inferred from ground-penetrating radar and optically stimulated luminescence ages. Sedimentology 61, 1240–1260. https://doi.org/10.1111/sed.12099

Roskin, J., Katra, I., Blumberg, D.G., 2014b. Particle-size fractionation of eolian sand along the Sinai-Negev erg of Egypt and Israel. Geol. Soc. Am. Bull. 126, 47–65. https://doi.org/10.1130/B30811.1

Różycka, M., Migoń, P., Michniewicz, A., 2017. Topographic Wetness Index and Terrain Ruggedness Index in geomorphic characterisation of landslide terrains, on examples from the Sudetes, SW Poland. Zeitschrift für Geomorphol. Suppl. Issues 61, 61–80. https://doi.org/10.1127/zfg_suppl/2016/0328

Ruggiero, P., Hacker, S., Seabloom, E., Zarnetske, P., 2018. The role of vegetation in determining dune morphology, exposure to sea-level rise, and storm-induced coastal hazards: A U.S. Pacific Northwest perspective, in: Barrier Dynamics and Response to Changing Climate. Springer International Publishing, Cham, pp. 337–361. https://doi.org/10.1007/978-3-319-68086-6_11

Salisbury, E., 1952. Downs & Dunes: Their Plant Life and Its Environment. G. Bell & Sons, Ltd., London.

Sankey, J.B., Glenn, N.F., Germino, M.J., Gironella, A.I.N., Thackray, G.D., 2010. Relationships of aeolian erosion and deposition with LiDAR-derived landscape surface roughness following wildfire. Geomorphology 119, 135–145. https://doi.org/10.1016/j.geomorph.2010.03.013

Sappington, J.M., 2012. Vector Ruggedness Measure (Terrain Ruggedness).

Sappington, J.M., Longshore, K.M., Thompson, D.B., 2007. Quantifying landscape ruggedness for animal habitat analysis: A case study using bighorn sheep in the Mojave Desert. J. Wildl. Manage. 71, 1419–1426.

Schaetzl, R.J., Baish, C., Colgan, P.M., Knauff, J., Bilintoh, T., Wanyama, D., Church, M., McKeehan, K., Fulton, A., Arbogast, A.F., 2020. A sediment-mixing process model of till genesis, using texture and clay mineralogy data from Saginaw lobe (Michigan, USA) tills. Quat. Res. 94, 174–194. https://doi.org/10.1017/qua.2019.82

Schaney, M.L., Kite, J.S., Schaney, C.R., Thompson, J.A., 2021. Evidence of Mid-Holocene (Northgrippian Age) Dry Climate Recorded in Organic Soil Profiles in the Central Appalachian Mountains of the Eastern United States. Geosciences 11, 477. https://doi.org/10.3390/geosciences11110477

Scheidegger, A.E., Langbein, W.B., 1966. Probability Concepts in Geomorphology, Geological Survey Professional Paper 500-C. Washington, D.C.

Schmid, G.L., 2013. 4.16 Soil Chronosequences, in: Treatise on Geomorphology. Elsevier, pp. 277–283. https://doi.org/10.1016/B978-0-12-374739-6.00076-2

Schmidt, J., Evans, I.S., Brinkmann, J., 2003. Comparison of polynomial models for land surface curvature calculation. Int. J. Geogr. Inf. Sci. 17, 797–814. https://doi.org/10.1080/13658810310001596058

Schumm, S.A., 1956. Evolution of drainage systems and slopes in badlands at Perth Amboy, N. J. Geol. Soc. Am. Bull. 67, 597–646.

Schwarz, C., Brinkkemper, J., Ruessink, G., 2018. Feedbacks between Biotic and Abiotic Processes Governing the Development of Foredune Blowouts: A Review. J. Mar. Sci. Eng. 7, 2. https://doi.org/10.3390/jmse7010002

Shao, Y., Yang, Y., 2005. A scheme for drag partition over rough surfaces. Atmos. Environ. 39, 7351–7361. https://doi.org/10.1016/j.atmosenv.2005.09.014

Sherman, D.J., Bauer, B.O., 1993. Dynamics of beach-dune systems. Prog. Phys. Geogr. Earth Environ. 17, 413–447. https://doi.org/10.1177/030913339301700402

Smith, A.B., Jackson, D.W.T., Cooper, J.A.G., Hernández-Calvento, L., 2017. Quantifying the role of urbanization on airflow perturbations and dunefield evolution. Earth's Futur. 5, 520–539. https://doi.org/10.1002/2016EF000524

Smith, M.W., 2014. Roughness in the Earth Sciences. Earth-Science Rev. 136, 202–225. https://doi.org/10.1016/j.earscirev.2014.05.016

Spearman, C., 1904. The Proof and Measurement of Association between Two Things. Am. J. Psychol. 15, 72. https://doi.org/10.2307/1412159

Stallins, J.A., Parker, A.J., 2003. The influence of complex systems interactions on barrier island dune vegetation pattern and process. Ann. Assoc. Am. Geogr. 93, 13–29.

Strypsteen, G., Van Rijn, L.C., Rauwoens, P., 2021. Comparison of equilibrium sand transport rate model predictions with an extended dataset of field experiments at dry beaches with long fetch distance. Aeolian Res. 52, 100725. https://doi.org/10.1016/j.aeolia.2021.100725

Suter-Burri, K., Gromke, C., Leonard, K.C., Graf, F., 2013. Spatial patterns of aeolian sediment deposition in vegetation canopies: Observations from wind tunnel experiments using colored sand. Aeolian Res. 8, 65–73. https://doi.org/10.1016/j.aeolia.2012.11.002

Sweeney, M.R., Lu, H.Y., Cui, M.C., Mason, J.A., Feng, H., Xu, Z.W., 2016. Sand dunes as potential sources of dust in northern China. Sci. China Earth Sci. 59, 760–769. https://doi.org/10.1007/s11430-015-5246-8

Tagil, S., Jenness, J., 2008. GIS-based automated landform classification and topography, landcover, and geologic attributes of landforms around the Yazoren Polje, Turkey. J. Appl. Sci. 8, 910–921.

Theuerkauf, E., Mattheus, C.R., Braun, K., Bueno, J., 2021. Patterns and processes of beach and foredune geomorphic change along a Great Lakes shoreline: Insights from a year-long drone mapping study along Lake Michigan. Shore & Beach 46–55. https://doi.org/10.34237/1008926

Thompson, T.A., Lepper, K., Endres, A.L., Johnston, J.W., Baedke, S.J., Argyilan, E.P., Booth, R.K., Wilcox, D.A., 2011. Mid Holocene lake level and shoreline behavior during the Nipissing phase of the upper Great Lakes at Alpena, Michigan, USA. J. Great Lakes Res. 37, 567–576. https://doi.org/10.1016/j.jglr.2011.05.012

Thornthwaite, C.W., 1948. An approach toward a rational classification of climate. Geogr. Rev. 38, 55–94.

Thornthwaite, C.W., Mather, J.R., 1957. Instructions and tables for computing potential evapotranspiration and the water balance. Publ. Climatol. X.

Tsoar, H., 2005. Sand dunes mobility and stability in relation to climate. Phys. A Stat. Mech. its

Appl. 357, 50–56. https://doi.org/10.1016/j.physa.2005.05.067

Tucker, C.J., 1979. Red and photographic infrared linear combinations for monitoring vegetation. Remote Sens. Environ. 8, 127–150. https://doi.org/10.1016/0034-4257(79)90013-0

Turner, M.G., O'Neill, R. V., Gardner, R.H., Milne, B.T., 1989. Effects of changing spatial scale on the analysis of landscape pattern. Landsc. Ecol. 3, 153–162.

USGS, 2019. USGS 13 arc-second n45w087.

van Denack, J.M., 1961. An Ecological Analysis of the Sand Dune Complex in Point Beach State Forest, Two Rivers, Wisconsin. Bot. Gaz. 122, 155–174. https://doi.org/10.1086/336104

van Dijk, D., 2014. Short- and long-term perspectives on the evolution of a Lake Michigan foredune, in: Coastline and Dune Evolution along the Great Lakes. Geological Society of America, pp. 195–216. https://doi.org/10.1130/2014.2508(11)

van Dijk, D., 2004. Contemporary geomorphic processes and change on Lake Michigan coastal dunes: an example from Hoffmaster State Park, Michigan. Mich. Acad. 35.

Walker, I.J., Davidson-Arnott, R.G.D., Bauer, B.O., Hesp, P.A., Delgado-Fernandez, I., Ollerhead, J., Smyth, T.A.G., 2017. Scale-dependent perspectives on the geomorphology and evolution of beach-dune systems. Earth-Science Rev. 171, 220–253. https://doi.org/10.1016/j.earscirev.2017.04.011

Walker, I.J., Hesp, P.A., 2013. 11.7 Fundamentals of Aeolian Sediment Transport: Airflow Over Dunes, in: Treatise on Geomorphology. Elsevier, pp. 109–133. https://doi.org/10.1016/B978-0-12-374739-6.00300-6

Weiss, A.D., 2001. Topographic Position and Landforms Analysis, in: Poster Presentation, ESRI User Conference, San Diego, CA.

Werner, B.T., 1999. Complexity in Natural Landform Patterns. Science (80-.). 284, 102–104. https://doi.org/10.1126/science.284.5411.102

Werner, C.M., Mason, J.A., Hanson, P.R., 2011. Non-linear connections between dune activity and climate in the High Plains, Kansas and Oklahoma, USA. Quat. Res. 75, 267–277. https://doi.org/10.1016/j.yqres.2010.08.001

Weymer, B.A., Houser, C., Giardino, J.R., 2015. Poststorm evolution of beach-dune morphology: Padre Island National Seashore, Texas. J. Coast. Res. 313, 634–644. https://doi.org/10.2112/JCOASTRES-D-13-00020.1

Wheaton, J.M., Gibbins, C., Wainwright, J., Larsen, L., McElroy, B., 2011. Preface: Multiscale Feedbacks in Ecogeomorphology. Geomorphology 126, 265–268. https://doi.org/10.1016/j.geomorph.2011.01.002

White, R.A., Piraino, K., Shortridge, A., Arbogast, A.F., 2019. Measurement of vegetation change in critical dune sites along the eastern shores of Lake Michigan from 1938 to 2014 with object-based image analysis. J. Coast. Res. 35, 842. https://doi.org/10.2112/jcoastres-d-17-00141.1

Wiernga, J., 1993. Representative roughness parameters for homogeneous terrain. Boundary-Layer Meteorol. 63, 323–363.

Wiernga, J., 1986. Roughness-dependent geographical interpretation of surface wind speed averages. Q. J. R. Meteorol. Soc. 112, 867–889.

Wilson, L., 1997. Land systems, in: Geomorphology. Kluwer Academic Publishers, Dordrecht, pp. 641–644. https://doi.org/10.1007/3-540-31060-6_220

Wilson, M.F.J., O'Connell, B., Brown, C., Guinan, J.C., Grehan, A.J., 2007. Multiscale terrain analysis of multibeam bathymetry data for habitat mapping on the continental slope. Mar. Geod. 30, 3–35. https://doi.org/10.1080/01490410701295962

Wolfe, S.A., Nickling, W.., 1993. The protective role of sparse vegetation in wind erosion. Prog. Phys. Geogr. 17, 50–68.

Wright, L.D., Thom, B.G., 1977. Coastal depositional landforms. Prog. Phys. Geogr. Earth Environ. 1, 412–459. https://doi.org/10.1177/030913337700100302

Xu, Z., Mason, J.A., Lu, H., 2015. Vegetated dune morphodynamics during recent stabilization of the Mu Us dune field, north-central China. Geomorphology 228, 486–503. https://doi.org/10.1016/j.geomorph.2014.10.001

Yizhaq, H., Ashkenazy, Y., Tsoar, H., 2009. Sand dune dynamics and climate change: A modeling approach. J. Geophys. Res. Earth Surf. 114, 1–11. https://doi.org/10.1029/2008JF001138

Yizhaq, H., Ashkenazy, Y., Tsoar, H., 2007. Why do active and stabilized dunes coexist under the same climatic conditions? Phys. Rev. Lett. 98, 98–101. https://doi.org/10.1103/PhysRevLett.98.188001

Yurk, B., Hansen, E., 2021. Effects of wind patterns and changing wind velocities on aeolian drift potential along the Lake Michigan shore. J. Great Lakes Res. 47, 1504–1517. https://doi.org/10.1016/j.jglr.2021.09.006

Zarnetske, P.L., Hacker, S.D., Seabloom, E.W., Ruggiero, P., Killian, J.R., Maddux, T.B., Cox, D., 2012. Biophysical feedback mediates effects of invasive grasses on coastal dune shape. Ecology 93, 1439–1450.

Zarnetske, P.L., Ruggiero, P., Seabloom, E.W., Hacker, S.D., 2015. Coastal foredune evolution: the relative influence of vegetation and sand supply in the US Pacific Northwest. J. R. Soc.

Interface 12, 20150017. https://doi.org/10.1098/rsif.2015.0017

Zeng, Z., Piao, S., Li, L.Z.X., Ciais, P., Li, Y., Cai, X., Yang, L., Liu, M., Wood, E.F., 2018. Global terrestrial stilling: does Earth's greening play a role? Environ. Res. Lett. 13, 124013. https://doi.org/10.1088/1748-9326/aaea84

Zhao, Y., Gao, X., Lei, J., Li, S., Cai, D., Song, Q., 2019. Effects of Wind Velocity and Nebkha Geometry on Shadow Dune Formation. J. Geophys. Res. Earth Surf. 124, 2579–2601. https://doi.org/10.1029/2019JF005199

Zhu, Z., Piao, S., Myneni, R.B., Huang, M., Zeng, Z., Canadell, J.G., Ciais, P., Sitch, S., Friedlingstein, P., Arneth, A., Cao, C., Cheng, L., Kato, E., Koven, C., Li, Y., Lian, X., Liu, Y., Liu, R., Mao, J., Pan, Y., Peng, S., Peñuelas, J., Poulter, B., Pugh, T.A.M., Stocker, B.D., Viovy, N., Wang, X., Wang, Y., Xiao, Z., Yang, H., Zaehle, S., Zeng, N., 2016. Greening of the Earth and its drivers. Nat. Clim. Chang. 6, 791–795. https://doi.org/10.1038/nclimate3004

CHAPTER 5.
CONCLUSIONS, THE GEOGRAPHY AND RECENT ACTIVITY OF LAKE MICHIGAN'S COASTAL SAND DUNES

5.1 Conclusions

This dissertation was organized into distinct chapters that were each geared toward assessing changes in Lake Michigan's coastal dunes in the modern era. Research of the last 25 years demonstrates that the region's coastal dunes began forming ~5.5ka, although in some locations, dune building may have started later (Lovis et al., 2012). According to the chronology constructed from several studies, the coastal dunes then underwent several periods of stability and instability along the entire shoreline. However, despite the detailed geochronology now available to researchers and a basic understanding of the landscape's geomorphic process-response regime, questions remain regarding the behavior of this unique dune system in the modern era. Specifically, this dissertation sought to address the gap in knowledge with regards to dune variability along Lake Michigan's eastern shoreline since ~1900, the time when our ability to observe and record our world began to improve. The goal of this dissertation was to determine if changes have occurred to the region's coastal dune systems in the last ~120 years and what might be driving those changes, especially with regards to the system's ecogeomorphic regime, where dune and vegetation interact.

The conclusions of each dissertation chapter show that vegetation is expanding in Lake Michigan's dunefields. This is the primary finding of this dissertation. Furthermore, this clear conclusion supports recent research from White et al. (2019) that demonstrated expanding vegetation in state park dunefields along Lake Michigan since 1938. It also comports with trends since ~1900 in Europe (Provoost et al., 2011) and globally (Gao et al., 2020) in which previously active coastal dunes stabilized due to an expansion of vegetation. This dissertation approached the question of vegetation and dune variability in the modern period from three different, but related, approaches. In the first dissertation study (Chapter 2), a semi-quantified process was

used to describe the expansion of vegetation seen in 20 repeat photography pairs. For the second and third dissertation studies, the processes were fully quantified. I mapped 435 dune blowouts along the eastern shore of Lake Michigan using repeat aerial photography, machine learning tools, and a STAMP model to quantify blowout behavior at three temporal periods as part of the second dissertation study (Chapter 3). For the final study in this dissertation (Chapter 4), I quantified terrain ruggedness and vegetation within the dunefield at Ludington State Park by calculating indices and attempted to find relationship between the two dune behavior variables.

In each of these studies, the results show the importance of vegetation to these coastal dune systems and how its expansion is changing dune behavior. In the first dissertation study, ground-level repeat photography documented how vegetation had stabilized dunes, while also altering their morphology. At many of the 20 sites analyzed for that study, dunes not only become more vegetated, but also seemed to grow through the accretion of aeolian sand, which had become trapped by grasses and woody shrubs. Likewise, in the second dissertation study, blowouts have reduced in size ~37% since 1938 and become increasingly fragmented, with vegetation becoming established in the deflation basins of many blowouts. In both studies, bare sand reduction in dunes was partially due to direct human intervention, such as development and planting programs. However, only a uniform control across the region can account for the largely spatial consistency in the expansion of vegetation north and south along the shoreline.

Moreover, the results of the third dissertation study, focusing on the relationship between terrain ruggedness and vegetation, illuminated the phenomenon of vegetation expansion in dunefields. I found that the values from two ruggedness indices – Riley's Terrain Ruggedness Index (TRI) and Sappington's Vector Ruggedness Measure (VRM) – and the values from the Soil-Adjusted Vegetation Index (SAVI) were not correlated overall, especially where one type of vegetation was dominant. However, when I examined the correlation results by land system, I found a

moderate-to-strong negative correlation between terrain ruggedness and vegetation amongst the dune barrens land system. Within the dune barrens, results indicated that ruggedness decreased with increasing SAVI, which was interpreted as an increasing incidence of woody vegetation along with density. Likewise, with grassy or patchy vegetation, terrain ruggedness increased within the dune barrens land system, which is characterized as by mixed vegetation and hummocky landforms. In other land systems at this scale where one type of vegetation is dominant, no relationship existed between terrain ruggedness and vegetation, including within the grass-dominated foredunes or in the mature woodland dunes farthest from the lakeshore.

While seeming somewhat disengaged from the results of the other dissertation chapters, this finding from the final dissertation study fits well with those of the other studies. Given favorable conditions and enough time, vegetation can overwhelm the other variables influencing the ecogeomorphic character of a dunefield. This is evident in the absence of a relationship between dune morphology, as expressed by terrain ruggedness, and vegetation in dunefield land systems where one vegetation type is dominant. By contrast, the dune barrens land system is a dunefield landscape characterized by variability and transition. As demonstrated in the chapter, the dune barrens areas of Ludington State Park were open dunes and swales with little if any vegetation in 1938. That area has now transitioned into land system with grasses, shrubs, common juniper (*Juniperus communis*), and jack pine (*Pinus banksiana*), with no one type of vegetation dominant within the land system. Grassy dunes within the dune barrens proved relatively rugged, suggesting that sand-trapping grasses are instrumental in the accretion of dunes. It also suggests that trees are inhabiting smooth, low-lying interdunal swale areas. Thus, in the dune barrens land system, it appears possible that critical thresholds within the ecogeomorphic process-response mechanisms have not yet been exceeded, driving a vegetation type toward dominance beyond the ability of other variables within the dune system to influence dune behavior. Yet, as the results

of the other dissertation chapters demonstrate, this current status in the dune barrens may not prevail much longer if the favorable conditions driving vegetation growth persist, given the concepts of ecogeomorphic hysteresis, bistability, and deterministic chaos.

In summary, vegetation is expanding over previously bare surfaces in coastal dunes along the eastern shore of Lake Michigan. Yet, while the expansion of vegetation in dunefields in the modern period is an important, singular finding, the question of the possible drivers responsible for these changes remains. Unfortunately, several possible drivers, or combination of drivers, within the dune system could be liable. As explored in this dissertation, especially in Chapter 2, an increase in annual precipitation of ~175mm since the 1930s at the central and southern portions of the lakeshore could be considered a prime, possible driver. These trends from meteorological stations at Muskegon and South Bend were moderately statistically significant, but the increase in annual precipitation farther north along the coast – at Traverse City – was smaller (~75mm), a finding which cast some doubt as to whether precipitation alone was driving the expansion of vegetation. Yet, it is also possible that a soil moisture threshold has been exceeded because of this increase in precipitation, no matter how modest. From the final dissertation study (Chapter 4), it is conceivable that interdunal moisture has played a role in the establishment of woody vegetation in the dune barrens landscape. Consequently, it is logical that an uptick in soil moisture, possibly from enhanced precipitation, is driving vegetation expansion in dunes and blowout fragmentation. This possibility, although not proven here, would be significant to regional dune systems, as annual precipitation is expected to continue to increase throughout the remainder of this century (Byun and Hamlet, 2018).

Other uniform controls are potential drivers of vegetation expansion. While local controls such as plantings, fire suppression, the introduction of invasive species, and logging certainly had an impact on dune behavior in the modern period, their influence was concentrated to their locality.

A uniform variable must be exhibiting some control regionally to account for the trend in vegetation. If not precipitation another factor combination of factors operating at meso- or macroscales must be responsible. One such potential uniform factor is the increased atmospheric concentration of CO_2 through anthropogenic means. As stated elsewhere in this dissertation, the leaf area index (LAI) had grown in 25-50% globally and in the Lower Peninsula of Michigan between 1982 and 2009 and that ~70% of that growth was due to increased CO_2 fertilization (Zhu et al., 2016). Functionally, increased atmospheric CO_2 drive photosynthesis and facilitate water efficiency in plants, potentially driving the spread of vegetation across previously bare sand dunes, although anthropogenically bolstered atmospheric CO_2 might derive negative physiological tradeoffs (Sperry et al., 2019). Similar to increased atmospheric CO_2, greater atmospheric nitrogen deposition from anthropogenic means might also be uniformly driving N enrichment of dune soils across the region. Greater atmospheric N deposition would foster plant growth and influence the composition of dune grassland ecosystems (van den Berg et al., 2005), although like increased atmospheric CO_2 its effects in North American dunefields is uncertain.

Still, there may be another intriguing possible explanation to the observations of these dissertation studies. It is possible the trend in vegetation growth in Lake Michigan's coastal dunes is a lagged response to an earlier climate event. In this case, the results from the blowout dissertation study are instructive. Recall that blowouts are erosional depressions or troughs which have "blown out" through existing dunes due to natural or anthropogenic forcing (Hesp, 2002) and are particularly sensitive to changes in their environment (Schwarz et al., 2018). Yet, these results demonstrate that no new natural blowouts meeting the identification criteria have formed since 1938. Thus, the conditions in which fostered blowout formation at over 400 sites along the eastern shore of Lake Michigan must not be present today. The most recent significant climate event was the Little Ice Age (LIA), a global cooling period roughly dated from ~0.1ka to ~0.7ka

(Nordstrom, 2015). The LIA was a period of episodic dune activity in Europe (Jackson et al., 2019; Provoost et al., 2011) and a period of cool, dry, droughty and possibly erosive conditions around the Great Lakes (Colman et al., 2000; Hupy and Yansa, 2009; Warner et al., 2021), while Lake Michigan water levels appear to be at or slightly above modern levels (Baedke and Thompson, 2000). Prior to the LIA, there were multiple warm periods within the late- and mid-Holocene, although their regional impact was nonlinear and uncertain. The Medieval Climate Optimum (MCO) (~1.2ka to ~0.7ka), the Roman Climate Optimum (RCO) (~2.3ka to 1.6ka), and the Holocene Climate Optimum (HCO) (~8.2ka to ~4.2ka (Schaney et al., 2021) all may have impacted the region's dune systems, possibly sparking the conditions necessary for blowout formation.

Some of these climate events coincide with periods of dune activity in the study area, according to analyses of the dating work performed on buried dune soils, aeolian sand, and other geochronological markers (Hansen et al., 2010; Lovis et al., 2012). It is not known if blowouts specifically formed during any particular climate event or during all of them. Nor is it known if the healing and fragmentation of blowouts is a response to processes of the past ~100 years or a lag from earlier periods of dune activity. This uncertainty holds true for all bare sand dune landforms which are beginning to stabilize under the ecogeomorphic influence of vegetation over the same time period. These landforms could be relics of earlier, more volatile conditions that are now responding in a lagged, nonlinear manner to changing climate, lake level, and ecogeomorphic conditions. Under this scenario, the result is a dune system in nonequilibrium and, with the relenting of certain drivers, eventually drifts towards its steady state, nonlinearly, and perhaps simply due to the "passage of time", as Salisbury (1952, pg. 161) observed. Alternatively, the coastal dune systems here could be responding now to current processes and increasingly mesic conditions which are driving the system toward an alternative state or a condition of

bistability, in which both stable and active dunes coexist. Of course, either scenario could encompass the idea of geomorphic deterministic chaos, in which the study area's dune systems are being forced toward a natural state, albeit chaotically with great variability of mode. This concept explains the heterogeneity which exists within dunefields that also exhibit a clear ecogeomorphic gradient as explained in the final dissertation chapter.

Clearly, the forcing mechanism(s) driving the current trend in vegetation growth in Lake Michigan's coastal dunes is more uncertain than the observed trend itself. Consequently, I feel the results of this dissertation call for an assortment of additional work, especially research focused on the causes of vegetation expansion in the study area. Particularly, the need exists for research into the components of the process-response mechanisms are driving stabilization, even if complex systems are difficult to parameterize and understand (Phillips, 2007, 2006). I propose research along two primary tracks. The first track should attempt to understand the process-response mechanisms which are driving dune and blowout stabilization now. This track includes further overall research into the soil moisture and precipitation regimes of these dunefields, along with a regional quantification of vegetative growth associated with increased concentrations of atmospheric CO_2 and controlled experiments investigating the response of native and invasive plant species to CO_2 and N fertilization.

For blowouts specifically, a similar focus is proposed, but through a longitudinal lens, which would involve field investigations at key indicator blowout sites to understand geomorphic changes and drivers. Such research should attempt to determine regional blowout soil moisture thresholds, the process by which blowouts are vegetated, the impact on CO_2 and N on dune plants, how foredune growth affects blowout sand supply and fragmentation, and how blowouts respond to human activity, especially in their deflation basins. Other field work could focus on the ecogeomorphic feedback mechanisms between terrain and vegetation operate.

The second proposed research track should focus on a longer spatiotemporal scale and seek knowledge regarding the macroscale drivers of dune behavior along the eastern shore of Lake Michigan. Included in this second track of research would be an effort to date blowouts origins, perhaps by concentrating on the depositional lobes of large, well-established trough blowouts. Blowout sites to be geochronologically dated should be spatially varied along the length of the lakeshore above and below the hinge line, as this dissertation research shows some divergence in the blowout response north and south of this geologic boundary. Further, additional optically stimulated luminescence (OSL) and radiocarbon dating of aeolian sand and buried dune soils is needed in several key dunefields to best ascertain if any periods of dune activity or stability can be linked to key climatic events, such as the LIA or the Medieval Climate Optimum (MCO) (~1.2ka to 0.7ka). This dating investigation would permit a more comprehensive timeline of aeolian, climate, and lake level activity across the region, illuminating the possible conditions which fostered dune building and maintenance. True, we currently have a geochronological picture of dune activity and stability thanks to the efforts of several workers (e.g., Arbogast et al., 2004; Hansen et al., 2010; Lovis et al., 2012), but I feel this is a framework from which to begin. Few efforts have been undertaken to link regional and global climate events to aeolian activity in the region, a gap in knowledge that should be filled given the relatively swift nature of change in aeolian systems (Delgado-Fernandez et al., 2018).

Other research areas, including the need for ruggedness indices better suited for dune systems, are also important. Yet, the primary new research should concern the micro- and mesoscale process-response mechanisms driving dune stabilization across the region and the longer macroscale drivers radiating from climate events and large lake level changes. Much is known with regards to the dunefields along the eastern shore of Lake Michigan, but questions remain regarding the changes we have observed. Determining the answers to these questions is of

importance for the state of Michigan, given the importance of the coastal sand dunes for many communities and the desire to protect or develop them (Arbogast et al., 2020). Land managers and planners in coastal Lake Michigan communities should also absorb the results of each chapter of this dissertation. Taken together, the results represent a challenge to those navigating the state of Michigan's critical dune regulatory guidelines and local planning ordinances. As demonstrated from this research, the condition of regional dune systems in which management decisions are being made is changing; dunes are becoming more vegetated and land systems are responding in complex ways. These results have implications for managers, whether they are tasked with protecting dune-dwelling endangered piping plovers (*Charadrius melodus*) or pitcher's thistles (*Cirsium pitcheri*). Maintaining a supply of sand to backdune and blowout areas may require excavating troughs or notches through vegetated, stabilized, accreting, foredunes to counteract vegetation expansion in a manner similar to European coastal managers (e.g., Laporte-Fauret et al., 2021). Additionally, managers may need to engage in plant-removal projects in order to preserve the "diversity" of dunes, which is one of the core purposes in the state's legislation guiding dune management (Arbogast et al., 2020). As Chapter 4 demonstrated, one type of vegetation has become dominant in some land systems, arguably limiting dune "diversity". As Arbogast et al. (2020) further demonstrated, the public's perceptions of the Lake Michigan dune system may diverge from this new vegetated and stabilized reality, prompting discussions about what role and goals land managers should adopt. Regardless of future policy pathways, Lake Michigan coastal dune systems are changing and land manager must be cognizant of it. After all, this expansive landscape might well represent the largest freshwater dune system in the world (Peterson and Dersch, 1981). It is a complex system. Answering these questions are crucial to understanding it.

REFERENCES

REFERENCES

Arbogast, A.F., Garmon, B., Sterrett Isely, E., Jarosz, J., Kreiger, A., Nicholls, S., Queen, C., Richardson, R.B., 2018. Valuing Michigan's Coastal Dunes: GIS Information and Economic Data to Support Management Partnerships.

Arbogast, A.F., McKeehan, K.G., Richardson, R.B., Zimnicki, T., 2020. Learning to Live in Dynamic Dunes: Citizen Science and Participatory Modeling in the Service of Michigan Coastal Dune Decision-Making. Lansing, MI.

Arbogast, A.F., Schaetzl, R.J., Hupy, J.P., Hansen, E.C., 2004. The Holland Paleosol: An informal pedostratigraphic unit in the coastal dunes of southeastern Lake Michigan. Can. J. Earth Sci. 41, 1385–1400. https://doi.org/10.1139/E04-071

Baedke, S.J., Thompson, T.A., 2000. A 4,700-year record of lake level and isostasy for Lake Michigan. J. Great Lakes Res. 26, 416–426. https://doi.org/10.1016/S0380-1330(00)70705-2

Byun, K., Hamlet, A.F., 2018. Projected changes in future climate over the Midwest and Great Lakes region using downscaled CMIP5 ensembles. Int. J. Climatol. 38, e531–e553. https://doi.org/10.1002/joc.5388

Colman, S.M., King, J.W., Jones, G.A., Reynolds, R.L., Bothner, M.H., 2000. Holocene and recent sediment accumulation rates in Southern Lake Michigan. Quat. Sci. Rev. 19, 1563–1580. https://doi.org/10.1016/S0277-3791(00)00007-X

Delgado-Fernandez, I., Smyth, T.A.G., Jackson, D.W.T., Smith, A.B., Davidson-Arnott, R.G.D., 2018. Event-Scale Dynamics of a Parabolic Dune and Its Relevance for Mesoscale Evolution. J. Geophys. Res. Earth Surf. 123, 3084–3100. https://doi.org/10.1029/2017JF004370

Gao, J., Kennedy, D.M., Konlechner, T.M., 2020. Coastal dune mobility over the past century: A global review. Prog. Phys. Geogr. Earth Environ. 44, 814–836. https://doi.org/10.1177/0309133320919612

Hansen, E.C., Fisher, T.G., Arbogast, A.F., Bateman, M.D., 2010. Geomorphic history of low-perched, transgressive dune complexes along the southeastern shore of Lake Michigan. Aeolian Res. 1, 111–127. https://doi.org/10.1016/j.aeolia.2009.08.001

Hesp, P., 2002. Foredunes and blowouts: Initiation, geomorphology and dynamics. Geomorphology 48, 245–268. https://doi.org/10.1016/S0169-555X(02)00184-8

Hupy, C.M., Yansa, C.H., 2009. Late Holocene vegetation history of the forest tension zone in Central Lower Michigan, USA. Phys. Geogr. 30, 205–235. https://doi.org/10.2747/0272-3646.30.3.205

Jackson, D.W.T., Costas, S., Guisado-Pintado, E., 2019. Large-scale transgressive coastal dune behaviour in Europe during the Little Ice Age. Glob. Planet. Change 175, 82–91. https://doi.org/10.1016/j.gloplacha.2019.02.003

Laporte-Fauret, Q., Castelle, B., Michalet, R., Marieu, V., Bujan, S., Rosebery, D., 2021. Morphological and ecological responses of a managed coastal sand dune to experimental notches. Sci. Total Environ. 782, 146813. https://doi.org/10.1016/j.scitotenv.2021.146813

Lovis, W.A., Arbogast, A.F., Monaghan, G.W., 2012. The Geoarchaeology of Lake Michigan Coastal Dunes. Michigan State University Press, East Lansing, Mich.

Nordstrom, K.F., 2015. Coastal dunes, in: Coastal Environments and Global Change. pp. 178–193. https://doi.org/10.1002/9781119117261.ch8

Peterson, J., Dersch, E., 1981. guide to sand dune and coastal ecosystem functional relationships, Michigan State University Extension Bulletin EMICHU-SG-81-501. East Lansing, Mich.

Phillips, J.D., 2007. The perfect landscape. Geomorphology 84, 159–169. https://doi.org/10.1016/j.geomorph.2006.01.039

Phillips, J.D., 2006. Deterministic chaos and historical geomorphology: A review and look forward. Geomorphology 76, 109–121. https://doi.org/10.1016/j.geomorph.2005.10.004

Provoost, S., Jones, M.L.M., Edmondson, S.E., 2011. Changes in landscape and vegetation of coastal dunes in northwest Europe: a review. J. Coast. Conserv. 15, 207–226. https://doi.org/10.1007/s11852-009-0068-5

Salisbury, E., 1952. Downs & Dunes: Their Plant Life and Its Environment. G. Bell & Sons, Ltd., London.

Schaney, M.L., Kite, J.S., Schaney, C.R., Thompson, J.A., 2021. Evidence of Mid-Holocene (Northgrippian Age) Dry Climate Recorded in Organic Soil Profiles in the Central Appalachian Mountains of the Eastern United States. Geosciences 11, 477. https://doi.org/10.3390/geosciences11110477

Schwarz, C., Brinkkemper, J., Ruessink, G., 2018. Feedbacks between Biotic and Abiotic Processes Governing the Development of Foredune Blowouts: A Review. J. Mar. Sci. Eng. 7, 2. https://doi.org/10.3390/jmse7010002

Sperry, J.S., Venturas, M.D., Todd, H.N., Trugman, A.T., Anderegg, W.R.L., Wang, Y., Tai, X., 2019. The impact of rising CO 2 and acclimation on the response of US forests to global warming. Proc. Natl. Acad. Sci. 116, 25734–25744. https://doi.org/10.1073/pnas.1913072116

van den Berg, L.J.L., Tomassen, H.B.M., Roelofs, J.G.M., Bobbink, R., 2005. Effects of nitrogen enrichment on coastal dune grassland: A mesocosm study. Environ. Pollut. 138, 77–85.

https://doi.org/10.1016/j.envpol.2005.02.024

Warner, S., Jeffries, S., Lovis, W., Arbogast, A., Telewski, F., 2021. Tree ring-reconstructed late summer moisture conditions, 1546 to present, northern Lake Michigan, USA. Clim. Res. 83, 43–56. https://doi.org/10.3354/cr01637

White, R.A., Piraino, K., Shortridge, A., Arbogast, A.F., 2019. Measurement of vegetation change in critical dune sites along the eastern shores of Lake Michigan from 1938 to 2014 with object-based image analysis. J. Coast. Res. 35, 842. https://doi.org/10.2112/jcoastres-d-17-00141.1

Zhu, Z., Piao, S., Myneni, R.B., Huang, M., Zeng, Z., Canadell, J.G., Ciais, P., Sitch, S., Friedlingstein, P., Arneth, A., Cao, C., Cheng, L., Kato, E., Koven, C., Li, Y., Lian, X., Liu, Y., Liu, R., Mao, J., Pan, Y., Peng, S., Peñuelas, J., Poulter, B., Pugh, T.A.M., Stocker, B.D., Viovy, N., Wang, X., Wang, Y., Xiao, Z., Yang, H., Zaehle, S., Zeng, N., 2016. Greening of the Earth and its drivers. Nat. Clim. Chang. 6, 791–795. https://doi.org/10.1038/nclimate3004